THE ROLE OF GABA IN FEAR AND ITS RELATIONSHIP TO EMOTION PROCESSING BRAIN NETWORKS

by Ilona Lipp

A Thesis

Submitted to the School of Graduate Studies

in Partial Fulfilment of the Requirements

for the Degree

Doctor of Philosophy

Cardiff University

Declaration

This work has not previously been accepted in substance for any degree and is not concurrently submitted in candidature for any degree.

Signed ..... (candidate) Date .....

Statement 1

This thesis is being submitted in partial fulfillment of the requirements for the degree of PhD.

Signed ..... (candidate) Date .....

Statement 2

This thesis is the result of my own independent work/investigation, except where otherwise stated. Other sources are acknowledged by explicit references.

Signed ..... (candidate) Date .....

Statement 3

I hereby give consent for my thesis, if accepted, to be available for photocopying and for inter-library loan, and for the title and summary to be made available to outside organisations.

Signed ..... (candidate) Date .....

Statement 4: Previously approved bar on access

I hereby give consent for my thesis, if accepted, to be available for photocopying and for inter-library loans after expiry of a bar on access previously approved by the Graduate Development Committee.

Signed ..... (candidate) Date .....

Summary

The aim of the project described in this thesis was to explore the relationship between the inhibitiory neurotransmitter gamma-aminobutyric acid (GABA) and fear-related brain activation, measured with functional magnetic resonance imaging.

The first part of the thesis deals with the question of how repeatable measures of fear-related brain activation can be obtained. Two paradigms were evaluated, a frequently used task using fearful and neutral faces and a newly developed paradigm using pictures of spiders, negative images from the international affective picture system, and carefully matched control stimuli.

In the main study latter paradigm was used to assess fear-related BOLD responses in two groups of participants, recruited for high vs. low levels of fearfulness. In the same participants, GABA concentration was measured using MRS in two brain regions relevant for emotion processing (left insula and left dorsolateral prefrontal cortex). Additionally, physiological parameters were recorded throughout the task, and a breath-hold task (to estimate vascular reactivity) as well as an arterial spin labeling aquisition (to estimate baseline cerebral blood flow) were included in the scanning session.

The main experimental chapters of the thesis deal with the questions whether fearfulness, GABA concentration and fear-related BOLD responses are associated, and how potential confounding factors - such as physiological task responses, vascular reactivity and baseline cerebral blood flow - might mediate this relationship. The last part of the main experimental part explores the relationship between fearfulness, GABA concentration and resting state functional connectivity in emotion processing networks.

In the general discussion, power of the study is estimated post-hoc, and limitations are outlined. Two chapters in the Appendix assess repeatability of the GABA MRS measures and vascular reactivity estimates.

Acknowledgements

This project would not have been possible without the contribution of a number of people.

Special thanks go to

- **Richard Wise** and **Xavier Caseras**, my two supervisors. Richard, thanks for your support in all matters, your encouragement and always constructive feedback. Xavier, thanks for regularly reminding me of the "goal of my PhD" and of being less pessimistic. Thanks to both of you for letting me do my own thing and making my own decisions, always ready to advise me with your expertise.

- **Kevin Murphy**, my non-official co-supervisor, and favourite second author. Thanks for providing me with your physiological noise correction scripts, and being a helpdesk for breath-holding problems.

- **John Evans**, my GABA coach, without who this project would simply not have worked out. Thanks for your crucial advice on setting up the aquisition, for rating all these spectra, for your optimism and for answering all my emails with the subject "just a quick question".

- **Caroline Lewis**, my data acqusition buddy. Thanks for your help with the least enjoyable part of this study (calling participants and asking them personal questions), and for making it possible to collect all this data so quickly by spending lots of evenings scanning with me.

- **Peter Hobden** for helping out with the scanning, the company during scanning and for adjusting your working hours to my scanning slots more than once.

- **Spiro Stathakis** and **Cyril Charron**, the "IT guys" for fixing things.

- **Mark Mikkelsen** for sharing experiences with spectroscopy, and to him and **Claire Hanley** for organizing the always useful insight into inhibition meetings.

- all the other people in **CUBRIC** for their input, support, and for providing the necessary distraction when needed. Special thanks go to **Claire Barnes** and **Sonya Bells** for our regular moaning and gossiping coffee breaks.
- all my **participants of the faces task repeatability study**, who only got paid in sweets.
- all my **participants of the main study** for looking at horrific pictures in the scanner and not running away.
- **Kacper Wieczorek** for our nerdy but stimulating science discussions, for sharing the up and downs of a PhD life and life outside the PhD.
- all my wonderful **friends outside work** and my basketball team(s) for reminding me that life is more than just science.
- **my family** for checking up on me regularly and providing me with Austrian chocolate and coffee to give me the necessary energy for finishing my thesis.

Abbreviations

Abbreviation	Description
ACC	anterior cingulate
ASL	arterial spin labeling
BOLD	blood-oxygen-level dependent
CO_2	carbon dioxide
DLPFC	dorsolateral prefrontal cortex
DTI	diffusion tensor imaging
fMRI	functional magnetic resonance imaging
FSS-II	Fear Survey Schedule-II
FSQ	Fear of Spiders Questionnaire
GABA	gamma-aminobutyric acid
GABA+	GABA plus coedited macromolecules
GAD	glutamic acid decarboxylase
HR	heart rate
HRF	hemodynamic response function
IAPS	international affective picture system
MPFC	medial prefrontal cortex
MRS	magnetic resonance spectroscopy
O_2	oxygen
OFC	orbitofrontal cortex
PET	positron emission tomography
PTSD	post-traumatic stress disorder
ROI	region of interest
RVT	respiratory volume over time
SC	signal change
SPECT	single photon emission computed tomography

Impact of this thesis

Please note that the following chapters have been amended for publication:

Chapter 2 resembles:
Lipp, I., Murphy, K., Wise, R.G., Caseras, X., 2014. Understanding the contribution of neural and physiological signal variation to the low repeatability of emotion-induced BOLD responses. NeuroImage 86, 335-342.

Chapter 4 resembles:
Lipp, I., Evans, C.J., Lewis, C., Murphy, K., Wise, R.G., Caseras, X., submitted for publication. The relationship between fearfulness, GABA+, and fear-related BOLD responses in the insula. PLoS ONE.

Chapter 10 resembles:
Lipp, I., Murphy, K., Caseras, X., Wise, R.G., submitted for publication. Agreement and repeatability of vascular reactivity estimates based on a breath-hold task and a resting state scan. NeuroImage.

Contents

Part I

Introduction

Chapter 1

A review of the literature

1.1 Outline

The brain imaging project described in this thesis deals with the question of how individual differences in fearfulness relate to brain function and chemistry. Two measures are of particular interest: fear-induced responses of brain structures known to be involved in emotion processing (as assessed by blood-oxygen-level dependent [BOLD] functional magnetic resonance imaging [fMRI]), and concentration of the inhibitory neurotransmitter gamma-amino butyric acid (GABA; as assessed by GABA sensitive magnetic resonance spectroscopy [MRS]).

In this literature review I aim to make the following points: 1) It is reasonable to assume the existence of biomarkers for fearfulness. 2) Potential biomarkers for fearfulness are a) hyperactivation of emotion processing brain regions in relation to negatively valenced stimuli, and b) a decrease of GABA concentration in fear-relevant brain structures. 3) The suggested biomarkers (fear-related brain activation and GABA concentration) might be associated with each other.

The literature review is structured in the following way: In **Section 1.2** I conceptualize the construct of fearfulness, discuss the development of fears and postulate that it is worth looking for biomarkers of fearfulness. In **Section 1.3** I review what is known about emotion and fear-processing networks in the brain, and then I introduce three regions that are of particular interest in this study: the insular cortex, the amygdala and the dorsolateral prefrontal cortex (DLPFC). In **Section 1.4** I give an introduction to the neurotransmitter GABA and provide evidence for its involvement in fear development and learning, in psychiatric disease, and in task-related BOLD responses. In **Section 1.5** I outline the challenges related to using BOLD fMRI and GABA MRS, and I discuss

a number of control measures that were included in this project to test for potential confounding factors. Last but not least I will summarize the hypotheses and research questions (**Section 1.6**).

1.2 Fear and fearfulness

1.2.1 An introduction to the constructs

Imagine coming home and finding a large snake on your kitchen table. How would you react? You might scream, you might freeze, you might run away. You will most likely experience something commonly described as fear. A useful definition of fear in this context is a strong reaction to a threatening stimulus, experienced as "anxious arousal" (Nitschke et al., 1999). Such a fear response has behavioural and physiological aspects, often including a facial expression characterized by opening of the eyes (e.g. Susskind et al., 2008), an increase in heart rate (HR) and perspiration (e.g. Davis, 1998), and an offensive or defensive behavioural response (fight or flight response) that depends on the particular situation (e.g. Blanchard et al., 2001). Darwin was the first to point out that some of these fear responses are comparable across various species (Darwin, 1782), and a considerable amount of research today is still based on the assumption that fear is a result of innate reactions of survival circuits existent in all mammalian brains (LeDoux, 2012; Panksepp, 1998).

However, not everyone experiences the same amount of fear. In fact, while a lot of people will run away at the sight of a snake, others might not be scared at all and approach it with curiosity. Individuals do not only differ in the intensity of fear responses but also in the tendency to show fear responses in relation to various objects and situations. It has been shown that people who show fear in one situation are more likely to also be afraid of other situations (Geer, 1965; Olatunji, 2006; Sawchuk et al., 2000), indicating that fearfulness can be considered a psychological trait. Being fearful can be useful for survival, since it prevents one from entering or staying in dangerous situations. However, high levels of fearfulness and anxiety can lead to lasting experience of stress, and impairments in daily life. In fact, most defined psychological disorders are characterized by symptoms related to emotion-processing and emotion perception, and in particular anxiety disorders[1] are characterized by an increased sensitivity to threat (Craske et al., 2011). In recent years,

[1] In the diagnostic system DSM-IV-TR these include panic disorder, social phobia, general anxiety disorder, simple phobia, obsessive-compulsive-disorder and post-traumatic stress disorder (PTSD; APA, 2000).

a trend has emerged to study biomarkers for such disorders and introduce specifically targeted strategies - such as biofeedback (e.g. Johnston et al., 2011; Linden et al., 2012) - to conquer the emotional symptoms.

Investigating subclinical variation in emotion-related traits can help to identify potential predisposing factors for developing clinical symptoms. The majority of subclinical studies in humans focus on trait anxiety rather than trait fearfulness. In contrast to fearfulness, which is related to the reactivity to stimuli in the present situation, trait anxiety is characterized by "anxious apprehension" and involves concern about things possibly happening in the future (Craske et al., 2011; Nitschke et al., 1999; Sylvers et al., 2011). Anxiety disorders are characterized by both, hightened fear reactions, and increased worry about future threat (Craske et al., 2011; Strelau and Zawadzki, 2011). Some researchers argue that the two constructs anxiety and fearfulness should be treated separately because there is only a moderate correlation between them (Sylvers et al., 2011) and some studies suggest different underlying brain mechanisms (Dien, 1999; Engels et al., 2010; Heller et al., 2008). However, in practice it is challenging to measure the constructs separately.

To measure fearfulness, typically questionnaires are used that rely on participants' awareness of their fear reactions. One example is the Fear Survey Schedule, which asks how much a person would avoid a variety of situations due to fear (e.g. Geer, 1965). The assumption behind this approach is that if someone has experienced a fear reaction towards a certain stimulus, this person will try to avoid exposure to the stimulus in the future. Whether a fearful person is also an anxious person might in fact depend on how easy it is to avoid the feared situations (Öhman, 2008). Because part of the strategy in this project is to confront participants with their fears, the construct fearfulness is measured using the Fear Survey Schedule-II (Geer, 1965). In the context of the literature review, studies using measures of fearfulness and studies using measures of trait anxiety will be discussed, as well as studies performed on clinical populations.

1.2.2 Development of fearfulness

Why do some people tend to react more strongly to negative stimuli than others? Research on how fears develop is predominantly conducted with phobic patients. Specific phobia is the most extreme form of fear, which is characterized as unreasonably excessive (APA, 2000). It is not clear how specific fears develop, and it is likely that several factors contribute. Early theories focus on the influence of learning and environment on fear development, and more recently, genetic contributions to fearfulness have been suggested.

For a long time, researchers assumed that fear conditioning was the assumed mechanism behind fear aquisition. When a neutral stimulus (e.g. a white rabbit) is coupled with an unconditioned stimulus that is able to produce an unconditioned response (e.g. loud sudden noise), the neutral stimulus acquires the capacity to induce a similar response as the unconditioned stimulus. This was first demonstrated by John Watson in a classical experiment in which a little boy was conditioned with a fear to a little white rabbit that he initially liked (Watson and Rayner, 1920).

However, not all individuals with fears report to have encountered situations in which this type of coupling could have happened (e.g. Poulton and Menzies, 2002). The extent to which conditioning plays a role in fear development might depend on the kind of fear (Coelho and Purkis, 2009), but is unlikely to be the only contributing factor. Another major theory, the prepared learning theory, focusses on the acquisition of fear of evolutionary relevant stimuli and was proposed by Seligman (1971). He postulated that by onto- or phylogenetic development certain stimuli have been prepared to be fearful stimuli, and that a single encounter with these stimuli is enough for fear acqusition. These include the common fears of heights, water, and spiders. In contrast to fears developed in laboratory settings through conditioning, these prepared fears are not easily extinguishable. It has in fact been shown that primates and humans get fear conditioned more easily when the conditioned stimuli are evolutionarily relevant (see review by LoBue and Rakison, 2013).

Bringing the two approaches together, the non-associative model of fear acquisition (Poulton and Menzies, 2002) postulates the existence of a limited number of innate, evolutionarily-relevant fears, and that all other fears are acquired by learning processes. Also this theory is not without critics (e.g. Muris et al., 2002) and it is still debated to what extent learning is necessary in fear development (Armfield, 2006; LoBue and Rakison, 2013). Furthermore, even though more and more is known about the neural processes involved in fear learning, it is unknown how evolutionary "preparedness" for certain stimuli might be manifested in the nervous system.

Another important aspect is social fear learning by observing or being informed about others experiencing fear (Olsson and Phelps, 2007). It might be the case that individuals who are exposed to fearful others also delevop more fears themselves (e.g. Gerull and Rapee, 2002). But environmental variance only accounts for some variability in fearfulness. Twin studies show that not only anxiety disorders have a significant genetic component (Hettema et al., 2001), but also specific fears are heritable. This has been found for specific fears such as fear of animals, social fear and agoraphobic fear (Skre, 2000), as well as general

fearfulness (Stevenson et al., 1992), with about 30-50% of the population variance being explained by genetic variance. Additionally, several subconstructs of fearfulness, such as briskness, perseveration and emotional reactivity have shown to be heritable to a similar degree (Strelau and Zawadzki, 2011). A number of specific genes have been suggested to contribute to fearful and anxious phenotypes in rodents and humans (Chen et al., 2006; Donner et al., 2008; Finn et al., 2003), including genes involved in GABA metabolism (e.g. Hettema et al., 2006; Thoeringer et al., 2009; also see Section 1.4.3).

How these genes influence fearfulness is not clear, and it is likely that genes have an influence on susceptibility factors for the development of fears, which is why the developmental and genetic contribution should not be seen as separate but as interacting (e.g. Lonsdorf et al., 2009). One possibility is that genes dictate the susceptibility to fear conditioning (Hettema et al., 2003). For example, people who report fear of flying show stronger conditioning effects for flying unrelated stimuli (Vriends et al., 2012), and individuals with anxiety disorders are more easily conditioned to fear (for a review see Lissek et al., 2005). It is also possible, however, that the presence of anxiety disorders influences the susceptibility for learning new fears, rather than the other way round. Other susceptibility factors might be the sensitivity to experience disgust, and behavioural inhibition (LoBue and Rakison, 2013; Muris et al., 2002). Others postulate that it might be a low threshold for the physiological part of the fear response that determines how easily individuals develop fears (Skre, 2000).

Research has started investigating what properties of the brain could mediate the effect between genes and fearfulness. The most commonly used brain imaging measure for that purpose is the activity in brain structures that are known to be involved in emotion processing. Gross and Hen (2004) postulate that one of the susceptibility factors for anxiety disorders is hyper-excitability of certain brain areas, and hypothesizes that this is caused by a lack of the inhibitory neurotransmitter GABA. However, this hypothesis has yet to be empirically tested; this being one of the aims of the present thesis. In the next two sections, evidence underlying this postulate will be discussed.

1.3 Investigating fear-related brain activation in humans: what we know from fMRI research

A major proportion of emotion research is done with animals, which is useful to understand the synaptic level mechanisms and cellular pathways that go hand in hand with fear

learning (e.g. Gross and Canteras, 2012). Most of these methods (such as introducing specific lesions) cannot be used in humans. Lesion studies in humans can be informative, however, naturally occuring lesions are not very spatially specific and usually only very few individuals with such lesions are available. This is why an important method in human emotion research is in vivo brain imaging.

The most commonly used brain imaging method to characterize fear processing in the human brain is BOLD fMRI. The advantage of fMRI over other brain imaging methods is that it has a good spatial resolution and can clearly identify signals from subcortical areas unlike electroencephalography or magnetoencephalography. Another advantage is that in comparison to positron emission tomography (PET) BOLD fMRI does not use radioactive tracers. The disadvantages are a low temporal resolution in the scale of seconds, and - as will be discussed later - the nature of the signal, making it susceptible to noise by unwanted factors (Section 1.5.1). Important knowledge about human emotion processing has been reached through fMRI, and I will first review what the main networks in emotion processing are, and then discuss three specific regions of interest.

1.3.1 Emotion processing brain networks

Findings regarding the localisation of emotion processing relevant areas are not consistent over different emotions and different tasks (Phan et al., 2002). Currently, two popular neuroscientific approaches try to explain fMRI findings from emotion studies. The first approach assumes a set of basic emotions[2]. and that each emotion goes hand in hand with specific brain activation and physiological responses. Quite a number of studies have tried to distinguish different emotional states using fMRI. In a meta-analysis combining studies that investigate various emotions and stimulus types, Vytal and Hamann (2010) managed to identify activation patterns specifically associated with each basic emotion. Regarding the emotion fear the authors describe a network composed of the bilateral amygdala, right insula, anterior cingulate (ACC) and left inferior frontal gyrus.

Not all meta-analyses found specific activation patterns for specific emotions (Lindquist and Barrett, 2012) and so a second model for emotions in the brain has been suggested, the constructionist approach (also see Hamann, 2012). It is based on the idea that the brain is organized in a number of basic functional networks that interact to produce a variety

[2]The concept of basic emotions has been proposed by Paul Ekman. He describes basic emotions as discrete emotions that meet certain criteria, such as the possession of distinctive universal signals and distinctive physiology. Basic emotions include anger, contempt, disgust, fear, happiness, sadness and surprise (see Ekman and Cordaro, 2011).

of different psychological states, such as attention, language, and also emotion (Lindquist and Barrett, 2012). These basic networks are often discovered by resting state fMRI and include the salience network, the default network, and the executive control network (e.g. Barrett and Satpute, 2013; Oosterwijk et al., 2012). Evidence for this approach comes from studies such as Oosterwijk et al. (2012)'s. They instructed their participants to imagine a negative situation, either focussing on thoughts, their bodily sensations or on emotions. For all three scenarios the same basic networks were involved, but contributed to different extents depending on the task instruction. Oosterwijk et al. (2012) conclude that there is no such thing as emotion processing circuit in the brain but that emotions are a result of the interplay of more general networks.

Independent of which of the approaches is more accurate, some brain areas are repeatedly reported to be involved in fear processing, such as the amygdala and insula (Phan et al., 2002). When individual differences and biomarkers are studied, the most commonly used approach is to look at individual regions and only a few studies look at network activity, even though this is becoming more and more common. In this project, both approaches are taken into account.

1.3.2 Fear-induced brain activation

Several strategies have been used to investigate fear-related brain responses. These include fear-conditioning, confrontation with generally fearful images and confrontation with stimuli specific to participants' fears.

One way to study fear responses in healthy participants is to performing fear conditioning in the scanner. Studies using this method usually find that the amygdala, anterior cingulate cortex (ACC), and the insular cortex are crucial structures for processing conditioned stimuli (for reviews see Büchel and Dolan, 2000; Kim and Whan, 2006; Sehlmeyer et al., 2009).

Another way is to confront participants with images of facial expressions or negative emotion-inducing images. Fearful faces induce activation in the amygdala, insula, cerebellum, fusiform gyrus, inferior parietal and inferior and medial frontal regions (meta-analysis by Fusar-Poli et al., 2009; Sabatinelli et al., 2011). Generally negative images, such as negative pictures from the international affective picture system (IAPS; Lang et al., 2008) are rated as more negative and more arousing than faces (Britton et al., 2006; Schäfer et al., 2005) and are often used to induce the experience of negative emotions in participants. However, resulting activation patterns cannot always be attributed to distinct emotions

such as fear. Confronting participants with negative emotion-inducing stimuli leads to activation in amygdala, orbitofrontal cortex (OFC), medial prefrontal cortex (MPFC) and occipital areas (meta-analysis by Sabatinelli et al., 2011).

A common approach to study fear responses in the brain is to confront phobic patients with phobia-related stimuli as compared to neutral control stimuli such as mushrooms. One typical example of such a study was conducted by Straube et al. (2006b). Twelve spider phobics and twelve controls were confronted with pictures of spiders and mushrooms as neutral controls. Only in phobics, increased activation during the spider vs. mushroom condition was found, in regions such as the ACC, insula and amygdala. Most studies have used spider phobia (e.g. Caseras et al., 2010; Schienle et al., 2005; Straube et al., 2004, 2006a,b; Wendt et al., 2008), but also social phobia (e.g. Klumpp et al., 2010; Stein et al., 2002) and snake phobia (e.g. Lueken et al., 2011) to study fear-induced brain activation. The areas that are commonly found during the contrast phobic stimulus vs. neutral stimulus are then assumed to be fear-relevant areas, and usually phobia patients show stronger activity in these areas than control participants. These areas include (amongst others) the amygdala (Caseras et al., 2010; Dilger et al., 2003; Etkin and Wager, 2007; Klumpp et al., 2010; Schienle et al., 2005; Straube et al., 2006b), the insula (Caseras et al., 2010; Dilger et al., 2003; Klumpp et al., 2010; Lueken et al., 2011; Stein et al., 2002; Straube et al., 2004, 2006a,b; Wendt et al., 2008), the DLPFC (Schienle et al., 2005; Straube et al., 2004), the ACC (Caseras et al., 2010; Lueken et al., 2011; Straube et al., 2006a,b), the inferior frontal gyrus (Caseras et al., 2010; Klumpp et al., 2010; Stein et al., 2002; Straube et al., 2004), and the fusiform gyrus (Schienle et al., 2005; Straube et al., 2006a). Therapy such as cognitive behavioural therapy can decrease activation in these areas, for example in the amygdala and insula (Goossens et al., 2007; Schienle et al., 2009; Straube et al., 2006a).

The finding that phobic participants show stronger BOLD responses to fear-specific stimuli is intuitive, since stronger fear reactions upon stimulus presentation can be expected. But there is also some evidence that participants with a strong fear respond more strongly to negatively valenced but fear-unrelated stimuli in fear-relevant brain structures. Most of this evidence comes from patient populations, such as patients with depression (Etkin and Schatzberg, 2011; Jaworska et al., in press), specific phobia (Wright et al., 2003), PTSD (Bruce et al., 2012) and general anxiety disorder (Etkin et al., 2010; Etkin and Schatzberg, 2011). In subclinical samples, trait anxiety was found to predict reactivity of the insula and amygdala to emotional faces (Etkin et al., 2004; Stein et al., 2007).

This suggests that fearful individuals might show a more general hyper-reactivity in the brain areas of interest. This hyper-reactivity might in fact be a predisposition for developing anxiety disorders, and it might explain behavioural findings such as that people with anxiety disorders show increased fear conditioning, elevated anticipation of stressors, and attentional bias to fear related information (Craske et al., 2011). However, not all studies find a more generalized hyper-reactivity (e.g. Wendt et al., 2008), therefore more research is needed to resolve to what extent this hyper-reactivity exists. The influence of fearfulness on activity upon generally negative IAPS images will be explored as part of this project.

1.3.3 Regions of interest

Based on the findings reported in the previous section, in this project three regions are of particular interest: the insular cortex, the amygdala, and the DLPFC. The insula and amygdala have been repeatably reported as hyper-reactive in fearful participants (see section 1.3.2). The DLPFC might be implicated in the downregulation of activity in these regions (Ray and Zald, 2012).

Insula

The insular cortex (insula) is part of the cerebral cortex and lies within the lateral sulcus, which makes it highly folded. The anterior part of the insula has three short gyri, while the posterior insula consists of two long gyri (Türe et al., 1999). Cytoarchitecturally, four areas are distinguished: the rostroventral agranular field consisting of two different areas, the transitional dysgranular field and the posterior granular field (Augustine, 1996). Important structural connections of the insula include its afferent and efferent projections to the amygdala, thalamus, ACC and prefrontal cortex and inferior frontal gyrus (Augustine, 1996; Catani et al., 2012; Mesulam and Mufson, 1982). Recent studies suggest that the anterior and posterior insula are part of two different structural networks. Findings from diffusion tensor imaging (DTI) studies indicate that the anterior insula is strongly connected to dorsal prefrontal, inferior frontal and temporal areas, while the posterior insula's main white matter tracts go to motor and somatosensory areas (Chia-Feng et al., 2012; Cloutman et al., 2012). This parcellation has also been supported by functional connectivity studies (Cauda et al., 2011; Chang et al., 2012; Deen et al., 2010).

The insula is involved in emotion processing (Lindquist et al., 2012; Phan et al., 2002; Schienle et al., 2002). A proposed mechanism underlying this function is that interocep-

tive sensations are integrated within the insula and based on the outcome, attention is regulated and an affective feeling is created (Lindquist et al., 2012). Craig (2009) proposed a model on how the integration is performed on a continuum from posterior to anterior insula, suggesting that the creation of the emotional feeling is based on the integration of homeostatic but also higher-level contribution such as environmental, hedonic, motivational, social and cognitive factors (see Figure 1.1). If the insula integrates interoceptive sensations, then it should also be involved in other mental states that go hand in hand with perception of bodily states. In fact, the insula has been found to play a crucial role in sexual arousal (Ortigue et al., 2007; Stoléru et al., 2012) and pain (Ciampi de Andrade et al., 2012; Wiech et al., 2010).

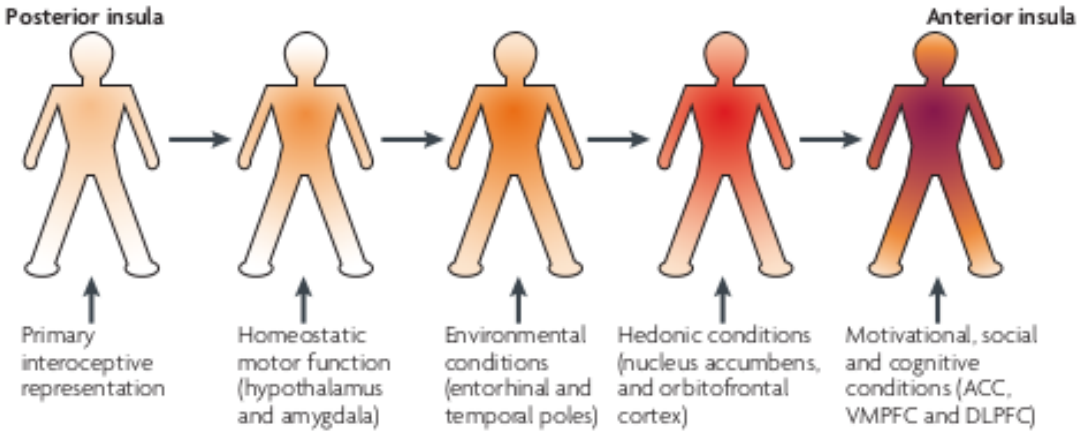

Figure 1.1: Integration of information is hypothesized to progress from posterior to anterior insula. Figure taken from Craig, 2009.

Another piece of evidence for this interoceptive integration model is that people with higher insula activation are better at perceiving their own heartbeat (Critchley et al., 2004). It has also been reported that there is an anatomical overlap of the insula activity during this kind of interoception and during the experience of fear (Caseras et al., 2013; Zaki et al., 2012). The role of the insula in processing one's own physiological reactions raises the question whether the increased insula activity in fearful participants might be mediated by their physiological reactions. This question will be addressed as part of this project.

Amygdala

Amygdala refers to a group of subcortical nuclei, whereby most commonly the superficial group, the centromedial and basolateral complexes are distinguished (Amunts et al., 2005). The amygdala is involved in emotion perception, perception of facial expressions, in par-

ticular fear (Calder et al., 2001; Costafreda et al., 2008), and fear conditioning (LeDoux, 2000). A model proposed by Stefanacci and Amaral (2002) postulates that the amygdala is a protective device that inhibits the approach of salient objects, evaluates whether the object determines a threat, and coordinates other brain regions to appropriately react, such as by generating autonomic physiological responses as suggested by animal research (e.g. Iwata et al., 1987). In fact, it has been shown that in threatening situations that lack a salient stimulus, or in situations where participants are asked to recall emotional situations, amygdala activity is less likely detected (Costafreda et al., 2008; Lindquist et al., 2012; Phan et al., 2002).

The amygdala has close bidirectional connections to the insula (Davis et al., 1994; Reynolds and Zahm, 2005). Paulus and Stein (2006) propose that the amydala passes on information about the valence of a stimulus to the insula, which integrates this with information about the interoceptive state. There is evidence that the connectivity between insula and amygdala is involved in emotion experience, as Baur et al. (2013) showed that anterior insula and amygdala connectivity explain 40 percent of variance in state anxiety.

DLPFC

The DLPFC is roughly equivalent to brodman areas 9 and 46 (Petrides, 2005; see Figure 1.2). The DLPFC has been assigned to the executive network (Carpenter et al., 2000; Niendam et al., 2012; Seeley et al., 2007), which also involves other frontal and parietal regions and is involved in executive functions such as flexibility, working memory, initiation and inhibition (Niendam et al., 2012). The DLPFC has direct connections to the insula (Chia-Feng et al., 2012; Cloutman et al., 2012), and it has been proposed that the salience network (which the insula is part of) regulates activity of the executive network (Menon and Uddin, 2010; Sridharan et al., 2008) depending on the outcome of the salience evaluation.

In emotion confrontation paradigmns, prefrontal activation is often reported (e.g. Schienle et al. 2005; Straube et al. 2004). Due to their involvement in the executive network, the particular role of prefrontal areas in emotion have been frequently discussed in the context of emotion regulation. Phillips et al. (2003) stated a theory on emotion processing, involving the three stages 1) appraisal and identification of emotional significance of a stimulus, 2) production of a specific affective state, 3) regulation of the affective state and emotional behaviour; steps 1 and 2 resemble the functions of insula and amygdala as

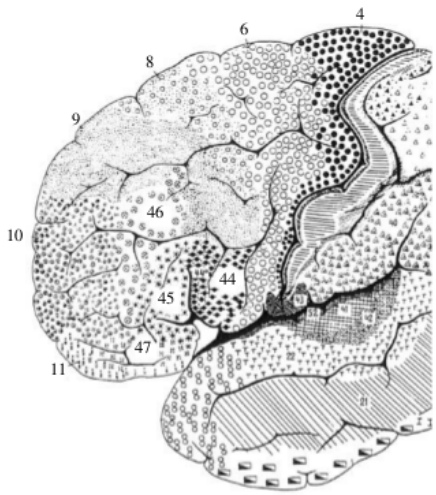

Figure 1.2: Cytoarchitectonic map of the lateral surface of the human cerebral cortex. The DLPFC corresponds roughly to Brodman areas 9 and 46. Figure taken from Petrides, 2005.

discussed above. Step 3 could involve mechanisms that downregulate the initial response of areas such as the amygdala and insula.

Different strategies of emotion regulation have been proposed (Gross and Barrett, 2011). One cognitive strategy of emotion regulation is reappraisal, such as reinterpreting the scene. Reappraisal recruits frontal areas including DLPFC, ventrolateral prefrontal cortext, MPFC and ACC, and is associated with reduction in amygdala and insula reactivity (Drabant et al., 2009; McRae et al., 2009; Ray and Zald, 2012). Goldin et al. (2008) found that early prefrontal responses go hand in hand with later reduction in amygdala and insula responses, and Eippert et al. (2007) showed that the DLPFC is involved in up- as well as downregulation of emotions. Unlike the MPFC, the DLPFC only has a limited number of direct projections to the amygdala (Ray and Zald, 2012; Stefanacci and Amaral, 2000), and probably plays a role in downregulation via indirect connections, through its close connections to other prefrontal regions (Ray and Zald, 2012; Yeterian et al., 2012). Phillips et al. (2008) furthermore suggests that the DLPFC is primarily involved in voluntary rather than automatic regulation of emotion.

In addition to amygdala and insula reactivity, individual differences in DLPFC recruitment have also been linked to individual differences in fear and anxiety. For example, Bishop et al. (2007) showed a negative correlation between trait anxiety and the extent to which the DLPFC reacts to fearful vs. neutral faces. On the other hand, it has also been reported that individuals with high anxiety activate frontal regions such as the DLPFC when presented with negative images more strongly than non-anxious people (Campbell-Sills et al., 2011). Different factors such as peceptual load (Bishop et al., 2007) seem

to have an influence on the relationship between anxiety and DLPFC activation. Also, some evidence suggests that individual differences in functional connectivity between the DLPFC and amygdala is stronger in individuals with high trait anxiety (Laeger et al., 2012).

1.4 The GABA system, its role in fear and its relationship to BOLD

This part of the review deals with the role of the neurotransmitter GABA in fear. First, I will provide a short introduction to the GABA system, then I will discuss different forms of evidence for its involvement in anxiety and fear, and its potential association with BOLD responses.

1.4.1 GABA is the inhibitory neurotransmitter

Functioning networks in the brain require balance between excitation and inhibition (e.g. Isaacson and Scanziani, 2011). While most neurons form excitatory connections with other neurons, only about 20-25 % of neurons release the inhibitory neurotransmitter GABA. These neurons are called interneurons and exist in all cortical layers. They show a variety of morphological, neurochemical and physiological characteristics, which makes classification challenging (Maccaferri and Lacaille, 2003). Most interneurons do have short axons, which means that they regulate locally, whereby they can target different parts of pyramidal cells. For example the parvalbumin-positive basket cells target the perisomatic region, Martinotti cells target the dendrites, and chandelier cells the axon initial segment (Fino et al., 2012). Inhibitory interneurons allow networks in the brain to self-organize, be more complex and increase temporal precision of firing. This allows neuronal networks to react to small stimulation but not over-react to massive stimulation (Buzsaki, 2006).

GABA is the main inhibitory neurotransmitter. It is produced by decarboxylating the amino acid L-glutamic acid. This reaction is catalyzed by the enzyme glutamic acid decarboxylase (GAD), which exists in two forms, GAD67 and GAD65. GAD's activity is the rate limiting step in the conversion of glutamate to GABA (Paredes and Agmo, 1992). GABA transaminase breaks down GABA into succinic semialdehyde, which is then further processed to succinate (for a review of GABA metabolism see Tillakaratne et al., 1995). GABA is stored in vesicles in the presynaptic cells until an action potential triggers exocytosis. After being released in the synaptic cleft, GABA can bind to three kinds of

GABA receptors on the postsynaptic membrane. Receptor A and C are chloride channels. Binding of GABA leads to conformational changes of these receptors, allowing chloride ions to influx into the postsynaptic cell. This causes hypopolarisation and a decrease in excitability (also see Nutt and Malizia, 2001). When GABA binds to type B receptors, the receptors trigger second messenger pathways that lead to slower and longer lasting inhibition (Chebib and Johnston, 1999). As it is the case with other neurotransmitters, neurons and glia cells reuptake GABA in order to inactivate it. GABA that goes to non-GABAergic cells cannot be used again for neurotransmission, which is why GABAergic neurons need to produce more GABA (Iversen et al., 2009).

1.4.2 GABA is important for fear learning and expression

Evidence that GABA is crucial for fear learning and fear expression comes from two types of studies: studies in which fear or fear learning is induced and changes in the GABA system are investigated, and studies in which changes in GABA transmission are induced and the effects on fear and fear learning are investigated. Due to practical, methodological and ethical reasons, the majority of these studies are conducted with animals, in particular rodents. I will include both animal and human literature in the following paragraphs.

Animal studies, in which fear is induced, have shown that fear does lead to changes in the GABA system, particularly in the amygdala. Heldt and Ressler (2007) and Stork et al. (2002) found that fear conditioning goes hand in hand with a decrease in messenger ribonucleic acid levels of a number of GABA related proteins in the amygdala, while fear extinction led to an upregulation. These findings suggest that fear learning leads to a downregulation of GABA transmission in order to allow excitatory neurotransmission in the amygdala to consolidate the fear memory (also see Maren and Quirk, 2004).

In humans, not many studies have investigated the effects of fear on GABA concentration. In one study, Hasler et al. (2010) told his participants that they would receive occasional electric shocks during the scan, and acquired GABA concentration measures from the medial prefrontal cortex throughout the scan duration. They found that GABA levels were significantly lower than in a no-threat control condition. This suggests that the effect of fear or stress triggers measurable GABA decreases in the human cortex.

Studies of the second type have been performed by influencing the GABAergic transmission with GABA agonists or antagonists. The effects of GABA agonists and antagonists in rodents have been demonstrated on a variety of behavioural fear measures. In general, it seems that GABA antagonists increase fear learning (e.g. Manzanares et al., 2005) and

fear reactions (e.g. Sanders and Shekhar, 1991), and that GABA agonists attenuate them (e.g. Muller et al., 1997; for reviews see Akirav and Maroun, 2007; Makkar et al., 2010; Malizia, 2002). This suggests that high levels of GABA transmission are disruptive for fear acquisition, which could lead to the hypothesis that individuals with low GABA concentration (possibly due to their genetic predisposition) are predisposed for fear learning. This postulate will be discussed in the Section 1.4.3.

Again, the number of studies in humans investigating GABA altering drugs are limited. Most evidence that changing GABA transmission leads to changes in fear and anxiety comes from the observation that anxiolytic drugs act on the GABA system (Kalueff and Nutt, 2007). Benzodiazepines have been a commonly used treatment for anxiety disorders since the 40s, but only decades later it was discovered that they are allosteric enhancers of GABA receptors (review by Nutt and Malizia, 2001). A number of studies in humans investigated the effects of GABA modulating drugs on specific behavioural outcomes. Diazepines have been shown to decrease startle responses and fear potentiation of the startle response response[3] (Baas et al., 2002; Bitsios et al., 1999; Graham et al., 2005; Grillon et al., 2006; Riba et al., 2001). The action probably happens by blocking the learning process rather than the expression of a previously learned response (Scaife et al., 2005, 2007). This again supports that GABA transmission levels are important for learning fear responses. In humans enhancing GABA transmission also decreases the ability to recognize fear as well as the subjective feeling of anxiousness (Bitsios et al., 1999; Del-Ben et al., 2012).

Bringing these findings together it seems that fear experiences influence GABA neurotransmission, and that by altering GABA neurotransmission fear-related behaviours can be influenced (for a review see Malizia, 2002 and Millan, 2003). A proposed mechanism for the action of GABA antagonists or agonists on fear is that they alter brain activation in emotion processing areas, which will be discussed below (Section 1.4.4).

[3]Startle response refers to a muscle contraction upon a strong stimulus. In humans this can for example be measured using electromyography. It has been found that the startle response is enhanced under presence of a stimulus that predicts an aversive event. This enhancement - the fear potentiation of the startle response - is often used as a measure of anticipatory anxiety, and has been related to traits of fearfulness and anxiety (e.g. see Vaidyanathan et al., 2009).

1.4.3 Why individual differences in GABA might explain individual differences in fear

So far, I discussed how changes in fear trigger changes in GABA, and how changes in GABA alter fear learning within individuals. However, this does not necessarily mean that individual differences in GABA are associated with individual differences in fearfulness. In this section I want to discuss evidence from two groups of studies: studies showing that different gene variants related to GABA influence fearfulness and anxiety, and studies measuring GABA concentration and relating it to clinical symptoms or patient populations.

Evidence from Genetics

As discussed in Section 1.2.2 fearfulness is heritable, and a few genes have been identified to play a role. Genes involved in the GABA system can code for receptor subunits, for metabolizing enzymes or for GABA reuptakers. Malfunctioning variants of these genes can lead to decreased efficiency in any of the GABA transmission related processes.

A lot of genetic studies are done with rodents, for example using the knock-out strategy to investigate effects of specific genes. Higher anxiety levels have been shown for mice with a GABA A receptor gamma subunit knockout (Smith and Rudolph, 2012), for mice with GABA B receptor subunit knockouts (Mombereau et al., 2005), and also for mice with knockout for a GABA reuptaker gene (Liu et al., 2007), and the GAD65 gene (Kash et al., 1999). Knocking out the GAD67 gene in the amygdala only shows effects on fear extinction but not conditioning or general anxious behaviour (Heldt et al., 2012).

In humans, the predisposition for affective disorders has been linked to mutations in genes coding for GABA metabolism proteins. The GAT-1 (GABA transporter, responsible for reuptake) gene has been linked to panic attacks (Thoeringer et al., 2009), and the gene for GAD67 linked to predisposition for depression and anxiety disorders (Hettema et al., 2006). GABA A receptor subunit genes have been associated with neuroticism and its sub facets anxiety, hostility, depression and vulnerability (Sen et al., 2004) as well as the somatic symptoms, anxiety and depression scales of a general health questionnaire (Feusner et al., 2001).

Evidence from brain imaging: PET, single photon emission computed tomography (SPECT) and MRS

Paulus and Stein (2006) suggested that anxious phenotypes might be a result of reduced

GABA concentration. In fact, GABA receptor density and GABA concentration have been studied in several clinical populations with a number of different methods.

GABA receptor density is not a direct measure of GABA concentration, but gives an indication of the number and strength of inhibitory synaptic connections (Kittler and Moss, 2003). Density of GABA A receptors in the brain is measured with either PET, or SPECT, by using radioactively labelled benzodiazepine antagonists such as Iomazenil. Studies using these methods in clinical population have revealed decreased benzodiazepine binding in patients with panic disorder only in the right prefrontal cortex (Brandt et al., 1998), across the whole brain including insula and DLPFC (Malizia et al., 1998), only in temporal cortices (Kaschka et al., 1995), and only in the insula (Cameron et al., 2007). For veterans with PTSD decreased binding has been reported in the hippocampus and prefrontal cortex (Bremner et al., 2000), across the cortex and also in the amygdala and hippocampus (Geuze et al., 2008). The general tendency seems to be a GABA decrease in patient populations. In a subclinical sample, Abadie et al. (1999) failed to find a relationship between anxiety and benzodiazepine binding. It has to be considered that most of these studies used very small sample sizes, which makes it hard to draw conclusions about the regional specificity.

While GABA receptor density might be an indicator of the abundance or importance of GABA in a region, GABA concentration can be directly measured from plasma and from the brain using MRS (described in Section 1.5.2). Measuring GABA concentration from plasma is indicative of a general GABA level, but does not allow to draw conclusions about levels in different brain regions. Nevertheless, studies still found evidence that mood disorders go hand in hand with a decrease in plasma GABA levels (Petty et al., 1992, 1993; Petty, 1994; Petty et al., 1995; Sanacora et al., 1999), suggesting that there might be a general GABA deficit in these populations. Vaiva et al. (2004) found decreased plasma GABA in panic disorder and Vaiva et al. (2006) found evidence that a decreased GABA level might be a predisposition for developing panic disorder.

MRS allows to measure GABA concentration from one location in the brain at a time (for a review see Puts and Edden, 2012). A number of studies have compared GABA levels between patient and control groups. They report lower GABA levels in prefrontal areas in patients with major depression (Hasler et al., 2007), as well as lower GABA levels in the ACC (Ham et al., 2007; Long et al., 2013), temporal cortex (Meyerhoff et al., 2014) and occipital lobe (Goddard et al., 2001, 2004a,b; Meyerhoff et al., 2014) in patients with panic disorder. Other studies show a reduction of GABA in patients with

social anxiety disorder in the hypothalamus (Pollack et al., 2008), and in the occipital lobe in patients recovered from mood disorders (Bhagwagar et al., 2007). Again, there is a general trend for a decrease in GABA in clinical populations, supporting the evidence from PET/SPECT studies. Again, because of the small sample sizes used in these studies, it is hard to tell whether there is a global GABA decific in clinical populations or whether it is restricted to certain brain structures. So far, no GABA MRS studies on participants with subclinical anxiety or fearfulness have been conducted. One study reported a negative correlation between state and trait anxiety and GABA in the right anterior insula, however the anxiety level was highly confounded with the presence of PTSD (Rosso et al., 2014). The relationship between subclinical levels of fearfulness and GABA concentration in two cortical regions will be investigated as part of this project.

1.4.4 GABA and BOLD might be associated

If GABA inhibits neural activity, and BOLD is a measure sensitive to neural activity, a negative relationship between the amount of GABA and BOLD signal amplitude can be expected. In a clever study with mice, Chen et al. (2005) showed that administration of a GABA transaminase inhibitor - so a drug that prevents the breakdown of GABA - leads to an increase in GABA concentration measured with MRS. This GABA increase was coupled with a decrease in BOLD response in the somatosensory cortex during forewpaw stimulation. This study does not only demonstrate that GABA MRS is sensitive to changes in GABA but also that there is a direct relationship between GABA concentration and BOLD reactivity.

The effects of drugs altering GABA transmission on BOLD responses have also been studied in humans. Because these drugs - such as benzodiazepines - are known for their effect on anxiety, their effects on emotion-related BOLD responses are of particular interest. Malizia (2000, as cited by Nutt and Malizia, 2001) for example found that anxiolytic effect of benzodiazepines go hand in hand with a decrease in brain metabolism (as measured using PET) in areas associated with emotion processing such as the insula and OFC. A study using emotional faces found that benzodiazepines decrease BOLD in the amygdala and insula, but not in prefrontal or occipital cortex (Paulus et al., 2005). In another face processing study, Del-Ben et al. (2012) report that benzodiazepine attenuates BOLD responses in right hemisphere amygdala, OFC, ACC and bilateral insula to fearful faces. Similarly, Wise et al. (2007) found that a benzodiazepine agonist decreased BOLD significantly in anterior insula during anticipation of pain. Pregabalin, another drug enhancing

GABA transmission, was also found to decrease BOLD responses in left amygdala and anterior insula during the anticipation of emotional stimuli, but to increase the BOLD response in the ACC (Aupperle et al., 2011). The authors suggest that the effects of anxiolytic drugs might actually be mediated by an attenuation of amygdala and insula reactivity.

In addition to manipulating GABA artificially, natural individual variation in GABA concentration has been linked to BOLD responses. A number of studies demonstrate a correlation between GABA measured with MRS and BOLD responses to a variety of stimuli. Muthukumaraswamy et al. (2009) found a negative correlation between BOLD signal amplitude and GABA level in the occipital cortex. Later, this was further explored, and a positive correlation between GABA and width of the hemodynamic response function (HRF), but a negative correlation between GABA and the amplitude was reported (Muthukumaraswamy et al., 2012). A negative correlation in the visual cortex was also reported by Donahue et al. (2010), but with a measure of task-related cerebral blood flow changes rather than the BOLD response. Northoff et al. (2007) found a negative correlation between negative BOLD and GABA concentration in the ACC during the presentation of emotional faces. Using a motor sequence learning task, Stagg et al. (2011) reported that participants with lower baseline GABA showed greater task-related BOLD responses. These results all point into the direction of a negative correlation between GABA and BOLD. Interestingly, Wiebking et al. (2014) found a positive correlation between activity related to interoceptive awareness in the insula and GABA level.

1.5 Methodological considerations

In this study, two extreme groups (participants with high vs. low levels of fearfulness) were recruited and fear-related BOLD responses and GABA concentration assessed. During the planning of this project, a number of possible confounding variables and challenges were considered. In the following, factors that are independent of neural activity but might influence task-related BOLD responses are discussed. Then the basic principles of GABA MRS are explained. Additionally the potential influence of menstrual cycle and hormonal contraception are outlined, and the rationale behind conducting repeatability studies of the measures involved is explained.

1.5.1 The challenge of BOLD as a measure of neural activity

The method used to study brain activation patterns in this project is BOLD fMRI. The idea behind this measure is that neural activation requires energy metabolism and oxygen, resulting in a greater oxygen delivery to activated regions, and as a consequence in a higher oxygenated/deoxygenated hemoglobin ratio, which is detected by the BOLD contrast (for a good introduction on BOLD FMRI see Huettel et al., 2009). However, it is not only neuronal activity itself that influences the BOLD signal. In this context, the influence of physiological noise, baseline cerebral blood flow and vascular reactivity will be discussed.

Physiological noise

Physiological parameters, including cardiac cycle, breathing cycle, carbon dioxide (CO_2), oxygen (O_2), heart rate (HR) and respiratory volume over time (RVT), have been shown to contribute to the BOLD signal (Birn et al., 2006, 2009; Chang et al., 2009; Dagli et al., 1999; Glover et al., 2000; Shmueli et al., 2007; Wise et al., 2004). The influence of physiological parameters on the BOLD signal is particularly important to consider in the context of studying emotions. This is because physiological reactions can be part of an emotional experience, if not crucial to it. Early theories on emotions already recognized this importance, starting with the James and Lange theory that postulated that emotional states are actually a result of perceiving and interpreting physiological processes rather than causing them (e.g. Kandel et al., 2013). Kreibig et al. (2007) and Kreibig (2010) reviewed literature on physiological reactions to emotional stimuli, and found a physiological profile for fear, characterized by an increase in HR, skin conductance, respiration rate, and a decrease in end-tidal CO_2.

The strategy of this study is to confront fearful vs. non-fearful participants with fear-inducing stimuli. Therefore, it might be the case that fearful participants show stronger physiological reactivity to the emotional stimuli, which could affect the BOLD signal and possibly be a confounding factor for fMRI group analysis. Even if the physiological fluctuations are not confounded with the task, increased physiological variability can introduce unwanted variance in the BOLD signal and decrease the power to detect BOLD responses of interest. Several methods have been developed to filter out signal related to physiological fluctuations from BOLD timeseries (Birn et al., 2009; Chang et al., 2009; Glover et al., 2000; Kay et al., 2013; Perlbarg et al., 2007). One potential problem with applying physiological noise correction is that if the physiological parameters are highly confounded with the task, regressing out their influence might also take out some task-related vari-

ance. The effect of physiological noise correction on emotion-related BOLD responses was investigated as part of this project.

Vascular reactivity and baseline cerebral blood flow

The BOLD signal depends on the cerebro-vascular reactivity, the responsiveness of the vascular system to vasodilative signals that are released with increased neural activity (Murphy et al., 2011; Thomason et al., 2005). If this vascular reactivity differs between people, task-related BOLD signals will also be different even if the underlying neural activity is the same. One method that has been introduced to measure this factor task-independently is to increase the CO_2 level by hypercapnic challenges (artificially regulating CO_2 level of the environment) or through breath-hold tasks. Using this method, cerebral blood flow (CBF) is modulated, under the assumption of an unchanged rate of oxygen consumption (Thomason et al., 2005). BOLD signal following an increase in CO_2 in a region has been found to explain up to 50 % of task-related (spatial and between participants) variability in BOLD responses in the same region (Biswal et al., 2007; Kannurpatti et al., 2012; Liu et al., 2013; Thomason et al., 2007).

Since the BOLD response reflects a change in cerebral blood flow, the baseline blood flow can also affect task-related BOLD responses (Cohen et al., 2002; Liu et al., 2012; Sicard and Duong, 2005; Vazquez et al., 2006). Cerebral blood flow has been associated with a number of personality and clinical traits (Coombs III et al., 2014; El-Hage et al., 2013; Schlegel et al., 1989; Takeuchi et al., 2011; Wolf et al., 2012), and might therefore be a confounding factor when individual differences are investigated. For this study, CBF is of particular interest because a number of studies show an association with GABA levels (Donahue et al., 2010, 2014; Franklin et al., 2011, 2012; Kajimura et al., 2004; Krause et al., 2014; Michels et al., 2012). Cerebral blood flow can be measured with a method called arterial spin labeling (ASL). Performing ASL, a magnetic label is applied to water molecules in the blood, changing their magnetic characteristics. At a certain amount of time after the labeling, the distortion of the signal caused by the label is measured and proportional to CBF (Buxton et al., 1998; Liu and Brown, 2007; Xu et al., 2010).

1.5.2 Measuring GABA using MRS

MRS allows to estimate concentration of molecules in predefined brain regions in vivo. The method makes use of the fact that resonance frequency of protons depends on their chemical environment. In an MRS experiment, a volume of interest voxel is defined, and

in this region the tissue is excited with radiofrequency pulses specific to the frequency of the nucleus of interest (for in vivo imaging this is usually the hydrogen nucleus due to the abundance of water molecules in the brain). The relaxation can be measured and resolved into a frequency spectrum with peaks that reflect the abundance of nuclei in different chemical environments. The chemical environments vary in the amount of nucleus shielding by electrons, which results in a chemical shift of the resonance frequency indicated in parts per million (ppm; Lambert and Mazzola, 2004; for a typical spectrum see Figure 1.3).

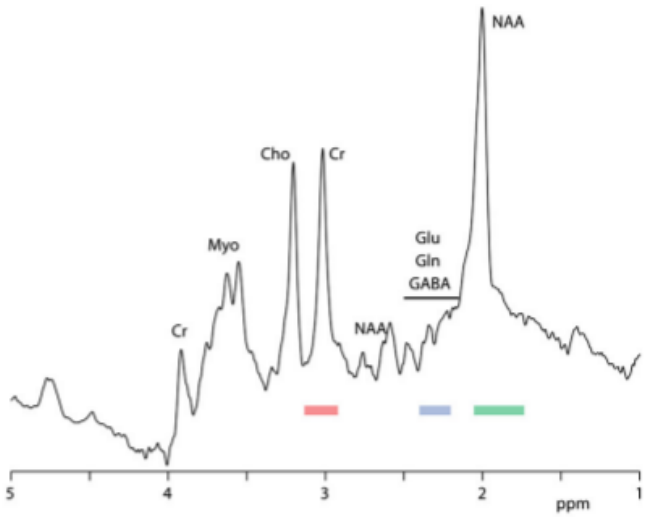

Figure 1.3: MRS spectrum. A spectrum acquired during a MRS sequence, showing peaks reflecting different brain metabolites. GABA contributes three of these peaks, as indicated by the red, blue and green stripes. Figure taken from Puts and Edden (2012).

GABA yields three peaks due to its three methylene group, at 1.0, 2.3 and 3 ppm (Puts and Edden, 2012; see Figure 1.3). All of the GABA peaks overlap with the peaks of other molecules, which is why GABA concentration cannot be deduced from a conventional spectrum. To get an estimate of GABA, special sequences are applied that make use of an effect called spin coupling (the effect that neighboring spins can influence each other). The GABA signal at 3.0 ppm is coupled to the signal at 1.9 ppm, whereas none of the other signals at 3.0 ppm are coupled to signals at 1.9 ppm. This allows to add a frequency selective pulse to the experiment, which affects only the signal at 1.9 ppm. Because of the coupling, this pulse will also have an effect on the GABA peak at 3 ppm. Effectively, this so called J-difference editing acquisition requires interleaved periods with this 1.9 ppm pulse on and off, so the difference in the 3 ppm peak between the two acquisitions should only resemble GABA. In this study, GABA+ (GABA plus coedited macromolecules) measures

are acquired. This means that some of the GABA signal is caused by macromolecules concentration due to similarly coupled spins (see also Henry et al., 2001).

Because the actual peak size depends on several factors and not just the concentration of a molecule, the concentration is estimated relative to a reference molecule. For GABA this is often water or creatin. The resulting arbitrary concentration units are called "institutional units", implying that the units of GABA concentration cannot be compared across different scanners.

The water concentration in a spectroscopy voxel is so high that the water peak would be substantially bigger than the peaks of other molecules. In this study, a MEGA-PRESS sequence is used, which includes pulses to suppress the water signal (Mescher et al., 1998). Water concentration to be used as a reference is acquired separately with a number of volumes. Because the amount of water in a voxel depends on the tissue composition, it is recommended to correct the GABA concentration for tissue types when water is used as a reference (Ernst et al., 1993).

Due to the low abundance of GABA relative to other molecules, and due to the necessity of spectral editing, big voxel sizes are used in order to maximize the signal to noise ratio. The disadvantage is a low spatial resolution. Even though GABA concentration from the amygdala would be of particular interest for this project due to known GABAergic pathways in the amygdala (e.g. Sah et al., 2003), methodological limitations did not allow this for this study. We acquired MRS spectra from the other two regions of interest, the left insula and left DLPFC, since this has been previously successfully done (Boy et al., 2011; Evans et al., 2013; Michels et al., 2012; O'Gorman et al., 2011; Wiebking et al., 2014; Wijtenburg et al., 2013).

1.5.3 Potential confounds: menstrual cycle and hormonal contraception

For practical reasons and due to gender differences in emotion processing (Stevens and Hamann, 2012) only females were tested in the main study. In females, steroid hormones such as estradiol and progesterone fluctuate with the menstrual cycle (e.g. Stricker et al., 2006), and there is evidence that steroid hormones can influence GABA concentration as well as anxiety.

Firstly, steroid hormones can directly influence and interact with GABA transmission (Schüle et al., 2011). This can also be manifested in GABA concentration as measured with MRS. Several studies found that in healthy women MRS GABA levels are highest in the follicular phase and decrease in the mid-luteal and late luteal phase (Epperson et al.,

2002; Harada et al., 2011; Silveri et al., 2013). On the other hand, behavioural and brain imaging studies show changes in emotion processing throughout the menstrual cycle (e.g. Frank et al., 2010; Gingnell et al., 2012).

Hormonal contraception works by administering either estradiol or progresteron (or precursers) or both, in order to prevent ovulation and other pregnancy preparing mechanisms. The oral intake of sex hormones has been shown to affect emotion-related BOLD responses (e.g. van Wingen et al., 2007, 2008), and might also influence GABA, even though this has not been investigated. For this reason, one aim of recruitment was to make sure that the groups recruited for fearfulness did not differ in the phase of their cycle, and had the same proportion of participants taking hormonal contraception.

1.5.4 Trait measuress and the importance of repeatability

GABA concentration as well as fear-related BOLD signals in this study are investigated in the context of individual differences and trait markes. In the literature review, it has been proposed that low GABA concentration and hyper-reactivity of brain areas involved in emotion processing might be predispositions for fearfulness. If this was the case, then measured GABA concentration and task-related BOLD responses should be relatively stable within individuals. This means, that if the same person was measured twice with the same scanning acquisition, the outcomes should be similar. How similar the outcomes are does not only depend on the stability of the construct but also on the reliability, so on how well the methods used can actually capture the construct of interest. If a measure shows both temporal stability and reliability, then it should be repeatable.

In this study, several repeatability estimates are made. Repeatability of BOLD signals of two emotion processing paradigms are estimated in Chapters 2 and 3, and repeatability of GABA measures and of vascular reactivity estimates are described in the Appendix in Chapters 9 and 10.

1.6 Research questions and overview of experimental chapters

The aim of this project was to investigate the relationship between individual differences in fearfulness, fear-related BOLD responses, and GABA concentration. As explained above, individual differences in physiological task-responses, or in baseline blood flow or vascular reactivity might be mediating associations between the measures and were

therefore included as control measures in the study. Figure 1.4 illustrates the investigated model in this project.

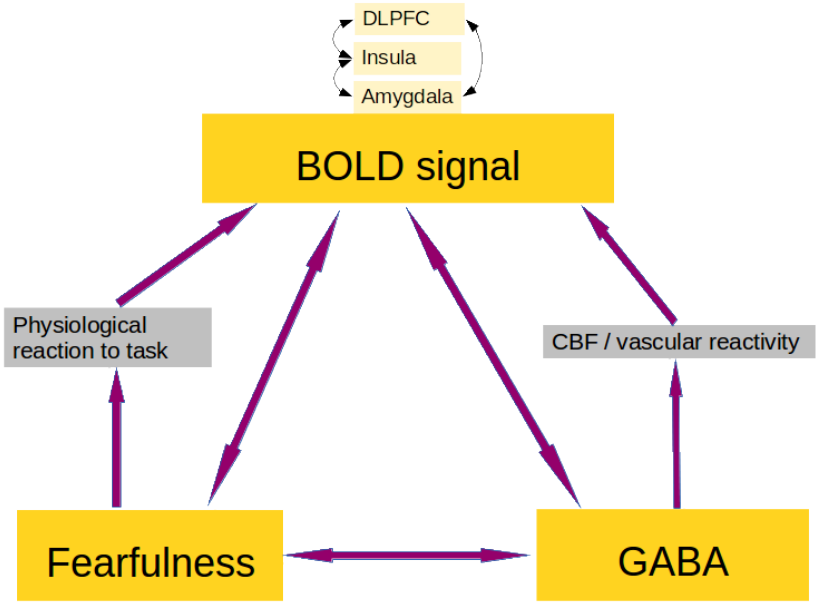

Figure 1.4: Illustration of the aim of the project. The main variables of interest are displayed in yellow boxes: GABA concentration, trait fearfulness and task-related BOLD signals, particularly in the DLPFC, insula, and amygdala. Also the connectivity between the regions was of interest, indicated by the arrows. As potential mediators, physiological task reactions, cerebral blood flow and vascular reactivity (in gray boxes) were included in the model. In the experimental chapters, associations between the main variables and control variables were investigated. Chapter 4 looks at the relationship between fearfulness, GABA and task-induced BOLD responses, in Chapter 5 the potential influence of physiological task reactions and in Chapter 6 the potential influence of CBF and vascular reactivity are investigated. Chapter 7 deals with the association between fearfulness, GABA and resting state functional connectivity.

The main experimental chapters (**Part III**) each investigate part of this model. The first two experimental chapters deal with establishing an emotion paradigm to be used in the main study (**Part II**). Each of the experimental chapters is written in the style of a scientific paper, with a short introduction, methods, results and a discussion. Due to the involvement of other researchers in the experimental work of this thesis, in the experimental chapter "we" will be used instead of "I".

In **Chapter 2** repeatability of task-related BOLD responses is evaluated with a faces task. The chapter demonstrates that the faces task used did not reveal significant emotion related BOLD activation, and that BOLD responses recorded from the amygdala and fusiform gyrus during this task were not repeatable in our subclinical sample.

For this reason another task was designed for this project, which is evaluated in **Chapter 3**. This task uses negative IAPS pictures and pictures of spiders, and was able

to elicit fear-related BOLD responses in the insula and amygdala.

Chapter 4 deals with the main question of the project: are fearfulness, BOLD responses and GABA correlated? It uses a sample of 44 female participants, recruited based on their level of fearfulness.

In **Chapter 5** the potential influence of task-related physiological responses was investigated. In particular, the effect of regressing out physiological variation on task-related BOLD responses is demonstrated.

Chapter 6 deals with the question whether baseline CBF or vascular reactivity can explain any of the individual differences in fearfulness, fear-related BOLD responses or GABA.

In **Chapter 7** the relationship between fearfulness, GABA and functional connectivity of two functionally defined regions of interest (ROI) in the left anterior insula and left DLPFC is investigated.

This is followed by a general discussion (**Chapter 8**), bringing all the findings together.

Appendix Chapters 9 and **10** discuss the repeatability of GABA concentration measures and of vascular reactivity measures. They are meant to improve the understanding of the imaging measures used in the study.

Part II

Developing a task to measure fear-related BOLD responses

Chapter 2

Understanding the contribution of neural and physiological signal variation to the low repeatability of emotion-induced BOLD responses during a task using faces

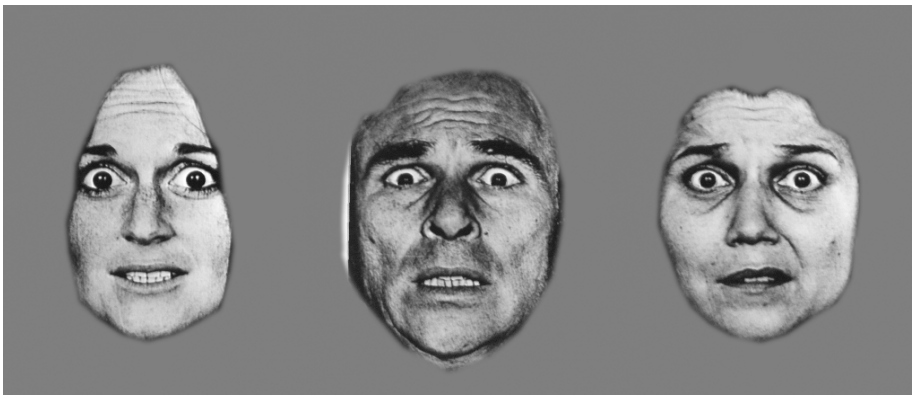

2.1 Abstract

Previous studies have reported low repeatability of BOLD activation measures during emotion processing tasks. It is not clear, however, whether low repeatability is a result of changes in the underlying neural signal over time, or due to insufficient reliability of the acquired BOLD signal caused by noise contamination. The aim of this study was to investigate the influence of cleaning the BOLD signal, by correcting for physiological noise and for differences in vascular reactivity, on measures of repeatability.

Fifteen healthy volunteers were scanned on two different occasions, performing an emotion provocation task with faces (neutral, 50% fearful, 100% fearful) followed by a breath-hold paradigm to provide a marker of vascular reactivity. Repeatability of signal distribution (spatial repeatability) and repeatability of signal amplitude within two regions of interest (amygdala and fusiform gyrus) were estimated by calculating the intraclass correlation coefficient (ICC).

Significant repeatability of signal amplitude was only found within the right amygdala during the perception of 50% fearful faces, but disappeared when physiological noise correction was performed. Spatial repeatability was higher within the fusiform gyrus than within the amygdala, and better at the group level than at the participant level. Neither physiological noise correction, nor consideration of vascular reactivity, assessed through the breath-holding, increased repeatability.

The findings lead to the conclusion that low repeatability of BOLD response amplitude to emotional faces is more likely to be explained by the lack of stability in the underlying neural signal than by physiological noise contamination. Furthermore, reported repeatability might be a result of repeatability of task-correlated physiological variation. This means that the emotion paradigm used in this study might not be useful for studies that require the BOLD response to be a stable measure of emotional processing, for example in the context of biomarkers.

2.2 Introduction

FMRI is a widely used tool for studying emotion in the human brain. Recent research in this area has highlighted the crucial role of the amygdala in the experience of emotion (Costafreda et al., 2008; Phan et al., 2002). Activity in the amygdala, measured through BOLD fMRI, has been suggested as a biomarker for different psychiatric disorders (Phillips et al., 2003). The assumption underlying the proposed biomarker is that the signal change (SC) measured in the amygdala is sufficiently strongly driven by inter-individual differences in neural activity induced by experimental challenges compared to other sources of fluctuations, or noise. However, previous studies have reported low repeatability of amygdala BOLD responses during emotion provocation (e.g. Johnstone et al., 2005; Manuck et al., 2007; Plichta et al., 2012), arguing against the suitability of this measure as a biomarker.

In order to obtain a quantitative estimate of repeatability, the intraclass correlation coefficient (ICC) is used most commonly (Caceres et al., 2009; Shrout and Fleiss, 1979), which reflects the ratio between the data variance of interest (inter-subject BOLD differences) and the total data variance. One way to use the ICC in the context of brain imaging is to extract the mean %SC from repeated measures in an area of interest and calculate the ICC for the obtained values, estimating repeatability of the signal amplitude (e.g. Johnstone et al., 2005). Another approach is to obtain spatial ICCs for particular regions of interest (ROIs). In this case, each voxel within the ROI is considered during ICC calculation, and for each participant, a single ICC is obtained. These ICCs reflect the repeatability of the signals spatial distribution (Plichta et al., 2012). Repeatability of the activity within the amygdala has been investigated in both ways, resulting in low to medium ICC values for signal amplitude (Johnstone et al., 2005; Manuck et al., 2007) and low values for signal distribution (Plichta et al., 2012; Stark and Kirsch, 2004; van den Bulk et al., 2013). Spatial repeatability at the group-level has been shown to be higher than that at the individual level (Plichta et al., 2012).

Low repeatability of BOLD responses can result from two factors or their combination: a) brain responses are too unstable to show temporal reliability (neural response variability); b) brain responses remain stable but cannot be measured accurately (measurement variability). If the former is true, BOLD responses in the amygdala would not be suitable as a stable biomarker for psychiatric disorders. However, if low repeatability is due to measurement error, or noise, there is the potential for improvement by refining the data acquisition and analysis methods.

One important factor that might introduce noise in the measurement of BOLD within the amygdala is the physiological reaction that also accompanies emotional responses. The recorded BOLD signal time-course is influenced by changes in breathing and heart rate (Birn et al., 2006, 2009; Chang et al., 2009; Wise et al., 2004). By recording and accounting for these changes, it is suggested that a cleaner measure of neural activation can be acquired (Chang et al., 2009). Another important aspect is that the stimulus-induced BOLD contrast depends on the vascular reactivity, blood volume and T2* (Clare et al., 2001), itself dependent on the local field gradients (Murphy et al., 2011; Thomason et al., 2005). Day-to-day differences in these factors might lead to day-to-day differences in the measured BOLD response even if the underlying neural activity were the same. One method that has been introduced to measure vascular reactivity independent of task is to increase the arterial CO_2 level with a hypercapnic challenge (artificially regulating the CO_2 level of the environment) or with voluntary breath-holding. Using this method, cerebral blood flow (CBF) is transiently increased without affecting the oxygen consumption rate throughout the whole brain (Thomason et al., 2005), producing a concomitant increase in BOLD signal.

The aim of this study was to investigate the between-session repeatability of the BOLD measure during the perception of emotional faces, and to assess whether repeatability can be enhanced by applying physiological noise correction and measures of BOLD vascular reactivity. Following previous studies, the amygdala was chosen as the main region of interest. The fusiform gyrus was selected as an additional region of interest because it has been reported to be involved in the perception of faces in general (e.g. McCarthy et al., 1997) as well as in emotion processing (e.g. Vuilleumier and Pourtois, 2007), and was expected to provide strong BOLD signal responses to our experimental stimuli.

2.3 Methods

2.3.1 Participants

Fifteen (8 male) participants with a mean age of 24 (SD = 1.6) voluntarily took part in the study having given informed, written consent. They undertook the scanning protocol twice with a mean interval of 23 days (range: 15-34; SD = 4.8). One participant was excluded from all analysis involving vascular reactivity due to a CO_2 trace that was unusable for analysis. The study was approved by the Cardiff University School of Medicine Research Ethics Committee.

2.3.2 Tasks

Emotion provocation task

The emotion perception paradigm was adapted from Surguladze et al. (2010) and has been widely used in clinical research to investigate emotional reactivity in mental disorders. Emotional faces selected from the Ekman and Friesen pool (FEEST, Young et al., 2002) of 10 identities (5 male: EM, JJ, NR, PE, WF; 5 female: C, MF, MO, PF, SW) were presented, showing 50% morphed fear-neutral expression, 100% fearful expressions or 25% morphed happy-neutral as neutral expressions (Morris et al., 1998). Each identity was presented six times, and each identity-emotion combination was presented twice during the task. In order to maintain participant attention on the presented stimuli, they were instructed to perform a male/female categorization task responding with a button press (index finger press for male, middle finger for female). Stimuli were presented for 2 seconds with a variable pseudorandomized inter-stimulus interval (fixation cross) between 3 and 8 seconds. Stimulus order was pseudorandomized with the same intensity of emotion not occurring more than twice in a row. The task took 8 minutes to complete.

Breath-holding task

The breath-holding task was adapted from Murphy et al. (2011). During the task, breathing instructions were presented on the screen, guiding the participant through six cycles of breath-holding and recovery, each with four different phases: paced breathing (alternating breathing in and breathing out for 3 seconds each) for 18 seconds, end-expiration breath-holding for 15 seconds, exhalation, and final recovery (spontaneous breathing with no breathing instructions) for 15 seconds. The task took 5 minutes to complete.

2.3.3 Recordings

The participants underwent gradient-echo echo-planar imaging at 3 T (GE HDx MRI System) with a T2* weighted imaging sequence (TR = 3 sec., TE = 35 ms, matrix = 64 x 64, FOV/slice = 220 mm, flip angle = 90, 53 slices of 2 mm with a 1 mm slice gap acquired in an interleaved order) using an eight-channel receive-only head coil. The orientation of the axial slices was parallel to the AC-PC line. During the emotion provocation task 154 functional image volumes were obtained, and 108 volumes were acquired during the breath-holding task. The tasks were presented using Presentation (Neurobehavioral Systems, Albany, CA) and rear-projected onto a screen behind the participant's head that was visible through a mirror mounted on the head RF coil.

A T1 weighted whole-brain structural scan was also acquired for purposes of image registration (1 x 1 x 1 mm resolution, 256 x 256 x 176 matrix size). The structural image was only acquired during session 1, and this image was used for registration for the functional images of session 1 and session 2.

During both scanning sessions, physiological parameters were recorded: a) the cardiac cycle was recorded using a pulse-oximeter placed on the left index finger, b) a respiration trace was recorded with a pneumatic belt around the chest, c) end-tidal CO_2 and end-tidal O_2 were recorded using a nasal cannula attached to rapidly responding gas analysers (AEI Technologies, PA) to provide representative measures of arterial partial pressures of both gases.

2.3.4 Data preprocessing and analysis

BOLD responses during the emotion paradigm were analyzed with and without physiological noise correction of the BOLD fMRI time-series data. This correction consisted of: first applying correction of cardiac and respiratory artifacts (RETROICOR, Glover et al., 2000) using two cardiac, two respiratory and one interaction component, followed by regressing out the variance related to CO_2 level, O_2 level, HR and RVT (Birn et al., 2006) using a general linear model framework. Both steps were performed using Matlab (The MathWorks Inc., vs. R2011a). Physiological noise correction was performed prior to preprocessing.

Both datasets (uncorrected and physiological noise corrected) were subsequently analyzed using FEAT (FMRIB Expert Analysis Tool, v5.98, http://www.fmrib.ox.ac.uk/fsl, Oxford University, UK). Preprocessing steps before model fitting were applied to each participants time-series, and included: highpass filtering of the data (100 seconds temporal cutoff), non-brain removal using BET (Smith, 2002), MCFLIRT motion correction (Jenkinson et al., 2002), spatial smoothing with a Gaussian kernel of full-width-half-maximum 5 mm and fieldmap-based EPI unwarping using PRELUDE + FUGUE (Jenkinson, 2003, 2004; for one person this was not performed due to problems during the acquisition of the fieldmaps). Due to the event-related design with a long TR of 3 seconds slice-time correction was performed as recommended by Sladky et al. (2011). Functional images were registered using FLIRT (Jenkinson and Smith, 2001) in a first step to the structural image with 6 degrees of freedom, and in the second step to the Montreal Neurological Institute (MNI) space with 12 degrees of freedom and FNIRT non-linear (10 mm) warp (Andersson et al., 2007a,b).

To model the emotion provocation task, three event types were defined, one for each emotion condition (i.e. neutral, 50% fear and 100% fear expressions); the fixation cross periods were used as the baseline. The model was convolved with the hemodynamic response function (gamma convolution), and the same temporal filtering was applied to the model as to the data. Temporal derivatives of the event-type regressors were included as regressors of no interest. The main effects for neutral, 50% fear and 100% fear were evaluated, as well as the contrast fear (average of 50 and 100% fear) > neutral. Group average maps were created with a fixed effects model using FLAME. The Z (Gaussianised T/F) statistic images were thresholded using clusters determined by $Z > 2.3$ and a (corrected) cluster significance threshold of $P < .05$ (Worsley, 2001).

A region of interest (ROI) analysis was performed for the amygdala and fusiform gyrus for both hemispheres. Anatomical masks were taken from the WFU-PickAtlas (Version 3.0.4, Wake Forest University, School of Medicine, Winston-Salem, North Carolina, www.ansir.wfubmc.edu). Percent SCs for whole brain maps and for ROIs were computed. For each region of interest, a repeated measures ANOVA was calculated for %SC within the ROI as the dependent variable, with the emotion condition and hemisphere as independent variables. Calculations were performed using SPSS (IBM SPSS v.19), with a chosen significance level of $P < .05$.

The breath-holding task was used to obtain a vascular reactivity map for each participant, based on BOLD %SCs. The recorded end-tidal CO_2 trace obtained during the breath-holding task was demeaned and entered as a regressor in a GLM along with its temporal derivative. In order to obtain a measure of BOLD %SC per unit change of CO_2, the range of the fitted timeseries (2^{nd}-98^{th} percentile to minimize the influence of outliers) was divided by the range of the end-tidal CO_2 trace (2^{nd}-98^{th} percentile). The resulting maps were concatenated across participants before demeaning and then entered as a voxelwise regressor in the group-level analysis (Murphy et al., 2011). Spatial repeatability analyses at the group level for the emotion provocation task were then conducted on the group activation maps with and without the inclusion of the vascular reactivity as a covariate across the group.

2.3.5 Repeatability analysis

The intraclass correlation coefficient (ICC[3,1]; Shrout and Fleiss, 1979 was used as a measure of repeatability. The ICC variant ICC(3,1) was chosen because it removes mean difference over the two times of measurement. For an overview of the repeatability analyses

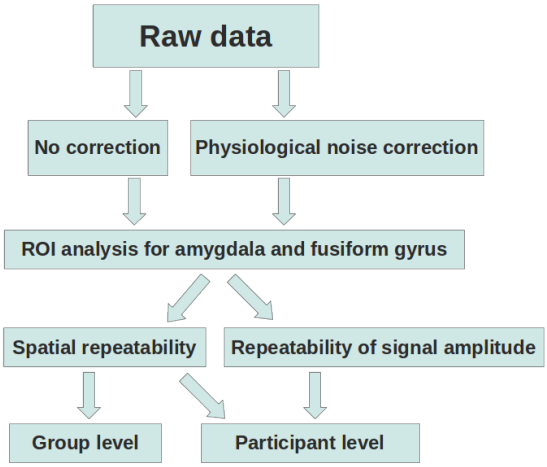

Figure 2.1: Overview of repeatability analysis. Raw data was either corrected for physiological noise or left uncorrected. For each ROI, spatial repeatability (at the group and at the participant level) as well as repeatability of the signal amplitude (at the participant level) was estimated.

see Figure 2.1. ICCs were interpreted according to commonly used guidelines (Cicchetti, 2001; see also e.g. van den Bulk et al., 2013) that classify values of $< .41$ as poor, values between .41 and .59 as fair, values between .60 and .74 as good and values $> .74$ as excellent.

Repeatability of the activation at the participant level: Repeatability of signal amplitude between sessions. The mean BOLD %SC for each ROI was extracted and ICCs as well as descriptive statistics were calculated using Matlab. ICCs were tested with a significance level set at $p < .05$. An additional analysis was conducted in order to control for changes in vascular reactivity that might influence the %SC in the emotion task. For each region, a linear regression was performed between %SC obtained during the breath-hold task and %SC obtained during the emotion task. The residuals from this regression constitute the %SC during the emotion task that cannot be explained by vascular reactivity. These values were then taken to compute ICCs having accounted for vascular reactivity. Since day-to-day variation in signal dropout within the ROIs could potentially influence the obtained repeatability measures, ICCs were also calculated for the mean signal intensity over time and space within the ROIs. Mean signal intensity was obtained from the time series image after all preprocessing steps have been performed.

Repeatability of the activation at the participant level: Spatial repeatability between sessions. For each participant and each region of interest, as well as for the whole brain, a spatial ICC was calculated for the unthresholded Z-score maps within the respective region from the two sessions.

Repeatability of the activation at the group level: Spatial repeatability. Spatial repeatability at the group-level was estimated by using the group level unthresholded Z-score maps for session 1 and session 2 and computing a spatial ICC over all voxels within each of the regions of interest.

Task-related variance in physiological parameters. We investigated the relationship between the stimulus paradigm and the recorded physiological parameters to uncover potential effects of the task on the volunteers physiology which may in turn influence BOLD signal responses. For each participant, a linear regression was performed between the HRF convolved stimulus time series and the physiological signals. These included the CO_2, O_2, HR, and RVT convolved with a HRF as well as the RETROICOR regressors. Since the latter differ significantly for each acquired slice, the regressor was generated for a slice passing through the amygdala (this was defined for each participant separately by visual inspection). The amount of task-correlated variation in physiological measures was defined as the shared variance (R^2) between the physiological regressors and the expected hemodynamic stimulus response model for each stimulus condition separately as well as for the complete task (HRF-convolved stimulus time series were summed with equal weight) and for the contrast fear > neutral (time series for the both fear conditions were summed and the time series for neutral stimuli was subtracted).

2.4 Results

2.4.1 Behavioral results

All participants responded to more than 97% (and over 88% correctly) of the face stimuli during both scanning sessions, indicating that they paid attention to the task. There were no differences in mean reaction times ($F[1,28] = 0.11$, ns) between scanning sessions but a trend for higher accuracy in the first scanning session than in the second session ($F[1,28] = 4.61$, $p = .05$). Fear intensity did not have an influence on the measures of task performance (accuracy: $F[2,28] = 1.01$, ns; reaction time: $F[2,28] = 1.45$, ns; see Figure 2.2).

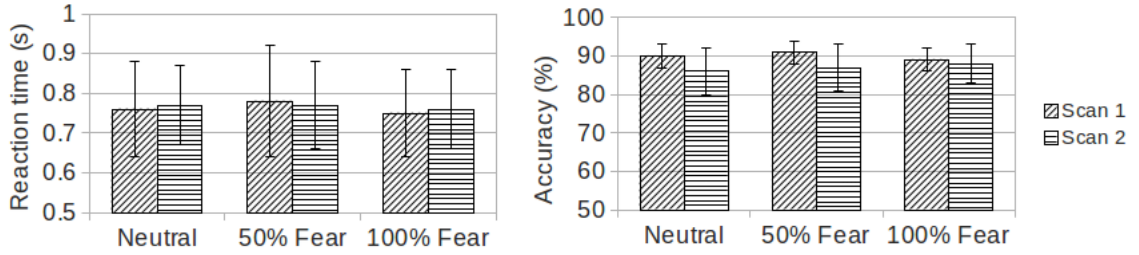

Figure 2.2: Behavioral results. Mean and standard deviation (error bar) of reaction time (left), and accuracy (right) are shown for each scan and condition.

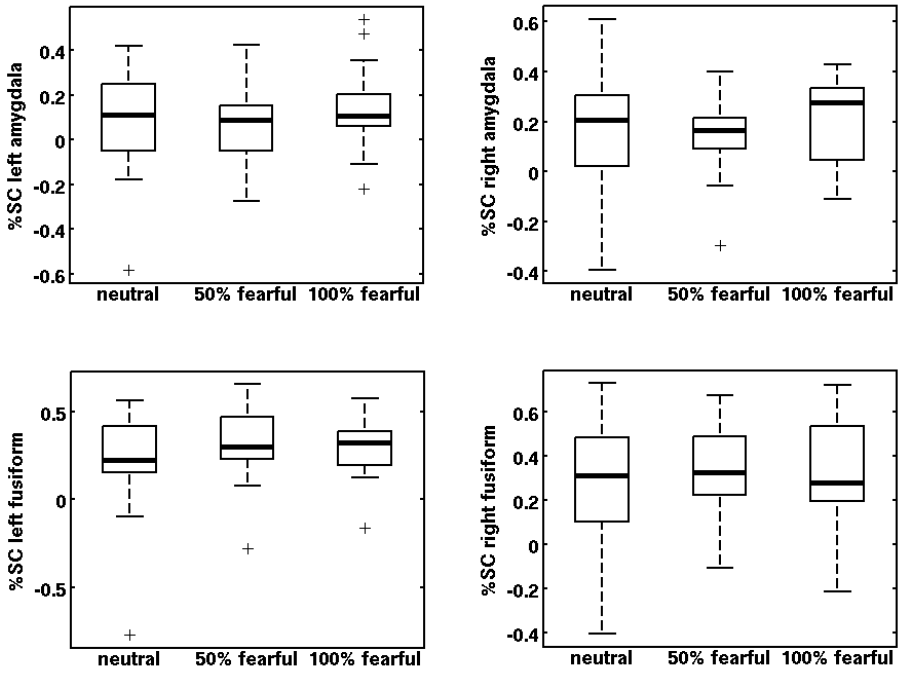

Figure 2.3: ROI activation. Percent SC within the left amygdala (top left), right amygdala (top right), left fusiform gyrus (bottom left) and right fusiform gyrus (bottom right) is shown for the three fear intensity conditions in session 1.

2.4.2 Task-related activation

ROI analysis

Percent SC relative to baseline were extracted for the amygdala and fusiform gyrus. In both ROIs, large variance between participants was observed. As expected, mean %SC were higher within the fusiform gyrus than within the amygdala. For descriptive statistics and between-session differences see Table 2.1 and Figure 2.3. Results for ANOVAS (influence of condition and hemisphere on %SC in the ROIs) can be found in Supplementary material.

Exploratory whole-brain analysis

Widespread significant BOLD activation was found during the presentation of the facial stimuli as compared to the baseline (for activation maps see Supplementary Figures A.1, A.2, and A.3). Using the whole brain approach, no areas appeared to be more strongly activated during the presentation of fearful faces (both intensities combined) than the presentation of neutral faces in either of the two scanning sessions and independent of physiological noise correction.

2.4.3 Repeatability of the activation at the participant level

Repeatability of signal amplitude

In order to obtain a value for repeatability for each ROI, %SC for the amygdala and fusiform gyrus in both hemispheres were extracted, and ICCs were computed. The highest repeatability was found in the right amygdala for moderately fearful faces with an ICC of .48 (p = .03). The same analysis was performed using the dataset corrected for physiological noise for which no significant ICC was found (for all values see Table 2.1). Regressing out breath-hold based vascular reactivity measures did not increase the ICCs (see Table A.1 and A.2 in Supplementary Material).

Table 2.1: ROI analysis for uncorrected as well as physiological noise corrected data. For each of the ROIs, mean and standard deviation of the %SC for both scanning sessions (scan 1 and scan 2), the significance of the between-session difference (paired t-test; indicated by p), the repeatability of the value (ICC) and its significance are provided. Amy = Amygdala, Fusi = Fusiform gyrus.

	No correction				**Physiological noise correction**			
Area/condition	$M(Std.)$ 1	$M(Std.)$ 2	p	ICC(p)	$M(Std.)$ 1	$M(Std.)$ 2	p	ICC(p)
Left amy.								
neutral	0.08 (0.25)	0.13 (0.20)	.46	.12 (.33)	0.07 (0.16)	0.13 (0.22)	.42	.01 (.49)
50% fearful	0.06 (0.17)	0.02 (0.30)	.61	.05 (.43)	0.10 (0.20)	0.06 (0.23)	.65	-.04
100% fearful	0.14 (0.20)	0.14 (0.16)	.99	.37 (.08)	0.09 (0.20)	0.12 (0.18)	.68	.29 (.14)
Fear > Neutral	0.04 (0.20)	-0.04 (0.19)	.37	-.56	0.04 (0.15)	-0.03 (0.24)	.52	-.68
Right amy.								
neutral	0.17 (0.23)	0.10 (0.22)	.38	.11 (.35)	0.14 (0.16)	0.09 (0.22)	.51	.06 (.41)
50% fearful	0.14 (0.16)	0.04 (0.26)	.10	.48 (.03)	0.16 (0.18)	0.06 (0.18)	.12	.25 (.17)
100% fearful	0.21 (0.17)	0.07 (0.15)	.01	.33 (.11)	0.14 (0.17)	0.05 (0.13)	.07	.19 (.24)
Fear > Neutral	0.03 (0.17)	-0.03 (0.18)	.42	-.51	0.03 (0.09)	-0.04 (0.17)	.33	-.42
Left fusi.								
neutral	0.21 (0.32)	0.25 (0.25)	.74	.12 (.32)	0.17 (0.24)	0.15 (0.20)	.83	.04 (.45)
50% fearful	0.31 (0.22)	0.13 (0.35)	.15	-.28	0.25 (0.28)	0.11 (0.20)	.17	-.21
100% fearful	0.30 (0.18)	0.20 (0.22)	.28	-.38	0.20 (0.20)	0.12 (0.17)	.32	-.24
Fear > Neutral	0.13 (0.32)	-0.06 (0.20)	.09	-.13	0.08 (0.18)	-0.02 (0.12)	.10	-.05
Right fusi.								
neutral	0.29 (0.30)	0.31 (0.24)	.82	.09 (.37)	0.26 (0.23)	0.19 (0.24)	.41	.12 (.32)
50% fearful	0.33 (0.20)	0.16 (0.30)	.11	-.06	0.30 (0.25)	0.12 (0.21)	.05	-.03
100% fearful	0.34 (0.25)	0.27 (0.20)	.44	-.14	0.25 (0.26)	0.17 (0.16)	.33	-.10
Fear > Neutral	0.08 (0.27)	-0.07 (0.25)	.14	-.04	0.05 (0.12)	-0.03 (0.17)	.13	.11 (.35)

In order to investigate whether signal dropout was the cause of this low repeatability in the regions of interest, the ICC was also calculated for the mean signal intensity over the whole length of the scan in these areas (see Methods section). The ICCs for left and right amygdala were .82 ($p < .001$) and .92 ($p < .001$), respectively; and .89 ($p < .001$) for the left fusiform, and .76 ($p < .001$) for the right fusiform, indicating excellent repeatability of mean BOLD signal intensity.

Spatial repeatability

In order to investigate whether the distribution rather than overall amplitude of BOLD activation is repeatable, a spatial ICC was calculated for each person, using the two Z maps within each region of interest. Table 2.2 shows the mean and standard deviation of the obtained ICCs. The ICCs for the fusiform indicate fair spatial repeatability for the main effect fear. Spatial repeatability in the amygdalae was poor for the contrast fear for the uncorrected dataset (ICC < 20) but could be slightly improved for the physiological noise corrected dataset (ICC > .40).

Table 2.2: 1st level spatial repeatability. Voxel-based ICCs for participant level SC-maps of the main effect fear, and the contrast fear > neutral. ICCs were converted to z(r) using the Fisher-z transformation before averaging across participants. Unc. = uncorrected, pnc: physiological noise correction. F > N = contrast Fear > Neutral.

		Left amygdala		Right amygdala		Left fusiform		Right fusiform	
Correction		Fear	F > N	Fear	F > N	Fear	F > N	Fear	F > N
unc.:	Mean	.15	.47	.13	.46	.56	.05	.57	.05
	Std.	.34	.08	.28	.08	.19	.20	.27	.20
pnc.:	Mean	.47	.20	.45	.24	.54	.04	.56	.04
	Std.	.05	.10	.04	.10	.25	.21	.26	.15

2.4.4 Repeatability of the activation at the group level

For determining the repeatability at the group level, ICCs between the two Z-maps of session 1 and session 2 were calculated for the two regions of interest. For both, the uncorrected and the physiological noise corrected datasets, the ICCs for the amygdala were in general poor. Repeatability values for the fusiform gyrus were excellent for both datasets (see Table 2.3).

2.4.5 Correlation between task and physiology

The shared variance between task-related %SCs and task-related physiological changes was estimated. All task conditions combined could explain on average 8% of the variance, while the three conditions separately could explain on average 12% (neutral stimuli), 9%

(50% fear stimuli), 9% (100% fear stimuli). All results for the analysis on task-related variance in physiological parameters can be found in Supplementary material (Table A.3).

Table 2.3: 2nd level repeatability. Voxelbased ICCs for group level Z-maps of the main effect fear, and the contrast fear > neutral. ** p < .001, * p < .05. unc. = uncorrected, pnc. = physiological noise correction, no VR: no vascular reactivity regressor included, with VR: vascular reactivity regressor included, F > N = contrast Fear > Neutral.

	Left amygdala		Right amygdala		Left fusiform		Right fusiform	
Correction	Fear	F > N	Fear	F > N	Fear	F > N	Fear	F > N
unc.- no VR:	.18**	.43**	.39**	-.04	.84**	.23**	.87**	.05
unc. - with VR:	.17**	.40**	.32**	.01	.84**	.18**	.86**	-.16
pnc. - no VR:	.34**	-.02	.47**	-.15	.86**	.22**	.86**	.03
pnc. - with VR:	.20**	.19**	.50**	-.09	.87**	.17**	.84**	-.03

2.5 Discussion

The aim of this study was to estimate the repeatability between sessions of BOLD signal changes obtained during a widely used emotion provocation task, and to investigate the effects of physiological noise correction and intra-individual and inter-individual differences in vascular reactivity on the repeatability indices. Overall, the repeatability indices of signal amplitude were poor at a participant-level for both the amygdala and the fusiform gyrus. At a group-level, the BOLD signal showed an excellent spatial repeatability within the fusiform gyrus. Correction for physiological noise and accounting for vascular reactivity appeared to have little effect on BOLD repeatability for the emotion task.

2.5.1 BOLD signal repeatability

A widely used emotional paradigm in clinical research (e.g. Almeida et al., 2010; Dannlowski et al., 2009; Rhodes et al., 2007; Surguladze et al., 2010) was implemented here. Participants responded accurately to most of the stimuli presented across emotional conditions. This suggests that overall, participants level of attention to the facial stimuli during both scanning sessions was adequate. We found high inter-individual variability of BOLD responses within the amygdala and fusiform gyrus. As predicted, the signal was stronger within the fusiform than within the amygdala. A whole-brain analysis revealed widespread activity throughout the brain for the main effect of fear, but the frequently reported contrast fearful > neutral faces did not reveal any significant clusters.

Repeatability of signal amplitude was low (< .40) for both regions of interest and effects considered, with an exception of BOLD within the right amygdala during the perception of 50% fearful faces (ICC = .48). Similar ICC values have been reported by Schaefer et al. (2000) in the left amygdala, and by Manuck et al. (2007) in the right amygdala. In

our data, however, physiological noise correction decreased this ICC value to .25, which suggests that the detected repeatability might be a result of repeatability of task-correlated physiological variation rather than repeatability of the neural signal in the amygdala. It is also important to notice that even the uncorrected repeatability index was no longer significant when correcting for multiple comparisons.

A cause for these low repeatability indices might lie in inhomogeneous activation within our ROIs. Therefore, the mean signal change within an anatomically defined region might not always be a useful measure for activation, especially when it comes to bigger regions such as the fusiform gyrus. For this reason, we also calculated the spatial repeatability, which provides an indication for how stable the distribution of activation is, independent of the mean signal amplitude. This analysis resulted in fair repeatability measures in the fusiform gyrus bilaterally, and poor results for the amygdala, which is comparable to previously reported outcomes (Plichta et al., 2012; Stark and Kirsch, 2004; van den Bulk et al., 2013). Spatial repeatability could be increased with physiological noise correction to an ICC of about .45 which is still lower than repeatability in the fusiform gyrus. However, it is important to acknowledge that the size of the fusiform gyrus mask favors spatial repeatability compared to the amygdala, since it largely extends beyond the active volume and therefore introduces more variability of the signal within the regarded ROI. Similar results were found when spatial repeatability was calculated for group-level activation. The ICC was higher within the fusiform gyrus (ICCs $> .80$) than in the amygdala (ICCs $< .51$). which might also be a result of more variability of group activation level within the fusiform gyrus. Our group-level repeatability in the amygdala is slightly lower than previously reported by Plichta et al. (2012) who used a different emotion task and implemented a block design.

2.5.2 Influence of physiological noise correction and vascular reactivity

Physiological noise correction did not improve repeatability of the BOLD response amplitude. The correction decreased the variance of the fMRI timeseries in the gray matter by about 15%, which means that physiological parameters are likely to have affected the BOLD response. There are several possible explanations for why the repeatability was not improved. Firstly, if physiological noise did not affect the estimated mean task-related BOLD signal in each session, even by accounting for this physiological noise contribution the BOLD signal changes across the group would not be affected. However, physiological

noise correction did lead an improvement of spatial repeatability for the main effect fear in the amygdala which suggests that it did have an effect on the data.

Secondly, it is possible that the physiological noise correction did improve the quality of the obtained signal, but also took out variance shared by neural responses and physiological measures (Birn et al., 2009). In fact we showed that physiological factors accounted for approximately 10% of variation in the predicted BOLD signal (i.e. the task regressor), which suggests that the task has an effect on the physiological measures. If this shared variance contributes to repeatability, then physiological noise correction might even decrease the ICC. In fact, this appeared to be the case for the right amygdala.

Thirdly, it is possible that physiological noise correction did improve the quality of the fMRI measure of neural activity, but that this neuronal response is not temporally stable. A lack of stability of the neural response to the stimuli might be partly caused by habituation effects. Significant decrease in activation from session 1 to session 2 was observed in the right amygdala during the perception of fearful images (Table 2.1). Habituation of the amygdala has been frequently observed, and it seems to be particularly strong in the right hemisphere (Phillips et al., 2001; Wright et al., 2001). The ICC(3,1) that we used to calculate repeatability takes systematic mean differences between the sessions into account, however, individual differences in habituation would still result in low repeatability indices. Additionally, the decrease of signal amplitude leads to a lower signal-to-noise ratio of the BOLD signal, which might affect repeatability. To further investigate whether habituation could have affected our repeatability measure, we re-ran our analyses only considering the first half of the emotional task (for results see Table A.4 in the Supplementary Material). The rationale behind this approach is that habituation can also happen throughout a scanning session (e.g. Wright et al., 2001) and therefore the first half of either session might be less affected by habituation and may provide a higher signal-to noise ratio (SNR) of the measure. Overall, this approach did not lead to an increase in repeatability, despite producing larger BOLD responses. This result also suggests that a lower signal-to-noise ratio is unlikely to be the cause of for the low repeatability result.

Adding our breath-hold based measure of vascular reactivity to the analysis did not result in higher estimates of repeatability. This suggests that low repeatability is not accounted for by day-to-day differences in our vascular reactivity measure.

2.5.3 Stability of neural response vs. reliability of measure

We showed that performing physiological noise correction and taking vascular reactivity into account does not improve repeatability. To investigate the possibility that low repeatability is caused by different amounts of signal dropout in the two sessions, repeatability was also calculated for the whole session-mean signal within the two ROIs. In this case, repeatability indices were high (ICCs $>$ .75). Taking all the results together, the low repeatability does not seem to be caused by physiological noise, signal-dropout or low signal-to-noise ratio of the scanner, but by either other sources of noise or by a lack of temporal stability of the neural response. If latter is the case, our results suggest caution in considering BOLD responses in the amygdala or fusiform gyrus triggered by emotional expressions as potential biomarker for psychiatric disorders.

2.5.4 Limitations and future directions

Participants of this study were all healthy young volunteers and even though considerable variability in the scores was observed, a more diverse sample (e.g. including patients) might have provided an even broader distribution of activation measures, thus allowing a more sensitive assessment of between session repeatability. Also for this particular sample the contrast fear $>$ neutral did not reveal the oft-reported activation within areas such as the amygdala (Costafreda et al., 2008). It is important to consider that our sample is not comparable to the high anxious samples that are often used in clinical research where this contrast is frequently investigated; although our group should not be much different from any control group included in clinical studies. Also, we implemented a fairly standard task design with regard to stimulus duration, interstimulus interval, number of stimuli, and MRI acquisition parameters (e.g. Fu et al., 2007; Lawrence et al., 2004; Surguladze et al., 2005, 2010). As it is the case for most study designs, we did not optimized for the detection of amygdala activation but rather for a whole-brain analysis. This might have affected the repeatability of the obtained amygdala activation, however, also triggers the question whether non-optimized designs should be used for an ROI analysis in the amygdala.

Another limitation of this study is that we assumed that the physiological noise correction would increase reliability of the measured neural responses. However, we were able to also demonstrate that physiological variation is correlated with the task, at least in some participants. This means that physiological noise correction may reduce the apparent significance of neurally driven signal changes. Methods need to be developed to distinguish

signals of neural origin from non-neuronal physiological effects of the task. However, overall we would recommend performing physiological noise correction since it may increase power to detect task-related activation, as suggested in the current data set and remains a conservative strategy only being likely to reduce false positives rather than increase them.

Furthermore, it has to be noted that our results apply to a specific emotion provocation task that has been widely used in the mental disorders field. However, a variety of other tasks that intend to trigger emotional responses have been developed and implemented in clinical research. It is possible, that BOLD responses elicited during these other paradigms show better repeatability indices than the ones reported here.

2.5.5 Summary and Conclusions

We found low repeatability of activation in the amygdala and fusiform gyrus during emotion processing, as had been previously reported. We also showed here that repeatability of the signal amplitude did not improve by accounting for physiological noise or day-to-day differences in vascular reactivity as assessed with a breath-holding task. This indicates that other unaccounted-for sources of noise are more influential than the ones here considered, or simply that neural activity underlying BOLD signal is not temporally stable, questioning the utility of these measures in the study of biomarkers for mental disorders. Further research is needed to identify other potential factors that could be accounted for in order to increase the repeatability of BOLD measures in these brain areas, and therefore make them more suitable biomarkers for mental conditions.

2.5.6 Next steps

For this study, we decided to assess repeatability of the BOLD responses in the amygdala, which have been frequently associated with the perception of fearful faces. Using this task, we could not detect activation associated specifically with fearful (vs. neutral) faces in the amygdala, or any other region. Additionally, activity in the amygdala during face processing as compared to a fixation cross baseline was low. For this reason, we decided to choose another emotion task for the main project. We designed a novel emotion paradigm that was better suited to elicit emotion related BOLD responses in our regions of interest by confronting participants with fear-eliciting stimuli. The next chapter describes how this paradigm was constructed, evaluates the resulting activation patterns and assesses repeatability of BOLD responses in functional as well as anatomical ROIs.

Chapter 3

Evaluation of a newly developed emotion paradigm: activation pattern and repeatability of BOLD responses

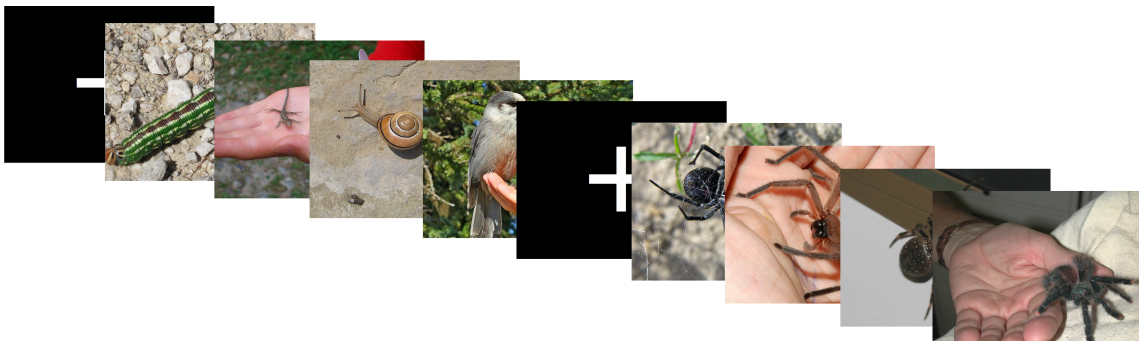

3.1 Abstract

The aim of this study was to construct and evaluate an emotion paradigm that elicits BOLD responses in emotion processing brain structures. Previous studies have shown low repeatability of BOLD responses in the amygdala during emotional face processing. We wanted to see whether more arousing stimuli, such as negative IAPS pictures and pictures of spiders elicit more repeatable BOLD signals.

An emotion paradigm was designed using two negative and two neutral stimulus conditions. In 37 female participants BOLD signals were assessed with an fMRI scan using this paradigm. Based on the results for a whole brain group analysis, functional ROIs in the amygdala and insula were constructed. 14 participants returned for a second scanning session. From data of these participants repeatability of the emotion-induced BOLD responses was assessed in the functional ROIs as well as in structural ROIs as a comparison. Repeatability was estimated with and without correcting for physiological noise.

We found that repeatability of the BOLD responses was higher in functional than in anatomical ROIs. BOLD was only repeatable when the negative conditions were contrasted to a fixation cross baseline but not when contrasted to the neutral condition. Physiological noise correction improved repeatability in these instances. This suggests that repeatability of emotion-induced BOLD responses depends on several factors, which should be considered when emotion paradigms are designed.

3.2 Introduction

The aim the main project was to investigate the relationship between fear-related BOLD responses, fearfulness and GABA concentration. To do this, we required a paradigm that elicts BOLD responses in areas involved in emotion processing, such as the amygdala and insular cortex (Phan et al., 2002). Several approaches to induce fear-related BOLD responses have been developed, including the presentation of fearful faces, of negative distressing pictures such as IAPS pictures (Lang et al., 2008) - and of fear-specific stimuli such as spiders.

Showing participants pictures of fearful faces assumes that these signal threat and therefore elicit activation in fear-processing structures (Morris et al., 1998; Phan et al., 2002). In fact, it has been shown that fearful faces elicit BOLD responses in the amygdala even when the emotional expression is not task-relevant and when the stimuli are not consciously perceived (Phan et al., 2002). A number of faces paradigms are frequently used, and include implicit gender-discrimination tasks (Surguladze et al., 2010), explicit emotion recognition tasks (Habel et al., 2007) and face-matching tasks (Hariri et al., 2002). Tasks also vary in the emotion intensity of the faces and whether a block or an event-related design is applied.

Amygdala reactivity is often investigated in the context of biomarkers for psychiatric disorders (Phillips et al., 2003). The assumption underlying the proposed biomarker is that the signal change measured in the amygdala is sufficiently strongly driven by temporally stable inter-individual differences in neural activity induced by experimental challenges. Repeatability of BOLD responses in the amygdala has been tested using several variants of the fearful faces paradigm. Johnstone et al. (2005) presented fearful and neutral Ekman faces in blocks, and instructed participants to passively view them on three separate occasions. They found low repeatability for activity in anatomically defined amygdalae, but repeatability of ICC $>$ .60 for a left functional ROI and lower - but still satisfactory - repeatability for a right functional amygdala. BOLD responses were only repeatable for the contrast fearful $>$ baseline but not for fearful $>$ neutral. In our recent study (Lipp et al., 2014, described in Chapter 2), we applied a gender discrimination task and found that BOLD responses to fearful faces in both anatomical amygdalae were not repeatable for either the contrast to baseline or the contrast to neutral faces. Studies looking at repeatability of amygdala during face matching task yielded inconclusive results. Manuck et al. (2007) found higher stability for a functionally defined right (ICC = .59) than for a functionally defined left amygdala (ICC = 0) when comparing BOLD responses to a face

matching vs. shape matching task, over retest interval of one year. Using a similar task, Plichta et al. (2012) found that BOLD responses in either amygdala were not repeatable, however, they used anatomical rather than functional amygdala masks. Sauder et al. (2013) reported significant but not high repeatability for the contrast faces > geometrical shapes and that it made no difference whether anatomical or functional regions of interest were used.

Due to the variety of tasks, contrasts, amygdala masks and retest intervals used, it is hard to draw a conclusion about when repeatable amygdala activity can be measured using face paradigms. Also, even though meta-analysis support a role of the amygdala in processing of fearful faces, not all studies find it (e.g. Lipp et al. 2014; Schäfer et al. 2005), which might be due to differences in the sample used and the challenge of detecting amygdala activation related to its size and signal to noise ratio. Additionally, it has been shown that the amygdala habituates to the presentation of emotional faces (Phillips et al., 2001; Wright et al., 2001). Therefore, lower reactivity in the second scanning session might contribute to low repeatability estimates. Paradigms with more variable stimuli than just faces, and paradigms eliciting stronger responses in the emotion processing network might be able to produce more repeatable activation in the amygdala.

Faces might signal threat but are not themselves the source of fear. One way to elicit stronger emotional responses is by using negative pictures from the international affective picture system (IAPS, Lang et al. 2008). Negative IAPS pictures are rated as more negative and more arousing than fearful faces (Britton et al., 2006; Schäfer et al., 2005). A direct comparison of face and IAPS paradigmns in the scanner was performed by Britton et al. (2006), Hariri et al. (2002) and Schäfer et al. (2005). Hariri et al. (2002) found stronger right amygdala activation for the face condition than for the IAPS condition, which was not replicated by Britton et al. (2006) or Schäfer et al. (2005). Britton et al. (2006) reported stronger BOLD responses in the superior temporal, insular and anterior cingulate cortices for faces and stronger responses in the visual cortex for IAPS pictures. On the other hand, Schäfer et al. (2005) found significant activations when using the IAPS pictures in areas such as the insula and OFC, but no activations using the face contrast. Again, whether faces or IAPS pictures induce stronger BOLD signals in fear-relevant structures might depend on the what stimuli and sample are used.

Another way to elicit BOLD responses in emotion-processing regions is to use stimuli that are specific to participants' fears. A lot of studies have used participants with spider phobia (Caseras et al., 2010; Dilger et al., 2003; Schienle et al., 2005; Straube et al., 2004,

2006a,b; Wendt et al., 2008), but also social phobia (Klumpp et al., 2010; Stein et al., 2002) and snake phobia (Lueken et al., 2011). The areas that are frequently found for the contrast phobic stimulus vs. neutral stimulus are assumed to be fear-relevant areas and include the amygdala (Caseras et al., 2010; Dilger et al., 2003; Klumpp et al., 2010; Schienle et al., 2005; Straube et al., 2006b; Stein et al., 2002), and the insula (Caseras et al., 2010; Dilger et al., 2003; Klumpp et al., 2010; Lueken et al., 2011; Straube et al., 2004, 2006a,b; Wendt et al., 2008).

So far repeatability of fear-related BOLD responses has predominantly been investigated in the amygdala and fusiform gyrus, using faces paradigm (Lipp et al., 2014; Plichta et al., 2012). In this study we developed a paradigm with negative IAPS pictures and fear-specific pictures of spiders to investigate whether 1) the stimuli can elicit activation in the amygdala and insula, 2) whether the BOLD responses are repeatable and whether repeatability depends on the nature of the ROIs (anatomical vs. functional) and the contrast (comparison to baseline vs. comparison to neutral condition), and 3) whether physiological noise correction influences repeatability of BOLD responses to fear-inducing stimuli that are reported to be more arousing than faces (Britton et al., 2006; Schäfer et al., 2005).

3.3 Methods

3.3.1 Participants

The sample used for task evaluation is equivalent to the sample that will be described in Chapter 4. The whole sample (consisting of both fearful and not fearful participants; N = 37[1]) was used to assess if the task elicited the expected activations in emotion processing areas, and to set up functional ROIs. A subsample of 14 participants (initial group assignment: 6 with high fearfulness, 8 with low fearfulness) was used to assess repeatability. These volunteers came for two scanning sessions between 2 and 10 weeks apart. As described in Chapter 4, participants were asked to come for the scanning session during a specific point in their menstrual cycle. This was also required for the second scanning session to keep cycle phase consistent throughout participants and throughout time points.

[1]Some participants from the original sample of N = 44 had to be excluded (see Chapter 4).

3.3.2 Emotion paradigm

The emotion paradigm that was presented during fMRI was designed in a way to 1) elicit fear reactions by showing fear-specific stimuli (pictures of spiders) as compared to control stimuli and 2) elicit more general negative emotion processing (unspecific negative pictures chosen from the IAPS (Lang et al., 2008) as compared to neutral pictures). The stimuli fall into four conditions: negative IAPS pictures, neutral IAPS pictures, spider pictures, and other animal pictures (neutral control). Two control conditions (neutral IAPS and other animals) were chosen in order to make fair contrasts ($IAPSnegative > IAPSneutral$, $SPIDERS > ANIMALS$) where the two conditions were designed in a way that they did not differ in any possible confounding factor other than their emotional/fear content. Confounding factors controlled for are: human content (Colden et al., 2008), brightness, contrast or spatial frequency (Carretié et al., 2007; Said et al., 2008; Vlamings et al., 2009; Vuilleumier et al., 2001), and complexity (Wiens et al., 2011). Spatial frequency was calculated for eight frequency bands and three colours with the scripts provided by Delplanque et al. (2007). Brightness was calculated as the average of pixels mean RGB (red/green/blue) values. Contrast scores were obtained by extracting the standard deviation of pixels mean RGB values in each pixel column and then computing the standard deviation of these values (also see Bradley et al. 2007, Ihssen and Keil 2012). Complexity was rated by the researcher on a scale of 1 to 10.

IAPS pictures were selected according to the valence reported in Lang et al. (2008)[2]. Negative IAPS pictures had valence ratings between 1 and 3 (mean = 1.9), neutral IAPS pictures had valence ratings between 4 and 6.5 (mean = 4.9). They were matched for content by broadly classifying the pictures into four categories and including 10 pictures of each category in the stimulus selection. The categories were: human bodies (definition: main aspect of picture is a human body), human faces (definition: human face looking at camera), animals, and environment (environmental situation, bodies - if visible - were not main aspect of image). Negative and neutral pictures did not differ in format (negative: 8 portrait, neutral 6 portrait), brightness (negative mean = 98 [std. = 36], neutral mean = 85 [std. = 34], $z = 1.6$ [$p = .10$]) or contrast (negative mean = 17 [std. = 9], neutral

[2]Picture numbers negative: 1052, 1111, 1525, 1932, 9140, 9181, 9183, 9185, 9187, 9571, 3001, 3005, 3015, 3063, 3140, 6825, 9040, 9362, 9412, 9413, 2095, 2800, 3059, 3168, 3180, 3266, 3301, 6231, 6250, 6563, 5971, 9280, 9611, 9620, 9622, 9630, 9908, 9911, 9930, 9940; Picture numbers neutral: 1112, 1350, 1390, 1616, 1661, 1670, 1675, 1726, 1820, 1908, 2272, 2357, 2377, 2396, 2400, 2410, 2411, 2480, 2749, 9210, 2190, 2210, 2215, 2221, 2230, 2440, 2441, 2495, 2499, 6837, 7130, 7180, 7242, 7491, 7500, 7510, 7546, 7560, 7595, 8211

mean = 17 [std. = 8], z = -0.43 [p = .67]), or in any of the eight frequency bands for red green or blue.

Spider images and images of the control animals were selected from the internet. For the control images, images of six categories butterflies, lady bugs, birds, lizards, snails and catterpillars were selected and presented to 20 female raters in line with a selection of spider images. Images showed the animal in different environments, in half of the finally selected stimuli, human hands were visible touching or in close distance to the animal. From the six preselected categories, four categories were selected based on the mean valence ratings for the images. The most neutrally rated categories were birds (mean valence = 6.4), lizards (mean valence = 5.2), caterpillars (mean valence = 4.7) and snails (mean valence = 4.4; overall mean = 5.2). As expected, the images of spiders were rated with a mean negative valence (mean = 2.6). The selected images for spiders did not significantly differ from the neutral animal images in format (all portrait), brightness (spiders mean = 117 [std. = 24], neutral mean = 124 [std. = 30], z = -0.88, p = .38) or contrast (mean spiders = 11 [std. = 4], neutrals = 10 [std. = 4], z = 0.60, p = .55) or in any of the eight frequency bands for red green or blue. Complexity was assumed to be balanced by the fact that all images showed an animal on a background.

The images were presented in short blocks of 10 seconds, with 4 images (presented for 2.5 sec.) each. A block design was chosen because block designs increase power to detect activation, the duration of 10 seconds was chosen to minimalize habituation effects within the blocks. In order to keep attention to the pictures and also to decrease habituation, the four images presented came from different categories (different IAPS categories, or different neutral animals) except for the spider blocks that exclusively showed spiders. In the animal blocks either all or none of the images within a block showed human hands. The blocks were arranged in superblocks (consisting of one block of each kind) whereby the blocks within the superblocks were pseudorandomized. Then, the superblocks were pseudorandomized. This assured that blocks of one kind could occur at most twice in a row. After half of the blocks a fixation cross appeared for either 7, 9, 11 or 13 seconds (there were no blocks of the same kind without a fixation period inbetween).

3.3.3 Imaging

Structural scans

A T1 weighted whole-brain structural scan was acquired for purposes of image and MRS voxel registration (1 x 1 x 1 mm resolution, 256 x 256 x 176 matrix size).

Functional scan: emotion paradigm

The participants underwent gradient-echo echo-planar imaging at 3 T (GE HDx MRI System) with a T2* weighted imaging sequence (TR = 3 seconds, TE = 35 ms, matrix = 64 x 64, FOV/slice = 220 mm, flip angle = 90, 46 slices of 2 mm with a 1 mm slice gap acquired in an interleaved order) using an eight-channel receive-only head coil. The orientation of the axial slices was parallel to the AC-PC line. Overall, the task took about 10 minutes and 204 functional images were aquired. The task was presented using Presentation (Neurobehavioral Systems, Albany, CA) and rear-projected onto a screen behind the participant's head that was visible through a mirror mounted on the head RF coil. Participants were asked to respond to the stimuli with a button box placed in their right hand.

The task instruction for participants was to judge whether they could detect a human or part of a human body on each picture. This task assured that response (yes or no) did not confound with emotion content since the amount of pictures with human parts in them was very similar in all four conditions. Participants were asked to rate the pictures after the scanning session, on the rating scale as used by Lang et al. (2008), from 1 = *very negative* to 9 = *very positive*.

3.3.4 Physiological parameters

The following physiological parameters were recorded during the scanning session: a) the cardiac cycle was recorded using a pulse-oximeter placed on the left index finger, b) a respiration trace was recorded with a pneumatic belt around the chest, c) end-tidal CO_2 and end-tidal O_2 were recorded using a nasal cannula attached to rapidly responding gas analysers (AEI Technologies, PA) to provide representative measures of arterial partial pressures of both gases.

3.3.5 Data preprocessing and analysis

The BOLD fMRI time-series data during the emotion paradigm were first corrected for physiological noise: this correction consisted of: first applying correction of cardiac and respiratory artifacts (RETROICOR, Glover et al., 2000) using two cardiac, two respiratory and one interaction component, followed by regressing out the variance related to CO_2 level, O_2 level (both HRF convolved), heart rate (HR; CRF convolved, Chang et al., 2009) and respiratory volume per time (RVT; RRF convolved; Birn et al., 2008), using a general linear model framework. Both steps were performed using Matlab (The MathWorks Inc.,

vs. R2011a). Physiological noise correction was performed prior to preprocessing. For seven participants physiological noise correction could only be partly performed, for two participants physiological recordings were missing altogether.

Both, the corrected and uncorrected datasets were analyzed using FEAT (FMRIB Expert Analysis Tool, v5.98, http://www.fmrib.ox.ac.uk/fsl, Oxford University, UK). Preprocessing steps before model fitting were applied to each participants time-series, and included: highpass filtering of the data (100 seconds temporal cutoff), non-brain removal using BET (Smith, 2002), MCFLIRT motion correction (Jenkinson et al., 2002), spatial smoothing with a Gaussian kernel of full-width-half-maximum 5mm and fieldmap-based EPI unwarping using PRELUDE + FUGUE (Jenkinson, 2003, 2004); for three participants this was not performed due to problems during the acquisition of the fieldmaps). Functional images were registered using FLIRT (Jenkinson and Smith, 2001) in a first step to the structural image with 6 degrees of freedom, and in the second step to the Montreal Neurological Institute (MNI) space with 12 degrees of freedom and FNIRT non-linear (10 mm) warp (Andersson et al., 2007a,b).

To model the emotion provocation task, four event types were defined, one for each picture condition (i.e. $IAPSnegative$, $IAPSneutral$, $SPIDERS$, $ANIMALS$). Fixation cross periods were used as the baseline. The model was convolved with the hemodynamic response function (gamma convolution), and the same temporal filtering was applied to the model as to the data. Temporal derivatives of the event-type regressors were included as regressors of no interest. Two main contrasts of interest were defined: a fear-specific contrast $SPIDERS > ANIMALS$, and a fear-unspecific contrast $IAPSnegative > IAPSneutral$ for more general emotion processing. Group average maps were created with a mixed effects model using FLAME1. The Z (Gaussianised T/F) statistic images were thresholded using clusters determined by $Z > 2.3$ and a (corrected) cluster significance threshold of $P < .05$ (Worsley, 2001).

3.3.6 ROI analysis

Anatomical ROIs used were the left and right insula, and the left and right amygdala, taken from the WFU-PickAtlas (Version 3.0.4, Wake Forest University, School of Medicine, Winston-Salem, North Carolina, www.ansir.wfubmc.edu). Functional amygdala ROIs were obtained by masking the group level maps for the contrast $IAPSnegative > IAPSneutral$ with the anatomical amygdala masks ("fear-unspecific left/right amygdala"). Functional insula masks were obtained by restricting the group level analysis

for the contrast $SPIDERS > ANIMALS$ ("fear-specific ROI") and $IAPSnegative > IAPSneutral$ ("fear-unspecific ROI") to the spectroscopy voxel in the left insula (see Chapter 4). Median %SC was extracted from the ROIs for all conditions and the two contrasts.

3.3.7 Repeatability analysis

The intraclass correlation coefficient (ICC[3,1]; (Shrout and Fleiss, 1979) was used as a measure of repeatability. ICCs were interpreted according to commonly used guidelines (Cicchetti, 2001) that classify values of $< .41$ as poor, values between .41 and .59 as fair, values between .60 - .74 as good and values $> .74$ as excellent.

For all ICCs we defined bivariate outliers based on the overall structure of the data using the Matlab toolbox provided by Pernet et al. (2012), and ICCs were computed with the remaining data points. Due to outlier removal, sample size changed slightly for each reported correlation. We therefore report correlations with respective sample size in brackets.

3.4 Results

3.4.1 Task evaluation

To elicit BOLD responses related to emotion processing, the fear-specific contrast $SPIDERS > ANIMALS$ and the fear-unspecific contrast $IAPSnegative > IAPSneutral$ were investigated. The group level analysis revealed significant BOLD responses in the left insula for both conditions, but BOLD responses in the amygdala only for the fear-unspecific contrast (see Table 3.1 and Figures 3.1 and 3.2).

3.4.2 ROIs

BOLD %SC were extracted for anatomical and functional ROIs for the 14 participants who came for a second scanning session. Mean and standard deviation for each session and between-session differences (investigated with a paired t-test between the two sessions) are reported in Table 3.2. For none of the regions, a significant change in %SC over the two sessions was found.

Table 3.1: Higher-level whole-brain analysis for the two contrasts $SPIDERS > ANIMALS$ and $IAPSnegative > IAPSneutral$. Significant clusters for the analysis over the whole sample (N = 37) are reported. The physiological noise corrected dataset was used for this analysis.

$SPIDERS > ANIMALS$			
Size	Peak (x,y,z)	Peak Z	Location
12117	-6, -56, 24	4.51	Cingulate, frontal gyrus
2297	-58, -40, 24	4.31	Temporal-occipital
2270	28, -78, -38	3.89	Cerebellum
1448	58, -40, 28	3.76	Angular, temporal gyrus
727	58, 10, -4	4.22	Right OFC, insula
582	-50, 8, -10	3.95	Left OFC, insula
$IAPSnegative > IAPSneutral$			
Size	Peak (x,y,z)	Peak Z	Location
12350	-50, -68, -4	5.53	Bilateral occipital/temporal
4879	0, -34, -10	5.12	Brain stem and thalamus
3740	-44, 18, -20	4.63	Left insula and OFC
3334	-4, 56, 18	4.72	Cingulate and frontal gyrus
1272	26, -4, -20	5.53	Right amygdala
520	46, 6, 16	4.08	Left amygdala

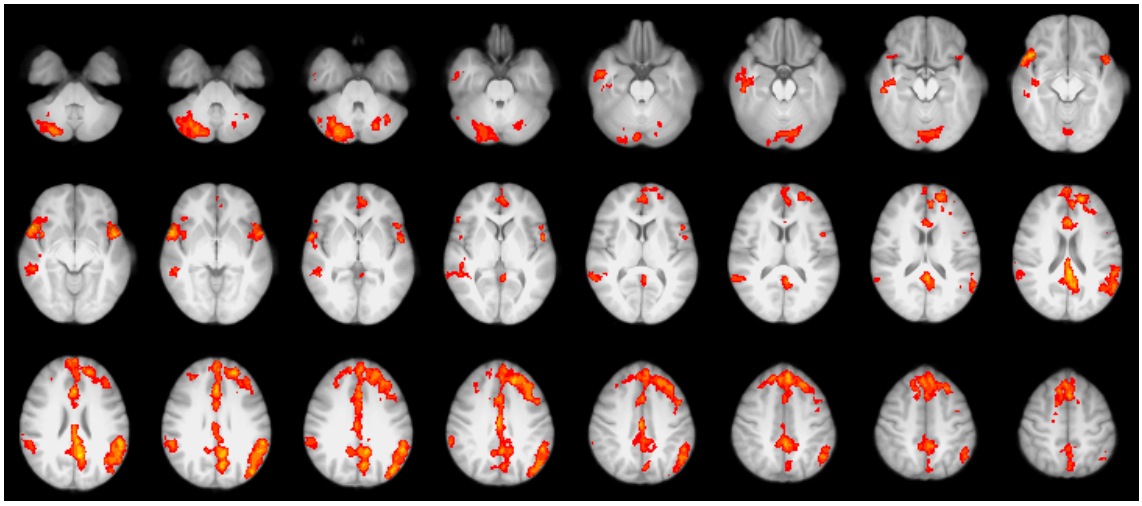

Figure 3.1: Group effect for the contrast $SPIDERS > ANIMALS$ (N = 37). The statistical threshold was set to Z > 2.3 and corrected cluster threshold of P < .05. Image displayed in radiological convention.

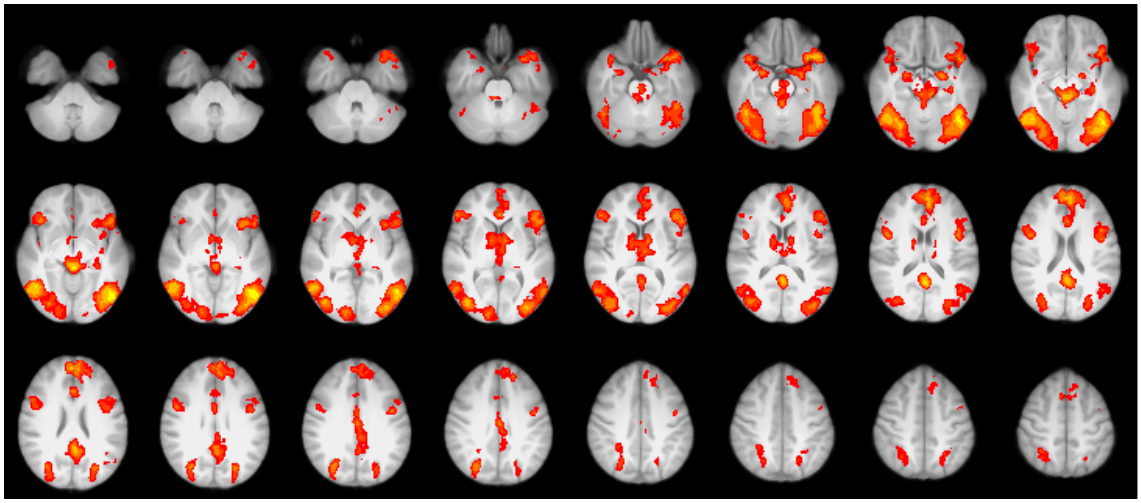

Figure 3.2: Group effect for the contrast $IAPSnegative > IAPSneutral$ (N = 37). The statistical threshold was set to Z > 2.3 and corrected cluster threshold of P < .05. Image displayed in radiological convention.

Table 3.2: ROI analysis for uncorrected as well as physiological noise corrected data. For each of the ROIs, mean and standard deviation of the %SC for both scanning sessions (scan 1 and scan 2) and the significance of the between-session difference (paired t-test; indicated by p) are provided. This was done using the data from the 14 participants who underwent two scanning sessions. IAPS neg = negative IAPS pictures, IAPS neu = neutral IAPS pictures, LI = Left insula, LA = Left amygdala, RA = Right amygdala, Spi. > An.: fear-specific contrast Spiders > Animals; Neg. > Neu.: fear-unspecific contrast IAPS negative > IAPS neutral.

	uncorrected			**physiological noise correction**		
Area / Condition	$M(Std)$ **1**	$M(Std)$ **2**	$t(p)$	$M(Std)$ **1**	$Mean(Std)$ **2**	$t(p)$
Left amygdala						
IAPS neg	0.42 (0.20)	0.33 (0.30)	1.18 (.26)	0.38 (0.20)	0.20 (0.34)	1.64 (.13)
IAPS neu	0.30 (0.29)	0.20 (0.40)	0.87 (.40)	0.23 (0.23)	0.09 (0.42)	1.24 (.24)
Spiders	0.24 (0.28)	0.08 (0.26)	1.46 (.17)	0.22 (0.28)	0.06 (0.30)	1.26 (.23)
Animals	0.24 (0.19)	0.24 (0.22)	-0.01 (.99)	0.22 (0.23)	0.20 (0.22)	0.24 (.82)
Neg. > Neu.	0.11 (0.26)	0.14 (0.30)	-0.29 (.78)	0.15 (0.20)	0.14 (0.31)	0.15 (.89)
Spi. > An.	0.01 (0.23)	-0.15 (0.26)	1.43 (.18)	0.00 (0.23)	-0.15 (0.31)	1.12 (.28)
Right amygdala						
IAPS neg	0.33 (0.22)	0.31 (0.33)	0.27 (.79)	0.28 (0.18)	0.26 (0.22)	0.46 (.65)
IAPS neu	0.22 (0.29)	0.23 (0.33)	-.10 (.92)	0.18 (0.19)	0.21 (0.32)	-0.38 (.71)
Spiders	0.17 (0.32)	0.14 (0.24)	0.38 (.71)	0.16 (0.26)	0.12 (0.24)	0.60 (.56)
Animals	0.23 (0.24)	0.19 (0.24)	0.44 (.67)	0.19 (0.20)	0.20 (0.16)	-0.23 (.82)
Neg. > Neu.	0.12 (0.20)	0.11 (0.18)	0.20 (.84)	0.11 (0.16)	0.07 (0.17)	0.48 (.64)
Spi. > An.	-0.05 (0.21)	-0.06 (0.12)	0.24 (.81)	-0.01 (0.18)	-0.10 (0.13)	1.72 (.11)
Left insula						
IAPS neg	-0.03 (0.17)	-0.06 (0.26)	0.34 (.73)	0.00 (0.15)	-0.06 (0.19)	0.77 (.45)
IAPS neu	-0.02 (0.11)	-0.07 (0.29)	0.57 (.58)	-0.02 (0.13)	-0.03 (0.20)	0.12 (.91)
Spiders	-0.01 (0.19)	-0.02 (0.18)	0.19 (.85)	-0.02 (0.16)	-0.01 (0.11)	-0.18 (.86)
Animals	0.00 (0.16)	0.01 (0.08)	-0.11 (.91)	0.00 (0.15)	0.02 (0.06)	-0.60 (.56)
Neg. > Neu.	0.00 (0.15)	0.01 (0.17)	-0.19 (.86)	0.03 (0.13)	-0.03 (0.11)	1.16 (.27)
Spi. > An.	-0.01 (0.12)	-0.03 (0.15)	0.70 (.50)	-0.01 (0.11)	-0.04 (0.15)	0.79 (.44)
Right insula						
IAPS neg	-0.06 (0.13)	-0.09 (0.20)	0.45 (.66)	-0.04 (0.10)	-0.09 (0.16)	0.93 (.37)
IAPS neu	-0.04 (0.11)	-0.10 (0.19)	1.07 (.30)	-0.04 (0.10)	-0.09 (0.15)	1.09 (.30)
Spiders	-0.03 (0.18)	-0.06 (0.12)	0.80 (.44)	-0.02 (0.15)	-0.04 (0.10)	0.60 (.56)
Animals	-0.04 (0.14)	-0.09 (0.09)	1.32 (.21)	-0.02 (0.11)	-0.07 (0.06)	1.44 (.17)
Neg. > Neu.	-0.01 (0.15)	0.00 (0.16)	-0.30 (.77)	0.01 (0.11)	-0.02 (0.11)	0.64 (.53)
Spi. > An.	0.01 (0.12)	0.03 (0.06)	-0.90 (.38)	0.01 (0.09)	0.03 (0.08)	-0.73 (.48)
fear - specific LI						
Spiders	0.14 (0.35)	-0.01 (0.47)	1.24 (.24)	0.12 (0.29)	0.01 (0.35)	1.46 (.17)
Animals	0.05 (0.25)	-0.09 (0.31)	1.32 (.21)	0.01 (0.25)	-0.07 (0.26)	0.81 (.43)
Spi. > An.	0.09 (0.27)	0.08 (0.36)	0.11 (.92)	0.12 (0.19)	0.09 (0.33)	0.31 (.76)
fear - unspecific LI						
IAPS neg	0.19 (0.12)	0.06 (0.29)	1.5 (.16)	0.17 (0.16)	0.00 (0.28)	1.82 (.09)
IAPS neu	0.05 (0.16)	-0.08 (0.34)	1.45 (.17)	0.03 (0.18)	-0.07 (0.30)	0.97 (.35)
Neg. > Neu.	0.12 (0.11)	0.13 (0.19)	-0.16 (.87)	0.13 (0.14)	0.08 (0.13)	0.91 (.38)
fear - unspecific LA						
IAPS neg	0.49 (0.26)	0.43 (0.37)	0.68 (.51)	0.44 (0.28)	0.29 (0.36)	1.31 (.21)
IAPS neu	0.36 (0.36)	0.25 (0.42)	0.83 (.42)	0.27 (0.30)	0.13 (0.45)	1.10 (.29)
Neg. > Neu.	0.14 (0.31)	0.19 (0.36)	-0.43 (.67)	0.20 (0.23)	0.19 (0.36)	0.08 (.94)
fear - unspecific RA						
IAPS neg	0.44 (0.25)	0.50 (0.42)	-0.68 (.51)	0.38 (0.23)	0.40 (0.30)	-0.39 (.70)
IAPS neu	0.24 (0.37)	0.33 (0.39)	-0.70 (.49)	0.21 (0.25)	0.26 (0.39)	-0.52 (.61)
Neg. > Neu.	0.20 (0.31)	0.21 (0.19)	-0.04 (.97)	0.17 (0.21)	0.15 (0.22)	0.31 (.76)

3.4.3 Repeatability

Significant repeatability was found for a number of regions (see Table 3.3). Scatter plots for some of the data are shown in Supplement Figures B.1-B.4.

Table 3.3: Repeatability analysis on the ROIs. ICC (p) are reported, significant ICCs are printed in bold. Outliers were removed for this repeatability analysis, the number of remaining participants (out of N = 14) is indicated in brackets for each ICC.

	uncorrected		**physiological noise correction**	
left amygdala:				
IAPS neg	**.68 (.004)**	(N = 13)	.32 (.16)	(N = 11)
IAPS neu	.07 (.41)	(N = 11)	-.03	(N = 12)
Spiders	.00 (.50)	(N = 12)	-.29	(N = 12)
Animals	.16 (.29)	(N = 13)	**.84 (.0001)**	(N = 12)
fear-unspecific contrast	-.24	(N = 11)	-.14	(N = 12)
fear-specific contrast	-.03	(N = 12)	-.63	(N = 14)
right amygdala:				
IAPS neg	**.48 (.04)**	(N = 13)	**.61 (.008)**	(N = 14)
IAPS neu	.09 (.38)	(N = 13)	**.49 (.04)**	(N = 13)
Spiders	.26 (.20)	(N = 12)	.36 (.13)	(N = 11)
Animals	.19 (.25)	(N = 13)	.35 (.11)	(N = 13)
fear-unspecific contrast	-.57	(N = 12)	-.08	(N = 12)
fear-specific contrast	-.05	(N = 12)	.23 (.22)	(N = 12)
left insula:				
IAPS neg	-.53	(N = 12)	.13 (.34)	(N = 12)
IAPS neu	.31 (.17)	(N = 11)	**.60 (.02)**	(N = 11)
Spiders	.18 (.30)	(N = 10)	.23 (.23)	(N = 12)
Animals	-.60	(N = 11)	-.03	(N = 11)
fear-unspecific contrast	.25 (.19)	(N = 13)	.39 (.10)	(N = 11)
fear-specific contrast	.16 (.30)	(N = 12)	.01 (.49)	(N = 11)
right insula:				
IAPS neg	.15 (.32)	(N = 11)	.37 (.12)	(N = 11)
IAPS neu	**.61 (.01)**	(N = 13)	.45 (.05)	(N = 13)
Spiders	.43 (.05)	(N = 14)	**.52 (.03)**	(N = 13)
Animals	.36 (.10)	(N = 13)	.45 (.06)	(N = 12)
fear-unspecific contrast	**.74 (.002)**	(N = 11)	.06 (.42)	(N = 11)
fear-specific contrast	**.51 (.04)**	(N = 12)	**.50 (.03)**	(N = 14)
fear-specific ROI (left insula):				
Spiders	.39 (.09)	(N = 12)	**.60 (.009)**	(N = 14)
Animals	-.19	(N = 13)	-.01	(N = 14)
fear-specific contrast	.41 (.07)	(N = 13)	.17 (.28)	(N = 13)
fear-unspecific ROI (left insula):				
IAPS neg	.24 (.20)	(N = 13)	**.49 (.04)**	(N = 12)
IAPS neu	.47 (.05)	(N = 12)	.09 (.38)	(N = 12)
fear-unspecific contrast	.17 (.27)	(N = 14)	.34 (.13)	(N = 12)
fear-unspecific ROI left amygdala:				
IAPS neg	**.48 (.03)**	(N = 14)	**.60 (.01)**	(N = 13)
IAPS neu	-.04	(N = 12)	-.41	(N = 10)
fear-unspecific contrast	-.06	(N = 12)	-.10	(N = 12)
fear-unspecific ROI right amygdala:				
IAPS neg	.43 (.06)	(N = 13)	**.66 (.005)**	(N = 13)
IAPS neu	-.26	(N = 12)	.11 (.36)	(N = 12)
fear-unspecific contrast	-.66	(N = 12)	-.03	(N = 12)

3.5 Discussion

3.5.1 Task evaluation

Fear-specific BOLD responses ($SPIDERS > ANIMALS$) were identified in the cingulate gyrus, but also regions in the frontal, temporal and insula gyri. This is in line with previous studies (Caseras et al., 2013; Lueken et al., 2011; Straube et al., 2006a). The fear-unspecific contrast ($IAPSnegative > IAPSneutral$) also yielded widespread activation, comprising cingulate, temporal, occipital and insular cortices, and bilateral amygdala. Previous studies report similar activation (Schäfer et al., 2009; Schienle et al., 2002; Wrase et al., 2003).

We did find significant activation in the amygdala for the fear-unspecific contrast but not for the fear-specific contrast. One reason for this might be that the amygdala does not only react to fear-specific animals but to all animals. Previous studies that reported amygdala activation used neutral stimuli such as mushrooms as control stimuli (e.g. Wendt et al. 2008). To our knowledge, only few studies have used exclusively animal pictures as a control condition, and the amygdala seemed to also react to the impages of control animals (see Table 3.2). A reason for this might be that the main role the amygdala has been assigned to is the detection and evaluation of potential threat (Costafreda et al., 2008). Even though the control animals were on average subjectively perceived as neutral, they might have still been automatically assessed for potential threat before this conclusion was reached. Another possibility is that individual pictures within the short blocks might have triggered a negative response in participants. Even though the control images were rated neutrally on average, there was substantial variance in the ratings (see Chapter 4). It also has to be considered that some of the participants included in this sample were not scared of spiders, which could contribute to why we could not find amygdala activation for the fear-specific contrast. However, we could not find an influence of fearfulness on activation in the amygdala (see Chapter 4) so this is unlikely to be the reason.

With regard to the insula, we found significant activation for both the fear-specific and fear-unspecific contrast. It was proposed that the insula's function is to "recognize and mark salient events for further processing" (Menon and Uddin, 2010). One proposed mechanism underlying this function is that interoceptive sensations are integrated within the insula and that based on that, attention is regulated and an affective feeling is created (Lindquist and Barrett, 2012). We found insula activity even after correcting for physiological noise, indicating that the significant BOLD responses are not just a result of higher physiological reactions to the task (also see Chapter 5).

Importantly, because we found significant task activation for the contrasts - in contrast to the previous study (Lipp et al., 2014) - we were able to create functional ROIs. In particular, we extracted a fear-specific ROI in the insula, a fear-unspecific ROI in the insula and bilateral fear-unspecific ROIs in the amygdala that could be used for repeatability analysis.

3.5.2 Repeatability

Higher repeatability for functional than for anatomical ROIs

We extracted signal changes from both structural and functional ROIs to calculate repeatability. The BOLD %SC to negative IAPS pictures was significantly repeatable in both amygdalae, but physiological noise correction lowered repeatability in the left amygdala, which suggests that this might have been caused by repeatability of physiological task reactions.

The anatomical insula did not seem to react to the task conditions much on average, probably because of its size and unspecificity. Surprisingly, BOLD %SC values for the right insula were significantly repeatable for a number of contrasts. This means that even though on average the right insula did not react to the paradigm, whether it did react and in which direction it reacted seems to be stable over time.

For the functional ROIs in the insula we found repeatable BOLD %SC for the fear-specific ROI during presentation of $SPIDER$ pictures, for the fear-unspecific ROIs in the insula and bilateral amygdala during presentation of $IAPSnegative$ pictures. Physiological noise correction seemed to improve repeatability in these instances. In agreement with Johnstone et al. (2005) these results suggest that repeatability is higher for functionally defined ROIs than for anatomical masks. Anatomical masks are probably too unspecific, and in many cases - such as the insula - too big and diverse within to obtain a meaningful average signal change.

Higher repeatability for comparison to baseline than for contrasts

Again in agreement with Johnstone et al. (2005), BOLD %SC for the contrasts were not repeatable, with the exception of %SC in the right anatomical insula. This suggests that even though the contrasts elicit group level activation patterns similar to previous studies, the participant level extracted BOLD %SC for the contrasts are not repeatable and might not be ideal to be used as trait markers. Interestingly, the BOLD %SC for main effects (contrast to baseline) were repeatable for the respective negative condition ($SPIDERS$

and $IAPSnegative$) but not for the control conditions ($ANIMALS$ and $IAPSneutral$). This suggests that constructing the functional ROIs based on the contrast is still a useful thing to do because the strong BOLD %SC elicited for the negative condition is repeatable - while the weaker BOLD % SC for the neutral condition is not much of interest anyway.

There might be several reasons for why the contrast values are not repeatable. One reason might be that by including two conditions in the calculation, additional noise is introduced. The contrast value consists of the response to the negative as well as the response to the neutral condition. We found that the response to the neutral condition (compared to baseline) is not repeatable, which might indicate some measurement noise, possibly because the BOLD responses are quite weak. It might also be that the response to the neutral condition is more dependent on the daily state of the participant, while the negative stimuli are quite strong and elicit more robust reactions. The contrast is designed to measure the emotion-specific BOLD signal. It is also possible that some aspect independent of emotion drives the repeatability of the negative stimuli, such as attention to the task. If this was the case, then one might expect also the main effect of the control condition should be repeatable, but we did not find this.

Between-session differences

In order to investigate potential effects of between-session habituation on the repeatability measures, differences between sessions were tested in the subsample of 14 repeatability participants. For these participants, no significance change in BOLD %SC was found from session 1 to session 2. This indicates that participants did not habituate to the stimuli over the retest interval. Low repeatability that was found for some of the ROIs and contrasts is more likely to be driven by other factors.

Limitations and future directions

We calculated repeatability over a number of regions and contrasts, and controlling for multiple comparisons would not lead to as many significantly repeatable results. However, we observed a pattern in the significant results (significant repeatability for functional ROIs and for comparison to fixation cross baseline). It is possible that the contrast to neutral condition includes more noise and therefore yields lower repeatability, and further research needs to be conducted to explore the possible explanations for this effect.

We did not find significant amygdala activity for our fear-specific contrast, which was in contrast to previous studies. Our explanation was that this might be due to amygdala

reactivity to our neutral condition. Again, further exploration of this phenomenon needs to be done to better understand the influence of the control condition used on detected activation.

Comparing the results to the results from our previous study (Lipp et al., 2014), it seems that using this newly developed paradigm allows to measure more repeatable emotion-related BOLD responses. The reason for this might lie in the nature of the stimuli, but also due to the recruitment process for this study a more diverse sample might have caused this difference. This suggests that paradigms should be developed and evaluated on a range of participants before being used to measure biomarkers.

Summary and conclusions

We investigated repeatability of emotion-related BOLD responses with a paradigm using IAPS pictures, fear-specific pictures of spiders and respective control stimuli. We found significant insula activation for the fear-unspecific and the fear-specific contrast, and significant amygdala activation for the fear-unspecific contrast. BOLD % SC were repeatable for the functionally defined ROIs in the negative condition vs. baseline when physiological noise correction is applied, but less repeatable for the anatomically defined ROIs and the contrasts. The findings suggest that repeatability of emotion-induced BOLD responses is dependent on several factors and that not all BOLD responses are suitable as biomarkers.

Next steps

In this study we evaluated a novel emotion paradigm, which was designed to elicit activation in the amygdala and insula. In order to address the main questions of this project, the influence of fearfulness and GABA+ (GABA plus coedited macromolecules) on this activation is assessed as a next step. Because the emotional aspect of the BOLD signal are of interest, to do this, the contrasts ($SPIDERS > ANIMALS$ and $IAPSnegative > IAPSneutral$) are used. Additionally, regarding the low repeatability we found for the contrasts, in a later step correlations are also calculated for the contrasts to fixation cross baseline, and differences in results will be discussed.

Part III

Investigating the role of GABA in fearfulness and fear-related BOLD responses

Chapter 4

The relationship between fearfulness, GABA, and fear-related BOLD responses in the insula and DLPFC

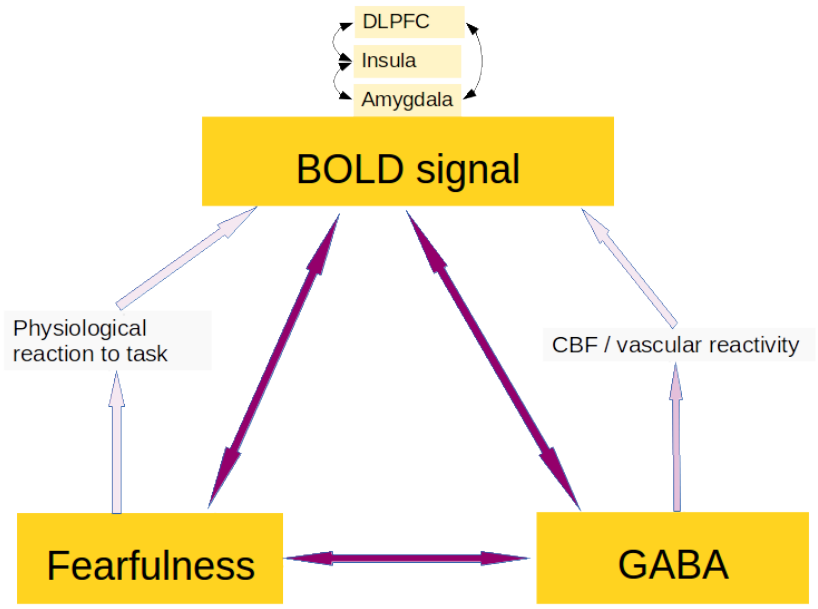

4.1 Abstract

The inhibitory neurotransmitter GABA plays a crucial role in anxiety and fear, but its relationship to brain activation during fear reactions is not clear. Previous studies suggest a decrease in GABA concentration in anxiety disorders, and that GABA agonists lead to attenuation of emotion-processing related BOLD signals in the amygdala and insula. The aim of this study was to directly investigate the relationship between fearfulness, GABA concentration and fear-related BOLD responses.

44 female participants with different levels of fearfulness were recruited for the imaging study. For the whole sample, BOLD signals were assessed using an fMRI scan with a fear-specific emotion paradigm, and GABA concentration measures were obtained from a GABA+ sensitive MRS scan using a voxel in the left insula and left DLPFC.

While fearfulness was not associated with GABA+ levels in our voxel, fear-related BOLD responses in the anterior insula were stronger in highly fearful participants than in less fearful participants. The BOLD signal in this cluster did not correlate with GABA+ concentration. However, we found a significant positive correlation between GABA and fear-related BOLD responses in a different cluster including parts of the left insula, amygdala and putamen. GABA+ in the DLPFC correlated with fear-related BOLD responses in the frontal cortex posterior to the spectroscopy voxel.

Our findings indicate a positive correlation between GABA and BOLD signals in brain-structures crucial for fear, while previous studies found negative correlations. This conflict in findings suggests that brain region, stimulus material and study design could influence whether and how GABA and BOLD might be associated.

4.2 Introduction

Fear is an acute behavioural and physiological reaction to perceived threat, which has been observed in all mammals and probably evolved because it is useful for survival and avoidance of pain (Panksepp, 1998). Recent research using fMRI has identified the amygdala and the anterior insula as key brain structures associated with the experience of fear (Büchel and Dolan, 2000; Costafreda et al., 2008; Phan et al., 2002). While the amygdala is important for the detection of environmental 'fear' cues (Öhman, 2002), the anterior insula seems to play the role of integrating internal bodily perceptions and external cues information to create the experienced emotional state (Paulus and Stein, 2006). Both these structures have shown increased levels of activity when phobic participants are presented with phobia related material (e.g. Caseras et al., 2010; Schienle et al., 2005; Straube et al., 2006a; Wendt et al., 2008), but also when healthy controls are confronted with negative images (Caseras et al., 2010; Etkin and Wager, 2007; Stein et al., 2007).

Studies using MRS have also shown that individuals suffering from anxiety disorders have reduced GABA concentration in the occipital cortex (Goddard et al., 2001), the ACC and basal ganglia (Ham et al., 2007), and the insula (Rosso et al., 2014). Also, by enhancing GABA transmission pharmacologically, fear responses (Nutt and Malizia, 2001; Panksepp, 1998) and emotion related BOLD responses in the insula and the amygdala are attenuated (Del-Ben et al., 2012; Paulus et al., 2005; Wise et al., 2007). All these suggest a relationship between GABA neurotransmission and fear-related BOLD responses. However, thus far, this hypothesis has not been directly tested. Previous studies have reported a negative relationship between BOLD and GABA in the visual cortex (Donahue et al., 2010; Muthukumaraswamy et al., 2009, 2012) and the ACC (Northoff et al., 2007). Our aim was to investigate the relationship between fear induced BOLD responses and GABA concentration in the insula. We recruited participants with either high or low fearfulness and confronted them with a paradigm designed to elicit fear-related BOLD responses. We expected stronger BOLD responses in the insula and amygdala of highly fearful participants, as well as lower GABA concentration in the insula. We also expected a negative correlation between fear-related BOLD changes and GABA concentration in the insula.

Additionally, we included a spectroscopy voxel in the DLPFC, a region that is often reported to play a role in emotion regulation (e.g. Ray and Zald, 2012). GABA concentration in the DLPFC has previously been related to working memory (Michels et al., 2012) and to individual differences in impulsivity (Boy et al., 2011), but this is the first time to study its potential involvement in emotion processing.

4.3 Methods

4.3.1 Participants

Screening

Five-hundred and seventy-four females (Mean[Std] age = 21[4]) from Cardiff University (students and staff) underwent an online screening, consisting of the Fear-Survey Schedule-II (FSS-II, Geer 1965) and the Fear of Spider Questionnaire (FSQ, Szymanski and Donohue, 1995). Both questionnaires show high internal consistency and retest-stability (Geer, 1965; Muris and Merckelbach, 1996; Szymanski and Donohue, 1995). The FSS-II (Geer, 1965) consists of 51 items assessing fear to a wide variety of potentially threatening stimuli/situations, including animals, social or interpersonal situations, tissue damage, illness or death, noises, other classical phobias, and miscellaneous (Wolpe and Lang, 1964). The FSQ consists of 18 items assessing fear of spiders; this questionnaire has also shown to discriminate among levels of spider fear within non-phobic population (Muris and Merckelbach, 1996), which was important for our recruitment strategy. Both questionnaires have previously shown adequate psychometric properties (Geer, 1965; Muris and Merckelbach, 1996; Szymanski and Donohue, 1995). Since our aim was to recruit a sample of high and low fearful participants and to induce fear in them via the presentation of still images of a specific feared stimuli, we invited candidates with the lowest and highest scores in both questionnaires to participate in the imaging study. Therefore, we aimed for a group of low fearful participants who were also not afraid of spiders, and a group of high fearful participants who all shared their fear of spiders. Figure 4.1 illustrates the recruitment criteria on both questionnaires.

Imaging participants

Candidates were screened over the telephone to ascertain their MRI compatibility, right-handedness, and absence of current or personal history of psychosis, mood or anxiety disorders other than potential specific phobia - according to the MINI International Neuropsychiatric Interview (MINI, Sheehan et al., 1998). On the day of the scan, participants were requested to complete again the FSSII and FSQ, along with the State and Trait Anxiety Inventory (STAI, Spielberger et al., 1970), Hospital Anxiety and Depression scale (HADS; Zigmond and Snaith, 1983), the General Health Questionnaire (GHQ-12, Goldberg, 1972). Table 4.1 shows the mean scores on all the questionnaires.

We scanned 44 participants, 22 in the high fear group and 22 in the low fear group.

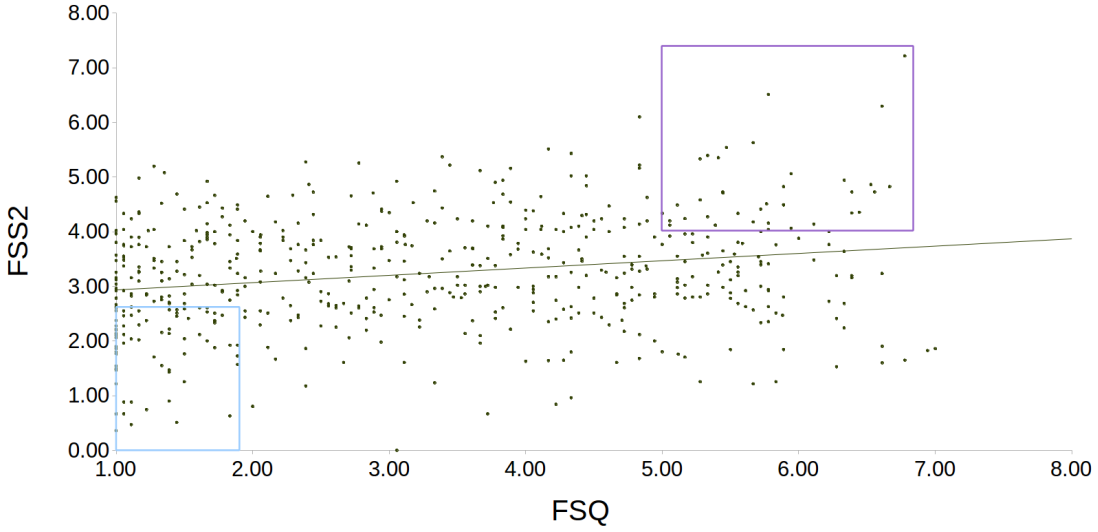

Figure 4.1: Recruitment of extreme groups. The scatter plot for the whole screening sample (N=574) is shown, with scores in the FSQ questionnaire on the x-axis, and the FSS-II on the y-axis. The purple box illustrates the recruitment thresholds for the high-fear group, the blue box the thresholds for the low-fear group. Correlation between the two measures was $r = .22$ ($p < .0001$).

Three participants from each group had to be excluded because their scores on the screening questionnaires at the time of scanning did not reflect their group assignment anymore (their score lay on the other side of the total median). One participant of the low fear group had to be excluded due to problems during the acquisition of the functional imaging data. The final sample consisted of 37 participants, 19 in the high fear group and 18 in the low fear group. Due to some evidence for an influence of the menstrual cycle on GABA levels (Epperson et al., 2002; Harada et al., 2011; Silveri et al., 2013), participants were asked to come for the imaging study during the first 9 days of their cycle; during this period the probability of being in the follicular phase - during which steroid hormone levels are most stable - is 95% (Stricker et al., 2006). Three participants did not comply with these instructions: one participant in the low fear group came on day 10, and two participants in the high fear group came on day 12 and day 14, respectively. Participants who were taking hormonal contraception (11 in the high fear and 11 in the low fear group) were asked to come for the scanning session outside their pill-free period, if applicable. The study was approved by the Cardiff University School of Psychology Ethics Committee. Participants were financially compensated for their time.

4.3.2 Imaging

Structural (T1) and functional imaging was performed as described in Chapter 3.

Table 4.1: Questionnaires. Questionnaire scores between the two groups are compared (N per group = 19; from each originally recruited group [N = 22], three participants had to be excluded because their scores on the questionnaires did not match their original initial group assignment). Mean (standard deviation) are listed separately for the high fear and the low fear group, the reported t and p value are obtained from a 2-sample-t-test.

Questionnaire	High fear	Low fear	t	p
Age	21.5 (3.1)	21.1 (2.9)	0.48	.63
FSQ	5.30 (0.85)	1.22 (0.40)	18.9	$< .001$
FSS-II	4.19 (0.71)	1.93 (0.80)	9.2	$< .001$
STAI state	1.60 (0.39)	1.55 (0.30)	0.46	.65
STAI trait	2.03 (0.14)	1.82 (0.11)	1.69	.10
GHQ	0.86 (0.34)	0.79 (0.30)	0.72	.47
HADS anxiety	1.07 (0.33)	0.84 (0.22)	2.46	.02
HADS depression	0.70 (0.30)	0.55 (0.16)	1.92	.06

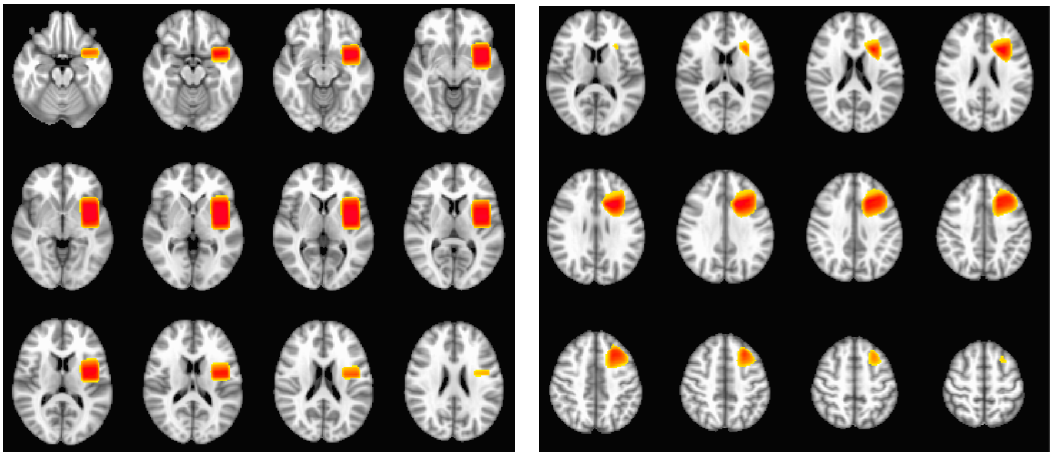

Figure 4.2: Left insula (left figure) and left DLPFC (right figure) voxel position. This shows the areas that a participant's voxel covered with 85% probability. This map was used for performing the restricted higher-level analysis.

4.3.3 GABA+ magnetic resonance spectroscopy

GABA+ was quantified from a 25 x 30 x 40 mm voxel located in the left insula and aligned with the insula cortex in the anterior-posterior direction. The DLPFC voxel (30 x 30 x 30 mm) was placed anterior to the precentral sulcus and aligned with the cortical surface (for both voxel locations see Figure 4.2). Two spectra from each region were aquired for each participant, in either the order insula-DLPFC-insula-DLPFC or DLPFC-insula-DLPFC-insula, counter-balanced within each fearfulness group.

GABA+ data (GABA plus coedited macromolecules) were acquired using a J difference editing technique (MEGA-PRESS, Mescher et al., 1998). Spectra were acquired with TR = 1800 ms, TE= 68 ms, 300 transients of 4096 data points were acquired in 9 minutes. Gaussian editing pulses (of 16 ms duration) were applied either to the GABA+ spins (1.9 ppm) or symmetrically about the water peak (7.5 ppm) in an interleaved manner. A further eight transients were acquired, without water suppression, as an internal concentration reference.

All spectra were analysed using Gannet (Edden et al., in press). GABA+ values were corrected for the tissue composition of the voxel. Tissue segmentation was performed using FAST, and tissue corrected according to Ernst et al. (1993). Prior to using GABA+ values for analysis, all spectra were visually inspected independently by two researchers, and rated using a 3-point scale ($0 = very\ good$, $1 = satisfactory$, $0 = reject$), to ensure the presence of artefacts did not affect the quantification of GABA. Spectra scoring below 1 were rejected resulting in the exclusion of 26/74 (insula) and 28/74 (DLPFC) spectra from the dataset. The GABA+ concentration estimations from the two scans per voxel were averaged for each participant if two spectra were available. Altogether, useable GABA+ data was acquired for 29 participants for the insula and 28 participants for the DLPFC (all used spectra can be seen in Supplementary Figures C.1 and C.2).

4.3.4 Data preprocessing and analysis

Data preprocessing, including physiological noise correction, was performed as described in Chapter 3. Group average and group difference (high fear vs. low fear) maps were created with a mixed effects model using FLAME1. For the analysis looking at the influence of GABA+ on the BOLD responses, the demeaned GABA+ measures were entered as a regressor in the group analysis model. For participants with no GABA+ data, the mean value was entered. The Z (Gaussianised T/F) statistic images were thresholded using

clusters determined by Z > 2.3 and a (corrected) cluster significance threshold of P < .05 (Worsley, 2001).

4.3.5 Statistical analysis

For all correlations we defined bivariate outliers based on the overall structure of the data using the Matlab toolbox provided by Pernet et al. (2012), and Pearson correlation coefficients were computed with the remaining data points. Due to outlier removal, sample size changed slightly for each reported correlation. We therefore report correlations with respective degrees of freedom in brackets.

ANOVAs were computed using the Matlab functions *anova*1 and *mixed_between_anova* (www.mathworks.co.uk/matlabcentral/fileexchange/27080-mixed-betweenwithin-subjects-anova/content/mixed_between_within_anova.m).

4.4 Results

4.4.1 Behavioural responses

Performance on the covert task was very high with a mean accuracy of 93% (Min. = 73%, Std. = 6%), suggesting that participants did pay attention to the stimuli. We did not find group differences in accuracy or reaction times (F[1,36] = 0.23, p = .64), and no interaction between group and stimulus category (F[3,108] = 0.36, p = .78). With regard to the picture ratings, we found a significant interaction between group and stimulus category (F[3,102] = 6.5, p = .0005). This interaction was driven by the group difference in the ratings for spiders (F[1,34] = 11.6, p < .01) but not for any of the other categories. Pictures of spiders were rated significantly less pleasant by participants in the high fear group (Mean = 2.2, Std. = 1.3) as compared to participants in the low fear group (Mean = 5.6, Std. = 2.9). Spiders were perceived as significantly more negative than the control animals in both of the groups (high fear: F[3,102] = 58, p < .01; low fear: F[3,102] = 9.08, p < .01), and the negative IAPS pictures as more negative than the neutral pictures (high fear: F[3,102] = 67, p < .01; low fear: F[3,102] = 9.08, p < .01).

4.4.2 Group differences in BOLD and GABA+ signal

The whole-brain analysis of the fear provocation paradigm showed significant BOLD responses in the orbitofrontal and cingulate cortex, posterior temporal and occipital regions, bilateral anterior insula, medial and lateral prefrontal cortices and cerebellum (see Ta-

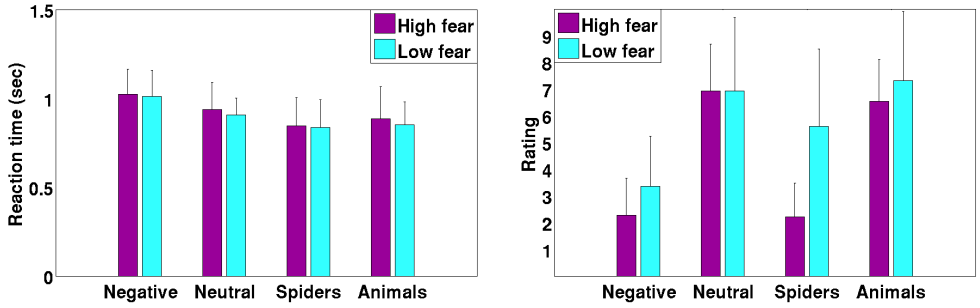

Figure 4.3: Behavioural results. Left: Reaction time for each stimulus category and fear group. Right: Ratings of the stimuli (high values indicate positive rating) for each stimulus category and fear groups. Bars indicate means, error bars standard deviations.

ble 4.3 and Figure 3.1 in Chapter 3) for the $SPIDERS > ANIMALS$ contrast. The contrast $IAPSnegative > IAPSneutral$ resulted in significant BOLD responses in the orbitofrontal and cingulate cortex, left insula, bilateral amygdala, and posterior temporal and occipital regions (see Table 4.4 and Figure 3.2 in Chapter 3). Furthermore, the exploratory whole brain analysis revealed stronger BOLD responses for participants in the high fear group in the cerebellum and ACC for the contrast $SPIDERS > ANIMALS$ (see Table 4.3 and Figure 4.4), and stronger BOLD responses for participants in the low fear group in the posterior cingulate for the contrast $IAPSnegative > IAPSneutral$ (see Table 4.4).

A voxelwise analysis restricted to the area of the brain covered by the insular voxel used in the spectroscopy acquisition showed significant BOLD responses for both the $SPIDERS > ANIMALS$ and the $IAPSnegative > IAPSneutral$ contrast. High and low fearful groups did only differ for the former contrast, with high fearful participants showing increased BOLD in the insular spectroscopy voxel compared to low fearful participants (see Table 4.2).

Based on these clusters, functional ROIs within the insula were defined: 1) a fear-specific ROI in the insula using the whole-group cluster of the contrast $SPIDERS > ANIMALS$, 2) a fear-unspecific ROI in the insula using the whole-group cluster contrast $IAPSnegative > IAPSneutral$, 3) a fear-specific ROI in the DLPFC using the whole-group cluster of the contrast $SPIDERS > ANIMALS$ that overlapped with the MRS voxel in the DLPFC.

GABA+ levels showed not to be different between low and high fearful participants (insula: $t[27] = -0.29$, $p = .78$, ns; DLPFC: $t[27] = -0.53$, ns). GABA+ in the insula was not significantly correlated with GABA+ in the DLPFC ($r[24] = .20$, $p = .34$).

Table 4.2: Higher level analysis, restricted to the regions covered by the spectroscopy voxel in the insula. Significant clusters are presented for the two regarded contrast.

Contrast $SPIDERS > ANIMALS$			
Group	Size	Peak (x,y,z)	Peak Z
All (N=37)	121	-48, 14, -8	3.73
High fear (N=19)	244	-46, 12, -6	4.52
Low fear (N=18)	No clusters		
High fear > low fear	175	-44, 12, -6	3.74
Low fear > high fear	No clusters		
Contrast $IAPSnegative > IAPSneutral$			
Group	Size	Peak (x,y,z)	Peak Z
All (N=37)	307	-46, 12, -16	3.91
High fear (N=19)	97	-34, 18, -2	3.24
Low fear (N=18)	No clusters		
High fear > low fear	No clusters		
Low fear > high fear	No clusters		

Table 4.3: Higher-level whole-brain analysis for the contrast $SPIDERS > ANIMALS$. Results are presented for the whole group, both groups separately, and group comparisons.

Group mean (N = 37)			
Size	Peak (x,y,z)	Peak Z	Location
12117	-6, -56, 24	4.51	Cingulate, frontal gyrus
2297	-58, -40, 24	4.31	Temporal-occipital
2270	28, -78, -38	3.89	Cerebellum
1448	58, -40, 28	3.76	Angular, temporal gyrus
727	58, 10, -4	4.22	Right OFC, insula
582	-50, 8, -10	3.95	Left OFC, insula
High fear (N = 19)			
Size	Peak (x,y,z)	Peak Z	Location
5487	-2, 26, 28	4.29	ACC
3104	-34, -62, -30	4.1	Cerebellum
1955	-2, -40, 20	3.97	Posterior cingulate
1069	46, -44, 6	3.76	Middle temporal gyrus
856	58, 10, -4	4.18	Right insula
779	-46, 12, -6	4.52	Left insula
753	-58, -42, 26	4.15	Left supramarginal
Low fear (N = 18)			
Size	Peak (x,y,z)	Peak Z	Location
2762	0, 66, 24	3.78	Frontal pole
2025	-10, -52, 28	4.28	Posterior cingulate
1756	-54, -58, 38	4.08	Left supramarginal
406	52, -68, 30	3.49	Right lateral occipital
379	54, -16, -16	3.50	Right middle temporal
High fear (N = 19) > low fear (N = 18)			
Size	Peak (x,y,z)	Peak Z	Location
3527	-20, -76, -28	3.49	Cerebellum
454	0, 0, 34	3.59	ACC
391	-44, 12, -6	3.74	Left anterior insula
Low fear (N = 18) > high fear (N = 19)			
no clusters			

Table 4.4: Higher-level whole-brain analysis for the contrast $IAPSnegative > IAPSneutral$. Results are presented for the whole group, both groups separately, and group comparisons.

Group mean (N = 37)			
Size	Peak (x,y,z)	Peak Z	Location
12350	-50, -68, -4	5.53	Bilateral occipital/temporal
4879	0, -34, -10	5.12	Brain stem and thalamus
3740	-44, 18, -20	4.63	Left insula and OFC
3334	-4, 56, 18	4.72	Cingulate and frontal gyrus
1272	26, -4, -20	5.53	Right amygdala
520	46, 6, 16	4.08	Left amygdala
High fear (N = 19)			
Size	Peak (x,y,z)	Peak Z	Location
3116	-50, -68, -4	4.45	Left occipital
2826	42, -76, 2	4.38	Right occipital
1070	-44, 16, -18	4.4	Left insula and OFC
578	-6, 52, 18	3.84	ACC
498	-2, -32, -8	4.52	Brain stem
Low fear (N = 18)			
Size	Peak (x,y,z)	Peak Z	Location
5589	-50, -68, -4	4.45	Left occipital
4836	42, -76, 2	4.38	Right occipital
4537	-44, 16, -18	4.4	Left insula and OFC
2859	-6, 52, 18	3.84	ACC
2790	-2, -32, -8	4.52	Brain stem
416	52, 32, 8	3.52	Right insula and OFC
High fear (N = 19) > low fear (N = 18)			
no clusters			
Low fear (N = 18) > high fear (N = 19)			
Size	Peak (x,y,z)	Peak Z	Location
374	8, -52, 24	3.48	Posterior cingulate

4.4.3 The relationship between GABA+ and fear-related BOLD responses

Insular GABA+ concentration did not correlate with %SC from either the $SPIDERS > ANIMALS$ in the fear-specific ROI (r[23] = .26, ns), or for the contrast $IAPSnegative > IAPSneutral$ in the fear-unspecific ROI (r[24] = -.01, ns). GABA+ concentration in the DLPFC did not correlate with BOLD responses in the fear-specific DLPFC ROI (r[24] = -.12, ns).

In order to further investigate the correlation of GABA+ and fear-related BOLD responses, we entered the GABA+ values as a regressor of interest in the whole-brain group level analysis of the fear provocation paradigm. For the contrast $SPIDERS > ANIMALS$, GABA+ predicted BOLD responses in a cluster covering parts of the left amygdala, insula, and ventral striatum (coordinates [x,y,z] = -28,-4,-12, cluster size = 420; see Figure 4.5), and in the frontal cortex (coordinates [x,y,z] = -46, -26, 58, cluster size = 649; for both clusters see Supplementary Figure C.3). DLPFC GABA+ correlated with BOLD responses in a frontal region ([x,y,z] = -32,-10,54, cluster size = 940) posterior to

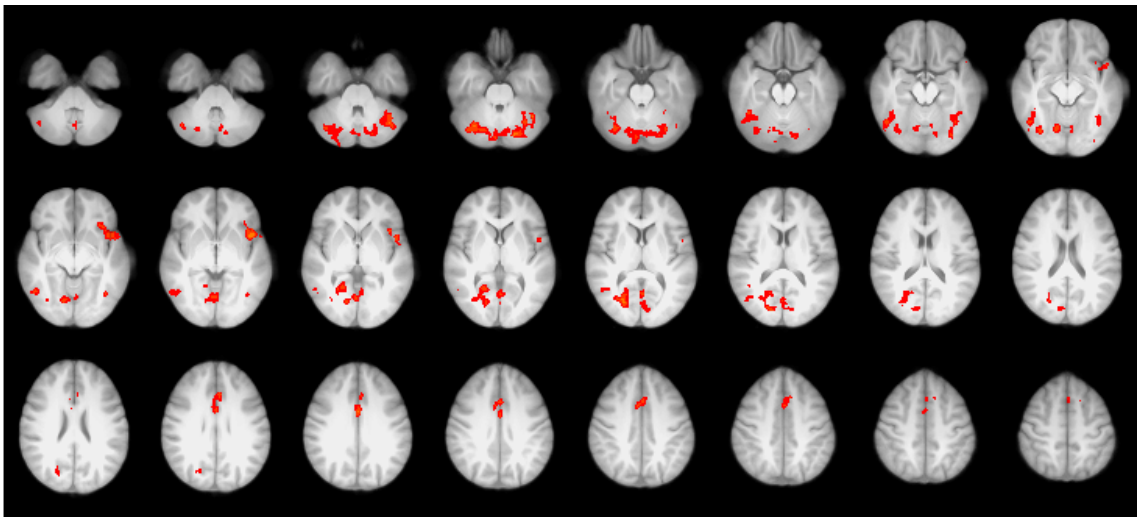

Figure 4.4: Group comparison (high fear (N = 19) > low fear (N = 18)) for the contrast $SPIDERS > ANIMALS$. The statistical threshold was set to Z > 2.3 and corrected cluster threshold of P < .05. Image displayed in radiological convention.

the MRS voxel (see Supplementary Figure C.4). No correlations between GABA+ and BOLD were found for the contrast IAPS negative > IAPS neutral.

4.5 Discussion

The goals of the present study were to investigate BOLD reactivity in the anterior insula and DLPFC during fear provocation, and the role of GABA+ concentration and fearfulness in this reactivity. We found increased BOLD responses during fear provocation, this being greater in individuals with high, relative to low, fearfulness. GABA+ concentration in the insular cortex or in the DLPFC did not differ between the fearfulness groups. Finally, GABA+ concentration predicted BOLD responses during the task in a cluster that included brain areas typically associated with the experience of fear, among them part of the insula. Similarly, GABA+ in the DLPFC predicted fear-related BOLD responses in the frontal cortex, posterior to the spectroscopy voxel.

4.5.1 The relationship between fearfulness and BOLD signals

Our fear provocation paradigm was designed to elicit fear-specific (pictures of spiders vs. control animals) and fear-unspecific (negative vs. neutral IAPS pictures) BOLD responses. In line with previous results (Caseras et al., 2013; Lueken et al., 2011; Straube et al., 2006a), our paradigm succeeded in eliciting BOLD responses in the anterior insula during both fear-specific and fear-unspecific conditions, along with responses in cingulate cortex, cerebellum and regions within the frontal, temporal and occipital cortices; only

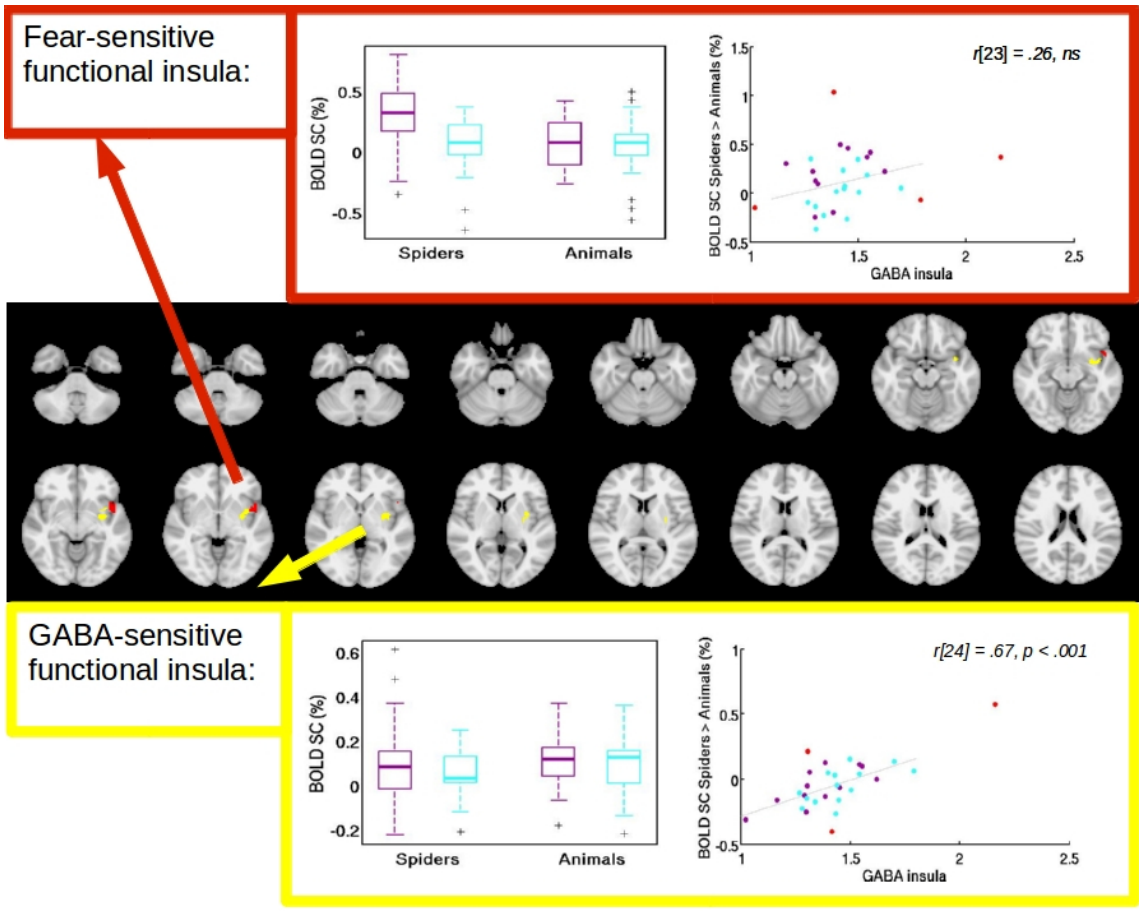

Figure 4.5: Two clusters within the spectroscopy voxel, both from contrast $SPIDERS > ANIMALS$, red: group result $SPIDERS > ANIMALS$, yellow: GABA-sensitive cluster. Median %SC from clusters were extracted. Data from participants in the high fear group is shown in purple, data from the low fear group in blue. Red dots in the scatter plots indicate participants that were identified as outliers for calculating the correlation.

the fear-unspecific images brought significant responses in the amygdala, though. Group differences were only observed for the fear-specific BOLD responses, with high fearful participants showing greater responses in cerebellum, ACC and left anterior insula. These results suggest that fearfulness only influences fear-specific, but not fear-unspecific, BOLD responses. This effect is also reflected at a behavioural level, since we only found group differences in the rating of spider pictures but not negative IAPS pictures. This finding somehow opposes previous results suggesting general increased responses in amygdala and insula to negative stimulation in anxiety prone participants (Stein et al., 2007) or in phobic participants to general negative - opposite to phobia related - stimulation (Schienle et al., 2005). However, the two groups in our sample differed more markedly in their scores to the SPQ than to the FSS-II, which could explain why group differences were also more substantial regarding the fear-specific than fear-unspecific stimulation. In any case, whether brain responses to fear related stimuli are qualitatively similar to responses to generally negative stimulation remains unresolved and would require further investigation.

We did, however, find stronger BOLD signals for the low fear group than for the high fear group in the posterior cingulate. The posterior cingulate is often investigated in the context of the default-mode and task-negative network (Greicius et al., 2003; Raichle et al., 2001). Task-related deactivation of this area was also the case in this study. The group difference we found was caused by less deactivation during presentation of negative vs. neutral IAPS pictures, in participants with low fearfulness only. We speculate that this might indicate that low fearful participants are using an emotion regulation strategy that involves upregulating their default mode network - Goldin et al. (2008) found the BOLD in the posterior cingulate associated with reappraisal - however, this needs further investigation.

Previous studies using clinical samples, such as patients with PTSD, have shown a GABA+ deficit in high fearful participants (Goddard et al., 2001; Ham et al., 2007; Rosso et al., 2014); however, we did not find this to be the case in our non-clinical sample. It is possible that reduced GABA+ levels are only a marker in clinical populations; although it could also be possible that lower GABA+ concentration is a clinical consequence or the disorder rather than a premorbid factor. In any case, our results suggest no association between GABA+ concentration in the insula or DLPFC and individual differences in fearfulness.

Recently, a few studies have suggested that GABA+ may be subject to changes induced by experimental manipulation, such as stress induction (Hasler et al., 2010). Also the

activation of a brain region can have an influence on later measured GABA+ levels, as shown by Michels et al. (2012). These findings indicate that GABA+ levels are not completely stable. In our scanning protocol, we performed the GABA+ spectroscopy at the end of the session. We cannot rule out that the functional paradigm or potentially even the scanning situation itself altered the GABA+ levels in our participants.

4.5.2 The relationship between GABA+ and fear-related BOLD signals

Even though the BOLD %SC obtained in the insula and DLPFC in response to the fear-specific stimuli did not correlate with GABA+ concentration, entering insular GABA+ as a regressor of interest in the higher level analysis of the fear provocation paradigm revealed a cluster covering parts of the insula, amygdala and striatum. Entering prefrontal GABA+ revealed a cluster in the frontal cortex, posterior to the spectroscopy voxel. Unlike most previous studies (Donahue et al., 2010; Muthukumaraswamy et al., 2009, 2012; Northoff et al., 2007), though, we found a positive rather than a negative correlation between BOLD and GABA+, both for the GABA+ regressor in the insula and in the DLPFC. This difference in the direction of the relationship could be explained by several factors: A) the voxel from which GABA+ concentration was extracted. Even though interneurons and inhibition are present throughout the cortex, their importance and role might differ from region to region. To our knowledge, there is no study investigating BOLD-GABA+ correlation in the DLPFC, and only one previous study using the insula (Wiebking et al., 2014). Like the present results, this study reported a positive correlation between both measures, which could indicate that GABA-BOLD relationship depends on the brain area investigated. B) our BOLD measure results from the contrast between two active conditions rather than the comparison to fixation cross baseline. We did match the stimuli in our conditions with regard to a number of features that could influence the BOLD response, in order to be left with the emotional aspect when contrasting the conditions. Even though there are unneglectable problems with setting up contrasts (Poldrack, 2010), BOLD responses compared to baseline could be contaminated by factors such as level of visual processing (e.g. how much attention to detail do participants pay), strategies to solve the simple task, and also more physiological factors such as vascular reactivity - factors that should play a reduced role for a contrast. This in mind, previous studies did show a negative correlation between GABA+ and BOLD, but the factors driving that correlation are not yet resolved.

To test whether looking at the contrast vs. main effect makes a difference with regard

to the effect of GABA, we calculated the correlation between GABA+ and BOLD for all four main effects. It turned out that there are no correlations in any but the $ANIMAL$ condition, and the correlation is negative (see Supplement Table C.1). Similarly, in the frontal cluster in which GABA in the DLPFC predicted the BOLD %SC for the contrast $SPIDERS > ANIMALS$ (with $r[25] = .74$, $p < .0001$), the correlation for $SPIDERS > fixation$ was not significant (r[26] = .06, ns), and a negative correlation between GABA and %SC for $ANIMALS > fixation$ was found ($r[26] = -.46$, $p = .02$). This suggests that the correlation between BOLD and GABA+ depends on the nature of the BOLD signal investigated. The BOLD signal in the anterior insula, which was found to be influenced by levels of fearfulness, was not influenced by GABA+ levels. The BOLD signal in the cluster sensitive to GABA+ was not influenced by fearfulness, and GABA+ was only associated with BOLD signal during the presentation of animal pictures but not fear-inducing spider pictures or IAPS images. It is possible that GABA-related processing plays different roles dependent on stimuli, and that the BOLD signal during the presentation of negatively valenced (Spiders and negative IAPS) or complex (IAPS pictures as compared to the pictures of animals) is more strongly influenced by other factors than GABA. The previous studies who demonstrated the negative correlation between GABA+ and BOLD used simple visual stimulus material without complex or emotional content to be processed (Donahue et al., 2010; Muthukumaraswamy et al., 2009, 2012), except for Northoff et al. (2007) using emotional faces, but looking at negative BOLD. The pictures of our control animals are also rather simple stimuli.

4.5.3 Limitations and future directions

Designing our paradigm, we aimed for two contrasts comparing the BOLD signal during the processing of negatively valenced images to the BOLD signal upon neutral stimuli. Participants were asked to rate the images after the scanning session, and as expected negative IAPS pictures were rated as significantly more negative than neutral IAPS pictures, while spider pictures were rated as significantly more negative than pictures of other animals. However, both neutral conditions (neutral IAPS pictures and control animal pictures) were rated as slightly positive with a median of around 7 on a scale from 1-9. Even though this indicates that our neutral conditions were in fact slightly positive conditions, we argue that the positive ratings are result of a contrast effect. In other words, because we did not include positive stimuli in the paradigm, participants might have tried to make use of the whole rating scale which resulted in positive ratings for the neutral stimuli. We

did select the control stimuli based on ratings in a previous study (Lang et al., 2008) and on a pilot we conducted, suggesting that the pictures were in fact neutral. To make sure neutral pictures are actually perceived as neutral, for future studies, it might therefore be an advantage to include positive stimuli, irrespective of the research question.

One limitation of this study, common to all research using MRS, is the unspecificity of the MRS signal with regard to the region of interest, but also to the origin of the signal. Due to low signal-to-noise ratio, MRS has very low spatial resolution as compared to the fMRI sequence. For example, the insula voxel was 25 x 30 x 40 mm, and covered areas surrounding the insula, such as frontal areas and the putamen. Also, spatial overlap of the spectroscopy voxel between participants is not exact. This means, we acquired GABA+ concentration from slightly different regions in each participant. Furthermore, within the measured regions, the origins of the GABA+ signal are not clear. The concentration measure is unspecific to whether GABA is intra- or extracellular, so it does not necessarily give an indication of GABA transmission. Low GABA concentration could either indicate a less established interneuron network, with less interneurons, or less connected interneurons. On the other hand, GABA concentration could be a state marker of interneuronal activity or current GABA availability. Last but not least, the GABA+ peak in the spectrum is also influenced by macromolecules (Henry et al., 2001), however, studies such as this investigating links between behaviour and GABA are less likely to be driven my the macromolecule signal than those comparing GABA+ levels patients and control groups (Mullins et al., 2014).

4.5.4 Conclusions

We found fear-related BOLD responses brain regions that have been previously associated with emotion processing. BOLD responses in the insula were stronger for participants with high fear than for participants with low fear, but we did not find any group differences in GABA+ concentration. We found a positive correlation between fear-related BOLD and insular GABA+ concentration in a cluster including insula, putamen and amygdala, and a positive correlation between fear-related BOLD and prefrontal GABA+ in a frontal cluster. This was in contrast to our expectations, and suggests that whether a positive vs. negative relationship between GABA+ and BOLD is found depends on the investigated region and the nature of the contrast.

4.5.5 Next steps

In this chapter we looked at the relationship between fearfulness, GABA+ and fear-related BOLD responses. We found stronger fear-related BOLD responses for participants with high fearfulness in a number of regions associated with emotion processing. However, BOLD is an indirect measure of neural activity and can be influenced by non-neuronal factors such as breathing and heart rate. Because we used a paradigm confronting fearful participants with their fears, it is possible that the emotional stimuli elicit physiological reactions that influence the BOLD response and might be a confound for our analyses. In the next chapter we assess what effect physiological noise correction had on our data and whether physiological reactions to the task might explain group differences in fear-related BOLD responses.

Chapter 5

Exploring the role of physiological reactions and physiological noise correction in fear-related BOLD responses

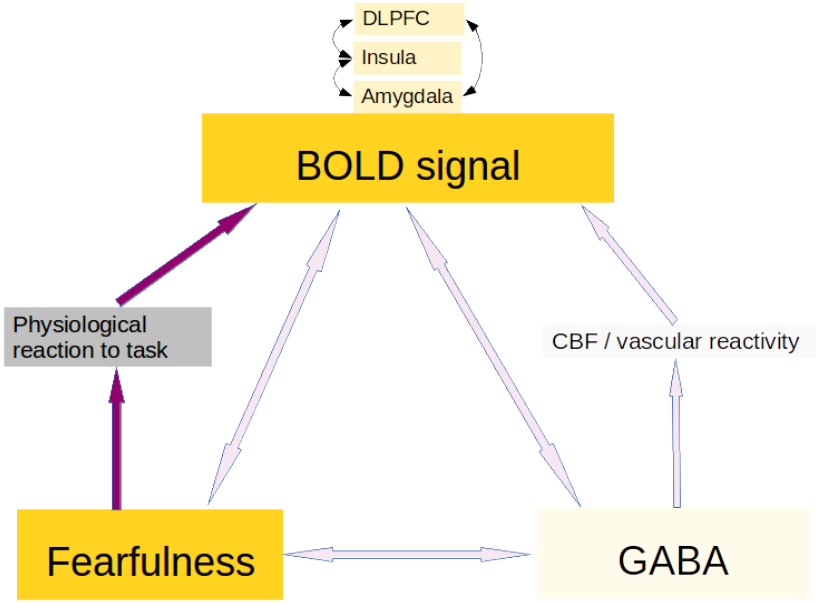

5.1 Abstract

The BOLD signal is not only influenced by neural activation but also by respiration and the cardiac cycle. Using an emotion task, we expected these physiological parameters to covary with the stimuli. The aim of this study was to quantify the physiological task responses and to explore the influence of physiological noise correction on the BOLD signal changes and the model fit. Furthermore, we investigated whether differences between fearfulness groups in physiological task reactions can explain the group differences in insula activity.

We found changes in HR, end-tidal CO_2, end-tidal O_2 and RVT during stimulus presentation and an influence of fearfulness on these changes. Comparing the results of the emotion task with vs. without physiological noise correction we demonstrate that correction leads to a decrease in model fit and a decrease in occipital activation when stimulus conditions were contrasted to fixation cross baseline. The amount of physiological task responses could significantly predict BOLD responses in the anterior insula but could not explain the difference between fearful and not fearful participants.

We demonstrated that physiological variation is confounded with the task, and that applying physiological noise correction makes the analysis more conservative. We concluded that the previously reported fearfulness group differences in anterior insula activation are not explained by differences in physiological task-responses.

5.2 Introduction

BOLD as an indirect measure of brain activation is not only influenced by neuronal changes but also by changes in respiration (Birn et al., 2008), the cardiac cycle (Chang et al., 2009), and fluctuation in CO_2 (Wise et al., 2004). If these physiological fluctuations are confounded with the task, it can be challenging to separate the physiological and neuronal sources of the BOLD signal (Birn et al., 2009). Since we are primarily interested in neuronally driven BOLD fluctuations, we performed physiological noise correction in the original analysis of the data (Chapter 4). But particularly when it comes to emotion tasks, some of the physiological parameters are likely to covary with the stimulus timecourse. Our paradigm was designed to elicit fear responses, which have been shown to induce cardiac acceleration, increased respiration and decreased CO_2 levels (Kreibig, 2010). Even though the physiological response functions are not identical to the HRF (Birn et al., 2009), it is still possible that the physiological noise correction removes some of the task-related BOLD responses.

A number of studies have reported differential activation between participants experiencing fear and participants not experiencing fear, in regions such as the amygdala, insula, anterior cingulate, fusiform and prefrontal aras (Caseras et al., 2010; Dilger et al., 2003; Klumpp et al., 2010; Lueken et al., 2011; Schienle et al., 2005; Stein et al., 2002; Straube et al., 2004, 2006a,b; Wendt et al., 2008). These studies have not performed physiological noise correction, so it cannot be excluded that some of these group differences can be attributed to group differences in physiological reactions to the task. Applying physiological noise correction, we found that highly fearful participants had higher BOLD responses in the insula, ACC and cerebellum. But it is not clear whether physiological noise correction prevented from finding additional group differences that might be influenced by group differences in physiological reactions, or whether it provided more power to find differences by cleaning up noise.

The insula is associated with processing information coming from bodily responses to guide attention (e.g. Craig, 2009; Lindquist et al., 2012). It is therefore possible that the amount of physiological reactions to the task influences the amount of processing necessary in the insula, and that the relationship between fearfulness and BOLD responses in insula is explained by higher physiological task responses in highly fearful participants. If this was the case, a correlation between physiological task responses and insula activation might be observed even after cleaning physiological noise.

One aim of this chapter is to explore what physiological noise correction does to fMRI

data obtained during an emotion task. We first estimate the physiological changes induced by the task. We then analyse the data without physiological noise correction, and compare the results to what we found with the corrected dataset, with regard to the activation patterns, the model fit, and the extracted BOLD percent signal changes. The second aim of this chapter was to test whether physiological task responses influences activation in the insula, and whether this relationship can explain differences between fearfulness groups in the anterior insula.

5.3 Methods

Methods are the same as in Chapter 4 with the following amendments and extensions:

5.3.1 Physiological parameter analysis

We investigated the relationship between the stimulus paradigm and the recorded physiological parameters to uncover potential effects of the task on the volunteers physiology. For each participant, HR, RVT, CO_2 and O_2 timecourses were demeaned, and then an average value was extracted for each stimulus condition. The average over baseline period (fixation cross) was substracted from the resulting value to get the change from baseline; then the change from baseline was divided by the baseline average to get the percent change from baseline. The investigated parameters are not fast changing signals (such as the parameters used for RETROICOR correction, Glover et al., 2000), which makes it possible to average over longer periods of time. Due to problems with acquisition or noise in the recordings, we did not have any physiological data from three participants. Additionally, we were not able to analyse CO_2 and O_2 in one participant, and cardiovascular and respiratory traces in five participants. These left 36 participants with intact physiological noise recordings. For analyses that involve group comparisons, 6 participants were excluded additionally due to problems with group assignment (see Chapter 4), leaving 15 participant in each of the two groups. To investigate the effects of stimulus category and fearfulness, mixed model ANOVAs were calculated using the Matlab function *mixed_between_anova* (www.mathworks.co.uk/matlabcentral/fileexchange/27080-mixed-betweenwithin-subjects-anova/content/mixed_between_within_anova.m).

5.3.2 fMRI data analysis

We analysed the fMRI dataset twice, once performing physiological noise correction, and once leaving out this step. Everything else was done exactly the same for both (the

corrected and the uncorrected) datasets. For this analysis, the same participants (N = 37) as in Chapter 4 were used (for participants with incomplete physiological recordings physiological noise correction was performed using the remaining parameters).

ROIs

Functional ROIs were defined based on the findings presented in Chapter 4: a fear-specific ROI (based on the whole-group results for the contrast $SPIDERS > ANIMALS$, masked with the insula spectroscopy voxel), a GABA-sensitive ROI (based on the whole-group results for the regressor insula GABA on the contrast $SPIDERS > ANIMALS$, masked with the insula spectroscopy voxel), and a fear-unspecific ROI (based on the whole-group results for the contrast $IAPSnegative > IAPSneutral$, masked with the insula spectroscopy voxel).

Additionally, anatomically defined ROIs in the insula and amygdala were used from the WFU-PickAtlas (Version 3.0.4, Wake Forest University, School of Medicine, Winston-Salem, North Carolina, www.ansir.wfubmc.edu).

5.3.3 Estimation of the model fit

The coefficient of determination (R^2) was used as an estimation of how well the applied model fits the data. This measure gives an indication of the amount of variance in the timeseries explained by the applied model. For each of the analysis methods (uncorrected vs. corrected) and each participant, an R^2 map was calculated by applying the following equation to each voxel:

$$\frac{MSS_{time-series} - MSS_{residuals}}{MSS_{time-series}}$$

, whereby the mean sum of squares (MSS) was calculated by squaring and temporally summing over the demeaned time series and residual time series, respectively. For each participant, the median R^2 was extracted from our regions of interest. Participants for who physiological recordings were incomplete were included in this analysis (physiological noise correction was performed using the remaining parameters), bringing the total number of participants included in the analysis to 41.

5.3.4 Correlating physiological responses with BOLD responses

In order to investigate the relationship between physiological task responses and BOLD %SC, we used the % changes from baseline during the $SPIDERS$ condition in HR,

RVT, CO_2 and O_2 (calculated as described above) as regressors in a linear model. In order to maximize the sample size, missing values were replaced with the mean of the remaining sample. Group membership was also included in the model, to see whether fearfulness has an effect on BOLD responses even when physiological task reactions are controlled for. The BOLD %SC for the contrast $SPIDERS > fixation$ in the fear-related ROI in the anterior insula was used as the dependent variable, and the linear regression (Matlab function *regstats*) was run for both, the corrected and the uncorrected dataset. Additionally, the cluster in the ACC, in which group differences were observed for the contrast $SPIDERS > ANIMALS$ (see Chapter 4) was used as a control region.

5.4 Results

5.4.1 Physiological responses to the task

We investigated the physiological reactions to the task with four physiological parameters, HR, RVT, end-tidal O_2 and end-tidal CO_2 (see Figure 5.1). In order see whether the parameters changed upon stimulus presentation, we calculated the percentage change to baseline for each stimulus category and performed a one-sample t-test, comparing to 0. We found that HR significantly decreases during the presentation of $IAPSnegative$ pictures (t[36] = -6.6, $p < .0001$), $IAPSneutral$ pictures (t[36] = -6.6, $p < .0001$), and $ANIMALS$ pictures (t[36] = -6.7, $p < .0001$), but not during the presentation of $SPIDERS$ pictures. Furthermore, end-tidal O_2 increased during the presentation of $SPIDERS$ pictures, (t[40] = 2.0, $p = .049$) but decreased during $ANIMALS$ pictures (t[40] = -3.0, $p = .005$). No other significant results were found.

Due to possible interactions with fearfulness, we additionally calculated mixed model ANOVAS, including the four stimulus conditions, and the two fearfulness groups (note that the sample size for each calculation decreased due to exclusion of six additional participants for group comparisons). For HR, there was no significiant interaction between condition and fearfulness (F(3,87) = 1.3, ns), but a significant main effect for stimulus condition (F(3,87) = 8.0, $p < .0001$). This was caused by a significant decrease of HR in all the stimulus conditions but the $SPIDERS$ condition (as reported above), independent of fearfulness. For the RVT and CO_2, we found significant and for O_2 a marginally significant interaction between condition and fearfulness group (RVT: F(3,87) = 7.85, $p = .0001$; O_2: F(3,99) = 2.7, $p = .05$, CO_2: F(3,99) = 4.5, $p = .005$). 2-sample t-tests revealed that this

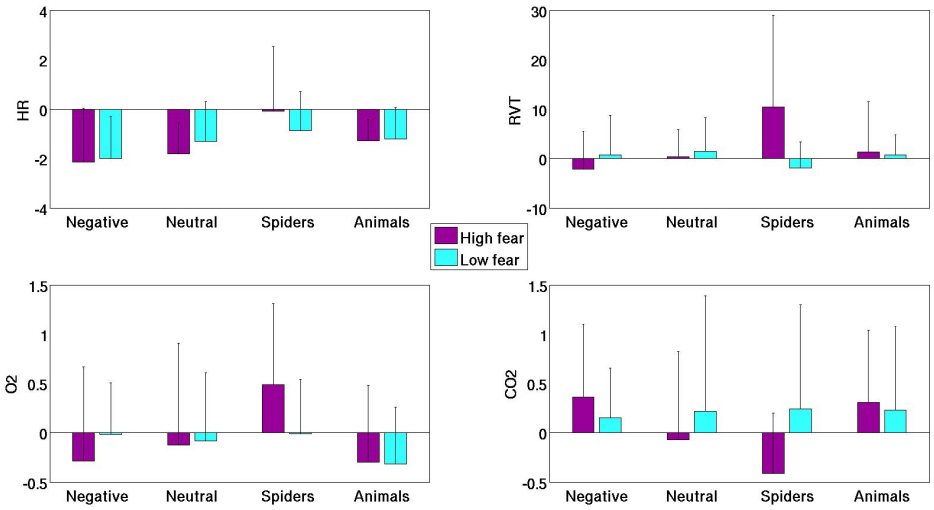

Figure 5.1: Task-related physiological changes. For each stimulus category, the average was calculated over the duration of the stimulus, and averaged over all stimuli of this category. Means and standard deviations of the percent change from baseline are plotted for both groups separately, and the four considered physiological parameters: HR (top left), RVT (top right), end-tidal O_2 (bottom left) and end-tidal CO_2 (bottom right).

Table 5.1: Effect of physiological noise correction on the model fit. For each of the regions of interest, the median (iqr) R^2 are shown, and the z and p values from a Wilcoxon signed rank test. Data from 41 participants was included in this analysis.

ROI	uncorrected	corrected	t-test
Left amygdala	.17 (.11)	.13 (.07)	$z[52] = 5.0$, $p < .0001$
Right amygdala	.16 (.13)	.12 (.06)	$z[52] = 5.4$, $p < .0001$
Left insula	.15 (.11)	.13 (.06)	$z[52] = 5.5$, $p < .0001$
Right insula	.15 (.10)	.12 (.07)	$z[52] = 5.5$, $p < .0001$
Fear-specific	.15 (.14)	.12 (.08)	$z[52] = 5.5$, $p < .0001$
GABA-sensitive	.14 (.08)	.10 (.06)	$z[52] = 5.3$, $p < .0001$
Fear-unspecific	.13 (.10)	.11 (.05)	$z[52] = 5.5$, $p < .0001$

interactions were caused by significant group differences for only the *SPIDER* condition (RVT: $t[28] = 2.4$, $p = .03$; O_2: $t[28] = 2.1$, $p = .049$; CO_2: $t[28] = -2.2$, $p = .04$).

5.4.2 Physiological noise correction and its effect on model fit

We extracted the median model fit (R^2) from each person and each region of interest. The model fit is an indicator of how well the observed BOLD responses (before and after physiological noise correction) fit the stimulus paradigm. In all the regions, the model fit was significantly higher in the uncorrected data set than in the corrected data set (see Table 5.1).

Table 5.2: Higher-level whole-brain analysis for the contrast $SPIDERS > ANIMALS$. Results are presented for the whole group, both groups separately, and group comparisons. This analysis was done using the dataset uncorrected for physiological noise.

Group mean (N = 37)			
Size	Peak (x,y,z)	Peak Z	Location
4431	-16, 38, 36	4.02	Superior frontal gyrus
2137	-10, -68, 32	4.11	Posterior cingulate
1546	-58, -40, 24	4.17	Left angular / supramarginal
993	46, -20, -22	3.57	Right temporal fusiform
894	34, -68, -34	3.38	Right cerebellum
745	50, 10, -6	3.76	Right insula
740	-36, -24, -8	3.44	Left temporal
626	-46, 6, -8	4.09	Left insula / temporal
High fear (N = 19)			
Size	Peak (x,y,z)	Peak Z	Location
2150	46, -64, -36	3.7	Cerebellum
1401	0, 28, 28	4.02	ACC
752	46, -20, -22	3.74	Inferior temporal
695	-28, 44, 36	3.69	Left frontal pole
548	50, 6, 4	3.67	Right insula / IFG
493	-46, 6, -8	4.08	Left insula / IFG
Low fear (N = 18)			
Size	Peak (x,y,z)	Peak Z	Location
1634	-4, -48, 22	3.6	Posterior cingulate
988	-54, -58, 34	3.79	Left angular gyrus
879	-16, 40, 36	3.38	Left frontal pole
486	58, -40, 30	3.22	Right angular gyrus
High fear (N = 19) > low fear (N = 18)			
Size	Peak (x,y,z)	Peak Z	Location
1122	-24, -78, -26	3.48	Cerebellum
Low fear (N = 18) > high fear (N = 19)			
no clusters			

5.4.3 Physiological noise correction and its effect on emotion-related BOLD responses

We ran all the analyses we had run with the physiological noise corrected set with the uncorrected set. Results of the whole-brain analysis for the contrasts $SPIDERS > ANIMALS$ and $IAPSnegative > IAPSneutral$ are displayed in Tables 5.2 and 5.3 and Figures 5.2 and 5.3 (compare to Tables 4.3 and 4.4 in Chapter 4 and Figures 3.1 and 3.2 in Chapter 3).

We also computed a whole-brain paired t-test on the uncorrected and corrected data sets to have a direct statistical comparison between them. Physiological noise correction did not influence the contrast ($SPIDERS > ANIMALS$, $IAPSnegative > IAPSneutral$) images, but significantly reduced occipital activation for all comparisons to fixation cross baseline (see Supplement Figure D.1).

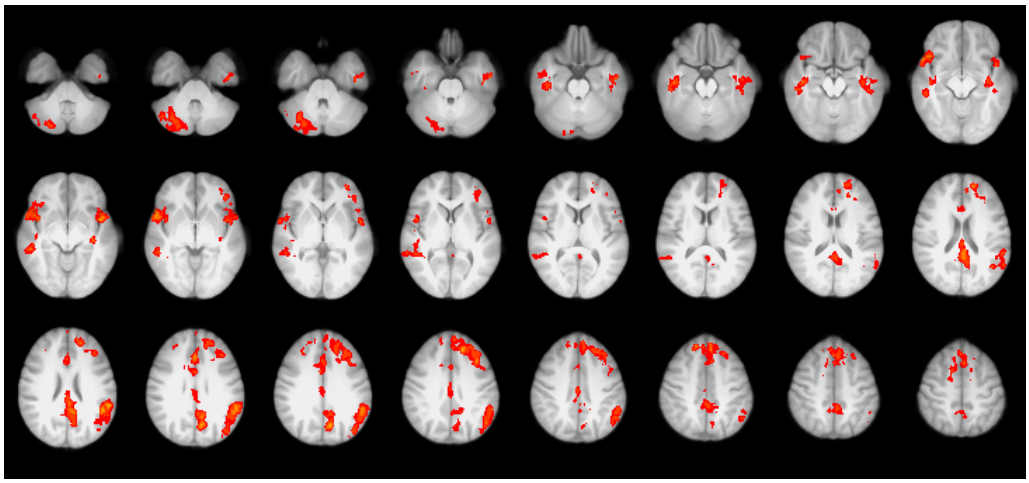

Figure 5.2: Group effect for the contrast $SPIDERS > ANIMALS$ (N = 37). The statistical threshold was set to Z > 2.3 and corrected cluster threshold of P < .05. Image displayed in radiological convention.

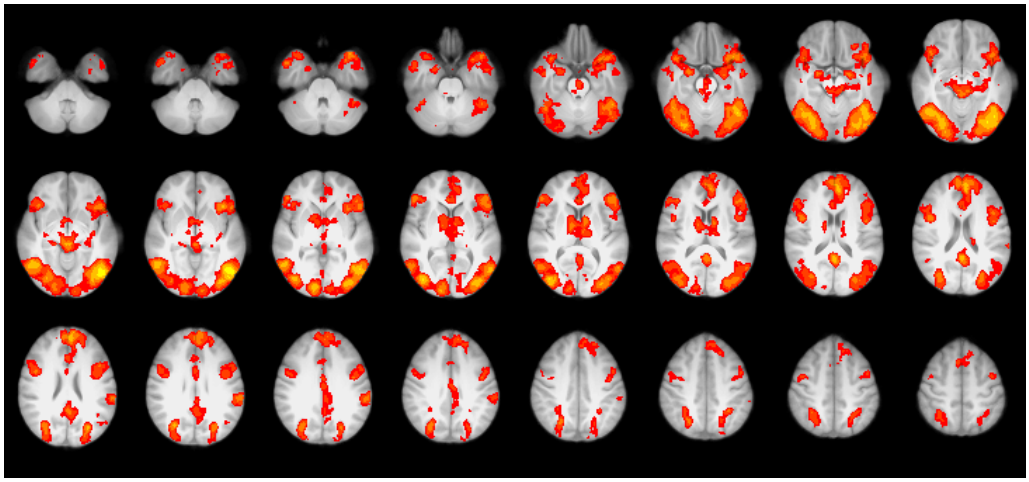

Figure 5.3: Group effect for the contrast $IAPSnegative > IAPSneutral$ (N = 37). The statistical threshold was set to Z > 2.3 and corrected cluster threshold of P < .05. Image displayed in radiological convention.

Influence of physiological noise correction on regionally extracted BOLD % SC

To check what influence physiological noise correction had on regionally extracted BOLD %SC values, we took the median %SC for each person and each data set. Data for the main effect $SPIDERS$ are shown in Table 5.4. For none of the investigated regions significant differences between the two analysis approaches could be found, and correlation coefficients between the two measures were very high.

Is amount of physiological reaction correlated to BOLD %SC?

In order to test whether the physiological task reactions can explain variance of the BOLD responses, we calculated a multiple regression, with the BOLD %SC upon presentation of

Table 5.3: Higher-level whole-brain analysis for the contrast $IAPSnegative > IAPSneutral$. Results are presented for the whole group, both groups separately, and group comparisons. This analysis was done using the dataset uncorrected for physiological noise.

Group mean (N = 37)			
Size	Peak (x,y,z)	Peak Z	Location
38470	-48, -68, -4	6.02	Widespread
499	-62, -30, 26	4.34	Left supramarginal
High fear (N = 19)			
Size	Peak (x,y,z)	Peak Z	Location
4860	40, -76, 2	4.85	Right occipital
4826	-50, -68, -4	4.87	Left occipital
1686	-6, 44, 18	4.27	ACC
1422	-54, 24, 4	4.18	Left IFG, also insula
657	42, 16, -18	4.09	Right insula, OFC
449	-44, -2, 36	3.5	Middle frontal
Low fear (N = 18)			
Size	Peak (x,y,z)	Peak Z	Location
15324	-48, -68, -6	5.67	Occipital and everywhere
10291	-38, 22, -32	4.61	OFC, frontal pole, insula
2897	0, 56, 24	4.85	Frontal pole
2271	0, -50, 20	5.06	Posterior cingulate
471	-66, -32, 26	4.27	Left supramarginal
High fear (N = 19) > low fear (N = 18)			
no clusters			
Low fear (N = 18) > high fear (N = 19)			
no clusters			

the $SPIDERS$ images (vs. fixation cross baseline) as dependent variable, and with the average changes from baseline during the $SPIDERS$ images in HR, RVT, CO_2 and O_2 as predictors. We also included group membership as a predictor to see if it can explain variance in the BOLD responses independently of the physiological reactions.

Using the uncorrected data set, 40% of the variance of BOLD %SC in the functional anterior insula could be explained by the physiological regressors and group membership ($R^2_{adjusted}$ = .40, $F(5,31) = 5.84$, $p < .001$), with O_2 (t = -2.2, p = .04), RVT (t = 2.6, p = .01) and group (t = -2.4, p = .02) significantly contributing to the model. CO_2 (t = 0.33, p = .75) or HR (t = 0.84, p = .41) did not have an independent effect on the

Table 5.4: Effect of physiological noise correaction on region-wise extracted BOLD %SC values, for the main effect $SPIDERS$. Median (Iqr.) values are shown for the uncorrected and corrected dataset, and a paired t-test was performed to test for mean differences. Results are presented for the anatomical and functional ROIs. The fear-specific ROI refers to the cluster in the anterior insula derived from the group level activation for the $SPIDERS$ contrast. GABA-sensitive ROI refers to the cluster derived from the analysis including the GABA+ regressor for the $SPIDERS$ contrast. Fear-unspecific ROI refers to the cluster in the anterior insula derived from the group level activation for the $IAPS$ contrast.

Area	uncorrected	corrected	t-test	correlation
Left amygdala	0.27 (0.43)	0.21 (0.32)	$z[42] = 1.7$, $p = .08$	$r[41] = .79$, $p < .0001$
Right amygdala	0.15 (0.39)	0.14 (0.33)	$z[42] = 0.3$, $p = .74$	$r[41] = .80$, $p < .0001$
Left insula	0.03 (0.16)	0.03 (0.13)	$z[42] = 1.2$, $p = .24$	$r[41] = .91$, $p < .0001$
Right insula	-0.02 (0.16)	-0.02 (0.16)	$z[42] = -0.58$, $p = .56$	$r[41] = .86$, $p < .0001$
Fear-specific ROI (insula)	0.22 (0.50)	0.17 (0.33)	$z[42] = 1.7$, $p = .10$	$r[41] = .92$, $p < .0001$
GABA-sensitive ROI (insula)	0.10 (0.26)	0.04 (0.16)	$z[42] = 1.3$, $p = .18$	$r[41] = .86$, $p < .0001$
Fear-unspecific ROI (insula)	0.11 (0.27)	0.09 (0.31)	$z[42] = 1.4$, $p = .15$	$r[41] = .86$, $p < .0001$

BOLD responses. After physiological noise correction the model fit was lower ($R^2_{adjusted}$ = .26, $F(5,31) = 3.57$, $p = .001$) and only O_2 (t = -2.2, $p = .03$) and group had significant independent effects (t = -2.7, $p = .01$).

As a control region we used a functional cluster in the ACC in which group differences were also found. Before noise correction all regressors explained 53% of the variance ($R^2_{adjusted}$ = .53, $F(5,31) = 9.16$, $p < .0001$) with RVT ($t = 2.52$, $p = .02$), HR (t = 2.81, $p = .01$) and group (t = -2.7, $p = .01$) significantly contributing to the model, and no independent effects of CO_2 (t = -1.40, $p = .17$) or O_2 ($t = 0.52$, $p = .61$). After physiological noise correction, the model fit was lower ($R^2_{adjusted}$ = .20, $F(5,31) = 2.81$, p = .03), and only group had a significant effect (t = -2.25, $p = .03$; other results: O_2: t = -0.68, $p = .50$; CO_2: t = -0.59. $p = .56$; RVT: $t = 0.73$, $p = .47$; HR: $t = 1.20$, $p = .24$).

5.5 Discussion

The aim of this chapter was to explore the interplay between task, physiological responses to the task, and BOLD responses. We demonstrated task-related changes in physiological parameters, and an influence of fearfulness on these responses. Correcting for physiological variation decreased the model fit, and correlations between physiological task responses and task-related BOLD responses.

5.5.1 Task and physiological variation are confounded

We investigated the percent change to baseline of four physiological parameters during the emotion paradigm (HR, RVT, end-tidal CO_2, and end-tidal O_2), and the influence of stimulus category and individual differences in fearfulness. We found that during the presentation of the stimuli of all conditions apart from $SPIDERS$, HR significantly decreased compared to baseline. HR during the presentation of $SPIDERS$ pictures did not increase as compared to baseline, but was higher than during the other stimulus categories, which was also reported by Wendt et al. (2008). Additionally, end-tidal O_2 increased compared to baseline when pictures of $SPIDERS$ were presented, and decreased when pictures of $ANIMALS$ were presented.

Individual differences in fearfulness influenced physiological task responses but only for the $SPIDERS$ condition. In particular, highly fearful participants showed an increase in RVT, and end-tidal O_2 and a decrease in end-tidal CO_2 upon presentation of $SPIDERS$ pictures while participants with low fearfulness did not undergo such changes. The changes in physiological parameters in highly fearful participants indicate increased breathing.

This corresponds well to a review by Kreibig (2010), showing that fear responses go hand with increased RVT and decreased CO_2.

Our results do indeed show that physiological parameters covary with the task, and that fearfulness has an influence on the extent of covariation. Therefore, not considering physiological fluctuations during the analysis of the fMRI data, some of the significant activation might be attributable to changes in physiology rather than changes in neural activity. In this study we explored the effects of physiological noise correction on the results.

5.5.2 Correcting for physiological variation decreases model fit

We performed physiological noise correction by filtering out all the variance in the BOLD signal attributable to physiological variation, and estimated the model fit by calculating the R^2 over a variety of brain regions for the dataset before and after this correction. It turned out that by applying physiological noise correction the model fit in all the regarded regions went down significantly. This might seem counterintuitive at the first sight, since noise correction aims to reduce noise and improve data quality, leading to a better model fit. However, as already speculated, controlling for task-correlated physiological parameters might also affect task-related BOLD changes. In our case this reduced the ability of the model to explain variance in the BOLD signal.

To demonstrate that the decrease in model fit is directly related to physiological variation confounded with the task, we calculated a Spearman rank correlation between the amount of task-confoundedness (as determined by the coefficient determination a regression of the convolved physiological parameters onto the convolved stimulus timecourse; see also Chapter 2) and the decrease in model fit. A significant positive correlation ($r[31] = .49$, $p = .004$ [8 outliers excluded]) indicates that participants with high task-confounded physiology also suffered the greatest loss in model fit.

Generally, a high model fit is preferred, and physiological noise correction might seem to be disadvantageous. On the other hand, by reducing the model fit, the analysis becomes more conservative since BOLD changes that are related to both physiology and task are no longer detected and we can be more confident that the BOLD changes that remain are not simply the effect of physiological changes that cooccur with the stimulus onset, but more directly related to neuronal changes.

5.5.3 Influence of physiological noise correction on BOLD responses

Performing the analysis with both, the corrected and uncorrected dataset, we found that using the physiological noise corrected data, less significant voxels are found for the fear-unspecific contrast, and more significant voxels are found for the fear-specific contrast. The group difference between the high and low fearfulness groups for the fear-specific contrast in the anterior insula is only found when physiological noise correction is used. Since this could be just due to just-not or just meeting the threshold, we also directly compared the results obtained from both methods.

First, we extracted the median BOLD %SC for the uncorrected and physiological noise corrected data set for a number of anatomical and functional regions relevant to the study. It turned out that for the areas no significant difference between corrected and uncorrected BOLD signal was found, and the corrected and uncorrected values are highly correlated. We found a marginal significant decrease of %SC in the amygdala after performing physiological noise correction, indicating that some of the uncorrected BOLD signal might be affected by physiological task-responses.

Second, we conducted a whole brain analysis, comparing corrected and uncorrected data with a paired t-test to see whether physiological noise correction significantly alters the detected BOLD responses. This was not the case for the contrasts $SPIDERS > ANIMALS$ or $IAPSnegative > IAPSneutral$. However, for all the main effects (comparison to fixation cross baseline), the BOLD response in the physiological noise corrected data set was significantly decreased in posterior parts of the brain, mostly occipital areas. This indicates that the physiological noise correction removes some task-correlated BOLD variation but to a similar extent for all four conditions. Occipital areas have in fact previously be found to be particularly sensitive to respiratory changes (Birn et al., 2008, 2009). Even though the emotion contrasts (fear-specific and fear-unspecific) and regions most commonly associated with emotion processing, such as amygdala and insula, did not seem affected by physiological task confounds, our results still suggest that in some cases physiological noise correction might be a crucial step in analysis. This is because some studies do use contrasts to fixation cross baseline when comparing groups that differ in fear (e.g. Dilger et al., 2003; Straube et al., 2004). Also, occipital regions, in particular the fusiform gyrus, are sometimes subject of research in emotion studies (e.g. McCarthy et al., 1997; Hoffmann et al., 2012). Furthermore, it might be the case that our stimulus conditions (negative vs. neutral) did not differ enough with regard to the elicited physiological responses to elicit an effect of physiological noise correction on the stimulus contrasts. It is

therefore possible that the data from other paradigms or from more reactive participants is even more susceptible to physiological task reactions.

Even though we did not find an effect of physiological noise correction on the emotion contrasts, the results in group level analysis still differed between the corrected and uncorrected data. This indicates that either there was a small, not significant, contributing effect of physiological noise correction or that the differences in results just happened by chance. Another possibility is that the way physiological noise correction affects the data differs between participants. In the same area physiological noise correction might lead to a higher BOLD response - due to noise reduction and increase in power - in some participants, in other participants it might lead to a lower BOLD signal - if the initial BOLD signal was purely a result of task-confound physiological reactions. If this was the case, we would not find a significant difference between the two conditions the way we conducted the analysis, but physiological noise correction might still lead to different results by making the BOLD response a better indicator for neural activity. The regionally extracted %SC for our regions of interest did highly correlate with each other (between $r = .79$ and $r = .92$), indicating high similarity but not perfect correspondance between the values.

5.5.4 BOLD responses in the insula are related to processing of physiological reactions to the task

We postulated that physiological task responses might mediate the relationship between fearfulness and task-related BOLD responses. Results from this study suggest that this is not the case. The group differences in activation in the left anterior insula (fear-specific ROI) were only found using the physiological noise corrected data, and not found using the uncorrected dataset.

The physiological noise correction aimed to filter out task confounded physiological variance, and therefore, the amount of physiological task responses should not have an influence on BOLD responses anymore, unless the correction did not work or the BOLD %SC is additionally related to the processing of the physiological reactions. Our results described above suggest that physiological noise correction removed physiological variation from the BOLD timecourse that was confounded with the task. The physiological parameters were modelled using physiological response functions, so our correction should have removed effects that these physiological parameters directly had on the BOLD response. It has been suggested that the anterior insula is related to perception of one's own bodily state. So even after physiological noise correction, participants with strong physiological

reactions might have stronger insula activity related to the processing of these stimuli, which could explain the influence of fearfulness on these responses.

In order to see if this was the case, we tested whether the stimulus-induced changes in physiological parameters from baseline during presentation of *SPIDERS* could independently from each other explain variance of the BOLD signal during the *SPIDERS* condition in the fear-related ROI in the anterior insula, and whether group assignment still had an influence on the BOLD response after accounting for physiological task reactions. We found that before physiological noise correction was applied more variance between participants in BOLD responses could be explained by physiological task reactions (40 vs. 26 %). Importantly, both before and after physiological noise correction, group assignment had a significant contribution to the BOLD %SC, independent of the physiological parameters, indicating that the group differences are not simply a result of different strength of physiological task reactions. After physiological noise correction, the amount of task-related O_2 change could still explain variance in BOLD responses in the insula. We used the cluster in the ACC, in which we found group differences for the fear-specific contrast as a control region. Here, individual differences in physiological task reaction could explain variance in the BOLD response to spiders only before noise correction was applied. After, only the group had a significant independent contribution. This is an important control because it again supports that physiological noise correction removes task-confound physiological reactions.

5.5.5 Limitations and future directions

How well physiological noise correction works is hard to test. In Chapter 3 we found that for some of the BOLD signals of interest, physiologically corrected data showed higher repeatability. This gives a hint that the noise correction produced a more reliable signal, however, since the true stability of emotion-related BOLD responses is not known, we cannot be certain of that.

We only demonstrated an impact of physiological parameters on fear-induced BOLD responses when they were contrasted to fixation cross baseline and not when contrasted to a neutral condition. It would be interesting to see whether the influence of physiological changes to the task is higher in paradigms that trigger even stronger physiological reactions or in samples with even stronger fear.

5.5.6 Conclusions

We demonstrated that physiological variation recorded during the task is confounded with stimulus onset, and that physiological task-reactions are dependent on stimulus condition and individual differences in fearfulness. Correcting for physiological variation led to a decrease in model fit, making the analysis more conservative. On average, task-related BOLD responses (as compared to fixation cross baseline) were significantly lower in the occipital cortex, confirming previous evidence that the occipital cortex is particularly sensitive to changes in breathing. We also demonstrated that the extent to which the task elicited physiological changes correlated with the BOLD %SC in the left insula when data was not cleaned for physiological influences. Findings from this chapter suggest that physiological noise correction is an important step of preprocessing data of an emotion paradigm.

5.5.7 Next steps

We concluded that the influence of fearfulness on fear-related BOLD responses in the anterior insula that we reported in Chapter 4 was not mediated by physiological task responses. Other factors that can influence the BOLD response independent of neural activity are baseline cerebral blood flow and vascular reactivity. These measures can differ between individuals, possibly affecting the amplitude of the BOLD response. In the next chapter the effects of the two variables on task-related BOLD responses are investigated, and potential associations with fearfulness or GABA+ explored.

Chapter 6

The role of baseline cerebral blood flow and vascular reactivity measures in fear-related BOLD responses, and in the GABA-BOLD relationship

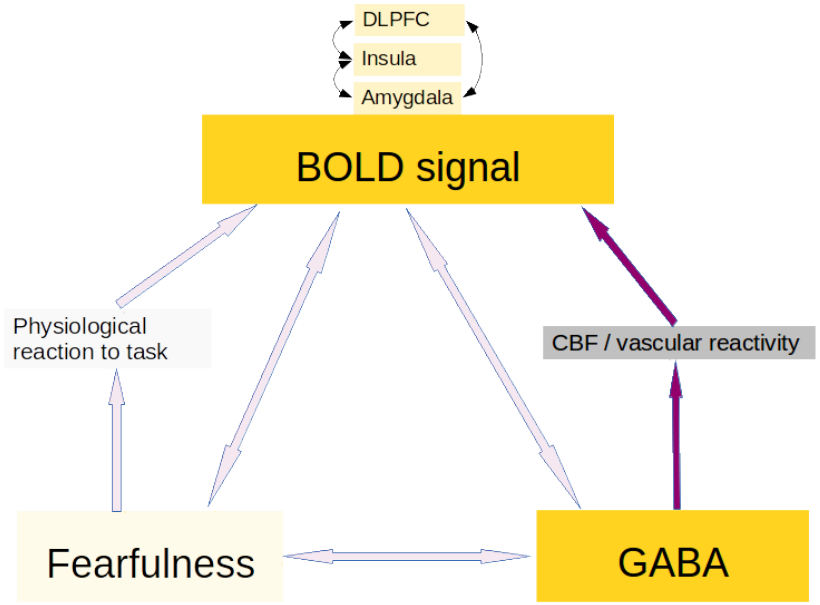

6.1 Abstract

Recently, we reported an influence of GABA and fearfulness on fear-related BOLD responses in the left insula and frontal cortex. The BOLD signal is only an indirect measure of neural activity, and also influenced by the vascular system. The aim of this study was to investigate the role of vascular reactivity and resting cerebral blood flow in the aforementioned correlations.

In addition to the emotion task and the spectroscopy scans, we assessed vascular reactivity through a breath-hold task, and CBF through ASL.

We found some, but not consistent, correlations between vascular reactivity, resting CBF and task-related BOLD responses. Fearfulness was not associated with either of the vascular measures. In the insula but not the DLPFC, GABA+ concentration was negatively correlated with vascular reactivity measures.

The results suggest an interplay between vascular factors, task-related BOLD responses and GABA, but did not indicate mediating effects in our previously presented results.

6.2 Introduction

In Chapter 4 we investigated the role of GABA and individual differences in fearfulness on fear-related BOLD responses, using a paradigm with fear-specific images ($SPIDERS$), fear-unspecific negative IAPS pictures ($IAPSnegative$) and respective control conditions ($ANIMALS$ and $IAPSneutral$). We found a cluster in the left insula for the fear-specific contrast $SPIDERS > ANIMALS$, and females with high fearfulness showed stronger BOLD responses in that region than females with low fearfulness. Insular GABA+ correlated with fear-specific BOLD responses in a cluster in the left insula, amygdala and putamen, and GABA+ in the DLPFC correlated with fear-related BOLD responses in a prefrontal cluster.

Interpreting these results, it is important to acknowledge that the nature of the BOLD response makes it an indirect measure of neural activity, and susceptible not only to neuronal changes but also to the state and to changes of the vascular system. In this study, we investigated two aspects of the vascular system: vascular reactivity (VR) and baseline cerebral blood flow (CBF). We wanted to see whether either of these factors might play a mediating role in the relationship between the BOLD signal and fearfulness or between the BOLD signal and GABA+.

Previous studies have demonstrated an influence of the reactivity of the cerebrovascular system on BOLD responses (for a review see Logothetis and Wandell 2004). One aspect of this vascular reactivity can be measured by changing the CO_2 content of the blood; CO_2 being a vasodilator. It has been shown that natural fluctuations in CO_2 during a resting state scan coincide with low frequency fluctuations in the BOLD signal (Wise et al., 2004). Furthermore, the BOLD signal following an increase in CO_2 in a region can explain up to 50 % of task-related variability in BOLD responses in that region (Biswal et al., 2007; Kannurpatti et al., 2012; Liu et al., 2013; Thomason et al., 2007). Neurotransmitters can have a modulatory role in vascular responses (Cauli and Hamel, 2010), but so far, noone has looked at the influence of GABA+ on vascular reactivity.

Changes in the BOLD signal reflect changes in CBF (Davis et al., 1998; Tak et al., 2014), and these changes might depend on the baseline CBF. A few studies investigated the influence of baseline CBF on BOLD responses by artifically up- or downregulating the CBF through CO_2 challenges. When baseline CBF is elevated, task-related BOLD responses become slower and weaker, while downregulating CBF has the opposite effect (Cohen et al., 2002; Sicard and Duong, 2005; Vazquez et al., 2006). These findings are based on intra-individual effects, but still indicate that inter-individual differences in baseline CBF

might explain some variance of BOLD responses. This was more directly tested by Liu et al. (2012) who measured resting CBF and task-related BOLD responses to emotional faces. Their findings indicate regional variation of the CBF-BOLD relationship, with some areas showing a positive correlation (e.g. prefrontal, fusiform, supramarginal areas) and some areas showing a negative correlation (e.g. left parietal areas).

Baseline CBF has been reported to be correlated with depression (Schlegel et al., 1989), gender and genes (El-Hage et al., 2013), borderline personality disorder (Wolf et al., 2012), and intelligence and creativity (Takeuchi et al., 2011). Furthermore, resting CBF can also be influenced by stress level (Wang et al., 2005), which could contribute to the CBF differences observed in clinical samples. Pharmacological studies found that GABA agonists diminishes blood flow in some areas, including amygdala, bilateral insula and orbito-frontal cortex, and increases blood flow in other areas, including the cingulate cortex (Franklin et al., 2011, 2012). Furthermore, a relationship between resting GABA concentration and CBF has previously been reported in the visual cortex (Donahue et al., 2010, 2014) and DLPFC (Michels et al., 2012). Krause et al. (2014) found a strong negative correlation between GABA in the ACC and cerebral blood flow over a number of brain regions.

In addition to our emotion paradigm and the spectroscopy scans, we included a breath-hold task (to estimate vascular reactivity) and an ASL aquisition (to estimate CBF) in our scanning protocol. The aim of this chapter was to investigated the relationship between these two measures with the task-related BOLD signal, GABA and fearfulness.

6.3 Methods

For group comparisons, the same participants were used as in Chapter 4. For analyses that did not compare the two fearfulness groups, the complete sample of 44 participants was considered. Eight participants had to be excluded for all analyses involving the breath-hold task due to a recorded CO_2 that suggested they were not performing the breath-hold task properly.

6.3.1 Breath-hold task

The breath-hold task was adapted from Murphy et al. (2011). During the task, breathing instructions were presented on the screen, guiding the participant through four cycles of breath-holding and recovery, each with four different phases: paced breathing (alternating breathing in and breathing out for 3 seconds each) for 18 seconds, end-expiration breath-

holding for 15 seconds, exhalation, and final recovery (spontaneous breathing with no breathing instructions) for 15 seconds. The task took less than four minutes to complete. End-expirational breath-hold was chosen because it has been shown that a shorter breath-hold duration is needed to obtain the same signal changes, and because the inspiration before a breath-hold varies between participant with regard to depth and intrathoracic pressure which introduces additional variability (Kastrup et al., 1998; Thomason and Glover, 2008).

6.3.2 Image acquisition

fMRI The participants underwent gradient-echo echo-planar imaging at 3 T (GE HDx MRI System) with a T_2* weighted imaging sequence (TR = 3s, TE = 35 ms, receive-only head coil). 78 volumes were acquired during the breath-hold task. The breath-hold task was presented using Presentation (Neurobehavioral Systems, Albany, CA) and rear-projected onto a screen behind the participant's head that was visible through a mirror mounted on the head RF coil. The orientation of the axial slices was parallel to the AC-PC line.

Arterial spin labelling (ASL) We positioned the labeling axis 74-94 mm below the AC-PC line (Aslan et al., 2010). Labelling duration and postlabeling delay were 1.5 s. A 3D pcASL technique acquired images using a fast spin echo acquisition with an interleaved stack of spirals (outward direction) readout and a centric ordering in the slice encoding direction. Each spiral arm included 512 sampling points in k-space and a total of 8 interleaves were acquired separately with a TR = 6 s and an echo train length of 60. The echo spacing was 7 ms and the effective echo time was 21 ms, and the bandwidth 125 kHz. The field of view (FOV) was 24 x 24 x 16 cm. Reconstruction was performed using a Fourier transform algorithm after the k-space data were regridded into 64 x 64 x 45 matrix. The total scan time was approximately 5 minutes. This method output three volumes (CBF map, mean subtraction volume and a calibration volume), as calculated from the data like in Xu et al. (2010). CBF maps were registered using FLIRT (Jenkinson and Smith, 2001). During the acquisition period, participants were presented with a black screen and instructed to keep their eyes open and to relax.

6.3.3 CO_2 recordings

During both scanning sessions end-tidal CO_2 and end-tidal O_2 were recorded using a nasal cannula attached to rapidly responding gas analysers (AEI Technologies, PA) to provide representative measures of arterial partial pressures of both gases.

6.3.4 Image data analysis and estimation of vascular reactivity

The acquired data were preprocessed using FEAT (FMRIB Expert Analysis Tool, v5.98, www.fmrib.ox.ac.uk/fsl, Oxford University, UK). Preprocessing steps before model fitting were applied to each participants timeseries, and included: highpass filtering of the data (100 seconds temporal cutoff), non-brain removal using BET (Smith, 2002), MCFLIRT motion correction (Jenkinson et al., 2002), spatial smoothing with a Gaussian kernel of full-width-half-maximum 5 mm and fieldmap-based EPI unwarping using PRELUDE + FUGUE (Jenkinson, 2003, 2004); for three people this was not performed due to problems during the acquisition of the fieldmaps. Functional images were registered using FLIRT (Jenkinson and Smith, 2001) in a first step to the structural image with 6 degrees of freedom, and in the second step to the Montreal Neurological Institute (MNI) space with 12 degrees of freedom and FNIRT non-linear (10 mm) warp (Andersson et al., 2007a,b). First-level analysis of the breath-hold task was performed using the recorded CO_2 trace including a temporal derivative due to a few participants with imperfect performance (Bright and Murphy, 2013a; Murphy et al., 2011). The residuals after model fitting were subtracted from the preprocessed time series in order to obtain a model-fitted timeseries. To estimate the BOLD %SC per unit change of CO_2, the range of this fitted BOLD timeseries was divided by the temporal mean and multiplied by 100 (to get %SC), and then divided by the range of the HRF convolved CO_2 trace (to get %SC / mmHg). In order to minimise the risk of outliers, a robust range was defined as the absolute difference between the 10th percentile and the 90th percentile (also see Chapter 10).

ROIs

Functional ROIs were defined based on the findings presented in Chapter 4: a fear-specific ROI in the left insula (based on the whole-group results for the contrast $SPIDERS > ANIMALS$, masked with the insula spectroscopy voxel), a fear-specific ROI in the left DLPFC (based on the whole-group results for the contrast $SPIDERS > ANIMALS$, masked with the DLPFC spectroscopy voxel), a GABA-sensitive ROI (based on the whole-group results for the regressor insula GABA+ on the contrast $SPIDERS > ANIMALS$,

masked with the insula spectroscopy voxel), a frontal gaba-sensitive ROI (based on the whole-group results for the regressor DLPFC GABA+ on the contrast $SPIDERS > ANIMALS$), a fear-unspecific ROI in the anterior insula (based on the whole-group results for the contrast $IAPSnegative > IAPSneutral$, masked with the insula spectroscopy voxel), and a fear-unspecific ROI in the left amygdala (based on the whole-group results for the contrast $IAPSnegative > IAPSneutral$, masked with the anatomical left amygdala).

Additionally, anatomically defined ROIs in the insula and amygdala were used from the WFU-PickAtlas (Version 3.0.4, Wake Forest University, School of Medicine, Winston-Salem, North Carolina, www.ansir.wfubmc.edu). For the analysis of vascular reactivity and CBF measures, these masks were additionally masked with a gray matter mask. For all ROIs, median vascular reactivity and CBF measures were extracted.

Statistical analysis

For all correlations we defined bivariate outliers based on the overall structure of the data using the Matlab toolbox provided by Pernet et al. (2012), and Pearson correlation coefficients were computed with the remaining data points. Due to outlier removal, sample size changed slightly for each reported correlation. We therefore report correlations with respective degrees of freedom in brackets.

6.4 Results

6.4.1 Breath-hold task evaluation

We calculated a vascular reactivity (BOLD %SC / change in mmHg CO_2) map for each person. The group average map is displayed in Figure 6.1. Average median over gray matter was 0.27 (Std. = 0.9) %SC / mmHg CO_2.

6.4.2 Perfusion map evaluation

We calculated a resting blood flow (ml/100g/min) map for each person. The group average map is displayed in Figure 6.1. Averages median CBF over gray matter was 48 (Std. = 5) ml/100g/min.

6.4.3 Correlation between vascular reactivity, resting CBF, and task-related BOLD responses

In none of investigated regions, CBF and VR were significantly correlated (see Table 6.1).

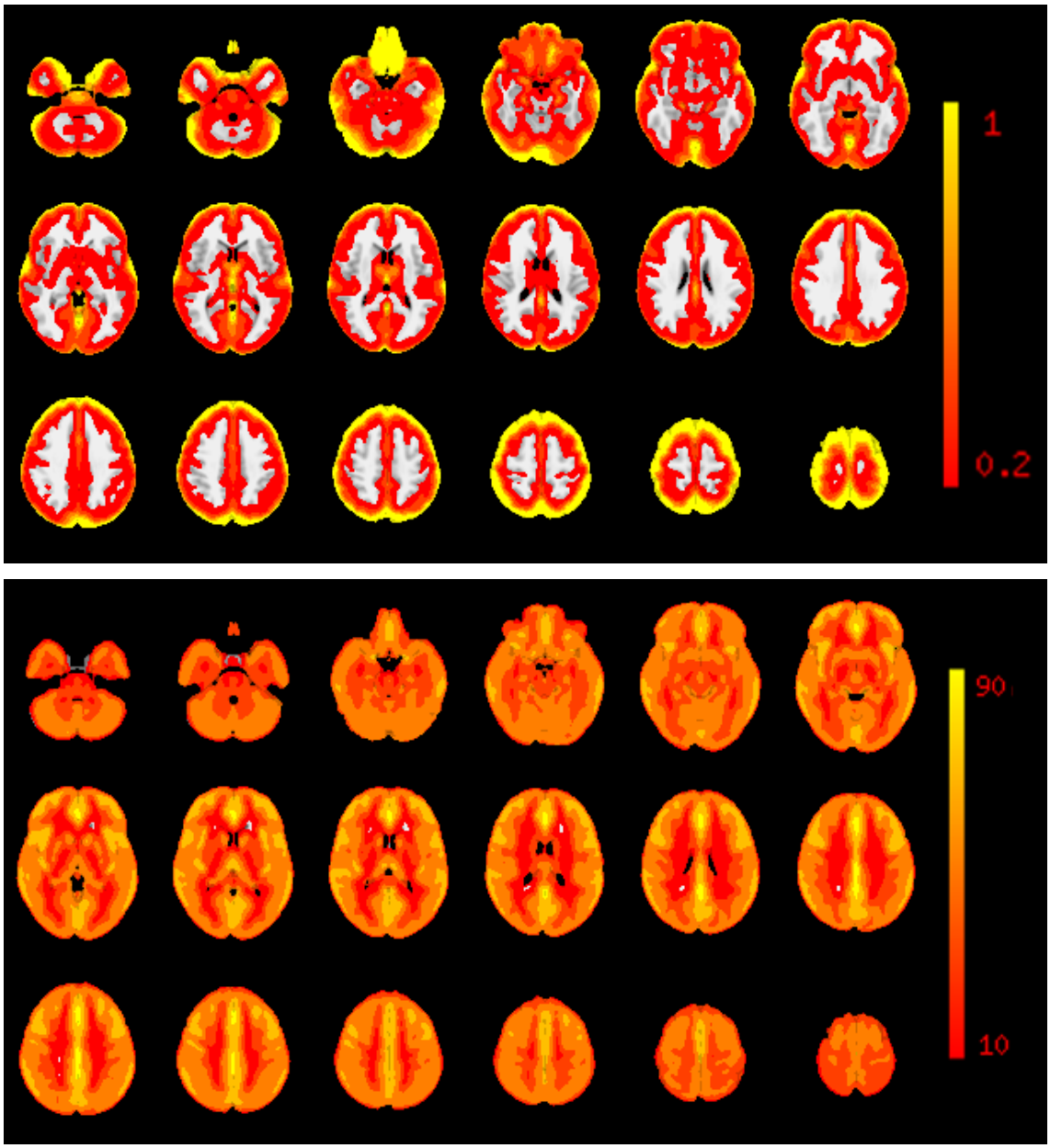

Figure 6.1: a): Average % BOLD SC / mmHg CO_2 map. The average map was calculated over N = 36 participants. Displayed are %SC in the range from 0.2 - 4. b): Average CBF (in ml/100g/min). The average map was calculated over N = 44 participants. Displayed are CBFs in the range from 0.2 - 80 ml/100g/min.

Table 6.1: Correlation between vascular reactivity and resting CBF for N = 36.

ROI	correlation
Left amygdala	$r[34]$ = -.04, *ns*
Right amygdala	$r[34]$ = -.06, *ns*
Left insula	$r[34]$ = -.05, *ns*
Right insula	$r[34]$ = -.13, *ns*
Fear-specific ROI (insula)	$r[34]$ = .01, *ns*
GABA-sensitive ROI (insula)	$r[34]$ = -.11, *ns*
GABA-sensitive ROI (frontal)	$r[34]$ = -.20, *ns*
Fear-unspecific ROI (insula)	$r[34]$ = .07, *ns*
Fear-unspecific ROI (amygdala)	$r[34]$ = -.02, *ns*

Table 6.2: Correlation between vascular reactivity and BOLD. Correlations were computed between participants. *SPIDER contrast*: $SPIDERS > ANIMALS$, *IAPS contrast*: $IAPSnegative > IAPSneutral$

Region	Contrast		
	$SPIDERS$	$ANIMALS$	$SPIDERcontrast$
Fear-specific ROI (insula)	$r[33] = -.08$, ns	$r[34] = -.35$, $p = .04$	$r[32] = .33$, $p = .06$
GABA-sensitive ROI (insula)	$r[30] = .13$, ns	$r[30] = .16$, ns	$r[30] = -.10$, ns
GABA-sensitive ROI (frontal)	$r[32] = .16$, ns	$r[33] = .12$, ns	$r[32] = -.12$, ns
Region	Contrast		
	$IAPSnegative$	$IAPSneutral$	$IAPScontrast$
Fear-unspecific ROI (insula)	$r[30] = -.11$, ns	$r[32] = -.15$, ns	$r[33] = .26$, ns
Fear-unspecific ROI (amygdala)	$r[31] = .14$, ns	$r[31] = .18$, ns	$r[32] = -.05$, ns

Table 6.3: Correlation between CBF and BOLD. Correlations were computed between participants with N = 43. *SPIDER contrast*: $SPIDERS > ANIMALS$, *IAPS contrast*: $IAPSnegative > IAPSneutral$

Region	Contrast		
	$SPIDERS$	$ANIMALS$	$SPIDERS$ *contrast*
Fear-specific ROI (insula)	$r[41] = .11$, ns	$r[41] = -.10$, ns	$r[41] = .21$, ns
GABA-sensitive ROI (insula)	$r[41] = .32$, $p = .04$	$r[41] = -.03$, ns	$r[41] = .34$, $p = .03$
GABA-sensitive ROI (frontal)	$r[41] = -.16$, ns	$r[41] = -.11$, ns	$r[41] = -.07$, ns
Region	Contrast		
	$IAPSnegative$	$IAPSneutral$	$IAPS$ *contrast*
Fear-unspecific ROI	$r[41] = -.06$, ns	$r[41] = -.01$, ns	$r[41] = -.14$, ns
Fear-unspecific ROI (amygdala)	$r[41] = .06$, ns	$r[41] = .12$, ns	$r[41] = -.03$

Correlations between task-related BOLD changes and vascular reactivity / CBF were calculated for each contrast and contrasts to fixation cross baseline. Vascular reactivity was negatively correlated with BOLD responses to $ANIMALS$ pictures (contrasted to fixation cross baseline), and showed a trend for a positive correlation with BOLD responses in the fear-specific ROI for $SPIDERS > ANIMALS$ contrast. No other correlations between vascular reactivity and task-related BOLD responses were found. In the GABA-sensitive functional ROI in the insula, a positive between-subject correlation between CBF and BOLD responses to $SPIDERS$ pictures (contrasted to fixation cross baseline as well as contrasted to $ANIMALS$ pictures) was found. For all numbers see Tables 6.2 and 6.3.

6.4.4 Fearfulness and vascular reactivity / CBF

In order to investigate the influence of fearfulness on measures of vascular reactivity and CBF, we performed 2-sample *t*-tests. None of them reached significance (Table 6.4).

6.4.5 GABA+ and vascular reactivity / CBF

We looked at the relationship between GABA+ concentration and vascular reactivity / CBF in functionally and anatomically defined regions of interest and within the spectroscopy voxels for the insula the DLPFC, respectively. While GABA+ did not correlate with CBF, we found negative correlations between GABA+ and vascular reactivity in the

Table 6.4: Group differences in vascular reactivity (VR) and cerebral blood flow (CBF). The median vascular reactivity / CBF was extracted for each person. To assess group differences, 2-sample *t*-tests were computed.

ROI	VR	CBF
Left amygdala	$t[29]$ = -0.80, *ns*	$t[36]$ = -1.71, *ns*
Right amygdala	$t[29]$ = 0.07, *ns*	$t[36]$ = -0.55, *ns*
Left insula	$t[29]$ = 0.06, *ns*	$t[36]$ = -1.31, *ns*
Right insula	$t[29]$ = 1.05, *ns*	$t[36]$ = -1.0, *ns*
Fear-specific (insula)	$t[29]$ = -0.72, *ns*	$t[36]$ = -0.50, *ns*
GABA-sensitive (insula)	$t[29]$ = 0.16, *ns*	$t[36]$ = -0.58, *ns*
GABA-sensitive (frontal)	$t[29]$ = 0.40, *ns*	$t[36]$ = -0.68, *ns*
Fear-unspecific (insula)	$t[29]$ = -0.12, *ns*	$t[36]$ = -0.60, *ns*
Fear-unspecific (amygdala)	$t[29]$ = -0.97, *ns*	$t[36]$ = -1.87, *ns*

Table 6.5: Correlation between GABA and vascular reactivity / CBF. Correlations were computed with insular GABA in insular regions, and with DLPFC GABA in DLPFC regions.

ROI	BH	CBF
Fear-specific (insula)	$r[26]$ = -.24, *ns*	$r[33]$ = .14, *ns*
GABA-sensitive (insula)	$r[25]$ = -.39, p = .04	$r[33]$ = .07, *ns*
Fear-unspecific (insula)	$r[25]$ = -.38, p = .05	$r[33]$ = .17, *ns*
Left anatomical insula	$r[26]$ = -.19, *ns*	$r[33]$ = .13, *ns*
Insula Voxel	$r[25]$ = -.43, p = .03	$r[35]$ = .10, *ns*
Dlpfc Voxel	$r[24]$ = .16, *ns*	$r[32]$ = .04, *ns*
Fear-specific (PFC)	$r[24]$ = .11, *ns*	$r[32]$ = .08, *ns*
GABA-sensitive (frontal)	$r[23]$ = .16, *ns*	$r[32]$ = -.16, *ns*

two functionally defined ROIs in the insula, and in the spectroscopy voxel around the insula (see Table 6.5 and Figure 6.2).

6.5 Discussion

We reported an influence of fearfulness and insular GABA+ on fear-related BOLD responses in the left insula. GABA+ in the DLPFC was associated with fear-related BOLD responses in a frontal cluster. Here, we aimed to investigate the potential role of vascular reactivity and baseline cerebral blood flow (CBF) in the previously discussed findings.

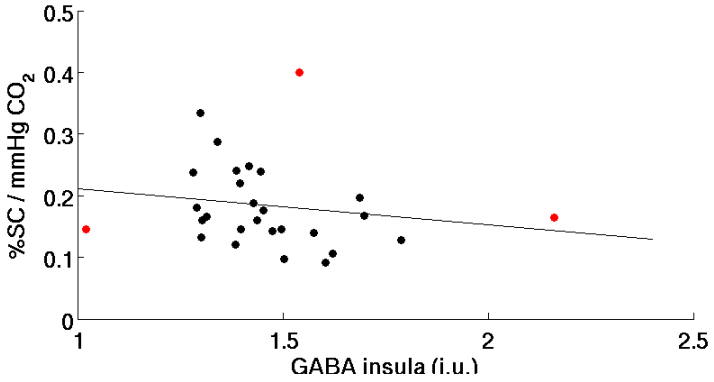

Figure 6.2: Scatter plot between GABA+ in insula and vascular reactivity in the spectroscopy voxel. Red dots were identified as outliers and not considered in calculating the correlation coefficient.

6.5.1 Vascular reactivity and CBF

In addition to the fMRI scan and the MRS scans, we applied a breath-hold task to measure vascular reactivity, and an ASL sequence to obtain resting cerebral blood flow levels. Over the gray matter we found average vascular reactivity measures of 0.27 %SC / mmHg CO_2 which is comparable to previously reported values (Kastrup et al., 2001; Lipp et al., submitted for publication; Liu et al., 2013). Average CBF was 48 ml/100g/min which is also comparable to previous literature (Aslan et al., 2010). We extracted median values for both vascular reactivity and CBF from anatomically and functionally defined regions of interest. CBF values did not correlate significantly with vascular reactivity values in any of the regions. This means that a participant's CBF in a region could not predict vascular reactivity in the same region, and that the two control measures we chose are independent from each other.

Findings from studies using gas challenges suggest that elevated CBF attenuates BOLD responses (Cohen et al., 2002; Sicard and Duong, 2005; Vazquez et al., 2006). Cohen et al. (2002) interpreted their findings as supportive for the hypothesis that the absolute BOLD response is stable, but appears as stronger or weaker depending on the baseline; this is because the relative increase in BOLD is the measure that is generally used. Our results do not support this. The important difference here is that we looked at inter-individual differences in baseline blood flow rather than within-participant differences. Inter-individual differences in resting blood flow did not contribute to inter-individual differences in vascular reactivity in our study. The amplitude of the BOLD responses in the breath-hold task is higher than BOLD responses to cognitive or emotional tasks. It might be the case that baseline CBF has a stronger impact when the BOLD responses in a task are weaker than breath-hold related BOLD responses.

6.5.2 Can vascular reactivity and resting CBF predict task-dependent BOLD responses?

We wanted to see to what extent vascular reactivity and baseline perfusion can explain the BOLD responses observed during the emotion task. Between-participant correlations between the measures could reveal whether any of the effects we found with the emotion paradigm might be mediated by vascular reactivity or CBF.

We calculated the correlations only for regions in which we found significant task-responses. In the fear-sensitive ROI we found a negative between-subject correlation between vascular reactivity and BOLD %SC during the presentation of $ANIMAL$ pic-

tures, and a trend for a positive correlation with the contrast $SPIDERS > ANIMALS$. We could not find differences between participants with high fearfulness and participants with low fearfulness in vascular reactivity in this region. This suggests, that the group difference we reported for the BOLD contrast is not caused by differences in vascular reactivity. None of the other between-subject correlations of vascular reactivity with BOLD reached significance. This is similar to what we previously reported with a different task (Lipp et al., 2014).

We found significant positive between-participant correlations between CBF and task-related BOLD responses, in the GABA-sensitive ROI for the main effects $SPIDERS$ and the contrast $SPIDERS > ANIMALS$. However, this is unlikely to explain the correlation between GABA and BOLD that we reported for this region, since GABA+ was not correlated with CBF. None of the other between-participants correlations between CBF and task-related BOLD reached significance. Again, the lack of consistent correlations does not support previous evidence from studies looking at the effects of up- or downregulating CBF, and might be related to lower power in between-participant designs.

6.5.3 The influence of GABA+ on vascular reactivity.

We found a negative correlation between insular GABA+ and vascular reactivity in the GABA-sensitive and in the fear-unspecific ROI, as well as in the spectroscopy voxel. The correlation was not significant in the fear-specific ROI or the anatomically defined insula, but the direction went in the same way. The correlation between GABA+ and BOLD in the GABA-sensitive ROI is unlikely to be mediated by vascular reactivity, since in this region vascular reactivity did not correlate with the task-dependent BOLD responses.

We could not replicate the GABA-vascular reactivity correlation using the DLPFC data. This finding cannot be explained by differences in variability in either the GABA+ measures (see Chapter 9) or the vascular reactivity measurese ($CV_{between}$ in DLPFC voxel: 39%, in insula voxel: 38%). One possibility for the discrepancy is that there are different mechanisms involved in vascular reactivity responses in the prefrontal cortex and in the insula. This seems unlikely, however, since both regions are cortical regions. It is also possible that the correlation found in the insula is related to the neural aspect of breath-holding rather than to vascular reactivity, since the insula has been associated with the feeling of breathlessness (Banzett et al., 2000; Evans et al., 2002). Last but not least we cannot explude the possibility that the GABA+ measures in the DLPFC are less reliable than the measures in the insula. We did not find better repeatability for the

insular GABA+ (see Chapter 9) but it is still possible that there are differences in what the obtained GABA measure actually represents, or differences in the macromolecule contribution to the signal.

The mechanisms behind which insular GABA+ might influence vascular reactivity is not clear. Our negative correlation indicates that a higher GABA+ concentration leads to a lower BOLD response to an increase in CO_2. As already speculated, this could be either explained by neural aspects of breath-holding, or might be related to the vasular reactivity of the system. GABAergic interneurons can lead to vasodilation or vasoconstriction (Cauli et al., 2004), depending on the interneuron type (Kleinfeld et al., 2011) and GABA receptor type (Fergus and Lee, 1997). Additionally, GABA receptors are sensitive to HCO_3- which can lead to an additional decrease in extracellular pH under the presence of CO_2 (Kaila and Voipio, 1987), proposing an additional pathway of CO_2-increase related BOLD responses. If the GABA+ concentration measure has to do with the number of interneurons and inhibitory connections in a region, then we might expect a positive relationship between GABA+ and vascular reactivity - but we actually found the opposite relationship. CO_2 leads to vasodilation through activating chemoreceptors and pH-receptors neurons in the brain stem (Putnam et al., 2004). However, it cannot be excluded that other neurons are also sensitive to these changes, one candidate are astrocytes. Recently, it has been discovered that astrocytes are GABAergic (Fraser et al., 1994), and that they have a role in regulating vasculature (Haydon and Carmignoto, 2006; Koehler et al., 2009).

6.5.4 The influence of GABA on CBF.

We did not find a correlation between GABA+ and resting CBF. This is consistent with Muthukumaraswamy et al. (2012), but in contrast to Donahue et al. (2010, 2014). Latter studies demonstrate that whether a correlation can be found and the direction of it is dependent on the CBF acquisition. While first a tendency for a positive correlation between CBF and GABA+ was found using a single inversion ASL, a negative correlation was reported for a VASO[1] sequence (Donahue et al., 2010). Donahue et al. (2014) used multiinversion time perfusion scan, and reported a negative correlation with GABA+, but no correlation if only one inversion time was used. In our study, we also only had one inversion time and did not find a relationship. The single inversion time has the disadvantage that a specified time between labeling and arrival is assumed to be adequate to model the CBF, however to what extent this time is a good estimate depends on partici-

[1]Vascular-space-occupancy (VASO) MRI is an alternative method to ASL for measuring CBF, using a contrast agent (see Lu et al., 2005).

pants, which might introduce additional variability in the CBF measure. Another factor to consider is that previous studies have looked at the visual cortex, and there might be regional differences in the correlation between GABA and CBF.

Inconsistent findings are also reported by pharmacological studies. Some studies have shown that GABA agonists (Caesar et al., 2003) do attenuate CBF responses to stimuli but not baseline CBF. Baseline might be more influenced by other factors such as stress (Wang et al., 2005), caffeine intake (Field et al., 2003; Laurienti et al., 2003), and anatomy of blood vessels (Sojkova et al., 2010). To what extent GABA has an influence on resting CBF might vary throughout the brain. Franklin et al. (2011, 2012) found that GABA agonists diminishes blood flow in some areas including amygdala, bilateral insula and orbito-frontal cortex, and increases blood flow in other areas, including the cingulate cortex.

6.5.5 Limitations and future directions

We investigated the interplay between vascular reactivity, CBF, task-related BOLD signals and GABA+ concentration. We could not find a clear pattern of correlations and due to the number of correlations calculated, the between-subject correlations would not survive correction for multiple comparisons.

We used a breath-hold scan to estimate vascular reactivity, which is a commonly used approach. However, it is impossible to disentangle vascular reactivity from neural aspects of breath-holding, which is particularly a problem for the insula, a region that has been associated with breathlessness (Banzett et al., 2000). An alternative to breath-holding is to increase CO_2 by applying gas-challenges, however, again this can lead to neural confounds with the perception of the CO_2 increase. It has been proposed to use resting state scans as an alternative method to estimate vascular reactivity, however, this method does not measure exactly the same thing (Lipp et al., submitted for publication). To test whether the correlation with GABA is related to the neural aspects of breath-holding, a study like Banzett et al. (2000)'s and Evans et al. (2002)'s could be applied, where CO_2 is held constant but the feeling of air-hunger is artificially elicited.

6.5.6 Conclusions

We found some between-participant correlations and some spatial correlations between vascular reactivity, CBF and task-related BOLD responses, but with large differences between participants. None of the correlations found indicate a mediation effect of vascular factors in our previously reported results. Fearfulness did not seem to have an influence on

either of the vascular factors, while GABA correlated negatively with vascular reactivity in the insula.

6.5.7 Next steps

This and the previous two chapters dealt with task-related BOLD responses during an emotion paradigm. Recently, a trend has emerged to study the connectivity between brain regions and individual differences in strength of so called resting state networks. In the next chapter, we investigate the influence of fearfulness on GABA+ on resting state connectivity of the anterior insula and the DLPFC.

Chapter 7

The relationship between fearfulness, GABA, and resting state connectivity of the insula and DLPFC

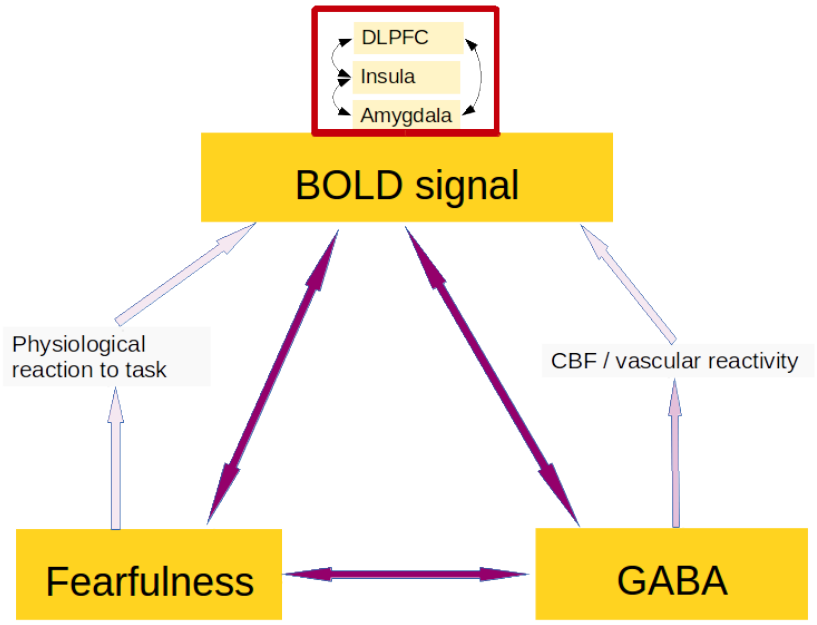

7.1 Abstract

To extend our findings on the influence of fearfulness and GABA+ on brain activation during the experience of fear, we also aimed to investigate the influence of these variables on the functional connectivity of the insula and DLPFC.

We computed seed analyses for functional ROIs in the left anterior insula and left DLPFC to explore their resting state functional connectivity, and to look at the potential influence of fearfulness and GABA+ (of the respective region) on the connectivity pattern. The left anterior insula was strongly connected to the right insula, the supplementary motor area, and ACC, with a connectivity pattern similar to what has been described as the salience network. The DLPFC ROI was strongly connected with regions associated with the default mode network.

High levels of fearfulness were related to stronger functional connecitivity of both seed regions. Only GABA+ in the insula was associated with functional connectivity, with a positive correlation between GABA+ and functional connectivity between anterior insula and caudate nucleus. Potential mechanisms behind the findings are discussed, and limitations and caveats in the field outlined.

7.2 Introduction

In a previous chapter we investigated the relationship between fearfulness, GABA+ and task-related BOLD responses in the insular cortex and DLPFC. Task-related BOLD responses reflect the extent to which a region responds to stimuli, and we found an influence of fearfulness and GABA+ on responses elicited during fear induction. In recent years, research has started to acknowledge that the brain operates as a network, and that investigating the connections between different regions can complement the understanding of brain mechanisms that have come from looking at individual regions. Particularly when it comes to emotion processing, it has been suggested that the interplay between different brain networks leads to the generation of emotional states (Oosterwijk et al., 2012) and that several of these networks, such as the salience and default mode network, might be dysfunctional in individuals with high anxiety (Sylvester et al., 2012).

One more specific hypothesis is that high levels of anxiety and fearfulness are a result of less successful emotion regulation (Amstadter, 2008; Phillips et al., 2008). Emotion regulation has been related to prefrontal-subcortical connections (Eippert et al., 2007; Lee et al., 2012; Phillips et al., 2008; Wager et al., 2008), and individuals with low anxiety levels have been found to recruit the DLPFC more strongly during emotional distractor tasks (Bishop et al., 2004; Bishop, 2009). Additionally, the structural (DTI) (Kim and Whalen, 2009) and functional connectivity between amygdala and prefrontal regions seems to be associated with subclinical and clinical levels of anxiety (Kim et al., 2011b; Prater et al., 2013) even during rest (Kim et al., 2011a). Furthermore, stronger connectivity between the insula and amygdala in highly fearful individuals has been reported in children (Qin et al., 2014), adolescents (Roy et al., 2013), and adults (Baur et al., 2013). Seeley et al. (2007) report stronger functional connectivity between anterior insula, ACC and left DLPFC for participants with high anxiety, interpreting it as stronger salience network activity in these participants. In summary, it seems that the interplay between amygdala, insula and DLPFC is important in fear and anxiety.

GABA might not only relate to neural activity in the area it is measured from, but also to the region's involvement in functional networks. Neurotransmitters have been shown to influence resting state connectivity. Several studies have demonstrated a relationship between glutamate or GABA concentration and resting state network strength (Duncan et al., 2013; Horn et al., 2010; Kapogiannis et al., 2013; Stagg et al., 2014). Additionally, there is evidence from pharmacological studies that manipulating GABA transmission has effects on resting state networks (Flodin et al., 2012; Greicius et al., 2008; Licata et al.,

2013). Flodin et al. (2012) and Greicius et al. (2008) looked at the effect of benzodiazepines on connectivity of the default mode network, and found both, increases and decreases. Licata et al. (2013) found that administration of a GABA agonists led to increased connectivity in a "limbic" network, containing basal ganglia, hippocampus, amygdala, OFC and prefrontal areas.

The main aim of this study was to investigate whether GABA+ and/or fearfulness have a significant impact on the strength of resting state functional connectivity maps from two key fear-related brain structures, the anterior insula and the DLPFC. Following the results from our fear induction paradigm, we focussed on the functionally defined left anterior insula and left DLPFC.

7.3 Methods

Sample and procedure are the same as described in Chapter 4. 100 volumes of resting state data were aquired with a T2* weighted imaging sequence (TR = 3s, TE = 35 ms, matrix = 64 X 64, FOV/slice = 220 mm, flip = 90, 46 slices of 2 mm with a 1 mm slice gap acquired in an interleaved order) using an eight-channel receive-only head coil. The orientation of the axial slices was parallel to the AC-PC line. During the resting state acquisition, participants were asked to keep their eyes open and relax. Physiological noise correction of the resting data was performed in the same way as it was done for the task (see Section 3.3.5). For three participants this could not be done due to technical problems with the physiological recordings, so their uncorrected data sets were used.

7.3.1 Seed analysis

The fear-specific functional ROIs in the anterior insula and DLPFC (see Chapter 4) served as seed regions. BOLD time-courses were extracted from the preprocessed resting state BOLD timeseries and entered as regressors in a whole-brain analysis. These regressors were not HRF convolved, no temporal filtering was applied and no further temporal derivatives were added. Six motion regressors were included in the first level analysis due to observed group differences in the absolute head displacement during the resting state scan, and the known effects of head motion on resting state analysis and (Power et al., 2012; Satterthwaite et al., 2013; van Dijk et al., 2012). Group average and group difference (high fearful vs. low fearful) maps were created with a mixed effects model using FLAME1. For the analysis including GABA+ as a regressor, the demeaned GABA+ measures from the voxel for the relevant region were entered as a regressor in the model. For participants

with no GABA+ data, the mean value was entered. The Z (Gaussianised T/F) statistic images were thresholded using clusters determined by $Z > 2.3$ and a (corrected) cluster significance threshold of $P < .05$ (Worsley, 2001). For the group average maps, a stronger threshold of $Z > 5$ was applied in order to identify only the areas most strongly correlated to the seed region. Because the influence of fearfulness on the connectivity between the seed regions and the amygdala was of particular interest, we additionally voxel-wise analysis (high fearful vs. low fearful maps) to the bilateral amygdala mask only (WFU-PickAtlas, Version 3.0.4, Wake Forest University, School of Medicine, Winston-Salem, North Carolina, www.ansir.wfubmc.edu).

7.4 Results

7.4.1 Connectivity of the functional anterior insula / prefrontal ROI

A whole-brain seed analysis was conducted for both the functional ROI in the left anterior insula, and the functional ROI in the DLPFC. The left anterior insula was most strongly connected to the right insula, the ACC, the supplementary motor cortex, and to regions in the occipital cortex (see Table 7.1 and Figure 7.1). Strong connectivity of the DLPFC ROI was found for bilateral medial frontal gyrus and posterior cingulate (see Table 7.2 and Figure 7.2).

7.4.2 Influence of fearfulness on connectivity

Fearfulness had an influence on the connectivity of both seed regions. In participants with high fearfulness the fear-specific ROI in the insula showed stronger connectivity to a cluster in the occipital and cerebellar cortex, and a cluster in the pre- and postcentral gyrus and precuneus (see Table 7.1). For the DLPFC cluster, highly fearful participants showed stronger connectivity to frontal white matter (see Table 7.2). For neither of the seed regions, the analysis restricted to the bilateral amygdala mask yielded group differences in connectivity.

7.4.3 Influence of GABA+ on connectivity

Entering GABA+ of the insula as a regressor in the group level analysis revealed that higher GABA+ goes hand in hand with higher connectivity of the anterior insula with a cluster in the right caudate, also spanning subcallosal cortex, ACC (coordinates [x,y,z]

Table 7.1: Seed analysis for fear-specific ROI (in left insula). For the group mean map, only clusters meeting the statistical threshold of Z > 5 and with a cluster size > 100 are reported. For the group comparisons, the statistical threshold was set to Z > 2.3.

Group mean (N = 37)			
Size	Peak (x,y,z)	Peak Z	Location
4006	0, -8, 62	6.92	SMA
2503	-46, 8, -8	8.79	Left insula
2174	44, 14, -6	7.11	Right insula
1067	64, -28, 20	6.52	Right planum temporale
797	14, -82, 20	5.76	Right cuneal cortex
740	-58, -42, 20	5.97	Left supramarginal
248	14, -20, 0	6.17	Right thalamus
217	-32, 46, 20	5.88	Frontal pole
128	2, -50, -12	5.84	Cerebellum
109	-10, -20, -2	5.44	Left thalamus
104	30, 42, 24	5.96	Right frontal pole
High fear (N = 19) > low fear (N = 18)			
Size	Peak (x,y,z)	Peak Z	Location
1311	-24, -68, -12	3.67	Occipital, superior cerebellum
1127	-24, -40, 60	3.73	Pre-/postcentral, precuneus, SMA
475	44, -64, -2	3.24	Right lateral occipital
Low fear (N = 18) > high fear (N = 19)			
no clusters			

Table 7.2: Seed analysis for fear-specific ROI (in left DLPFC). For the group mean map, only clusters meeting the statistical threshold of Z > 5 and with a cluster size > 100 are reported. For the group comparisons, the statistical threshold was set to Z > 2.3.

Group mean (n = 37)			
Size	Peak (x,y,z)	Peak Z	Location
1721	-30, 24, 36	8.9	Seed region
1281	-6, -42, 36	6.18	Posterior cingulate, precuneus
257	34, 30, 34	5.87	Left middle frontal gyrus
101	-52, -50, 40	5.42	Left angular gyrus
High fear (N = 19) > low fear (N = 18)			
Size	Peak (x,y,z)	Peak Z	Location
438	26, 18, 18	3.34	Right frontal white matter
Low fear (N = 18) > high fear (N = 19)			
no clusters			

= 6,20,4, cluster size = 739, see Figure 7.3). GABA+ in the DLPFC did not influence connectivity of the seed ROI in the DLPFC.

7.5 Discussion

The aim of this study was to look at the resting state connectivity profile of the functional regions in the insula and DLPFC, and at whether GABA+ or fearfulness has an influence on this connectivity. Both ROIs showed extended connectivity across the whole brain at a $Z > 2.3$ threshold; so a more restrictive threshold was applied to limit our results to the most connected brain areas.

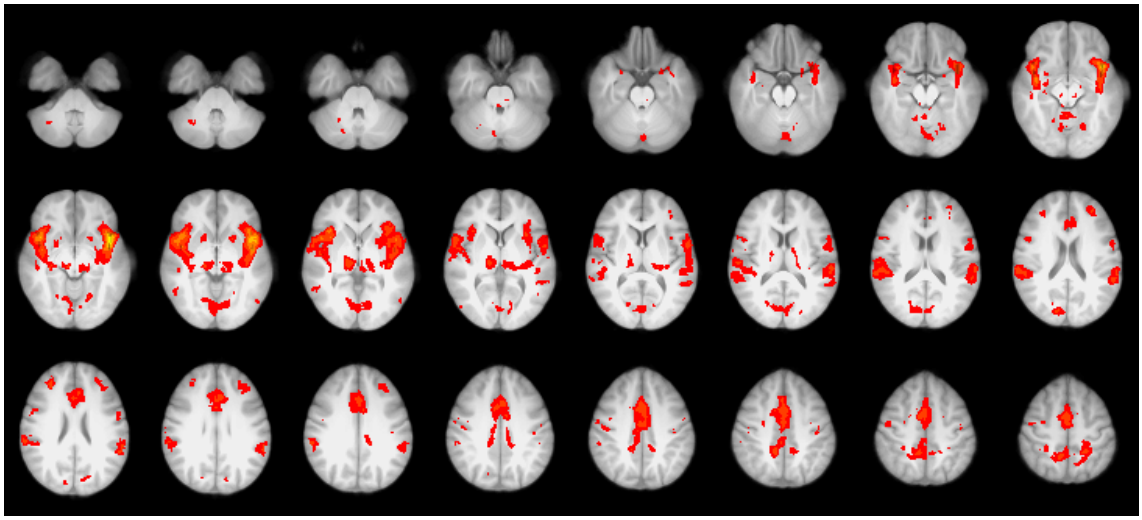

Figure 7.1: Seed analysis for fear-specific ROI (in left insula). The statistical threshold was set to Z > 5 and corrected cluster threshold of P < .05. Image displayed in radiological convention.

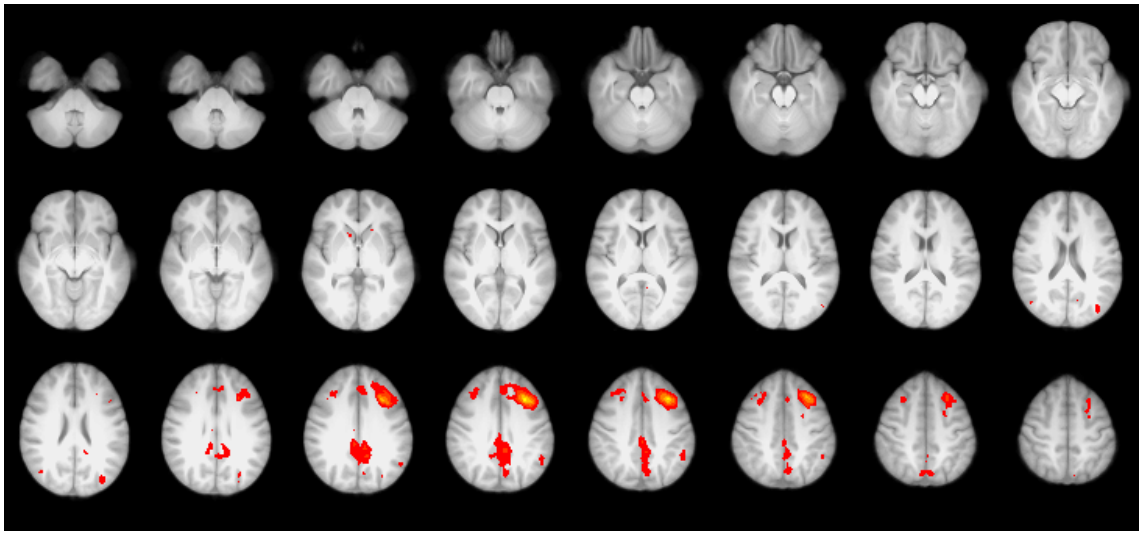

Figure 7.2: Seed analysis for fear-specific ROI (in left DLPFC). The statistical threshold was set to Z > 5 and corrected cluster threshold of P < .05. Image displayed in radiological convention.

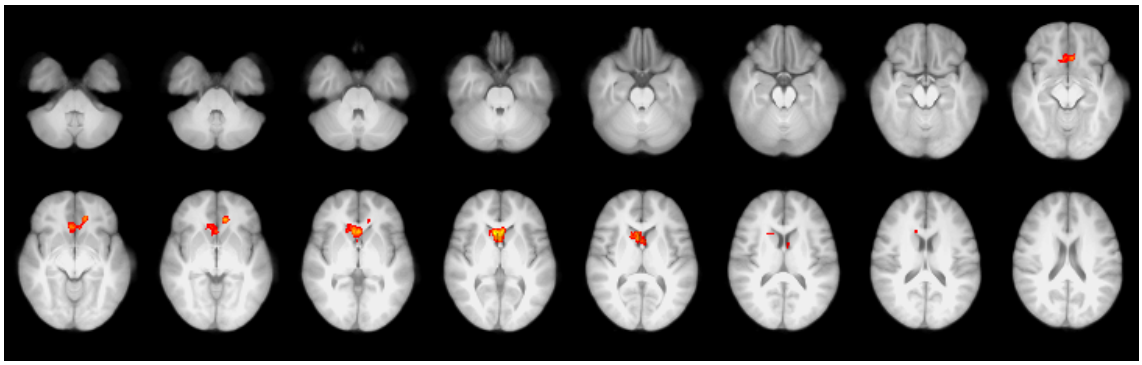

Figure 7.3: Influence of insular GABA+ on whole brain connectivity of fear-specific ROI (in left insula). The statistical threshold was set to Z > 2.3 and corrected cluster threshold of P < .05. Image displayed in radiological convention.

7.5.1 Resting state connectivity of the insula cluster

Our ROI in the anterior insula was most strongly connected to the right insula, the ACC, to frontal and also occipital regions. In fact, the network we found was comparable to what Yeo et al. (2011) described as ventral attention network - also called "salience network" (e.g. Oosterwijk et al., 2012; Seeley et al., 2007) - which also includes regions in the ACC, SMA and subcortical regions (Seeley et al., 2007).

The insular cortex is a large structure and previous connectivity studies suggest that it can been parcellated into two to three main functional domains (posterior, ventral anterior and dorsal anterior) that differ in their connectivity profiles (Cauda et al., 2011; Chang et al., 2012; Deen et al., 2010). DTI findings suggest that the anterior insula is strongly connected to dorsal prefrontal and inferior frontal areas and that the posterior insula is strongly connected to motor and somatosensory areas, while both parts are equally connected to limbic structures (Chia-Feng et al., 2012). Previous resting state connectivity studies report a similar segregation, and additional functional connections between the ventral anterior insula and the amygdala, OFC and temporal regions, and between the dorsal anterior insula to ACC and DLPFC (Cauda et al., 2011; Chang et al., 2012; Deen et al., 2010). The ROIs used for this study would be anatomically categorized as part of the anterior compartment defined by Cauda et al. (2011) and Chang et al. (2012), with both dorsal and ventral contribution.

The connectivity maps we obtained for our functional ROI include connections that have previously been reported for both anterior and posterior compartments. One major difference from our study to previous studies is that previous studies applied global signal regression (Cauda et al., 2011; Chang et al., 2012; Deen et al., 2010). This might account for the fact that we found this relatively unspecific and widespread connectivity throughout the brain. Additionally, our seed region was derived functionally from a task, and might therefore be a functional entity with a specific set of functional connections, that cannot be mapped exactly to what has been previously found with anatomically defined regions.

7.5.2 Resting state connectivity of the DLPFC cluster

When the functional cluster in the DLPFC was used as a seed region, the most strongly connected regions turned out to be a region around the posterior cingulate and precuneus, the middle frontal gyri and left angular gyrus. The DLPFC is generally associated with an executive control network, that includes fronto-parietal regions (e.g. Seeley et al., 2007). The connectivity pattern of our functional ROI in the DLPFC resembles more the

default mode network, which involves posterior cingulate, precuneus and medial frontal cortex (Greicius et al., 2003; Raichle et al., 2001). However, connectivity between the left DLPFC and posterior cingulate has also been found in other studies in the context of the default mode network (Greicius et al., 2003). In fact, during the task our functional ROI was deactivated compared to the fixation cross baseline, but more so during the animal condition than during the spider condition (which is why it appeared for the contrast $SPIDERS > ANIMALS$). It might be the case that this particular part of the DLPFC is less relevant for executive functioning or as hypothesized voluntary emotion regulation, and more to functions related to default mode activity, such as being self-conscious (Northoff et al., 2006). However, the MPFC, which is also part of the default mode network, is known to regulate amydala activations through direct anatomical connections (e.g. Marek et al., 2013; Ray and Zald, 2012).

The results from the two seed analyses show two different connectivity patterns of anterior insula and DLPFC ROIs, suggesting that the two seed regions are not part of the same network. While the insula is often associated with the salience network, our DLPFC cluster was strongly connected with regions from the default mode network. Menon and Uddin (2010) propose that the salience network switches between default mode network and executive network, depending on evaluation of the salience of stimuli. All these networks have been related to emotion processing (Pannekoek et al., 2013; Qiu et al., 2011; Zhao et al., 2007), and newer theories on emotion assume that the state of emotion is a result of the interplay of basic networks in the brain (Oosterwijk et al., 2012), rather than a distinct emotion processing network. In this study, we looked at the influence of fearfulness and GABA+ on the strength of the two networks obtained through seed analyses.

7.5.3 Influence of fearfulness on resting state connectivity

We found higher task-related BOLD responses in the fear-related ROI in the left anterior insula for highly fearful participants, similarly, higher fear participants showed stronger resting state connectivity of the same ROI. Simmons et al. (2011) compared participants with high vs. low anxiety with regard to functional connectivity of the left anterior insula during anticipation of emotional stimuli. They also found increased connectivity in highly anxious people in a number of regions, including the cerebellum, precuneus, and various frontal regions. We found increased connectivity during rest, extending Simmons et al. (2011)'s findings. Regions that were more strongly connected to the anterior insula in

highly fearful participants were the pre- and postcentral gyrus and occipital cortex and cerebellum.

Analysing the emotion paradigm, we found that highly fearful participants had stronger fear-related BOLD responses in parts of the cerebellum (see Chapter 4). There is some overlap between that cluster and the significant cluster in the functional connectivity analysis, indicating that the abnormal functional connectivity might indeed be related to circuits important for emotion-processing. In fact, the role of the cerebellum in cognition and emotion control has started to receive more and more attention (Schmahmann and Sherman, 1998; Schmahmann and Caplan, 2006; Schutter and van Honk, 2005). In particular, the cerebellum might play an important role in emotion regulation (Schutter and van Honk, 2009), and has been found activated during processing of a number of emotions (Baumann and Mattingley, 2012). Additionally, altered functional connectivity of the cerebellum for individuals with high fear or anxiety has been previously reported, such as increased connectivity between the cerebellum and basolateral amygdala in adolescents with generalized anxiety disorder (Roy et al., 2013), and increased connectivity between cerebellum and putamen in depressed adults (Alalade et al., 2011). These and our findings for participants with high fearfulness levels suggest that the cerebellar cortex is an important part of networks involved in emotion processing. We also found increased connectivity between anterior insula and pre- and postcentral gyrus and occipital areas for highly fearful participants. The significant clusters in these regions also overlap with the task-related activation patterns. It seems that high fear is associated with stronger connectivity between the anterior insula and a number of other areas that are involved in fear processing. One hypothesis resulting from these findings is that group differences in task-related activition in such areas during tasks that recruit the insula could be partly driven by differences in functional connectivity of the insula.

Previous studies have shown stronger functional connectivity between insula and amygdala in participants with high fear (Baur et al., 2013; Qin et al., 2014; Rabinak et al., 2011; Roy et al., 2013; Sripada et al., 2012). We could not replicate this result, even when we restricted the analysis to the amygdala, and this might be due to a number of different reasons. For once, in contrast to other studies we looked at subclinical levels of fearfulness rather than anxiety or anxiety disorders. The study by Baur et al. (2013) found a correlation with state anxiety (and only a tendency for trait anxiety), and our groups selected for fearfulness did not differ in state anxiety at the time of scanning (see Chapter 4). The study by Qin et al. (2014) looked at childhood trait anxiety, but it might be the

case that children with high trait anxiety also show higher state anxiety to the scanning situation. Roy et al. (2013) used a sample of adolescents with generalized anxiety disorder and Rabinak et al. (2011) and Sripada et al. (2012) used a sample of veterans with PTSD, so samples not comparable to ours. The lack of group differences in insula - amygdala in our study might be related to the recruitment strategy that was based on subclinical levels of fearfulness rather than clinical fear / anxiety.

Due to its role of the DLPFC in emotion regulation, functional connectivity differences between participants with high fearfulness and participants with low fearfulness were expected. We did not find a group difference in the functional connectivity between our DLPFC ROI and the amygdala (even when restricting the analysis to the amygdala), which could be partly due to the nature of the DLPFC ROI, which is strongly connected to regions of the default mode network. Our DLPFC seed region was functionally defined from the task, but it is not clear what exact role it plays in the tasks, and it might simply be the case that it does not have anything to do with emotion regulation. Previously, lower functional connectivity between amygdala and prefrontal regions have previously been reported for patient groups, such as PTSD (Stevens et al., 2013), depression (Lu et al., 2012; Tang et al., 2013), and social anxiety disorder (Prater et al., 2013). However, other studies have found the opposite, that high anxiety is associated with stronger coupling between prefrontal areas and amygdala, and this was interpreted as an amplification of amygdala responses by prefrontal areas in individuals susceptible to fear (Robinson et al., 2012, also see Vytal et al., 2014). It might depend on the circumstances under which functional connectivity is assessed, and whether participants are instructed to detect aversive stimuli, to ignore them or do not have a task at all. In this study, functional connectivity was assessed during rest, so during the absence of fear-inducing stimuli or threat. It is possible that prefrontal-amygdala connectivity differences between fearful and non-fearful participants only become apparent in situations that do require regulation of attention to or from these stimuli, which could explain why we did not find group differences.

During rest, we did find stronger connectivity for the DLPFC region in highly fearful participants, but in a cluster in right frontal white matter. Interpreting BOLD signal in white matter has to be done carefully, since it is theoretically not straightforward (Logothetis and Wandell, 2004), even though some claim that the HRF is similar in gray and white matter (Fraser et al., 2012). Either way, interpretation of this result is challenging, and whether it reflects something important or is simply a chance finding remains to be discovered in future studies.

7.5.4 Influence of GABA+ on resting state connectivity

In order to assess the influence of GABA+ on the resting state networks, we used insular GABA+ as a regressor for the seed analysis with the anterior insula seed region, and GABA+ in the DLPFC as a regressor for the seed analyis with the DLPFC seed region.

GABA+ had an influence on resting state connectivity of the anterior insula seed region, in a cluster in the right caudate and nearby regions. This region is relatively close to but not overlapping with the spectroscopy voxel in the left insula. The finding suggests that higher GABA+ concentration in the insula is associated with stronger connectivity between the anterior left insula and the right caudate. The role of connectivity between anterior insula and caudate in emotion is not clear though. Previous studies found decreased connectivity between insula and caudate in patients with major depression (Ma et al., 2012; van Tol et al., 2013), which suggests that the connectivity between the two regions might have some functional role for emotion. The caudate nucleus itself has been related to processing of negative stimuli (Carretié et al., 2009), and also for our unspecific contrast ($IAPSnegative > IAPSneutral$) the group activation extended to parts of the caudate.

Interestingly, the two studies that previously investigated the relationship between GABA concentration and resting state network strength have demonstrated a negative rather than a positive correlation; one study for the default mode network (Kapogiannis et al., 2013) and one study for the motor network (Stagg et al., 2014). Kapogiannis et al. (2013) postulated that "regional balance between glutamate and GABA may determine the synchronized portion of neuronal activity in that region and, therefore, correlate with functional connectivity." (p.117). However, we observed the opposite, a positive correlation between GABA+ and functional connectivity, and in fact, one role of GABAergic interneurons is to orchestrate microcircuits in the brain, and as a result to produce oscillations by coordinated inhibition (see e.g. Kann et al., in press). Considering this, the positive correlation between GABA concentration and functional connectivity also seems plausible. In fact, there are different ways in which GABA and functional connectivity might influence each other. One possibility is that the level of GABA in region A dictates the level of inhibition of the input from region B, and therefore to what extent region A has a similar activation timecourse to region B. On the other hand, GABA in region A might influence the output of region A into region B and therefore to what extent region B reacts to region A with a similar timecourse. In both these cases, assuming that GABA concentration reflects the level of inhibition, a negative correlation between GABA

and functional connectivity makes sense. It has to be considered that GABA generally acts locally rather than through long-distance connections. So another option is that the GABA concentration might simply determine the connectivity within small microcircuits that would not be measurable with current fMRI techniques. However, if connectivity within microcircuits is related to connectivity between these circuits, and possibly to the connectivity within a whole network, then correlation between GABA and long-distance functional connectivity might be observed. For this scenario, it is not clear in which direction the relationship should go, since more GABA transmission might lead to more inhibition of the circuits but also to stronger synchronization between nodes. Due to the current technical limitations of measuring GABA and small-scale functional connectivity in living humans, the interpretation of available data is also limited. At the moment, exploratory studies like this can provide first clues to what might be happening. Whether the correlation between GABA and functional connectivity we found is meaningful, remains to be tested and replicated with improved methods in the future.

7.5.5 Limitations and future directions

In contrast to previous studies, we did not apply global signal regression for the functional connectivity analysis. Global signal regression, which is used to reduce noise in the data, has been found to artificially introduce negative correlations (Murphy et al., 2009), which is why we decided against using it. This might be one of the explanations why, in contrast to previous studies, we did not find any significant negative correlations with our seed regions. In order to reduce noise we applied physiological noise correction instead, which reduces variation in the BOLD signal related to variation in breathing and HR. The difference in noise correction might be one reason why we could not replicate some of the previous findings.

We investigated the relationship between GABA+ in the insula and DLPFC and functional connectivity of functionally defined seed regions in the anterior insula and DLPFC. The spectroscopy voxels used to measure GABA+ were very large compared to the seed regions used. Therefore, the actual contribution of the seed region to the GABA+ measure is not known. If the GABA+ concentration in the entire insula / entire DLPFC is relatively homogeneous, this is not a problem, however, how homogeneous the concentration is has not been tested.

Functional connectivity is a statistical construct based on temporal correlations between regions. High resting state network strength does not necessarily mean that the

regions of a network are highly activated. There is evidence that functional connectivity does partly reflect structural connectivity (e.g. Hagmann et al., 2008; Greicius et al., 2009), but whether high connectivity can be found also depends on the variance of the signal, possibly reflecting how variant and changable the thoughts during rest are in a participant. Functional connectivity has been found to reflect the cognitive state a participant is in (Shirer et al., 2012), and it is possible that group differences between fearfulness groups reflect differences in how participants "rest" during scanning rather than robust differences in functional connectivity.

7.5.6 Summary and Conclusions

The connectivity of our functional ROI in the anterior insula is comparable to what has been previously reported. The functional ROI in the DLPFC was most strongly connected to regions of the default mode network. We found that fearfulness had an influence on both resting state networks. Participants with high fearfulness had stronger connectivity between anterior insula and regions in the occipital lobe, cerebellum and SMA. We found a positive correlation between GABA+ in the insula and connectivity between anterior insula and right caudate nucleus. GABA+ in the DLPFC did not influence resting state connectivity of the DLPFC ROI. We conclude that with the current knowledge and methods available it is hard to predict and interpret a GABA-resting state functional connectivity relationship, but that exploratory analyses like this one can shed first light on possible mechanisms.

Part IV

General discussion

Chapter 8

Bringing all the findings together...

8.1 Summary of the findings

The aim of this thesis was to investigate the interplay between fearfulness, GABA and fear-related BOLD responses. Previous studies have shown GABA deficits in clinical populations, hyper-activation of emotion processing brain regions in individuals with high fear, and a direct negative relationship between GABA concentration and BOLD responses. This was the first study to combine measures of BOLD responses during a fear provocation task with measures of fearfulness and GABA concentration in structures related to fear processing. Additionally, we collected a number of control measures that could have a potential impact on any of the relationships of interest and which could lead to a better understanding of the methodology in the field.

Prior to investigating the main research questions, two emotion paradigms were evaluated for usability in this project. The first paradigm consisted of frequently used emotional faces (**Chapter 2**), but failed to elicit BOLD responses specific to the emotional content of the faces. Additionally, the BOLD responses were not repeatable over a retest scanning interval. In **Chapter 3** a novel emotion paradigm was developed, aimed to elicit activation in fear-relevant brain structures such as the amygala and insula. Two contrasts were set up, a fear-specific ($SPIDERS > ANIMALS$) and an unspecific ($IAPSnegative > IAPSneutral$) contrast. Based on the results, we concluded that this novel paradigm was more suitable for the main project.

In **Chapter 4** the main hypotheses were tested. We did not find an association between fearfulness and GABA+ levels, but demonstrated that highly fearful participants

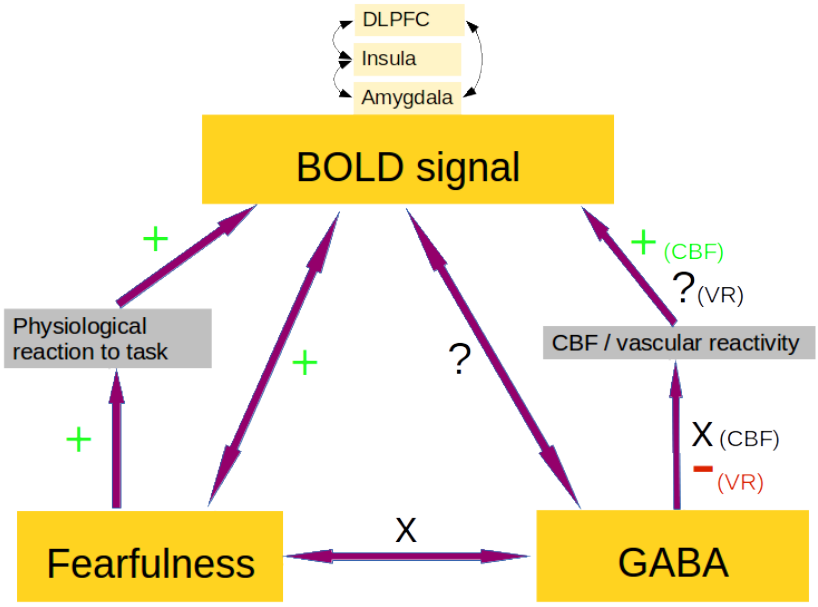

Figure 8.1: Summary of findings. While fearfulness was not associated with GABA+ concentration, we found a positive relationship between fearfulness and physiological responses to the task, as well as an influence of physiological task reponses on emotion-related BOLD responses. The relationship between GABA+ and BOLD signals was inconclusive. Insular GABA+ was associated with vascular reactivity in the insula but not in the DLPFC and not with baseline CBF. The influence of vascular reactivity and baseline CBF was also not conclusive and depended on the region and contrast investigated.

had stronger fear-related BOLD responses in the anterior insula, and in other regions that are frequently associated with emotion processing, replicating the findings from previous studies. We did not find a correlation between GABA+ and fear-specific BOLD responses in functionally defined regions in the anterior insula and DLPFC, however, a positive correlation between insular GABA and BOLD responses for the fear-specific contrast in a cluster encompassing insula, amygdala and putamen, as well as a positive correlation between GABA+ in the DLPFC and fear-specific BOLD responses in a frontal cluster posterior to the spectroscopy voxel. GABA+ concentration was not associated with the level of BOLD responses for the fear-unspecific contrast.

In **Chapter 5** the potential mediating role of physiological responses to the task was investigated. We demonstrated that stimuli elicited physiological changes during the task, and that applying physiological noise correction had an effect on the analysis of the emotion paradigm, making it more conservative and reducing the common effect of physiology and task.

Other potential mediating factors investigated were vascular reactivity and baseline cerebral blood flow (**Chapter 6**). We did not find evidence for either of the measures being

responsible for the previously discovered results, however, we demonstrated a negative correlation between GABA+ and vascular reactivity in the insula.

Finally, the association between fearfulness and GABA+ and functional connectivity of fear-related regions in the left anterior insula and left DLPFC were investigated **(Chapter 7)**. We found stronger connectivity of both regions for highly fearful participants, and a positive correlation between insular GABA+ and connectivity between the anterior insula and the caudate. Figure 8.1 illustrates all the findings.

8.2 Considerations for interpretation

A number of issues have to be considered when the above findings are discussed.

8.2.1 Recruitment

We used a subclinical sample for this study. Results from subclinical samples are informative, since they can give clues about potential predispositing factors for clinical disorders, without the risk of treatment confounds or that brain correlates might in fact be results of the disorder rather than a predisposition. This might be a reason why we could not replicate some of the previous findings that were reported with clinical samples, such as decreased GABA concentration in fearful participants. On the other hand, subclinical populations might have protective factors that keep them from developing clinical disorders despite having high fear. For example, it is possible that whether highly fearful individuals develop a psychiatric disorder is dependent on their GABA level. If this was the case, highly fearful individuals that do not develop psychiatric conditions (such as our sample) would have comparable GABA levels to healthy controls (but altered GABA concentration would be found in individuals with psychiatric conditions). This is a speculative scenario, but outlines the limitation of using subclinical samples for investigating predispositions.

Because we aimed for healthy participants with high vs. low subclinical levels of fearfulness, we had to conduct screening prior to recruitment. Screening questionnaires were the FSS-II and the FSQ, both of which have previously been shown to have good reliability and validity in non-clinical samples. We picked extreme groups from a screening sample of around 600 females, and we observed that the scores in the two screening questionnaires did not correlate very highly ($r = .22$, $p < .0001$). This was unexpected since fear of spiders has previously been found to be correlated with other fears (Olatunji, 2006; Sawchuk et al., 2000). One reason for our low correlation might be that the items of

the FSS-II span a big variety of stimuli of various categories. Fear of spiders might only predict fear of certain other stimuli and not fearfulness in general.

The low correlation between the screening questionnaires made recruitment challenging. Additionally, the screening took place a few months before scanning for some participants, which is why all participants were given the screening questionnaires again at the time of scanning, even though it was not expected that the scores would change much. However, six participants had to be excluded because they filled out the questionnaires the opposite way than at the time of the screening. In general, particularly for the FSS-II a regression to the mean was observed, and in our final sample the FSQ seemed to differentiate groups better than did the FSS-II. This might be one of the reasons why we found most group differences in spider-related contrasts (rating of the images, BOLD activation), and potentially also influenced the fact that we did not find group differences in GABA+ concentration.

Our sample consisted of young female members (students and staff) of Cardiff University. On one hand, in such a homogeneous sample it is less likely that fearfulness is confounded with other factors such as age or gender. On the other hand, recruiting from wider population might have led to higher variance / more extreme extreme groups in fearfulness and therefore to more power to detect potential associations.

8.2.2 High GABA, low BOLD: is it too simplistic?

Most previous studies have reported negative rather than a positive correlation between GABA and BOLD, which does suggest that the measured GABA concentration indicates the level of inhibition in a brain region. However, even though a negative relationship between GABA levels and BOLD signal seems intuitive, it is probably not as simple. It is in fact not well understood what role GABA and GABAergic interneurons play in the generation of the BOLD signal (for good reviews see Buzsáki et al., 2007; Lauritzen et al., 2012; Logothetis, 2008). The current understanding is that even though postsynaptic activity in excitatory synapses but not in inhibitory synapses drives the BOLD response, "the balanced proportional changes in excitation-inhibition activity, which occur as a result of neuromodulatory input, are likely to strongly drive the haemodynamic responses" (Logothetis, 2008, p.873). This means that whether a lot of GABA transmission leads to a lower BOLD response depends on the level of excitation. In fact, some studies have found positive correlations between GABA and glutamate measures (Kegeles et al., 2012; Stagg et al., 2011), which is not surprising considering that GABA is a metabolic prod-

uct of glutamate. However, it might suggest that both neurotransmitter concentrations reflect the level of complexity in a region. How much glutamate gets transformed into GABA depends on GAD, and individual differences in GABA concentration are related to genes for GAD67 (Brealy et al., unpublished findings; Marenco et al., 2010). Because the GABA MRS measure is sensitive to intra- and extracellular GABA, it is not clear at this point whether high GABA concentration actually indicates high GABA transmission. Interestingly, benzodiazepine administration in humans has been shown to decrease measured GABA concentration (Goddard et al., 2004a). This might mean that if GABA transmission is efficient - because of high receptor number, well functioning receptors or benzodiazepine abundance - maybe not as much GABA is needed for successful transmission. This adds another level of complexity when it comes to investigating individual differences in GABA concentration measures.

Even though most of the previous studies looking at GABA and BOLD report negative correlations, recently two studies reported the opposite (this study and Wiebking et al., 2014). It is unclear how many studies did not find a correlation (since negative findings are less likely to be published), one example is Robson (2012) who could not replicate findings by Muthukumaraswamy et al. (2009)/Muthukumaraswamy et al. (2012). In addition to that, within some of the studies GABA did not correlate with BOLD responses for all the contrasts, and in some cases only in one out of a number of conditions (e.g. Stan et al., in press and also this study), which leads to problems with multiple comparisons and potential chance findings. Furthermore, it is not clear why GABA should only correlate with BOLD responses under certain conditions in the same region (given that BOLD responses are found for all conditions). We tried to come up with an explanation for our findings (GABA contribution is higher in simple, non-emotional stimuli) but this needs to be further explored with studies designed for that purpose.

8.2.3 Were we measuring trait markers?

In this project, we were interested in predisposing factors or biomarkers for high levels of fearfulness. We suggested both fear-induced BOLD responses and GABA+ concentration measures as potential biomarkers, which assumes that the measures are relatively stable over time and more strongly driven by individual differences rather than daily state of the participant. In order to test this, we conducted repeatability analyses for both, the fMRI paradigm, and the GABA spectroscopy scans.

We evaluated two emotion paradigms for repeatability. The first paradigm was an

emotional faces task and did not produce repeatable BOLD responses, or the expected activation patterns. The second task was self-constructed and gave more repeatable results, and also demonstrated that repeatability depends on factors such as how ROIs are defined and what contrast is being used. Repeatability was lower for the contrast to the neutral condition than for the contrast to fixation cross baseline, indicating that it is harder to capture the emotional aspect reliably with this emotion paradigm. This makes it more challenging to investigate the relationship between the emotional-related BOLD response and GABA, and might be a reason why we did not find a correlation when we used functionally defined ROIs and the contrast $SPIDERS > ANIMALS$ or $IAPSnegative > IAPSneutral$. We did find a correlation between GABA+ and BOLD responses for the contrast $SPIDERS > ANIMALS$ in a different cluster, but it turned out that the correlation was in fact highly influenced by the contrast of neutral condition to fixation cross baseline.

The reason why contrasts between two active conditions do so badly could be several. For one, there might be lower signal-to-noise ratio because the %SC change is substantially lower. Also, even though in our study stimuli were very carefully matched, no contrast is perfect and it is unlikely that it ever ONLY captures the emotional aspect. Comparison to fixation cross has other problems. For example, we demonstrated that physiological parameters have an influence on BOLD responses contrasted to fixation cross baseline, independently of the stimulus condition. This was found mostly for visual areas, but we cannot exclude that other areas are also affected to some extent. Furthermore, individual differences in vascular reactivity could predict BOLD responses contrasted to fixation but not contrasted to the neutral condition in the amygdala (data not shown in this thesis). This demonstrates that the contrast to fixation cross is influenced by a number of unwanted factors, that might be hard to control for, and some of them might even be unknown. It is not clear whether the low repeatability of the contrast measures are due to low reliability of the measurement or due to temporal fluctuation of emotional aspect of the BOLD signal. Resolving this issue would be very important for future emotion research.

In the Appendix, a study is described in which the repeatability of the GABA+ measures was estimated. This was done using the same participants as in the main experimental chapters. Since two spectra were obtained from each participant and each region, and some participants came back for a second scan, we could estimate repeatability of a 9 min. spectrum acquisition, but also of the average of two such spectra over a longer period of time. We found that averaging over two spectra yielded higher repeatability even

though data for this analysis was collected in two separate sessions a few weeks apart. This suggests that measuring GABA+ several times and averaging gives better measures of GABA+, but also that GABA+ is somewhat stable over a few weeks. This supports recent findings by Near et al. (2014) who found good repeatability of occipital GABA+ measures over a 7 day interval. In our main project we had to exclude several participants because they had no acceptable GABA+ spectrum, and for a number of participants we only had one acceptable spectrum and could not take average over two spectra. This means that the GABA concentration estimates that were used in this study are noisy, which influences the power of the study.

Taking the results from BOLD repeatability and GABA repeatability together, we conclude that BOLD contrast to fixation cross (but not contrast to neutral condition) and GABA+ in our regions of interest are possibly trait markers, but measurement of these is noisy. Considering the low sample sizes of other studies, but also the sample size of this study - which suffered from additional exclusion of participants - it is possible that we did not have enough power to detect all true effects (a general problem in Neuroscience, also see Button et al., 2013). In the following, we estimate the power of this study post-hoc.

8.2.4 Post-hoc power analysis of this study

The low repeatability of some of the measures suggests that the power of this study might be not high enough to detect some of the expected effects. This is demonstrated using the correlation between BOLD and GABA+ in our functionally defined fear-specific cluster in the anterior insula. We could not find a significant correlation between the two measures in a sample of 29 participants. In order to estimate the power of this analysis, the approach used in Robson (2012) was adapted. We used the BOLD %SC data from the 14 retest participants to estimate the noise in the BOLD data. The mean of the %SC from the contrast $SPIDERS > ANIMALS$ from session 1 was 0.12, std. from session 1 was 0.19, and estimated noise was 0.86 (calculated the absolute percent change from session 1 to session 2 averaged across participants, and multiplied by the sample mean to end up with the same units). In order to estimate noise of GABA+ data, data was used from 22 participants with two accepted GABA+ spectra in the insula in the first scanning session. Mean from scan 1 was 1.43, std. 0.23, and noise (calculated as described above) 0.29. It has to be noted that the noise calculation for BOLD data was a bit stricter since it involved a retest interval of a few weeks, while the GABA+ noise was calculated with data from the same session.

Data for a population of people (N = 10000) was simulated with a "true" effect size between $r = 0$ and $r = 1$. For a variety of sample sizes (N = 2-100) a random sample was drawn and normally distributed noise was added (by creating random numbers with a standard deviation equivalent to half of the noise calculated above). Then the correlation in the respective sample (using the noisy data) was calculated. This was done in 10000 iterations, and from the 10000 resulting values for each sample size and each true effect size the probability of getting a significant result was calculated, as well as the average detected correlation coefficient.

As illustrated in Figure 8.2 (top), independent of the real correlation coefficient, in a randomly drawn sample the detected correlation coefficient does not exceed $r = .34$. The power of 80% to detect an existing correlation is only given when the real correlation exceeds $r = .80$ and with sample size of around 100 participants, or when the real correlation approximates $r = 1$ and the participant number exceeds 64. This indicates that the power in this study to detect a correlation between BOLD in the functional anterior insula and insular GABA+ was very low, given the noise of the measures. As noted above, the noise estimation of the BOLD contrast %SC was strict, assuming that the value should be constant over time. This power analysis probably underestimates power slightly, but illustrates an important issue. As a comparison, we ran the same simulation using the more repeatable contrast $SPIDERS > fixation$. Figure 8.2 (bottom) shows the results. Here, with a sample size like ours (N = 29), power of 80% can already be reached with a real correlation of .65. With a true correlation of 1, the average detected correlation is .80. This indicates again, that the comparison to fixation cross baseline for this paradigm seems to be less noisy and more powerful, but it is still harder to interpret than the contrasts to neutral conditions.

8.3 Conclusions

The aim of this thesis was to investigate the relationship between fearfulness, GABA concentration and fear-related BOLD responses. We assumed a trait fearfulness and that GABA concentration and fear-related BOLD responses are relatively stable over time, being potential predispositions for clinical disorders characterized by a high level of fear. Repeatability studies conducted in the context of the thesis suggest that how stable the variables actually are over time depends on the way they are measured. For example stability of the BOLD responses depended on the emotion paradigm used, contrast used and region of interest used (Chapters 2 and 3). Repeatability of the GABA measures

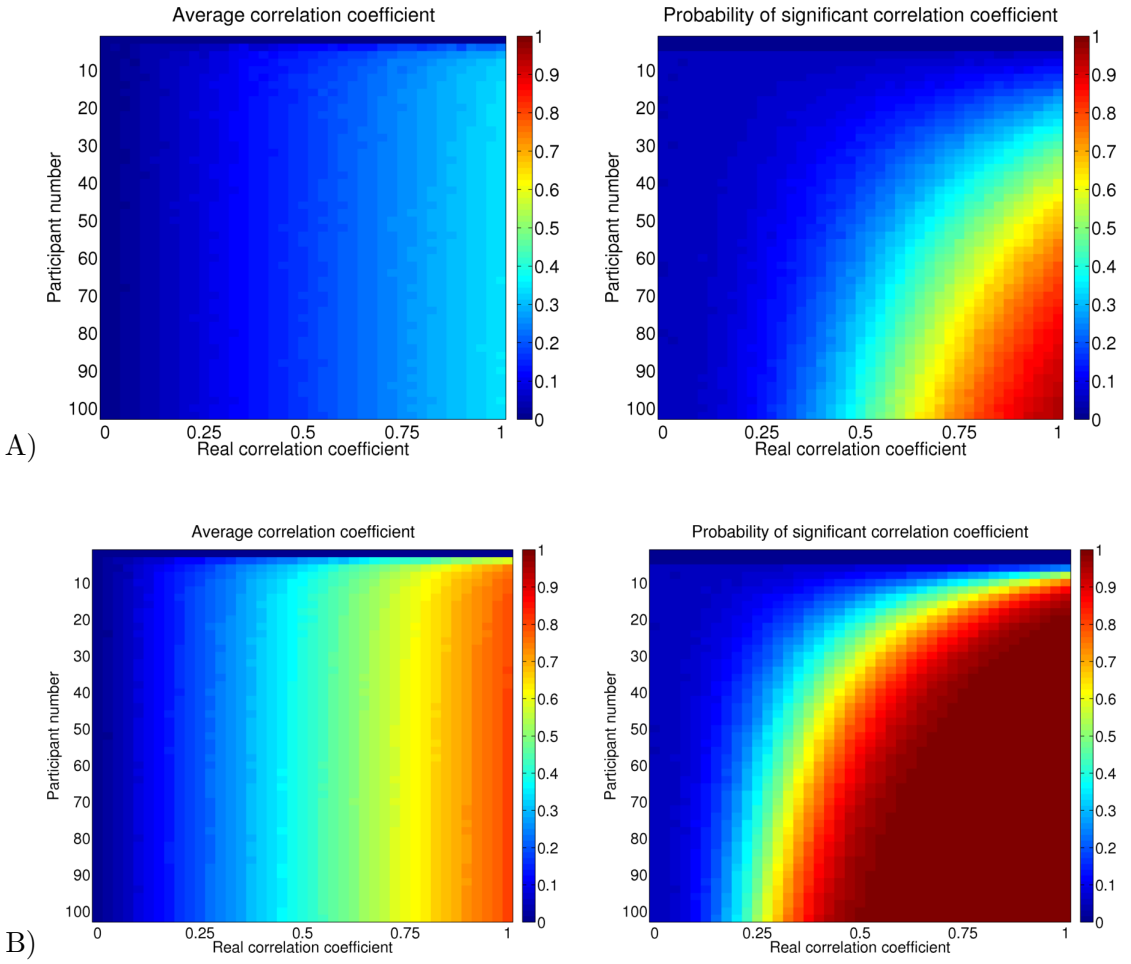

Figure 8.2: Simulations for GABA+-BOLD correlation. Left plots: average detected correlation coefficients in randomly drawn samples (with sample sizes between 0 and 100 [y-axis] from a simulated population with true effect sizes between $r = 0$ and $r = 100$ [x-axis]. For each scenario, 100000 iterations were run. Right plots: probability of detecting a significant correlation, using the same data. Row A) Simulations were done for BOLD %SC of the contrast $SPIDERS > ANIMALS$ in the fear-specific functional ROI in the left anterior insula. Row B) Simulations were done for BOLD %SC of the contrast $SPIDERS > fixation$ in the fear-specific functional ROI in the left anterior insula.

depended on the criterion for excluding participants based on data quality (Chapter 9). Measures of fearfulness have previously shown to be temporally stable, but we had to exclude a number of participants for inconsistent answers on the questionnaires. All these findings suggest that our variables of interest are potentially trait variables, but measures of the variables are characterized by a considerable amount of noise. Post-hoc power analyses described above demonstrate that in order to correlate noisy measures as ours with each other, big sample sizes are needed.

The main conclusions from this thesis are summarized as follows: a) FMRI task construction and analysis influences the repeatability of the BOLD %SC measures, and the BOLD response associated with the emotional content of the stimuli does not seem to be a repeatable measure. b) The BOLD response to pictures independent of emotional content contrasted to fixation cross baseline is influenced by non-neural factors such as physiological reactions to the task, which is why physiological noise correction is recommended. c) Physiological reactions to the task are dependent on fearfulness, however, they do not explain the influence of fearfulness on BOLD responses in the anterior insula. d) GABA+ in a region correlates with task-related BOLD responses and functional connectivity of that region, however, interpretation of such correlations is restricted by the unspecificity of the GABA+ measure. e) Due to noise in measures such as BOLD responses and GABA+ measures studies using these measures, are likely to be limited in terms of power. Issues with power of this and of previous studies might be the reason for some of the conflicting findings.

This does not mean that research in this field should not be continued. Recently, a lot of effort is being made in improving GABA MRS measures (e.g. Evans et al., 2013; Harris et al., in press), and in understanding and correcting for non-neuronal sources of variance in the BOLD signal (e.g. Bright and Murphy, 2013b). It is likely that the trend to measure with higher field strengths will also contribute to the improvement of some of the measures used in this study. When conducting projects aimed at investigating individual differences and trait measures it is highly recommended to estimate noise in the data and repeatability of the measures, in order to be able to assess the power and to be aware of the limitations of any resulting study.

Part V

Appendix: Methodological explorations

Chapter 9

Measuring GABA: Repeatability of GABA+ concentration measures in the insula and dorsolateral prefrontal cortex

9.1 Abstract

There is an increasing body of research relating inter-individual differences in behaviour and clinical symptoms to GABA+ concentration in frontal brain regions. These regions (such as the insula and DLPFC) can be prone to low signal-to-noise ratio and increased artefacts, due to the effect of magnetic field inhomogeneity. Although data quality can be variable, we still lack consensus on objective criteria to evaluate whether a spectrum is "good enough" to provide a reliable GABA+ concentration measure. In this study, we aim to demonstrate how excluding spectra based on different criteria affects the repeatability of GABA+ concentration measures.

We collected GABA+ spectra in the left insula and left DLPFC from 44 females between 18-27 years of age. For each participant, two spectra (9 min. acquisition time each) from each voxel were obtained within one scanning session. Voxels were placed based on anatomic landmarks. Additionally, 14 participants underwent a second scanning session following the same protocol. Spectra were acquired on a 3T MR scanner, using MEGA-PRESS spectral editing. The GABA+ data was analysed in Gannet.

We compared exclusion criteria that were based on two data quality indices: the fit error (%) of GABA+ (standard deviation of fit residuals / GABA+ peak height), and expert ratings of spectrum quality. For spectra that met the applied criterion, within-session and between-session repeatability was estimated using the intraclass correlation coefficient (ICC) and the coefficient of variance (CV). Within-session repeatability was lower than previously reported repeatability estimates for the occipital voxel, but and could be increased with very strict exclusion criteria. Between-session repeatability was calculated over the averaged concentration measures over two runs, and turned out higher than within-session repeatability, suggesting that increasing the number of acquisition runs can improve repeatability. Furthermore, expert ratings seemed to be more sensitive measures of data quality than fit error.

Our findings support the assumption that GABA+ spectra obtained from the insula and DLPFC are noisy and show low repeatability when data is not carefully inspected with regard to data quality. Based on our results we recommend applying strict quality control and acquiring and averaging over several spectra if GABA+ concentration in the insula and DLPFC are of interest.

9.2 Introduction

GABA is the brain's major inhibitory neurotransmitter, released by interneurons in order to establish a balance between excitation and inhibition (Buzsaki, 2006; Isaacson and Scanziani, 2011). Pharmacological, genetic and animal studies found evidence that GABA metabolism and transmission is altered in psychiatric disease, such as schizophrenia (e.g. Guidotti et al. 2005). MRS, a method based on magnetic resonance imaging, obtains GABA concentration measures from human brains in vivo. Scientists have started applying this method to address clinical questions and GABA MRS measures have successfully been linked with psychiatric symptoms (e.g. Ham et al. 2007; Rosso et al. 2014) and even personality traits (e.g. Boy et al. 2011).

But even though GABA MRS has proven a very useful tool, several limitations are hard to overcome. Firstly, because of the low signal-to-noise ratio (SNR), spatial resolution is very low compared to other MRI methods. A typical spectroscopy voxel is about 3 x 3 x 3 cm^3 big, making the measures quite unspecific with regard to the region of interest. Secondly, the placement of the voxel in a participant's brain is done by the researcher using anatomical landmarks, but due to differences in size and shape of individuals' brains, the part of the brain covered by the voxel varies between participants. Thirdly, data quality is sensitive to field inhomogeneity. Most studies place the voxel in the occipital lobe, which yields spectra of good quality (Puts and Edden, 2012). Obtaining GABA measures from other, more inhomogeneous, areas such as the insular and prefrontal cortex can lead to noisy spectra and artefacts.

Currently, no clear guidelines exist for excluding bad quality spectra, and the process varies between studies. In some papers the exclusion criterion is not even reported (e.g. Streeter et al., 2005). The most commonly stated criterion is based on the Cramer bound, an index calculated by some, but not all, analysis packages. Even though it might be a reasonable indicator for data quality (Cavassila et al., 2001), we do not know how good a spectrum has to be so that the researcher can confidently use it for answering questions about the brain. Particularly for studies investigating the relationship between GABA concentration and other measures, it is crucial that inter-individual differences are due to actual differences in GABA concentration and not measurement error. The extent to which this requirement holds true can be estimated by looking at the repeatability of the measures - given the assumption that what one is trying to measure is stable over the retest interval.

A number of studies have assessed repeatability of GABA spectroscopy across different

regions by comparing variance between participants to variance within participants, using the coefficient of variation (CV_{within}, $CV_{between}$), and the intraclass correlation coefficient (ICC) which quantifies the ratio of between-subject variance to total variance (Shrout and Fleiss, 1979). GABA obtained from the occipital voxel seems to be repeatable (Evans et al., 2010), while for the DLPFC somewhat lower repeatability has been reported (Evans et al., 2013; O'Gorman et al., 2011; Wijtenburg et al., 2013).

In this study, we directly addressed the question '"How good is good enough?"'. We measured GABA+ (GABA coedited macromolecules) concentration in the insula and the DLPFC, twice in each region and each participant. Our aim was to assess overall data quality, using two repeatability indices, the intraclass correlation coefficient (ICC) and the coefficient of variation (CV). We assessed within-session and between-session repeatability (by asking some participants back for a second scanning session). Then we applied exclusion criteria to the aquired spectra based on subjective expert ratings, and on the objective GABA+ fit error, and looked at the effect of the strictness on repeatability of the remaining data. Our aim was to find the exclusion criterion that brings the best balance between retaining sample size and obtaining satisfying repeatability. Furthermore, we investigated the similarity of voxel placement between participants.

9.3 Methods

9.3.1 Participants and GABA+ acquisition

For this repeatability study, the data from the main project was used (see Chapter 4). All 44 participants were considered for this analysis.

For the first session, one participant did not produce a second insula scan, and three participants did not produce a second DLPFC scan. During the second session, one participant did not produce a second insula scan. Spectra with fit error above 20% were excluded from all analyses, as were spectra with GABA+ estimation of > 3 i.u. (> 0.5 i.u. for GABA+/Cr) since they turned out to be outliers in all repeatability analyses. This left 33 participants with two GABA+ spectra for the DLPFC voxel, and 36 participants with two GABA+ spectra for the insula voxel.

9.3.2 Anatomical overlap of voxels

We calculated the amount of anatomical overlap between a participant's spectroscopy voxel with the spectroscopy voxels from the same region of all other participants. The

Table 9.1: Reliability of spectrum rating. Intra-rater reliability for Rater1(R1) and Rater2(R2), and inter-rater reliability calculated by ICCs are shown as well as the correlation between the ratings and the fit error, and between the ratings on the three-point and five-point scale.

	3 point scale	5 point scale
ICC_{intra}	.85 (R1), .84 (R2)	.92 (R1), .84 (R2)
ICC_{inter}	.77	.81
Correlation with fit error	$r = -.53$	$r = -.50$
Correlation between scales	$r = .90$	

percent overlap was calculated by dividing the volume shared between both spectroscopy voxels by the average number of volume of the two spectroscopy voxels. Therefore, for each participant, 43 overlaps were calculated and averaged. This was done for data from the first scanning session only.

The anatomical mask for the left insula was taken from the WFU-PickAtlas (Version 3.0.4, Wake Forest University, School of Medicine, Winston-Salem, North Carolina, www.ansir.wfubmc.edu). Insula coverage was estimated by dividing the volume shared between spectroscopy voxel and insula mask, by 2123 (volume of insula mask [in voxels]). In order to assess the percentage an individual's spectroscopy voxel that is filled by the insula, the shared volume between spectroscopy voxel and anatomical insula was divided by the volume of the spectroscopy voxel. This was done for session 1. This procedure could not be performed for the DLPFC since there is no equivalent mask.

9.3.3 Data quality indices

Ratings were performed on two different rating scales in order to investigate whether a broader classification system has an advantage. Two expert raters rated the unfitted spectra twice on each of the scales, independently from each other. Using a 3 point scale, the images were rated on the scale from 0 (*unusable*), 1 (*borderline*), 2 (*good*). The 5 point scale compromised the classifications 1 (*unusable*), 2 (*borderline*), 3 (*average*), 4 (*good*), 5 (*very good*). Intra- and inter-rater reliability were high for both the 3 point, and the 5 point scale. The scales correlated highly with each other (Table 9.1). For futher analysis the 5 point scale was used. Figure 9.1 shows examples for spectra rated as *unusable*, *average*, and *very good*, respectively.

The second indicator of data quality used was the fit error of the GABA+ peak model fit, as provided by Gannet. It constitutes the standard deviation of the fit residuals of the GABA+ fit and water fit. For the analysis with GABA+/Cr, a combined fit error of GABA+ and Creatin peak was used.

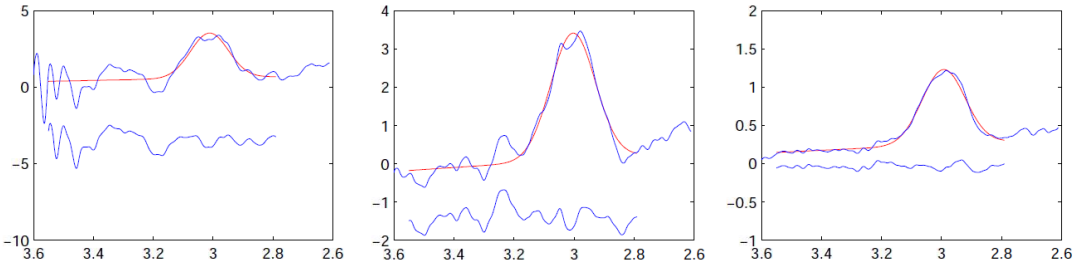

Figure 9.1: Examples for spectrum ratings. Shown are examples for spectra rated as *unusable* (left), as *average* (middle) and as *very good* (right). The blue line shows the data, the red line the fitted model. The blue line below plots the residuals. X-axis: ppm (GABA+ is located at 3 ppm), y-axis: arbitrary units.

9.3.4 Repeatability estimations

The intraclass correlation coefficient (ICC[3,1]; Shrout and Fleiss 1979) was used as a measure of repeatability. ICCs were interpreted according to commonly used guidelines (Cicchetti, 2001) that classify values of $< .41$ as poor, values between .41 and .59 as fair, values between .60 - .74 as good and values $> .74$ as excellent. Negative ICCs are reported as 0. Within-session ICCs were calculated using single spectra, and ICCs for the average of two spectra (indicates the repeatability of the average of two measures with the given repeatability) were estimated using the Spearman-Brown Prophecy formula: $ICC_{average}$ = 2 * ICC / (1 + ICC).

A CV_{within} were calculated for each person by dividing the standard deviation of the two GABA+ estimates by their mean. CVs_{within} were averaged over all participant to report a single CV_{within} value. $CV_{between}$ was calculated for both sessions (by dividing the standard deviation by the mean of all participants' GABA+ estimates) and averaged over the two sessions.

In order to find a useful exclusion criterion, different thresholds for excluding spectra were applied. For the fit error, thresholds from 1 percent to 20 percent were applied with steps of 0.5. For the ratings, criteria were applied from 1 to 5, with steps of 0.25. All analyses were performed using MATLAB (MathWorks, Natick, MA).

9.4 Results

9.4.1 Within-session repeatability of GABA+ irrespective of data quality

Before excluding spectra, CV_{within} for DLPFC and insula were 12% and 15%, respectively. $CV_{between}$ was 18% for both voxels. ICCs were .11 ($p = .26$) for the DLPFC and ICC =

.18 ($p = .15$) for the insula. Scatter plots are shown in Figure 9.2, with colour and size of the dots indicating the two data quality indices.

9.4.2 Influence of data quality on within-session GABA+ repeatability

For spectra from session 1, mean and std. fiterror were 8.8 (0.19) for the DLPFC, and 9.3 (0.99) for the insula, respectively. Mean ratings were 3.1 (1.2) for the DLPFC, and 2.6 (1.3) for the insula.

We calculated ICC and CVs for different inclusion thresholds, based on both quality indices (see Figure 9.3 and Table 9.2 for all numbers). For the insula, within-session repeatability could not be improved when spectra were excluded based on fit error or ratings. For the DLPFC, applying a strict inclusion criterion based on the fit error led to high (ICC $> .80$) repeatability. Applying strict inclusion criteria also decreased the CV_{within} to $< 10\%$.

Only expert ratings (mean of two spectra) could predict the absolute difference between the two obtained measures (DLPFC: $r[31] = -.48$, $p = .005$; Insula $r[34] = -.39$, $p = .02$), but not fit error (DLPFC: $r[31] = .27$, $p = .13$; Insula $r[34] = .04$, $p = .80$; see Figure 9.4).

Between-session repeatability of GABA+

Between-session repeatability was estimated based on the 14 participants who came for a second scanning session. For participants who had two spectra per session passing the applied exclusion criterion, the concentration estimate was averaged. Before excluding spectra, CV_{within} for DLPFC and insula was 12% and $CV_{between}$ was 17% for both voxels. ICCs were .09 ($p = .39$) for the DLPFC and ICC = 0 for the insula. Again, we calculated ICC and CVs for different inclusion thresholds, based on both quality indices (see Figure 9.5 and Table 9.3 for all numbers). For both, DLPFC and insula, significant ICCs $> .80$ were obtained when exclusion was based on expert ratings.

Results for GABA+/Cr

The same analyses were performed using GABA+ with Creatin as a reference. It turned out that larger between-subject variance was observed for both the insula and the DLPFC (see Supplementary Tables E.1 and E.2, and Figure E.1). Results are fairly similar, apart from that fairly high ICCs were obtained for the insula when rating criteria were applied (however, the CV_{within} was still above 10% for these cases). Again, between-session repeatability was higher for DLPFC and insula when the spectra rated worst were excluded.

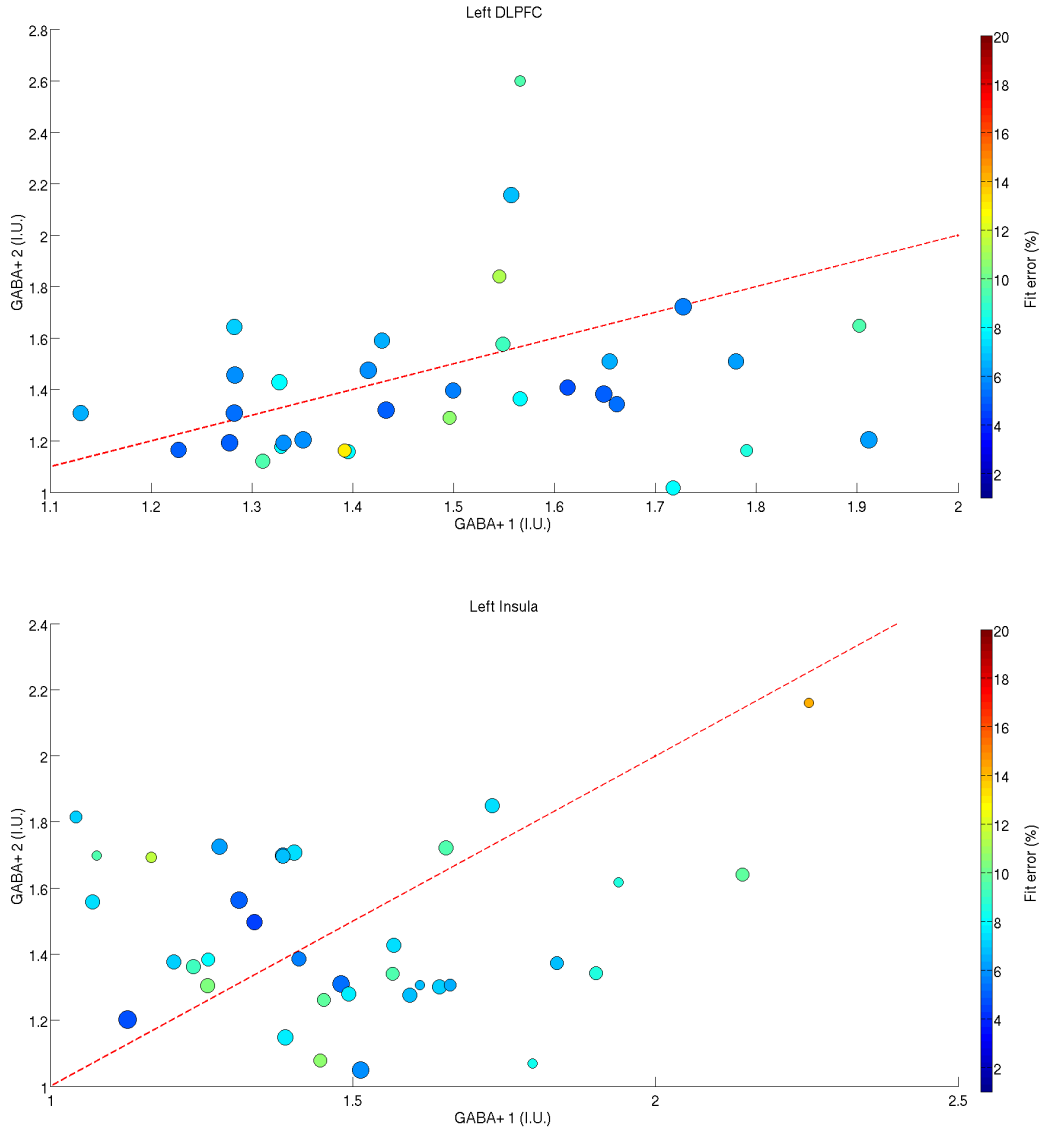

Figure 9.2: Within-session repeatability. Scatter plot of GABA+ measure obtained in run 1 with GABA+ measure obtained in run 2 (top: DLPFC, bottom: insula). The colour of the dot refers to the mean fit error, the size of the bubble to the mean rating (the bigger, the better rated the spectrum quality). The red line indicates the ideal slope of data.

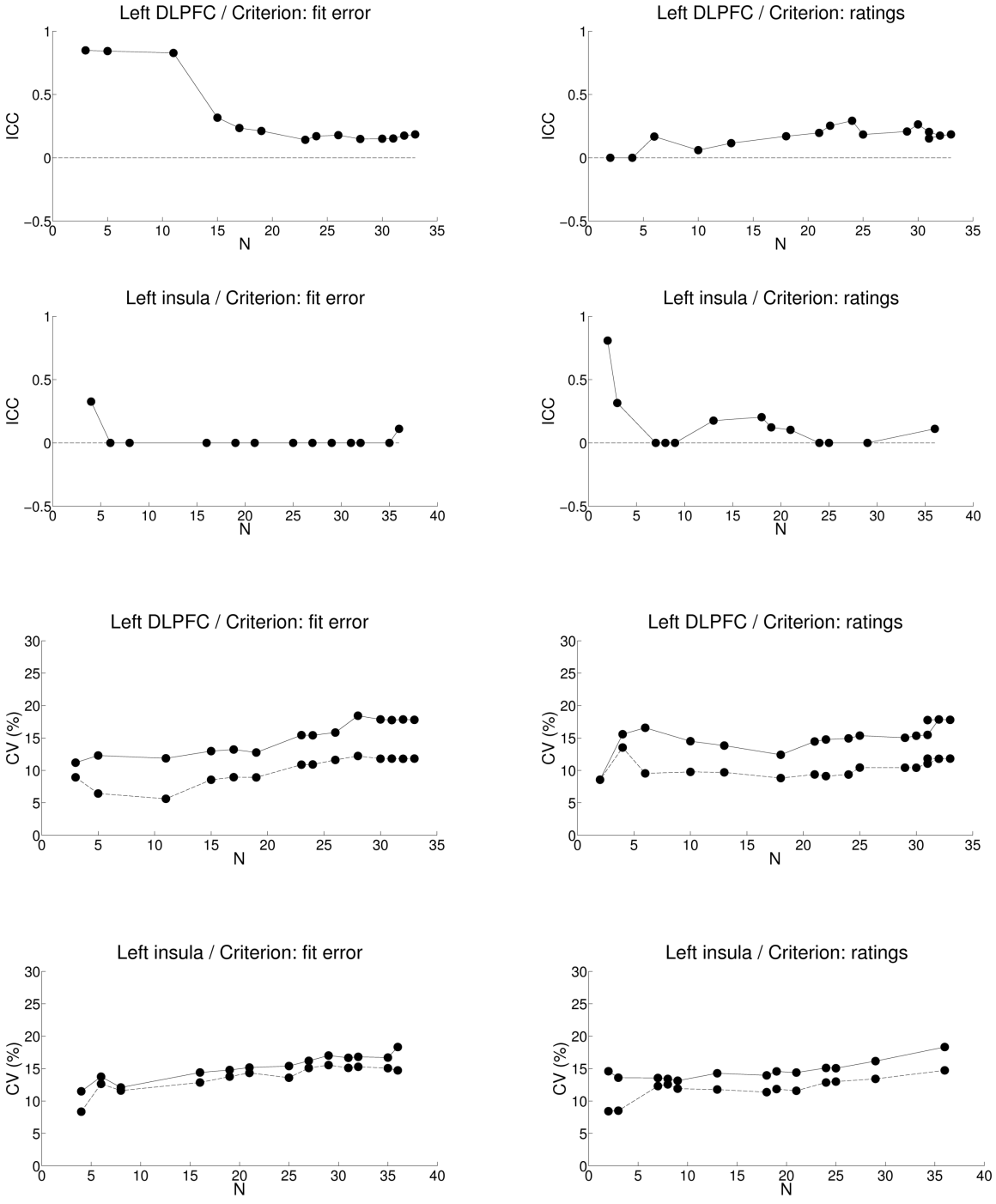

Figure 9.3: Within-session repeatability dependent on spectrum exclusion criteria. Plotted are within-session ICCs (top plots) and CVs (bottom plots) as a function of the number of participants retained in the sample after excluding spectra based on fiterror (left plots) or ratings (right plots). Dashed lines show CV_{within}, non-dashed lines $CV_{between}$.

Table 9.2: Within-session repeatability dependent on spectrum exclusion criteria. For each exclusion criterion (top rows: based on fit error; bottom rows: based on ratings), the number of remaining participants, the ICC and its significant value, as well as CV_{within} and $CV_{between}$ based on the remaining sample are shown. ICC(av) refers to the estimated ICC for averaged measures (based on Spearman-Brown).

Fit error

	DLPFC						Insula					
thr.	N	ICC	p(ICC)	ICC(av)	CV_{ws}	CV_{bs}	N	ICC	p(ICC)	ICC(av)	CV_{ws}	CV_{bs}
20.0	33	0.18	0.15	0.31	11.82	17.80	36	0.11	0.26	0.20	14.73	18.33
19.5	33	0.18	0.15	0.31	11.82	17.80	36	0.11	0.26	0.20	14.73	18.33
19.0	33	0.18	0.15	0.31	11.82	17.80	36	0.11	0.26	0.20	14.73	18.33
18.5	33	0.18	0.15	0.31	11.82	17.80	36	0.11	0.26	0.20	14.73	18.33
18.0	32	0.18	0.16	0.30	11.79	17.85	36	0.11	0.26	0.20	14.73	18.33
17.5	32	0.18	0.16	0.30	11.79	17.85	36	0.11	0.26	0.20	14.73	18.33
17.0	32	0.18	0.16	0.30	11.79	17.85	36	0.11	0.26	0.20	14.73	18.33
16.5	32	0.18	0.16	0.30	11.79	17.85	36	0.11	0.26	0.20	14.73	18.33
16.0	32	0.18	0.16	0.30	11.79	17.85	36	0.11	0.26	0.20	14.73	18.33
15.5	32	0.18	0.16	0.30	11.79	17.85	36	0.11	0.26	0.20	14.73	18.33
15.0	32	0.18	0.16	0.30	11.79	17.85	36	0.11	0.26	0.20	14.73	18.33
14.5	32	0.18	0.16	0.30	11.79	17.85	35	0.00	N.A.	0.00	15.06	16.70
14.0	32	0.18	0.16	0.30	11.79	17.85	35	0.00	N.A.	0.00	15.06	16.70
13.5	31	0.15	0.20	0.26	11.82	17.76	35	0.00	N.A.	0.00	15.06	16.70
13.0	31	0.15	0.20	0.26	11.82	17.76	32	0.00	N.A.	0.00	15.28	16.81
12.5	31	0.15	0.20	0.26	11.82	17.76	32	0.00	N.A.	0.00	15.28	16.81
12.0	30	0.15	0.21	0.26	11.80	17.86	32	0.00	N.A.	0.00	15.28	16.81
11.5	30	0.15	0.21	0.26	11.80	17.86	31	0.00	N.A.	0.00	15.10	16.67
11.0	28	0.15	0.22	0.26	12.22	18.43	29	0.00	N.A.	0.00	15.54	17.01
10.5	28	0.15	0.22	0.26	12.22	18.43	27	0.00	N.A.	0.00	15.09	16.20
10.0	26	0.18	0.19	0.30	11.61	15.84	25	0.00	N.A.	0.00	13.60	15.39
9.5	24	0.17	0.21	0.29	10.91	15.42	21	0.00	N.A.	0.00	14.33	15.16
9.0	23	0.14	0.25	0.25	10.88	15.44	21	0.00	N.A.	0.00	14.33	15.16
8.5	23	0.14	0.25	0.25	10.88	15.44	19	0.00	N.A.	0.00	13.76	14.78
8.0	19	0.21	0.19	0.35	8.92	12.76	16	0.00	N.A.	0.00	12.86	14.40
7.5	17	0.24	0.17	0.38	8.95	13.22	8	0.00	N.A.	0.00	11.61	12.09
7.0	15	0.32	0.12	0.48	8.55	12.97	6	0.00	N.A.	0.00	12.65	13.75
6.5	11	0.83	0.00	0.91	5.62	11.86	6	0.00	N.A.	0.00	12.65	13.75
6.0	5	0.84	0.02	0.91	6.43	12.30	4	0.33	0.30	0.49	8.36	11.50
5.5	3	0.85	0.08	0.92	8.93	11.19	1	N.A.	N.A.	N.A.	N.A.	N.A.
5.0	0	N.A.	N.A.	N.A.	N.A.	N.A.	1	N.A.	N.A.	N.A.	N.A.	N.A.

Rating

	DLPFC						Insula					
thr.	N	ICC	p(ICC)	ICC(av)	CV_{ws}	CV_{bs}	N	ICC	p(ICC)	ICC(av)	CV_{ws}	CV_{bs}
1.0	33	0.18	0.15	0.31	11.82	17.80	36	0.11	0.26	0.20	14.73	18.33
1.2	32	0.18	0.16	0.30	11.79	17.85	29	0.00	N.A.	0.00	13.42	16.16
1.5	31	0.20	0.13	0.34	11.04	15.48	25	0.00	N.A.	0.00	13.00	15.06
1.8	30	0.26	0.08	0.42	10.41	15.35	24	0.00	N.A.	0.00	12.86	15.10
2.0	29	0.21	0.14	0.34	10.42	15.03	21	0.10	0.32	0.19	11.58	14.39
2.2	25	0.18	0.18	0.31	10.44	15.36	19	0.12	0.30	0.22	11.85	14.57
2.5	24	0.29	0.08	0.45	9.36	14.94	18	0.20	0.20	0.34	11.37	13.95
2.8	22	0.25	0.12	0.40	9.11	14.76	13	0.18	0.27	0.30	11.78	14.28
3.0	21	0.20	0.19	0.33	9.37	14.46	9	0.00	N.A.	0.00	11.91	13.13
3.2	18	0.17	0.24	0.29	8.82	12.41	8	0.00	N.A.	0.00	12.57	13.41
3.5	13	0.12	0.35	0.21	9.70	13.83	7	0.00	N.A.	0.00	12.30	13.56
3.8	10	0.06	0.43	0.11	9.77	14.50	3	0.32	0.34	0.48	8.51	13.60
4.0	6	0.17	0.36	0.29	9.54	16.57	3	0.32	0.34	0.48	8.51	13.60
4.2	4	0.00	N.A.	0.00	13.52	15.58	2	0.81	0.20	0.89	8.43	14.60
4.5	2	0.00	N.A.	0.00	8.57	8.56	1	N.A.	N.A.	N.A.	N.A.	N.A.
4.8	1	N.A.	N.A.	N.A.	N.A.	N.A.	1	N.A.	N.A.	N.A.	N.A.	N.A.
5.0	0	N.A.	N.A.	N.A.	N.A.	N.A.	0	N.A.	N.A.	N.A.	N.A.	N.A.

Table 9.3: Between-session repeatability dependent on spectrum exclusion criteria. For each exclusion criterion (top rows: based on fit error; bottom rows: based on ratings), the number of remaining participants, the ICC and its significant value, as well as CV_{within} and $CV_{between}$ based on the remaining sample are shown. ICC(av) refers to the estimated ICC for averaged measures (based on Spearman-Brown).

Fit error

	DLPFC						Insula					
thr.	N	ICC	*p*(ICC)	ICC(av)	CV_{ws}	CV_{bs}	N	ICC	*p*(ICC)	ICC(av)	CV_{ws}	CV_{bs}
20.0	12	0.09	0.39	0.16	12.16	17.20	14	0.00	N.A.	0.00	11.91	17.01
19.5	12	0.10	0.38	0.18	11.89	17.09	14	0.00	N.A.	0.00	11.91	17.01
19.0	12	0.10	0.38	0.18	11.89	17.09	14	0.00	N.A.	0.00	11.91	17.01
18.5	12	0.10	0.38	0.18	11.89	17.09	14	0.00	N.A.	0.00	11.91	17.01
18.0	12	0.09	0.38	0.17	11.41	16.76	14	0.00	N.A.	0.00	11.91	17.01
17.5	12	0.09	0.38	0.17	11.41	16.76	14	0.00	N.A.	0.00	11.91	17.01
17.0	12	0.09	0.38	0.17	11.41	16.76	14	0.00	N.A.	0.00	11.91	17.01
16.5	12	0.09	0.38	0.17	11.41	16.76	14	0.00	N.A.	0.00	11.91	17.01
16.0	12	0.09	0.38	0.17	11.41	16.76	14	0.00	N.A.	0.00	11.91	17.01
15.5	12	0.09	0.38	0.17	11.41	16.76	14	0.00	N.A.	0.00	11.91	17.01
15.0	12	0.09	0.38	0.17	11.41	16.76	14	0.00	N.A.	0.00	11.91	17.01
14.5	12	0.09	0.38	0.17	11.41	16.76	14	0.00	N.A.	0.00	11.91	17.01
14.0	12	0.09	0.38	0.17	11.41	16.76	14	0.00	N.A.	0.00	11.91	17.01
13.5	12	0.09	0.38	0.17	11.41	16.76	14	0.00	N.A.	0.00	11.91	17.01
13.0	12	0.09	0.38	0.17	11.41	16.76	14	0.00	0.49	0.01	11.80	16.96
12.5	11	0.16	0.31	0.27	10.15	16.59	14	0.00	N.A.	0.00	11.54	16.75
12.0	11	0.16	0.31	0.27	10.15	16.59	14	0.00	N.A.	0.00	11.54	16.75
11.5	11	0.16	0.31	0.27	10.15	16.59	14	0.00	N.A.	0.00	11.54	16.75
11.0	11	0.16	0.31	0.28	10.59	16.91	13	0.00	N.A.	0.00	12.20	18.60
10.5	9	0.22	0.27	0.36	11.47	18.24	13	0.01	0.49	0.01	12.00	17.41
10.0	8	0.20	0.30	0.34	12.30	18.92	13	0.01	0.49	0.01	12.00	17.41
9.5	8	0.20	0.30	0.34	12.30	18.92	13	0.01	0.49	0.02	11.74	17.24
9.0	6	0.41	0.18	0.58	8.09	11.43	13	0.01	0.49	0.02	11.74	17.24
8.5	5	0.42	0.20	0.60	8.04	12.66	13	0.04	0.45	0.08	11.88	17.52
8.0	4	0.42	0.24	0.59	8.50	12.60	11	0.17	0.30	0.29	12.92	20.03
7.5	3	0.48	0.26	0.65	8.36	14.82	10	0.21	0.26	0.35	13.60	20.03
7.0	3	0.48	0.26	0.65	8.36	14.82	9	0.23	0.26	0.38	14.99	20.93
6.5	3	0.58	0.21	0.74	7.37	14.34	6	0.24	0.31	0.38	11.24	14.20
6.0	2	0.95	0.10	0.97	5.33	20.94	5	0.18	0.37	0.30	11.27	14.65
5.5	1	N.A.	N.A.	N.A.	1.17	1.17	2	0.00	N.A.	0.00	12.84	12.82
5.0	1	N.A.	N.A.	N.A.	5.30	5.30	1	N.A.	N.A.	N.A.	12.23	12.23

Rating

	DLPFC						Insula					
thr.	N	ICC	*p*(ICC)	ICC(av)	CV_{ws}	CV_{bs}	N	ICC	*p*(ICC)	ICC(av)	CV_{ws}	CV_{bs}
1.0	12	0.09	0.39	0.16	12.16	17.20	14	0.00	N.A.	0.00	11.91	17.01
1.2	12	0.12	0.35	0.22	11.09	16.72	14	0.00	N.A.	0.00	11.70	16.96
1.5	12	0.12	0.35	0.22	11.09	16.72	14	0.02	0.47	0.04	12.14	18.29
1.8	11	0.26	0.21	0.41	9.61	12.74	13	0.04	0.45	0.07	11.72	17.79
2.0	11	0.26	0.21	0.41	9.61	12.74	13	0.00	N.A.	0.00	13.01	18.54
2.2	10	0.27	0.21	0.43	10.56	13.41	12	0.03	0.46	0.06	12.28	18.28
2.5	8	0.60	0.04	0.75	7.40	14.25	12	0.00	N.A.	0.00	13.29	18.32
2.8	6	0.76	0.02	0.87	6.44	15.73	11	0.11	0.36	0.20	11.62	16.69
3.0	6	0.78	0.02	0.88	6.49	15.90	10	0.13	0.35	0.23	11.06	17.04
3.2	4	0.84	0.04	0.91	6.85	17.83	9	0.33	0.18	0.50	8.35	11.21
3.5	3	0.75	0.12	0.86	8.43	18.13	6	0.82	0.01	0.90	4.77	12.61
3.8	3	0.53	0.24	0.69	10.57	15.64	5	0.67	0.07	0.80	5.80	12.34
4.0	2	0.30	0.40	0.46	14.86	12.03	4	0.01	0.49	0.02	5.43	5.98
4.2	1	N.A.	N.A.	N.A.	6.75	6.75	2	0.00	N.A.	0.00	8.86	2.26
4.5	1	N.A.	N.A.	N.A.	6.75	6.75	2	0.00	N.A.	0.00	8.86	2.26
4.8	0	N.A.	N.A.	N.A.	N.A.	N.A.	1	N.A.	N.A.	N.A.	14.41	14.41
5.0	0	N.A.	N.A.	N.A.	N.A.	N.A.	1	N.A.	N.A.	N.A.	12.23	12.23

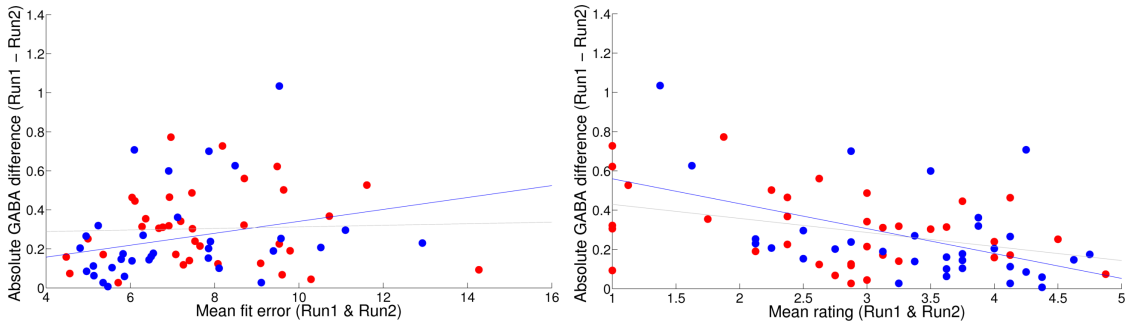

Figure 9.4: Relationship between spectrum quality and within-session difference between measures. Left: Fit error as quality criterion. The mean fit error of both spectra is plotted against the absolute difference between the two obtained GABA+ concentration measures. Right: Expert rating as quality criterion. The mean expert rating of both spectra is plotted against the absolute difference between the two obtained GABA+ concentration measures. Blue dots represent DLPFC data, red dots data from the insula.

Table 9.4: Anatomical overlap between spectroscopy voxels. "Insula coverage" refers to the amount of the anatomical insula covered by the spectroscopy voxel, "percent of voxel filled with insula" refers to the relative volume of the spectroscopy voxel that includes the anatomical insula, "between-participant overlap" refers to the ratio of the spectroscopy voxel overlapping with other participants' voxels on average, "between-session overlap" refers to the overlap between the spectroscopy voxels of a participant that were placed in two different sessions. For each value, minimum (min.), maximum (max.), median and interquartile range (iqr.) are provided. An estimation of between-participant overlap of an occipital voxel was included as a comparison, data was borrowed from (Mikkelsen et al., in preparation).

	Min.	Max.	Median	Iqr.
Insula coverage	39%	89%	70%	11%
Percent of voxel filled with insula	12%	25%	20%	2%
Between-participant overlap DLPFC	35%	71%	62%	9%
Between-participant overlap insula	57%	83%	77%	7%
Between-participant overlap Occipital (N=6)	59%	74%	70%	7.8%
Between-session overlap DLPFC	30%	87%	62%	18%
Between-session overlap Insula	42%	91%	68%	18%

9.4.3 Spectroscopy voxel positioning

Anatomical overlap of spectroscopy voxel position was calculated between participants to see how similar voxel positions are in different participants. Furthermore, we looked at the repeatability of the voxel position by calculating the between-session overlap for participants who came for a second session. Average overlap was 62% for the DLPFC, and 77% for the insula. On average 70% of the anatomical insula were covered by the spectroscopy voxel (see Table 9.4 for all values).

9.5 Discussion

We investigated the within-session and between-session repeatability of GABA+ concentration measures in the left insula and DLPFC, and the influence of different exclusion criteria on the repeatabilty estimates.

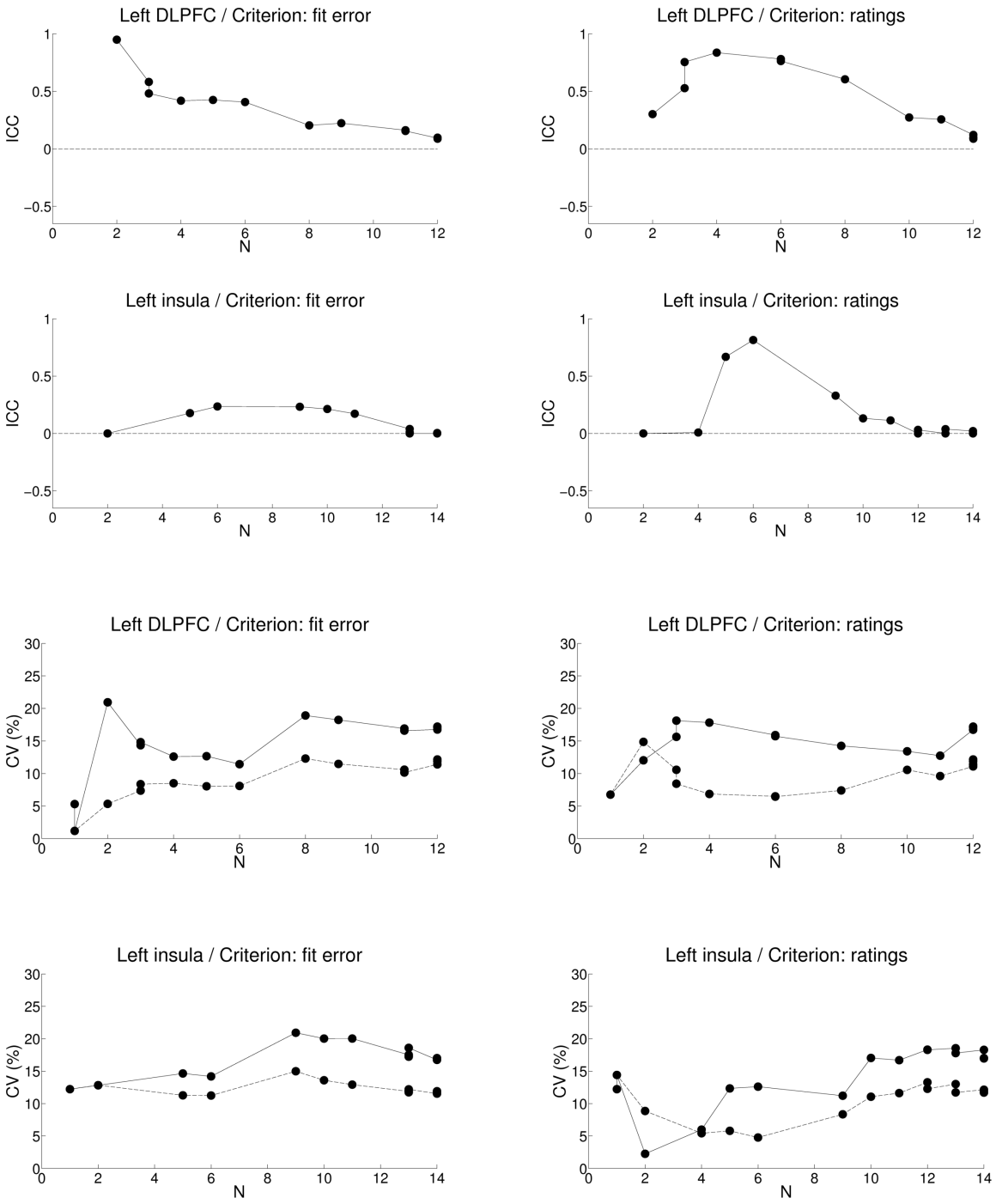

Figure 9.5: Between-session repeatability dependent on spectrum exclusion criteria. Plotted are between-session ICCs (top plots) and CVs (bottom plots) as a function of the number of participants retained in the sample after excluding spectra based on fiterror (left plots) or ratings (right plots). Dashed lines show CV_{within}, non-dashed lines $CV_{between}$. If both spectra of a participant and session met the inclusion criteria, the GABA+ estimate for this participant was averaged across the two spectra.

9.5.1 Within-session repeatability of GABA+

Repeatability was estimated using CVs, as well as ICCs. CVs_{within} give an indication of measurement error by calculating the variance of multiple measures within a person. Small CVs_{within} indicate that similar measures were acquired within a person. If inter-individual differences are investigated, the average CV_{within} should be lower than the $CV_{between}$ (which gives an indication of variance between participants). When all data sets were included, we found CV_{within} of 12% for the DLPFC, and of 15% for the insula. The CV_{within} were lower than the $CV_{between}$ (18% for the DLPFC and insula), but higher than CVs_{within} that were previously reported for the occipital lobe (4%, Mikkelsen et al., in preparation; 10%, Robson, 2012; 6.5%, Evans et al., 2010), the ACC (9%, Napolitano et al., 2013; 15% Mikkelsen et al., in preparation).

Three studies have estimated CVs for GABA in the DLPFC using a MEGA-PRESS sequence, reporting values of 12% (O'Gorman et al., 2011), 12% (Evans et al., 2013) and 13% (Wijtenburg et al., 2013). Latter study estimated GABA rather than GABA+ repeatability using a 7T 8 minute acquisition. These CVs are similar to our estimates. So far, no study has reported CVs_{within} for the insular cortex. Our estimates suggest that repeatability is even lower than in the DLPFC.

In order to be able investigate inter-individual differences in the concentration estimates, the between-participant variance has to significantly exceed the within-participant variance. The ICC provides a quantification of the ratio of between vs. total variance. Even though variance between participants was larger than variance within participants in our measures, retest correlations estimated by the ICC indicated low repeatability of the measures (.18 for the DLPFC, .11 for the insula). In other words, the GABA+ concentration in run 1 could not predict the concentration in run 2, for either of the inspected regions. Previously reported ICCs for the occipital voxel were .77 (Muthukumaraswamy et al., 2012), .64 (Mikkelsen et al., in preparation), for the ACC .79 (Geramita et al., 2011), and .17 (Mikkelsen et al., in preparation). This again suggests that GABA+ concentration estimates are more repeatable in the occipital cortex than in the DLPFC or insula.

9.5.2 Influence of the exclusion criterion on repeatability

We tried to improve repeatability of the measures by excluding bad spectra. Two data quality indices were compared with regard to their usefulness as exclusion criteria: expert ratings of the spectrum quality, and the fit error of the GABA+ peak. Intra- and interrater reliability for the ratings were very high. The ratings showed a medium correlation ($r =$

-.50) with the fit error, confirming a relationship between the two quality indices but also indicating that the ratings were not only based on the shape of the GABA+ peak but also other possible characteristics of the spectrum, such as baseline fluctuations or artifacts. Based on both criteria, we excluded spectra, applying increasingly strict thresholds. Along with the increase in threshold, both CV_{within} and $CV_{between}$ showed declining values, suggesting that some of the variance between participants is caused by measurement error. For the DLPFC, a CV_{within} below 10% was only achieved when 30-40% of participants were excluded from analysis, for the insula this was only achieved after excluding 90% of participants (This has to be interpreted with caution, however, since the confidence of the estimates also decreases with the decrease of sample size). With regard to the ICC, for the DLPFC, a significant ICC of above $> .40$ was only obtained when the spectra of 2/3 of participants were excluded from analysis, using an exclusion of 6.5% fit error. For the insula, independently of how strict the exclusion criteria were, the threshold of .40 was not even met with the strictest inclusion criteria. Again, since sample size decreases with strictness of the criterion, this might be partly due to decreased power in the repeatability estimation.

Even though we used fairly standard aquisition methods, our within-session repeatability estimates suggests that obtaining a GABA+ concentration with a 9 minute acquisition does not yield in a GABA+ concentration measure that is a useful correlate to other variables, unless very strict exclusion criteria are applied to the spectra. Otherwise most of the variance in the measure is caused by within-subject variance, so external variables can not account for much of the variance anymore.

9.5.3 Between-session repeatability of GABA+

It is not clear whether increasing the length of aquisition would always lead to better data quality and repeatability. Increased scan duration could also lead to increased motion artifacts and scanner drift (Harris et al., in press) throughout the session. Therefore, it might be beneficial to acquire two spectra and average the obtained concentration estimate. We calculated within-session repeatability with a single spectrum, and only estimated how much repeatability would increase when two spectra are averaged (using the Spearman-Brown Prophecy formula). We then went on to calculate the actual repeatabilty of averaged values for the proportion of participants who came for a second scanning session. Again, without exclusion of spectra, between-session repeatability as measured

by the ICC was around 0, and CVs comparable to what was found for within-session repeatability.

When spectra were then excluded based on different thresholds, ICCs were somewhat larger than it was the case for within-session repeatability, however, due to the smaller sample size, significance was harder to reach. When excluding based on ratings, for both the insula and DLPFC, significant ICCs of $> .80$ (indicating "excellent repeatability") were reached when about 50% of participants were excluded. Even though this suggests that very strict inclusion criteria are needed to obtain repeatable GABA+ estimates, the increased ICCs as compared to the within-session ICCs indicates that averaging over several spectra does increase repeatability. Even more so when the limitations to the between-session comparison are taken into consideration, such as the shift in voxel position and potential day-to-day fluctuations of GABA+.

9.5.4 Fit error or expert ratings?

For within-session repeatability, exclusion based on fit errors was more successful for the DLPFC than based on ratings, and unsuccessful for the insula altogether. For between-session repeatability, exclusion based on ratings was able to increase repeatabiliy of the remaining measures for both areas, while exclusion based on fit error was not. When we correlated the absolute difference between the two GABA+ measures obtained during a single session, we only found a correlation with the average rating but not with the average fit error. This suggests that expert ratings are somehow more sensitive in indicating data quality than the fit error. Possibly other characteristics of the spectra than the GABA+ peak fit - such as baseline fluctuation (which does not necessarily have a strong influence on the fit error) - are a better predictor of data quality. The overall better performance suggests that experts inspection of the data might be a good enough indicator for whether a spectrum should be included or excluded. However, the rating scale used in this study ranged from 1 (*unusable*) to 5 (*very good*), and only excluding spectra rated as *unusable* was not sufficient to increase repeatability. Our results suggest that if a CV_{within} below 10% is aimed for, then all spectra have to be rated with an average of 2.5 for the DLPFC, and even higher for the insula. Another obstacle with using expert ratings is that the experience of the rater with different kinds of artifacts will have an influence on the ratings, which is not a problem when objective quality indeces such as the fit error or the Cramer bound are used.

9.5.5 Spectroscopy voxel positioning

The positioning of the voxel can influence variability between subjects and also between-session repeatability. We wanted to estimate the variation in voxel positioning, by calculating the spatial overlap between participants' spectroscopy voxel. It turned out that the overlap was on average 62% for the DLPFC, and 77% for the insula. This is comparable to an estimation based on a different dataset for the occipital voxel (average of 70%). The limited spatial overlap of tissue covered is due to different head sizes and shapes between participants, but also due to variation caused by the researcher manually selecting the voxel position. Surprisingly, the overlap of two spectroscopy voxels placed in a single participant in two different sessions was similar to between-participant overlap (DLPFC: 62%, insula: 68%), which suggests that this manual placing is somehow arbitrary and not only dependent on the participant's brain. This variation in placement can have an impact in the interpretation of data. In this case, the amount of insular cortex covered by the spectroscopy voxel varied form 39% to 90%, and on average only 20% of the voxels' volume was actually insular cortex. This somewhat restricts the interpretation of the spatial origin of the spectrum. However, we found good between-session repeatability for high-quality spectra despite low repeatability of the voxel position. It is therefore possible that the shift of the voxel position does not have a strong influence on the GABA+ estimation, possibly due to similar concentrations in surrounding tissue.

9.5.6 Limitations and future directions

We reported low within-session repeatability for GABA+ estimates in the DLPFC and insula. In our analyses we assumed that repeatability is mainly a measure of reliability, however, we cannot exclude the possibility that low frequency GABA+ fluctuations contribute to the within-participant variability. There is some evidence that GABA+ can be experimentally manipulated (Hasler et al., 2010; Michels et al., 2012). However, if actual GABA+ fluctuations are responsible for low repeatability, then GABA+ concentration is not very useful as a marker for individual differences anyway. The fact that repeatability was better after applying very strict inclusion criteria, and after averaging over two spectra suggests, however, that at least a big proportion of the low repeatability is due to data quality and noise.

We only investigated the influence of two quality indices on repeatability, and it is possible that other indices such as the Cramer bound, or SNR etc. perform better in predicting the difference between two measurements. Depending on the data analysis

method and package, different quality measures are provided. The advantage of expert ratings is that they can be applied independently of the analysis package, but on the other hand ratings are more subjective and might be dependent on the experience of the rater. More advanced objective algorithms to determine data quality based on different spectral criteria could be very useful for researchers without a lot of experience.

We looked at GABA+ measures. Recently, more and more studies apply macromolecule suppressed acquisition to obtain a purer measure of GABA (e.g. Aufhaus et al. 2013). A recent study demonstrated comparable repeatability of the GABA+ and GABA measures (Mikkelsen et al., in preparation) in the occipital lobe. However, high repeatability for GABA+ in the occipital voxel has been frequently reported, and MM suppression might only be beneficial to repeatability in more problematic areas, such as the DLPFC and insula. Therefore, it remains to be discovered whether MM suppression leads to higher repeatability in these regions.

We found that in order to assure high repeatability of the GABA+ measures very strict inclusion criteria have to be applied. However, this substantial data loss is not feasable in most cases because scanning is expensive, and recruitment can be challenging, especially when clinical populations are investigated. Rather than post-hoc exclusion of spectra, it would be beneficial to identify predictors for spectrum quality measurable prior to the spectroscopy acquisition, and to find ways to assure good spectrum quality during the scan (e.g. by selectively applying advanced shimming procedures). In the case of DLPFC, head and ventricle size are potential predictors for spectrum quality since small head movements could cause skull and cerebrospinal fluid contribution to the signal. Individually changing the voxel size could help overcome difficulties related to these factors.

We reported the number of participants included after applying different exclusion thresholds. This number referred to the number of participants who produced two spectra meeting this threshold. Even though the quality of spectrum 1 can predict quality of spectrum 2 (fiterror retest correlation $r = .42$, $p = .0002$, retest correlation ratings $r = .60$, $p < .0001$), the number of participants with one spectrum meeting the criterion is higher than the number of participants with two matching spectra (see Table E.3 in Supplement). Therefore, acquiring several spectra might also have the advantage that the probability is higher to get at least one meeting a criterion.

9.5.7 Conclusions

GABA+ measures from the insula and DLPFC can be noisy. We show that repeatability of these measures is low when the measure is based on a 9 min. acquisition. Our results suggest that averaging the measures of two subsequent runs yield in more repeatable measures. In order to achieve this quite strict exclusion criteria have to be applied. Therefore, we recommend to acquire several spectra from each person, and average over those with are judged as good by expert raters.

Chapter 10

Agreement and repeatability of vascular reactivity estimates based on a breath-hold task and a resting state scan

10.1 Abstract

FMRI BOLD responses to changes in neural activity are influenced by the reactivity of the vasculature. By complementing a task-related BOLD acquisition with a vascular reactivity measure obtained through breath-holding or hypercapnia, this unwanted variance can be statistically reduced in the BOLD responses of interest. Recently, it has been suggested that vascular reactivity can also be estimated using a resting state scan.

This study aimed to compare three breath-hold based analysis approaches (block design, sine-cosine regressor and CO_2 regressor) and a resting state approach (CO_2 regressor) to measure vascular reactivity. We tested BOLD variance explained by the model and repeatability of the measures. Fifteen healthy participants underwent a breath-hold task and a resting state scan with end-tidal CO_2 being recorded during both. Vascular reactivity was defined as CO_2 - related BOLD %SC / mmHg change in CO_2.

Maps and regional vascular reactivity estimates showed high repeatability when the breath-hold task was used. Repeatability and variance explained by the CO_2 trace regressor were lower for resting state data based approach, which overestimated vascular reactivity. We conclude that breath-hold based vascular reactivity estimations are more repeatable than resting-based estimates are, and that there are limitations with replacing breath-hold scans by resting state scans for vascular reactivity assessment.

10.2 Introduction

The BOLD signal that is acquired during fMRI is commonly used as a measure of neural activity in the brain. The nature of the BOLD signal makes it susceptible not only to changes in neural activity but also depends in part on the reactivity of the cerebrovascular system (for a review see Logothetis and Wandell, 2004). One aspect of this vascular reactivity can be measured by changing the CO_2 content of the blood; CO_2 being a vasodilator. It has been shown that natural fluctuations in CO_2 during a resting state scan coincide with low frequency fluctuations in the BOLD signal (Wise et al., 2004). Furthermore, the BOLD signal following an increase in CO_2 in a region can explain up to 50% of variance between participants in task-related BOLD responses in that region (Kannurpatti et al., 2012; Liu et al., 2013). This confound can cause problems for studies investigating task-dependent BOLD signals, in particular if group differences in vascular reactivity exist, for example, in the case when comparing older and younger participants (Handwerker et al., 2007; Riecker et al., 2003; Thomason et al., 2005).

One approach to this problem is to estimate vascular reactivity in a separate scan and to set up a statistical design that controls for regional or inter-individual differences in vascular reactivity (Murphy et al., 2011). This can reduce unwanted variability between participants, leaving variability that better reflects differences in the neural responses (Liu et al., 2013; Murphy et al., 2011; Thomason et al., 2007). A common way to estimate vascular reactivity is to increase CO_2 by inducing hypercapnia through respiratory challenges (artificially regulating the CO_2 level of the environment) or through breath-hold tasks. With both of these methods, the CO_2 level and as a result the cerebral blood flow (CBF) can be modulated, under the assumption of an unchanged rate of oxygen consumption (Poulin et al., 1996). When breath-hold or respiratory challenges are used to estimate vascular reactivity, the increase in CO_2 leads to wide-spread BOLD responses throughout all of gray matter (e.g. Bandettini and Wong, 1997).

Increasing inspired CO_2 and breath-holding are the most commonly used approaches to measure vascular reactivity, and Kastrup et al. (2001) showed that both yield comparable results. However, there are some problems related to the two methods. Using the respiratory challenge approach is logistically challenging, and not all participants are compliant with the breathing apparatus. Breath-holds are more easily implemented, however, participants may vary in their ability to hold their breath. One way to compensate for performance differences is to record the end-tidal CO_2 and use the traces for modeling the BOLD response (Bright and Murphy, 2013a). Another way of assessing vascular reac-

tivity avoiding this problem has been proposed by Kannurpatti and Biswal (2008). They define a resting state physiological fluctuation amplitude (RSFA) which is calculated as the temporal standard deviation of the BOLD time-series obtained during a resting state scan. This method has been used to scale task-related BOLD responses (e.g. Kannurpatti et al. 2011), and Kannurpatti and Biswal (2008) found very high similarity between RSFA maps and maps showing the temporal standard deviation of the BOLD time-series obtained during breath-hold or a 5 % CO_2 challenge. However, it is not clear whether RSFA is a specific measure of vascular reactivity, since it is ignorant of underlying changes in CO_2 and undoubteldly incorporates BOLD signal changes originating from fluctuations in neural activity rather than purely vasoactive stimulation. During a breath-hold scan the changes in CO_2 are induced and happen during specified periods of time. This gives the researcher several options for modeling the BOLD data. Murphy et al. (2011) compared a number of models with regard to how well they fit a BOLD-timecourse obtained during six cycles of 20 second breath-holds. The simplest model is a block model convolved with the HRF. Another option is a sine-cosine waveform regressor at the task frequency. Using these two models, one assumes that participants follow task instructions and can manage to hold their breath for the specified amount of time. A way to avoid this assumption is to model the end-tidal CO_2 measured during the scan convolved with the HRF. Murphy et al. (2011) found that the sine-cosine model outperforms the block design and that using the recorded CO_2 trace regressor leads to a better model fit than using the sine-cosine regressors, but not in all brain regions. However, when participants vary in their breath-hold performance, the CO_2 regressor can substantially improve the quality of vascular reactivity estimations (Bright and Murphy, 2013a).

If end-tidal CO_2 is acquired during a resting state scan, the CO_2 regressor approach could in principle also be used for resting scan data to evaluate vascular reactivity. This allows to look at CO_2 related BOLD fluctuations and could lead to a more specific measure of vascular reactivity during rest than the temporal standard deviation of the BOLD signal, potentially reducing the confounding effect of fluctuations in neural activity contribution to a vasculare reactivity estimate. In this study, we measured end-tidal CO_2 during a breath-hold task and a resting state scan to obtain scaled BOLD signal changes as vascular reactivity measures (CO_2-related percent change in BOLD / mmHg CO_2; also see Wise et al. 2004). This enabled us to investigate whether the breath-hold approach and the resting state approach result in measures of vascular reactivity, and how well the model established using the CO_2 traces fits the BOLD data.

The model fit gives an indication of the quality of a method used. Another quality index is the repeatability of the obtained results. In a number of studies different ways of breath-hold acquisition are compared with regard to repeatability as measured by inter-trial variability (Magon et al., 2009; Scouten and Schwarzbauer, 2008; Thomason and Glover, 2008). Comparing inter-trial and inter-individual variance over different conditions makes it possible to define the most repeatable condition. The intraclass correlation coefficient (ICC) reflects the ratio between the data variance of interest (between-participant differences) and the total data variance (Shrout and Fleiss, 1979), and has frequently been applied to fMRI data (Bright and Murphy, 2013a; Caceres et al., 2009). The ICC can be applied to extracted percent signal change from an area of interest, as well as to voxels in order to obtain an estimate of spatial repeatability (repeatability of the signals spatial distribution; e.g. Lipp et al. 2014). Magon et al. (2009) applied a similar approach to breath-hold data, calculating Pearson's correlation coefficient over the t values of all voxels in the gray matter. Mean correlations in the 11 participants for a 21 second long breath-hold was .70, which indicates good repeatability (Cicchetti, 2001). Recently, Bright and Murphy (2013a) reported high repeatability of spatial maps as well as locally extracted averages of vascular reactivity when end-tidal CO_2 regressors were used to analyse breath-hold data.

The aim of this study was to compare the vascular reactivity estimates obtained during breath-holding and during rest on three levels: the estimates in %SC / mmHg CO_2, the model fit of the CO_2 regressor and between-session repeatability of the vascular reactivity maps and regionally averaged vascular reactivity. To allow direct comparison to previous studies, we also included measures of temporal standard deviation (RSFA and temporal standard deviation of the BOLD timeseries during breath-holding) in the analysis. Furthermore, we aimed to investigate whether between-session repeatability is influenced by the model used to analyse the breath-hold data (block design vs. sine-cosine regressor vs. CO_2 regressor). An additional aim of this study was to establish the minimum number of breath-hold cycles needed to obtain repeatable vascular reactivity maps.

10.3 Methods

10.3.1 Sample

Fifteen (8 male) participants with a mean age of 24 (range: 21-28) voluntarily took part in the study. They underwent the same scanning protocol twice with a mean interval of

23 days (range: 15-34). One participant was excluded from analysis due to problems with the acquired CO_2 trace. All participants gave written consent. The study was approved by the Cardiff University School of Medicine Research Ethics Committee.

10.3.2 Breath-hold task

The breath-hold task was adapted from Murphy et al. (2011). During the task, breathing instructions were presented on the screen, guiding the participant through six cycles of breath-holding and recovery, each with four different phases: paced breathing (alternating breathing in and breathing out for 3 s each) for 18 s, end-expiration breath-holding for 15 s, exhalation, and final recovery (spontaneous breathing with no breathing instructions) for 15 s. The task took 5 minutes to complete. End-expirational breath-hold was chosen because it has been shown that a shorter breath-hold duration is needed to obtain the same signal changes, and because the inspiration before a breath-hold varies between participant with regard to depth and intrathoracic pressure which introduces additional variability (Kastrup et al., 1998; Thomason and Glover, 2008).

10.3.3 Image acquisition

The participants underwent gradient-echo echo-planar imaging at 3 T (GE HDx MRI System) with a T_2* weighted imaging sequence (TR = 3 s, TE = 35 ms, receive-only head coil). 140 volumes were acquired during the resting state period, 108 during the breath-hold task. The breath-hold task was presented using Presentation (Neurobehavioral Systems, Albany, CA) and rear-projected onto a screen behind the participant's head that was visible through a mirror mounted on the head RF coil. The orientation of the axial slices was parallel to the AC-PC line. During the resting state period, participants were presented with a black screen and instructed to keep their eyes open and to relax.

A T1 weighted whole-brain structural scan was also acquired for purposes of image registration (1 x 1 x 1mm resolution, 256 x 256 x 176 matrix size). The structural image was only acquired during session 1, and this image was used for registration for the functional images of session 1 and session 2.

10.3.4 CO_2 recordings

During both scanning sessions end-tidal CO_2 and end-tidal O_2 were recorded using a nasal cannula attached to rapidly responding gas analysers (AEI Technologies, PA) to provide representative measures of changes in arterial partial pressures of both gases.

10.3.5 Image data analysis

The acquired data were preprocessed using FEAT (FMRIB Expert Analysis Tool, v5.98, www.fmrib.ox.ac.uk/fsl, Oxford University, UK). Preprocessing steps before model fitting were applied to each participant's timeseries, and included: highpass filtering of the data (100 s temporal cutoff), non-brain removal using BET (Smith, 2002), MCFLIRT motion correction (Jenkinson et al., 2002), spatial smoothing with a Gaussian kernel of full-width-half-maximum 5 mm and fieldmap-based EPI unwarping using PRELUDE + FUGUE (Jenkinson, 2003, 2004); for one person this was not performed due to problems during the acquisition of the fieldmaps. Functional images were registered using FLIRT (Jenkinson and Smith, 2001) in a first step to the structural image with 6 degrees of freedom, and in the second step to the Montreal Neurological Institute (MNI) space with 12 degrees of freedom and FNIRT non-linear (10 mm) warp (Andersson et al., 2007a,b). First-level analysis of the breath-hold task was performed in three different ways using different sets of regressors: 1) a boxcar regressor with a lag of 9 s, 2) a sine and cosine wave at the task frequency (0.02 Hz) and 3) the recorded CO_2 trace (HRF convolved) including a temporal derivative (Murphy et al., 2011). The resting state data were analysed with the recorded CO_2 (convolved with a HRF) trace as a regressor, also including a temporal derivative. The CO_2 traces were temporally filtered by FEAT for both, the breath-hold and the resting state analysis. We will refer to these approaches as BH_{Block}, $BH_{\text{Sine-cosine}}$, $BH_{\text{CO2 trace}}$ and $Resting_{\text{CO2}}$.

10.3.6 RSFA calculation

To create RSFA maps, the temporal standard deviation of the BOLD timeseries was calculated for each voxel (Kannurpatti and Biswal, 2008) for the resting state data. This was performed after all the preprocessing steps described above. To be able to compare results to previous studies, the temporal standard deviation of the BOLD timeseries was also calculated for the breath-hold scan. We will refer to these approaches as $Resting_{\text{RSFA}}$ and BH_{Tsd}.

10.3.7 Estimation of the model fit

The coefficient of determination (R^2) was used as an estimation of how well the applied model fits the data. This measure gives an indication of the amount of variance in the timeseries explained by the applied model. For each of the analysis methods and each participant, an R^2 map was calculated by applying the following equation to each voxel:

$$\frac{MSS_{time-series} - MSS_{residuals}}{MSS_{time-series}}$$

, whereby the mean sum of squares (MSS) was calculated by squaring and temporally summing over the demeaned time series and residual time series, respectively. For each participant, the median R^2 was extracted from gray matter over the whole brain as well as for gray matter within a number of anatomical masks selected from the WFU-PickAtlas (Version 3.0.4, Wake Forest University, School of Medicine, Winston-Salem, North Carolina, www.ansir.wfubmc.edu).

10.3.8 Calculation of the BOLD %SC / mmHg CO_2

For each analysis method, the residuals after model fitting were subtracted from the preprocessed time series in order to obtain a model-fitted timeseries. To estimate the BOLD %SC per unit change of CO_2, the robust range of this fitted BOLD timeseries was divided by the temporal mean and multiplied by 100 (to get %SC), and then divided by the robust range of the HRF convolved CO_2 trace (to get %SC / mmHg). In order to minimise the risk of outliers, a robust range was defined as the absolute difference between the 10th percentile and the 90th percentile. The median %SC was then extracted for the gray matter mask and for the additional anatomically defined regions.

10.3.9 Statistical analysis

Repeatability analysis The intraclass correlation coefficient (ICC[3,1]; Shrout and Fleiss 1979) was used as a measure of repeatability. ICCs were interpreted according to commonly used guidelines (Cicchetti 2001; see also e.g. van den Bulk et al. 2013) that classify values of $< .41$ as "poor", values between .41 and .59 as "fair", values between .60 - .74 as "good" and values $> .74$ as "excellent".

In order to determine the repeatability of vascular-reactivity maps, voxel-wise $ICC_{spatial}$ were calculated for each participant separately. This was performed using the %SC/ mmHg maps and all voxels in gray matter. The same approach was used to estimate the agreement between vascular-reactivity maps obtained using different analysis approaches, but for this analysis Pearson correlation coefficients ($r_{spatial}$) were used. All repeatability analyses were performed using in-house MATLAB (MathWorks, Natick, MA) scripts.

Statistical comparisons between analysis methods We compared the extracted median values for R^2, BOLD %SCs, and spatial repeatability ICCs for the three breath-

hold based methods and the resting approach by calculating Friedman's tests, using the function implemented in MATLAB (MathWorks, Natick, MA). This nonparametric test was chosen due to the nature of the values used and due to problems with the assumption for sphericity. Pairwise comparisons were performed, for which uncorrected p values are reported.

10.4 Results

Average vascular reactivity maps and RSFA maps are shown in Figure 10.1.

10.4.1 Model fit

In order to examine the model fit, data from session 1 was used. The amount of variance explained by the four methods was calculated for each participant. There is a significant difference in the variance explained between the methods ($\chi[3] = 23.2$, $p < .0001$, see Figure 10.2a). Pairwise comparisons revealed that the BH_{Block} design explains the BOLD time course significantly worse than the $BH_{\text{Sine-cosine}}$ and the $BH_{\text{CO2 trace}}$ design (BH_{Block} vs. $BH_{\text{Sine-cosine}}$: $p = .0002$, BH_{Block} vs. $BH_{\text{CO2 trace}}$: $p = .0013$). The model fit in the $Resting_{\text{CO2}}$ set is significantly lower than in all breath-hold based approaches ($Resting_{\text{CO2}}$ vs. BH_{Block}: $p = .030$, $Resting_{\text{CO2}}$ vs. $BH_{\text{Sine-cosine}}$: $p = .0075$, $Resting_{\text{CO2}}$ vs. $BH_{\text{CO2 trace}}$: $p = .0075$). No significant difference was found between the $BH_{\text{Sine-cosine}}$ and $BH_{\text{CO2 trace}}$ regressors ($p > .99$).

An example for a model fit for each of the analysis methods is given in Figure 10.3. Since the variance explained by each of the models is expected to differ between regions, the median model fit was extracted on a regional basis as well. In all of the regions, either the sine-cosine or the CO_2 trace model explain the most variance (see Supplementary Figure F.1).

10.4.2 Estimations of vascular reactivity

Estimations for the mean %BOLD / mmHg CO_2 throughout the gray matter differed between analysis methods ($\chi[3] = 22.7$, $p < .0001$). Pairwise comparisons reveal significant differences between all the methods, except for the comparison between $BH_{\text{Sine-cosine}}$ and $BH_{\text{CO2 trace}}$ regressors (BH_{Block}: vs. $BH_{\text{Sine-cosine}}$: $p = .0002$, BH_{Block} vs. BH_{CO2}: $p = .0013$, BH_{Block} vs. $Resting_{\text{CO2}}$: $p = .0075$, $BH_{\text{Sine-cosine}}$ vs. BH_{CO2}: $p > .99$, $BH_{\text{Sine-cosine}}$: vs. $Resting_{\text{CO2}}$: $p = .030$, $Resting_{\text{CO2}}$ vs. BH_{CO2}: $p = .0075$). Estimations are lowest for the BH_{Block} design and highest for the $Resting_{\text{CO2}}$ analysis (see

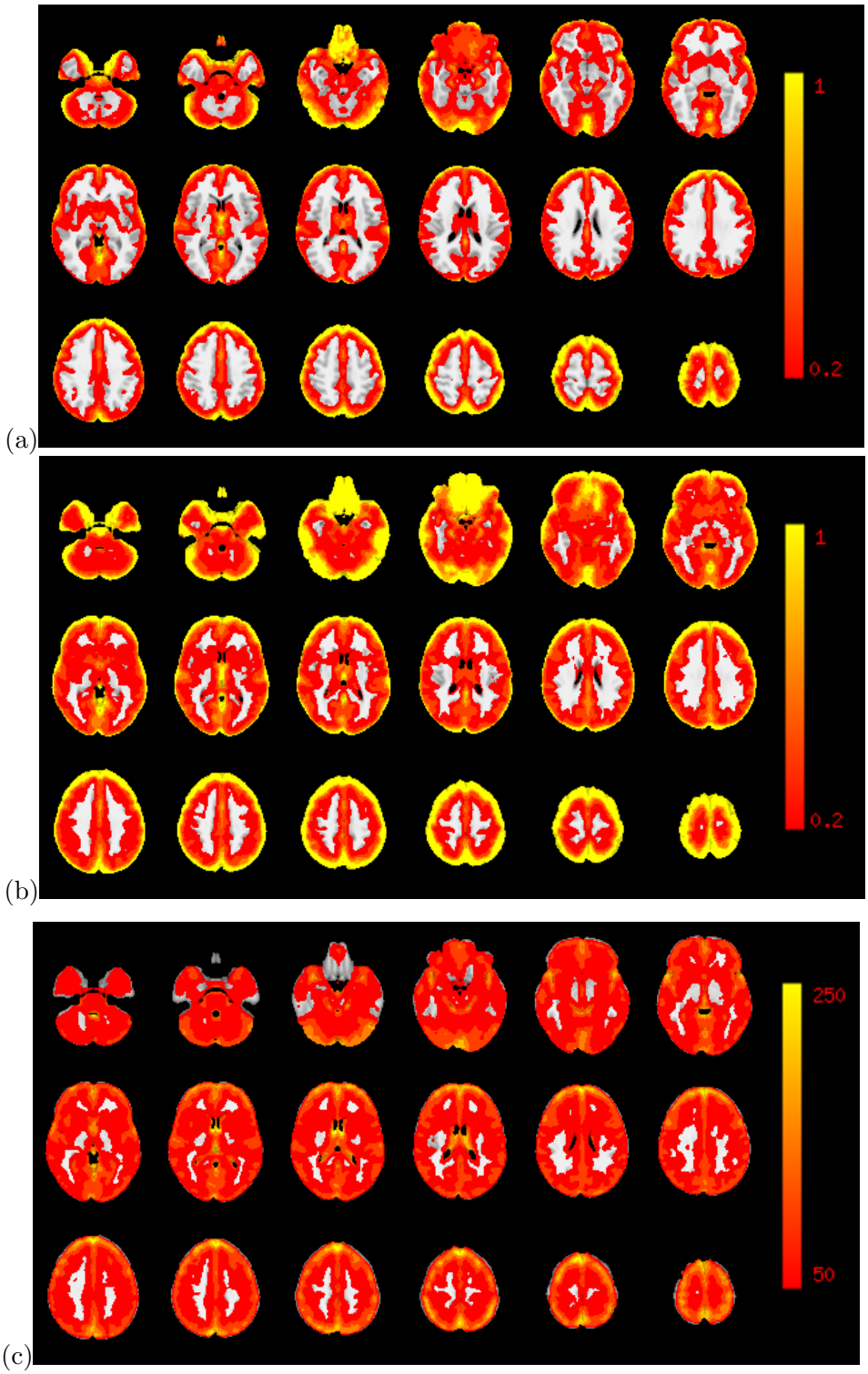

Figure 10.1: Average vascular reactivity maps, calculated with a) the BH_{CO2} method (in % SC / mmHg CO_2), b) the $Resting_{CO2}$ method (in % SC / mmHg CO_2), and c) the RSFA approach (in arbitrary units). The average was calculated over 14 participants.

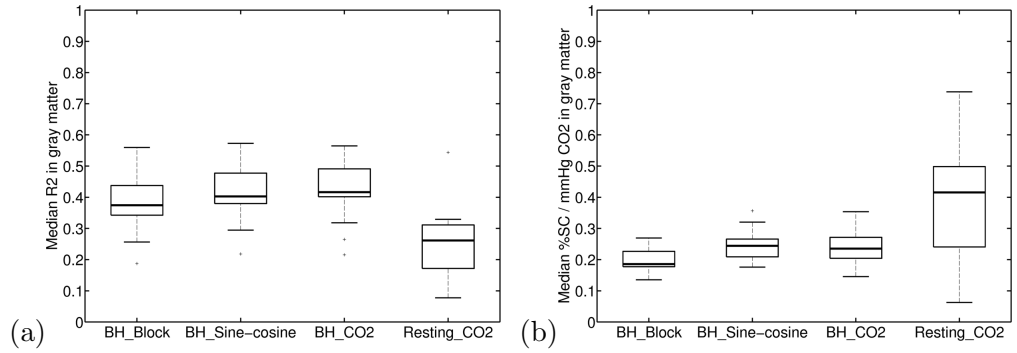

Figure 10.2: a) Comparison of the analysis methods with regard to the model fit as estimated by the median R^2 in gray matter. b) Comparison of the analysis methods with regard to median BOLD % signal change / mmHg CO_2 estimations in gray matter.

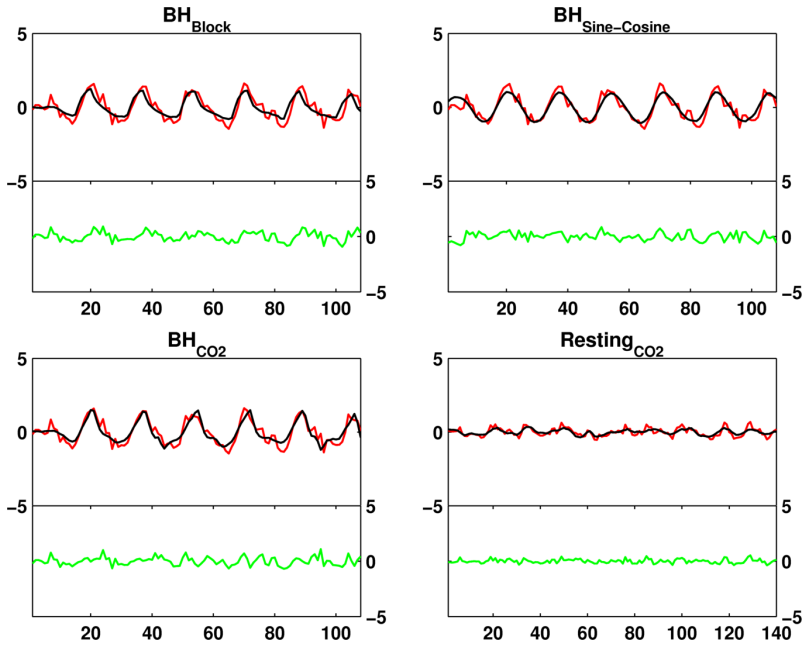

Figure 10.3: For each method an example of a model fit of an average participant is provided. The BOLD timeseries (averaged over the gray matter) is plotted in red, the model in black. Residuals are plotted in green.

Figure 10.2b). This pattern holds true in most of the considered individual regions (see Supplementary Figure F.2). Estimations of the median extracted percent signal change / mmHg CO_2 in the gray matter show high between-participant correlations with each other when the three breath-hold analysis approaches are used. The values obtained with the $Resting_{\mathrm{CO2}}$ are only significantly correlated with the BH_{CO2}, and with the BH_{Tsd} method, while $Resting_{\mathrm{RSFA}}$ does not correlate with any of the breath-hold based approaches (Table 10.1). Scatter plots for all correlations are shown in Supplementary Figure F.3.

Table 10.1: Between-participant Pearson correlation coefficients between the median vascular reactivity estimates (BOLD % signal change / mmHg CO_2) in gray matter obtained through the three breath-hold based approaches (BH_{Block}, $BH_{\text{Sine-cosine}}$ and BH_{CO2}) and the resting state based approach ($Resting_{\text{CO2}}$). Additionally, the two approaches based on the temporal standard deviation of the BOLD signal ($Resting_{\text{RSFA}}$ and BH_{Tsd}) were included to allow direct comparison to findings of previous studies. $^{*}p < .05$ $^{**}p < .001$

	BH_{Block}	$BH_{\text{Sine-cosine}}$	BH_{CO2}	$Resting_{\text{CO2}}$	$Resting_{\text{RSFA}}$	BH_{Tsd}
BH_{Block}	1	.90**	.89**	.44	.19	.49
$BH_{\text{Sine-cosine}}$		1	.86**	.31	.17	.59*
BH_{CO2}			1	.54*	.33	.51
$Resting_{\text{CO2}}$				1	.61*	.49
$Resting_{\text{RSFA}}$					1	.59*
BH_{Tsd}						1

10.4.3 Comparison of vascular reactivity maps obtained during breath-hold vs. resting state scans

In order to quantify agreement between the vascular reactivity maps produced using the breath-hold data vs. the resting state data, the r_{spatial} values between the maps were obtained for session 1 for each person. Vascular reactivity maps created with the BH_{Block} and $BH_{\text{Sine-cosine}}$ regressor show high agreement (median $r_{\text{spatial}} > .97$) with the maps created with the BH_{CO2} regressor in all participants, whereas the maps created using the $Resting_{\text{CO2}}$ show more variable but on average high correspondance to the breath-hold created map (median $r_{\text{spatial}} = .73$, min. $= .60$, max. $= .86$). The $Resting_{\text{RSFA}}$ data set shows only low agreement with the breath-hold based maps (Figure 10.4). However, the two standard deviation based measures ($Resting_{\text{RSFA}}$ and BH_{Tsd}) are highly similar (median $r = .84$, min. $= .68$, max. $= .90$), while the BH_{CO2} and BH_{Tsd} maps only show medium agreement (median $r = .54$, min. $= .29$, max. $= .64$). For the resting state data, the $Resting_{\text{CO2}}$ method and $Resting_{\text{RSFA}}$ maps have very low agreement (median $r = .26$, min. $=$ -.05, max. $= .62$).

If vascular reactivity can be measured with a resting state scan, day-to-day differences in vascular reactivity as measured by breath-hold should correspond to day-to-day differences in vascular reactivity as measured by the resting data. An r_{spatial} was calculated for each person using a day-to-day difference map from BH_{CO2} and $Resting_{\text{CO2}}$ data. The maps did not appear to be related, with a median r_{spatial} of .20 (min. $= .02$, max $= .49$).

10.4.4 Repeatability of vascular reactivity estimates

Repeatability for the median %SC extracted from gray matter is good using the BH_{Block} design (ICC $= .67$, $p = .003$), $BH_{\text{Sine-cosine}}$ (ICC $= .68$, $p = .003$) and using the BH_{CO2} (ICC $= .65$, $p = .004$), and poor using the $Resting_{\text{CO2}}$ data (ICC $= .32$, $p = .12$) but

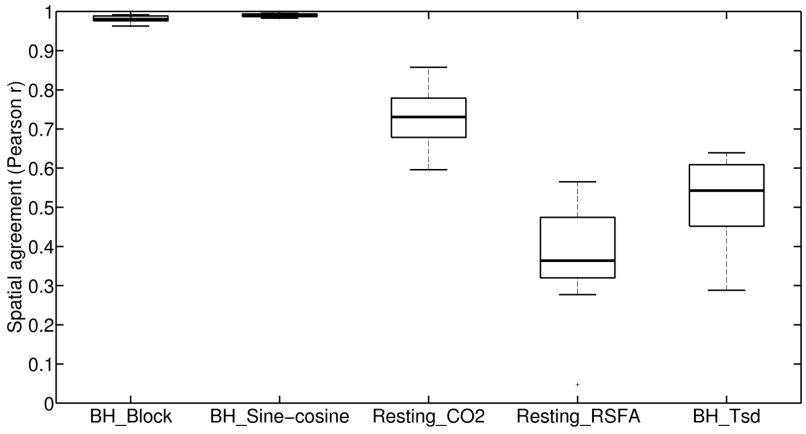

Figure 10.4: Spatial agreement between the vascular reactivity map using BH_{CO2} method and $Resting_{\mathrm{CO2}}$ method. As a comparison, agreement is also plotted between the maps using BH_{CO2} and the maps obtained with the BH_{Block} design and $BH_{\mathrm{Sine\text{-}cosine}}$ regressor.

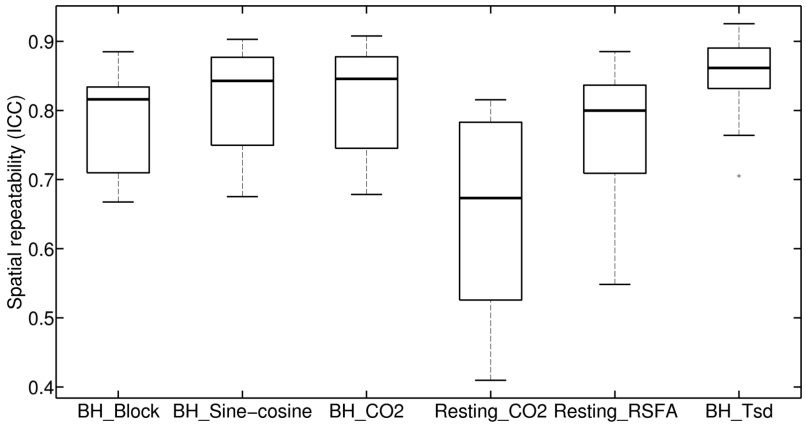

Figure 10.5: Comparison of spatial ICCs of vascular reactivity maps obtained with the six methods. ICCs were calculated over voxels in gray matter only.

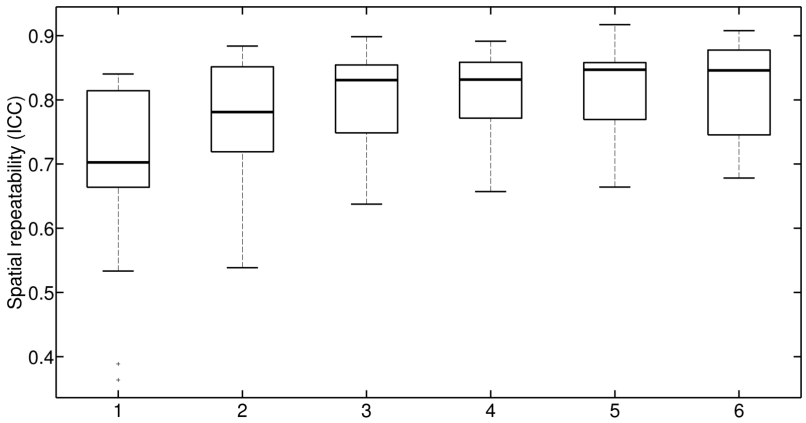

Figure 10.6: Spatial repeatability dependent on how many cycles of breath-hold are included in the analysis. Data for the CO_2 trace regressor are presented.

excellent for the $Resting_{\mathrm{RSFA}}$ data (ICC = .79, $p < .001$. Scatter plots are shown in Supplementary Figure F.4. ICCs were also calculated on a regional level (see Figure 10.7). In most of the regions, either the BH_{Block} or the $BH_{\mathrm{Sine\text{-}cosine}}$ and in some cases the $Resting_{\mathrm{RSFA}}$ data show the highest repeatability.

Spatial repeatability was calculated for each person and each analysis method (see Figure 10.5). Spatial repeatability depends on analysis method ($\chi[3] = 32.4$, $p < .0001$). Pairwise comparisons reveal that highest repeatability is found for the $BH_{\mathrm{Sine\text{-}cosine}}$ and BH_{CO2} models with no significant difference between them. Repeatability is lowest for the resting state data set (BH_{Block} vs. $BH_{\mathrm{Sine\text{-}cosine}}$: $p = .0013$, BH_{Block} vs. BH_{CO2}: $p = .0002$, BH_{Block} vs. $Resting_{\mathrm{CO2}}$: $p = .0013$, $BH_{\mathrm{Sine\text{-}cosine}}$ vs. BH_{CO2}: $p = .29$, $BH_{\mathrm{Sine\text{-}cosine}}$ vs. $Resting_{\mathrm{CO2}}$: $p = .0002$, $Resting_{\mathrm{CO2}}$ vs. BH_{CO2}: $p = .0013$). Spatial repeatability was also calculated for the temporal standard deviation approaches. Repeatability of $Resting_{\mathrm{RSFA}}$ maps was on average excellent, but varied between participants, with some having only fairly repeatable maps. BH_{Tsd} maps showed good to excellent repeatability in all participants.

10.4.5 How many cycles of breath-hold are needed to get reproducible vascular reactivity maps?

Repeatability was calculated for the maps obtained using different numbers of breath-hold cycles included in analysis. The number of cycles significantly influences the $\mathrm{ICC}_{\mathrm{spatial}}$ values obtained ($\chi[5] = 44.7$, $p < .0001$; see Figure 10.6). Comparing subsequent numbers of cycles shows that implementing two cycles yields higher repeatability than one cycle ($p = .0013$), three higher repeatability than two ($p = .0013$), five higher repeatability than four ($p = .030$), but there is no difference between three and four ($p = .59$), or five or six ($p = .29$). Six cycles give a more repeatable estimates than three ($p = .030$) or four ($p = .0013$).

10.4.6 Repeatability of breath-hold performance

In order to examine performance differences between the two sessions, an ICC was calculated for each person over the time course of the CO_2 regressor. A median of ICC = .81 (min. = 26, max. = .93) suggests that performance is highly repeatable in most participants (see Supplementary Figure F.5a). The range of the physiological trace used to scale the BOLD response showed fair repeatability for the breath-hold based approach (ICC = .41, $p = .06$; see Supplementary Figure F.5b) as well as for the resting based approach

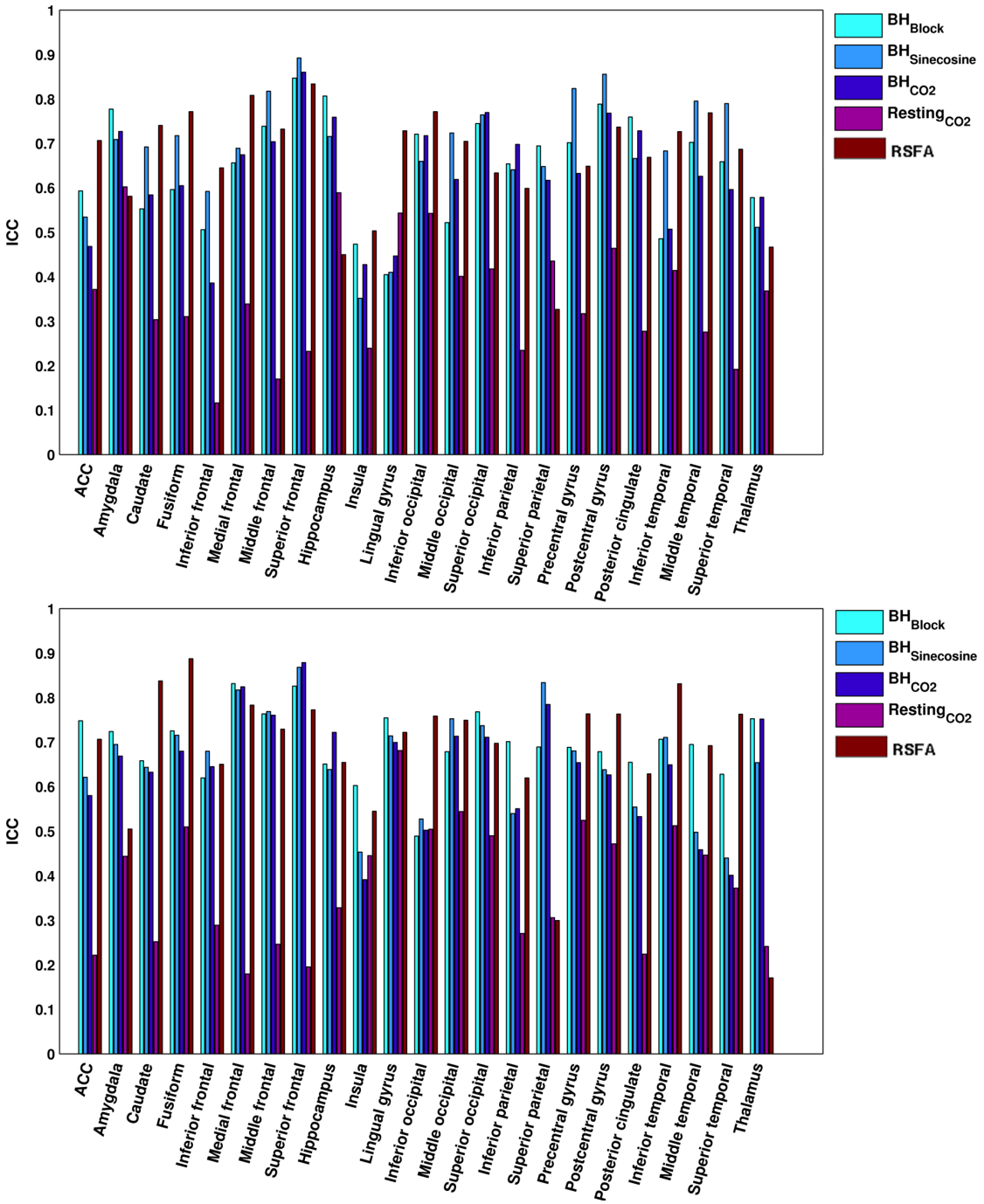

Figure 10.7: The repeatability (ICC) of the estimated vascular reactivity by each of the methods in each region of interest in the left hemisphere (left) and right hemisphere (right). An ICC of < 40 indicates "poor" repeatability, .40-.59 "fair" repeatability, .60-.74 "good" and $> .74$ "excellent" repeatability.

(ICC = .54, p = .02; see Supplementary Figure F.5c), indicating that the extent of CO_2 increase in session 1 only shows a fair relationship to the CO_2 increase in session 2.

10.5 Discussion

In this study, we compared three different ways of analysing a breath-hold scan (BH_{Block}, $BH_{\text{Sine-cosine}}$, and BH_{CO2}) and an approach using resting state data set ($Resting_{\text{CO2}}$) with regard to different aspects of measuring vascular reactivity: model fit of the regressors, repeatability of obtained vascular reactivity maps, and repeatability of regionally extracted vascular reactivity estimates. We compared vascular reactivity maps obtained during the breath-hold scan to the maps obtained during the resting scan to see whether resting state scans could be potential replacements for breath-holds when it comes to estimating vascular reactivity. Additionally, we extracted RSFA ($Resting_{\text{RSFA}}$) and the temporal standard deviation of the breath-hold data (BH_{Tsd}) set to make results directly comparable to previous studies, and to investigate the effects of modeling the data by using recorded CO_2 traces.

10.5.1 Model fit and estimations of vascular reactivity

The model fit of each regressor was assessed by calculating the amount of variance in the BOLD time-series explained by the regressor. In gray matter, the BH_{Block} design accounted for significantly less variance than the $BH_{\text{Sine-cosine}}$ or BH_{CO2} trace regressors, which on average explained about 40 % of the BOLD time-series (min. = 19%). These values are comparable with those previously reported by Murphy et al. (2011). In the resting state data, the CO_2 regressor could on average only explain less than 30 % of the variance (min. 9%) which is also comparable to previous studies (Chang et al., 2009; Wise et al., 2004). Within the gray matter, the amount of variance explained by the models varies substantially between regions, with particularly good model fits in the frontal cortex, and poorer model fits in other regions such as insula and thalamus. Lower model fits for the resting state data than for the breath-hold data were found in most of the considered regions. In other words, the BOLD time-course during rest is not as strongly influenced by CO_2-related physiological changes as it is during the breath-hold scan. This was expected since the change in CO_2 during the breath-hold scan is bigger (median range in CO_2: 8 mmHg) than during a resting scan with no other task-instruction than to relax (median range in CO_2: 2 mmHg). The difference in model fit between breath-hold data and resting

data suggests that the proportion of neuronally-driven fluctuations is higher in the resting state data, which makes it more challenging to measure vascular reactivity.

However, also for the breath-hold task the regressors are not sufficient to explain all variance in the BOLD time-series. For this reason, in order to obtain a measure of vascular reactivity it is important to identify the CO_2 related signals in the BOLD time-course. Estimating vascular reactivity by simply using the temporal fluctuation of the BOLD time-series, as suggested by Kannurpatti and Biswal (2008), gives a good indication of how much the BOLD signal fluctuates but disregards the influence of the source of fluctuation. In this study we used a different approach, by defining vascular reactivity as the amplitude of the model fitted dataset divided by the CO_2 change. This allowed to specifically look at CO_2-related BOLD fluctuations. In regions with high vascular reactivity, a good model fit was obtained. Using a BH_{Block}, fit estimations of vascular reactivity were lower than for the $BH_{\text{Sine-cosine}}$ and BH_{CO2} trace model. The vascular reactivity estimates in BOLD signal change / mmHg CO_2 values are comparable to previous studies (Kastrup et al., 2001; Liu et al., 2013).

The resting state analysis ($Resting_{\text{CO2}}$) - for which model fit was lower than in any of the breath-hold based methods - provided the highest vascular reactivity estimates, which were highly variable between participants. In participants with lower model fit, lower vascular reactivity is estimated; but in participants for which the CO_2 regressor explains a considerable amount of the BOLD timecourse, a small change in CO_2 seems to result in a big change in BOLD, resulting in estimates of vascular reactivity about twice as high as the estimates obtained through breath-holding and higher than previously reported (Wise et al., 2004). Since the same participants were used in both scans, there must be another reason for this difference in estimation than actual differences in vascular reactivity. One explanation for that finding is that in the resting state scan CO_2 fluctuations might be correlated with neuronal fluctuations. This would result in a higher BOLD response than caused by the CO_2 increase only. Confounded neural fluctuations might be related to arousal, which affects the breathing pattern and as a consequence the BOLD response. The over-estimation of vascular reactivity makes it difficult to interpret the findings for the resting state scan and suggests that breath-hold tasks cannot simply be replaced by resting state scans if adequate measures of vascular reactivity are the aim.

10.5.2 Agreement of vascular reactivity measures and maps obtained during breath-hold vs. resting state scans

Kannurpatti and Biswal (2008) found that vascular reactivity maps obtained during a resting scan are very similar to the maps obtained during breath-hold scans, using the temporal standard deviation approach. We replicated this finding using the temporal standard deviations ($Resting_{\mathrm{RSFA}}$ and BH_{Tsd}), however, using the CO_2 modeling approach the agreement between breath-hold and resting state derived maps was slightly lower with a mean correlation of .75. There was no agreement between $Resting_{\mathrm{RSFA}}$ maps and $Resting_{\mathrm{CO2}}$ maps, and only medium agreement between BH_{Tsd} and BH_{CO2} trace maps. This means that temporal standard deviations are not strongly related to the CO_2 modelled data and are probably driven by more than changes in CO_2.

In order to be able to replace breath-hold scans with resting state scans when measuring vascular reactivity, not only the spatial agreement of the resulting maps is required, but also between-participant correlations. This is because vascular reactivity measures are used to decrease between-participant variance. At the participant-level, we found a relationship between the extracted vascular reactivity in gray matter obtained through BH_{CO2} and the $Resting_{\mathrm{CO2}}$ values of $r = .55$. This is similar to what has been reported by Kannurpatti et al. (2012). In comparison, we found correlations of around $> .85$ between the three breath-hold based approaches (however, it has to be noted that these measures were all derived from the same scan). Vascular reactivity measured with the $Resting_{\mathrm{RSFA}}$ method did not correlate significantly with any of the breath-hold based approaches. Another study that looked at the relationship between RSFA and vascular reactivity (as measured by hypercapnia) in the whole-brain found a correlation of .36 (Liu et al., 2013). This correlation coefficient is similar to ours ($r = .33$), which did not reach significance with our sample size. However, the small effect size does indicate vascular reactivity assessed through breath-holding and RSFA are not interchangable.

10.5.3 Repeatability of vascular reactivity estimates and maps

Repeatability was estimated in order to obtain an indication for how reliable and stable the vascular reactivity measures are. Repeatability was calculated for the extracted vascular reactivity (%BOLD / mmHg CO_2) in all considered regions. In most regions, repeatability of breath-hold based vascular reactivity can be classified as good (.60 - .75), while most of the ICCs obtained during the resting state data would be classified as poor or fair ($< .40$ / $< .60$). Which breath-hold resulted in the highest repeatability was region-

dependent, but in most regions the BH_{CO2} regressor resulted in lower repeatability than the BH_{Block} or $BH_{\mathrm{Sine\text{-}cosine}}$ regressors. This was the case even though the model fit for the BH_{CO2} trace regressor was found to be higher than for the BH_{Block} regressor and no different from the $BH_{\mathrm{Sine\text{-}cosine}}$ regressor. It is possible that by recording the CO_2 trace during both sessions, additional measurement error was induced that resulted in slightly lower repeatability. These findings are in contrast with what Bright and Murphy (2013a) reported, comparing a CO_2-based approach with a HRF convolved ramp regressor. However, their study was specifically designed to induce variability in task-performance between participants. In our study most participants managed to hold their breath for 15 seconds without problems, which might be the reason why the CO_2 analysis did not lead to higher repeatabiliy than the other regressors. The vascular reactivity measures obtained with the BH_{Block} or $BH_{\mathrm{Sine\text{-}cosine}}$ regressor are influenced by performance, and performance turned out to be highly repeatable in most participants. This might have led to a boost in repeatability when either of these two regressors are used.

How repeatable the vascular reactivity measures were, varied from region to region. This reflects regional differences in the size and reliability of the vascular reactivity estimates (also reflected by regional differences in the model fit), as well as differences in the stability of vascular reactivity over time. Day-to-day differences in factors such as tiredness or caffeine intake might influence vascular reactivity more in some regions than in others. In some regions, such as the insular cortex (Banzett et al., 2000; Evans et al., 2002) the vascular reactivity measures are likely to be influenced by neural confounds, which might also lead to less reliable estimates of vascular reactivity. Indeed, the insular cortex was the region with the least repeatable estimates in this study.

$Resting_{\mathrm{RSFA}}$ appeared to be highly repeatable in most of the regarded regions. However, due to the lack of agreement with breath-hold based and spatial agreement with $Resting_{\mathrm{CO2}}$ based vascular reactivity, it is unclear what this method actually measures. During the breath-hold, the strong BOLD responses to the task can be assumed to be strongly driven by the arterial CO_2 changes, even though neural aspects of breath-holding might still influence the BOLD signal change to a certain extent (e.g. Banzett et al. 2000; Evans et al. 2002). During the resting state scan, no such intense physiological changes are present. Resting state scans are widely used to assess cognitive networks, assuming the BOLD signal variations largely originate from fluctuations in neuronal activity rather than fluctuations in CBF associated with underlying non-metabolically demanding variations. Even after correcting for physiological changes (such as variations in breathing),

neural networks can still be detected (for reviews see Birn, 2012; van den Heuvel and Hulshoff Pol, 2010). This means, that in the resting state dataset neural aspects are likely to have a bigger influence on the BOLD signal than is the case during breath-hold scans. Using only the temporal standard deviation over the whole time-series makes it impossible to study the source of this signal fluctuation, even though some of the variance can be explained by CO_2 reactivity, as indicated by a medium between-participant correlation between $Resting_{\mathrm{RSFA}}$ and $Resting_{\mathrm{CO2}}$. Also, the amount of physiological BOLD fluctuations - irrespective of the underlying vascular reactivity - might vary between participants, reducing the interpretability of vascular reactivity in resting state data.

The change in CO_2, which directly influences the vascular reactivity estimates, only shows fair repeatability, suggesting that there might be day-to-day differences in the CO_2 increase during breath-holding. An additional analysis was performed to determine the repeatability if BOLD %SCs are not divided by the change in CO_2. ICCs increase for all analyses (BH_{Block}: ICC = .85, $p < .001$; $BH_{\mathrm{Sine\text{-}Cosine}}$: ICC = .63, $p = .006$; BH_{CO2}: ICC = .71, $p = .001$; $Resting_{\mathrm{CO2}}$: ICC = .89, $p < .001$) but most substantially for the $Resting_{\mathrm{CO2}}$ data set. This is an another indicator for the possibility that the CO_2 trace might be confounded with other factors leading to a boost in the BOLD response independent of the actual change in CO_2. Interestingly, not dividing by the CO_2 range also gave slightly better ICC values for the breath-hold related BOLD changes, which indicates that CO_2 measurement error probably does play a role. In this particular sample breath-hold performance and CO_2 changes might not have been variable enough to detect the benefit from recording and using the end-tidal CO_2 trace as reported by (Bright and Murphy, 2013a).

Since repeatability of vascular reactivity values (BOLD signal change / mmHg CO_2) is not only influenced by the quality of the method but also by possible day-to-day differences in vascular reactivity, spatial repeatability of the vascular reactivity maps might be a better indicator for reliability. Also, the performance of breath-hold will affect all voxels in the same way, and repeatability of the maps should be less dependent on day-to-day differences in performance. We found that the BH_{Block} design leads to lower mean spatial repeatability than the $BH_{\mathrm{Sine\text{-}Cosine}}$ or BH_{CO2} trace regressors, but all median ICCs for the breath-hold data sets are above .80 which can be classified as excellent. Spatial repeatability of the vascular reactivity maps using resting state data was very variable between participants, with a median classified as good for the $Resting_{\mathrm{CO2}}$ and a median classified as excellent for the $Resting_{\mathrm{RSFA}}$ analysis. This means that vascular reactivity

maps obtained with resting state data are repeatable in most but not all participants. The lower repeatability in some participants could result from session-to-session differences in what participants were doing during the resting state scans and from activation of different networks on each occasion. This again suggests that resting state data are harder to interpret when it comes to vascular reactivity.

How many cycles of breath-hold are needed to get reproducible vascular reactivity maps?

To answer the question how many cycles are necessary to obtain repeatable vascular reactivity, we analysed the BOLD timeseries several times, each time including a different number of breath-hold cycles. Only including one or two cycles of breath-holding does not result in repeatable maps in most participants. Based on our results, we recommend implementing at least three cycles to guarantee repeatable maps in all participants, when a breath-hold duration of 15 seconds is used. It is possible that using longer duration less cycles are needed, whilst shorter duration more cycles might be necessary.

10.5.4 Limitations and future directions

Even though we obtained good repeatability for regional vascular reactivity estimates, and high spatial repeatability of the maps, we need to be careful with the interpretation of the findings. Other factors than what we addressed as vascular reactivity - such as task performance - can play a role in the repeatability estimates. On one hand, using the BH_{Block} design and $BH_{\text{Sine-cosine}}$ regressors, task-performance plays a big role. If performance is bad, these regressors do not fit the data very well and lead to a unreliable vascular reactivity estimates. This problem is addressed by using the BH_{CO2} regressor, however, in our sample this regressor gave slightly lower repeatability values than the other two breath-hold regressors. In our sample, participants did not have problems performing the task, and the BH_{CO2} method is particularly useful for participants who have problems holding their breath (Bright and Murphy, 2013a). In our study, overall good performance but slight variation between participants might have led to higher repeatability in the performance-dependent regressors.

Another problem that affects all three regressors is the fact that some neural confounds with breath-holding are likely to be present (Banzett et al., 2000; Evans et al., 2002). If this neural activity are repeatable, then vascular reactivity estimates will automatically show higher repeatability as well. Neural confounds are even more likely to affect the

resting state scan, and we have shown over-estimation of vascular reactivity estimates that could be driven by neuronally driven fluctuations coinciding with CO_2 fluctuations. One difference in our estimates in resting state - data based vascular reactivity measures to previous attempts is that we used an eyes-open resting state scan rather than an eyes-closed scan. Eyes-open aquisition has been shown to yield more repeatable resting state networks but no difference in network strength (Patriat et al., 2013). McAvoy et al. (2008) reported higher frequency of CO_2 fluctuations in the eyes-open vs. eyes-closed condition and Peng et al. (2013) found that in the eyes open condition the time lag between change in CO_2 and BOLD response is longer than in the eyes closed condition than in the eyes open condition. However, they reported no significant difference in the model fit of the CO_2 trace on the BOLD timeseries between the two conditions, indicating that both eyes open and eyes closed acquisition can be used to assess vascular reactivity. It is not clear whether the aquisition method (eyes open or closed) has an influence on the repeatability vascular reactivity estimates, and remains to be investigated.

10.5.5 Conclusions

We found good repeatability of vascular reactivity estimates in most of the regions analysed and excellent repeatability of vascular reactivity maps, when the breath-hold scan is used for estimation. Also, at least three breath-hold cycles are necessary in order to obtain repeatable maps.

Analysing the resting state scan with a CO_2 regressor in order to obtain vascular reactivity measures could not compete with the breath-holding with regard to model fit or repeatability. Also, vascular reactivity estimates in % change BOLD / mmHg CO_2 were considerably higher with the resting state analysis, indicating the presence of some neural confounds. Vascular reactivity maps obtained with $Resting_{\mathrm{CO2}}$ and with BH_{CO2} revealed good spatial agreement but % change BOLD / mmHg CO_2 only showed medium correlation, suggesting that it is not straight-forward to replace breath-holding with resting state scans in the assessment of vascular reactivity.

Part VI

References

Bibliography

Abadie, P., Boulenger, J.P., Benali, K., Barré, L., Zarifian, E., Baron, J.C., 1999. Relationships between trait and state anxiety and the central benzodiazepine receptor: a PET study. The European Journal of Neuroscience 11, 1470–8.

Akirav, I., Maroun, M., 2007. The role of the medial prefrontal cortex-amygdala circuit in stress effects on the extinction of fear. Neural Plasticity 2007, 30873.

Alalade, E., Denny, K., Potter, G., Steffens, D., Wang, L., 2011. Altered cerebellar-cerebral functional connectivity in geriatric depression. PloS ONE 6, e20035.

Almeida, J.R.C., Versace, A., Hassel, S., Kupfer, D.J., Phillips, M.L., 2010. Elevated amygdala activity to sad facial expressions: a state marker of bipolar but not unipolar depression. Biol Psychiatry 67, 414–421.

Amstadter, A., 2008. Emotion regulation and anxiety disorders. Journal of Anxiety Disorders 22, 211–21.

Amunts, K., Kedo, O., Kindler, M., Pieperhoff, P., Mohlberg, H., Shah, N.J., Habel, U., Schneider, F., Zilles, K., 2005. Cytoarchitectonic mapping of the human amygdala, hippocampal region and entorhinal cortex: intersubject variability and probability maps. Anatomy and Embryology 210, 343–52.

Andersson, J.L.R., Jenkinson, M., Smith, S.M., 2007a. Non-linear optimisation. FMRIB technical report TR07JA1. .

Andersson, J.L.R., Jenkinson, M., Smith, S.M., 2007b. Non-linear registration, aka Spatial normalisation. FMRIB technical report TR07JA2. .

APA, 2000. Diagnostic and statistical manual of mental disorders. 4th, text revision ed., American Psychiatric Association.

Armfield, J.M., 2006. Cognitive vulnerability: a model of the etiology of fear. Clinical Psychology Review 26, 746–68.

Aslan, S., Xu, F., Wang, P.L., Uh, J., Yezhuvath, U.S., Van Osch, M., Lu, H., 2010. Estimation of labeling efficiency in pseudocontinuous arterial spin labeling. Magnetic Resonance in Medicine 63, 765–771.

Aufhaus, E., Weber-Fahr, W., Sack, M., Tunc-Skarka, N., Oberthuer, G., Hoerst, M., Meyer-Lindenberg, A., Boettcher, U., Ende, G., 2013. Absence of changes in GABA concentrations with age and gender in the human anterior cingulate cortex: a MEGA-PRESS study with symmetric editing pulse frequencies for macromolecule suppression. Magnetic Resonance In Medicine 69, 317–20.

Augustine, J.R., 1996. Circuitry and functional aspects of the insular lobe in primates including humans. Brain Research Reviews 22, 229–244.

Aupperle, R.L., Ravindran, L., Tankersley, D., Flagan, T., Stein, N.R., Simmons, A.N., Stein, M.B., Paulus, M.P., 2011. Pregabalin influences insula and amygdala activation during anticipation of emotional images. Neuropsychopharmacology 36, 1–12.

Baas, J.M.P., Grillon, C., Böcker, K.B.E., Brack, A.A., Morgan, C.a., Kenemans, J.L., Verbaten, M.N., 2002. Benzodiazepines have no effect on fear-potentiated startle in humans. Psychopharmacology 161, 233–47.

Bandettini, P., Wong, E.C., 1997. A hypercapnia-based normalization method for improved spatial localization of human brain activation with fMRI. NMR in Biomedicine 10, 197–203.

Banzett, R.M., Mulnier, H.E., Murphy, K., Rosen, S.D., Wise, R.J., Adams, L., 2000. Breathlessness in humans activates insular cortex. Neuroreport 11, 2117–2120.

Barrett, L.F., Satpute, A.B., 2013. Large-scale brain networks in affective and social neuroscience: towards an integrative functional architecture of the brain. Current Opinion in Neurobiology 23, 361–372.

Baumann, O., Mattingley, J.B., 2012. Functional topography of primary emotion processing in the human cerebellum. NeuroImage 61, 805–11.

Baur, V., Hänggi, J., Langer, N., Jäncke, L., 2013. Resting-state functional and structural connectivity within an insula-amygdala route specifically index state and trait anxiety. Biological Psychiatry 73, 85–92.

Bhagwagar, Z., Wylezinska, M., Jezzard, P., Evans, J., Ashworth, F., Sule, A., Matthews, P.M., Cowen, P.J., 2007. Reduction in occipital cortex gamma-aminobutyric acid concentrations in medication-free recovered unipolar depressed and bipolar subjects. Biological Psychiatry 61, 806–12.

Birn, R.M., 2012. The role of physiological noise in resting-state functional connectivity. NeuroImage 62, 864–70.

Birn, R.M., Diamond, J.B., Smith, M.A., Bandettini, P.A., 2006. Separating respiratory-variation-related fluctuations from neuronal-activity-related fluctuations in fMRI. NeuroImage 31, 1536–48.

Birn, R.M., Murphy, K., Handwerker, D.A., Bandettini, P.A., 2009. fMRI in the presence of task-correlated breathing variations. NeuroImage 47, 1092–104.

Birn, R.M., Smith, M.A., Jones, T.B., Bandettini, P.A., 2008. The respiration response function: The temporal dynamics of fMRI signal fluctuations related to changes in respiration. NeuroImage 40, 644–654.

Bishop, S., Duncan, J., Brett, M., Lawrence, A.D., 2004. Prefrontal cortical function and anxiety: controlling attention to threat-related stimuli. Nature Neuroscience 7, 184–8.

Bishop, S.J., 2009. Trait anxiety and impoverished prefrontal control of attention. Nature Neuroscience 12, 92–8.

Bishop, S.J., Jenkins, R., Lawrence, A.D., 2007. Neural processing of fearful faces: effects of anxiety are gated by perceptual capacity limitations. Cerebral Cortex 17, 1595–603.

Biswal, B.B., Kannurpatti, S.S., Rypma, R., 2007. Hemodynamic Scaling of fMRI-BOLD signal: Validation of low frequency spectral amplitude as a Scalability Factor. Magnetic Resonance Imaging 25, 1358–1369.

Bitsios, P., Philpott, A., Langley, R.W., Bradshaw, C.M., Szabadi, E., 1999. Comparison of the effects of diazepam on the fear-potentiated startle reflex and the fear-inhibited light reflex in man. Journal of Psychopharmacology 13, 226–34.

Blanchard, D.C., Hynd, A.L., Minke, K.A., Minemoto, T., Blanchard, R.J., 2001. Human defensive behaviors to threat scenarios show parallels to fear- and anxiety-related defense patterns of non-human mammals. Neuroscience and Biobehavioral Reviews 25, 761–70.

Boy, F., Evans, C.J., Edden, R.A.E., Lawrence, A.D., Singh, K.D., Husain, M., Sumner, P., 2011. Dorsolateral prefrontal gamma-aminobutyric acid in men predicts individual differences in rash impulsivity. Biol Psychiatry 70, 866–872.

Bradley, M.M., Hamby, S., Löw, A., Lang, P.J., 2007. Brain potentials in perception: picture complexity and emotional arousal. Psychophysiology 44, 364–73.

Brandt, C.A., Meller, J., Keweloh, L., Höschel, K., Staedt, J., Munz, D., 1998. Increased benzodiazepine receptor density in the prefrontal cortex. Journal of Neural Transmission 105, 1325–1333.

Bremner, J., Innis, R.B., White, T., Fujita, M., Silbersweig, D., Goddard, A.W., Staib, L., Stern, E., Cappiello, A., Woods, S., Baldwin, R., Charney, D.S., 2000. SPECT [I-123]iomazenil measurement of the benzodiazepine receptor in panic disorder. Biological Psychiatry 47, 96–106.

Bright, M.G., Murphy, K., 2013a. Reliable quantification of BOLD fMRI cerebrovascular reactivity despite poor breath-hold performance. NeuroImage 83, 559–568.

Bright, M.G., Murphy, K., 2013b. Removing motion and physiological artifacts from intrinsic BOLD fluctuations using short echo data. NeuroImage 64, 526–37.

Britton, J.C., Taylor, S.F., Sudheimer, K.D., Liberzon, I., 2006. Facial expressions and complex IAPS pictures: common and differential networks. NeuroImage 31, 906–19.

Bruce, S.E., Buchholz, K.R., Brown, W.J., Yan, L., Durbin, A., Sheline, Y.I., 2012. Altered emotional interference processing in the amygdala and insula in women with Post-Traumatic Stress Disorder. NeuroImage. Clinical 2, 43–9.

Büchel, C., Dolan, R.J., 2000. Classical fear conditioning in functional neuroimaging. Current Opinion in Neurobiology 10, 219–223.

Button, K.S., Ioannidis, J.P.A., Mokrysz, C., Nosek, B.A., Flint, J., Robinson, E.S.J., Munafò, M.R., 2013. Power failure: why small sample size undermines the reliability of neuroscience. Nature Reviews. Neuroscience 14, 365–76.

Buxton, R.B., Frank, L.R., Wong, E.C., Siewert, B., Warach, S., Edelman, R.R., 1998. A general kinetic model for quantitative perfusion imaging with arterial spin labeling. Magnetic Resonance in Medicine 40, 383–96.

Buzsaki, G., 2006. Rhythms of the Brain. Oxford University Press.

Buzsáki, G., Kaila, K., Raichle, M., 2007. Inhibition and brain work. Neuron 56, 771–83.

Caceres, A., Hall, D.L., Zelaya, F.O., Williams, S.C.R., Mehta, M.A., 2009. Measuring fMRI reliability with the intra-class correlation coefficient. NeuroImage 45, 758–68.

Caesar, K., Thomsen, K., Lauritzen, M., 2003. Dissociation of spikes, synaptic activity, and activity-dependent increments in rat cerebellar blood flow by tonic synaptic inhibition. PNAS 100, 16000–5.

Calder, A.J., Lawrence, A.D., Young, A.W., 2001. Neuropsychology of fear and loathing. Nature Reviews. Neuroscience 2, 352–63.

Cameron, O.G., Huang, G.C., Nichols, T., Koeppe, R.A., Minoshima, S., Rose, D., Frey, K.A., 2007. Reduced gamma-aminobutyric acid A - benzodiazepine binding sites in insular cortex of individuals with panic disorder. Arch Gen Psychiatry 64, 793–800.

Campbell-Sills, L., Simmons, A.N., Lovero, K.L., Rochlin, A.A., Paulus, M.P., Stein, M.B., 2011. Functioning of neural systems supporting emotion regulation in anxiety-prone individuals. NeuroImage 54, 689–96.

Carpenter, P.A., Just, M.A., Reichle, E.D., 2000. Working memory and executive function: evidence from neuroimaging. Current Opinion In Neurobiology 10, 195–9.

Carretié, L., Hinojosa, J.A., Lopez-Martin, S., Tapia, M., 2007. An electrophysiological study on the interaction between emotional content and spatial frequency of visual stimuli. Neuropsychologia 45, 1187–1195.

Carretié, L., Ríos, M., de la Gándara, B.S., Tapia, M., Albert, J., López-Martín, S., Alvarez-Linera, J., 2009. The striatum beyond reward: caudate responds intensely to unpleasant pictures. Neuroscience 164, 1615–22.

Caseras, X., Mataix-Cols, D., Trasovares, M.V., López-Solà, M., Ortriz, H., Pujol, J., Soriano-Mas, C., Giampietro, V., Brammer, M.J., Torrubia, R., 2010. Dynamics of brain responses to phobic-related stimulation in specific phobia subtypes. The European Journal of Neuroscience 32, 1414–22.

Caseras, X., Murphy, K., Mataix-Cols, D., López-Solà, M., Soriano-Mas, C., Ortriz, H., Pujol, J., Torrubia, R., 2013. Anatomical and functional overlap within the insula and anterior cingulate cortex during interoception and phobic symptom provocation. Human Brain Mapping 34, 1220–9.

Catani, M., Dell'acqua, F., Vergani, F., Malik, F., Hodge, H., Roy, P., Valabregue, R., Thiebaut de Schotten, M., 2012. Short frontal lobe connections of the human brain. Cortex 48, 273–91.

Cauda, F., D'Agata, F., Sacco, K., Duca, S., Geminiani, G., Vercelli, A., 2011. Functional connectivity of the insula in the resting brain. NeuroImage 55, 8–23.

Cauli, B., Hamel, E., 2010. Revisiting the role of neurons in neurovascular coupling. Frontiers in Neuroenergetics 2, article 9.

Cauli, B., Tong, X.K., Rancillac, A., Serluca, N., Lambolez, B., Rossier, J., Hamel, E., 2004. Cortical GABA interneurons in neurovascular coupling: relays for subcortical vasoactive pathways. The Journal of Neuroscience 24, 8940–9.

Cavassila, S., Deval, S., Huegen, C., van Ormondt, D., Graveron-Demilly, D., 2001. Cramer-Rao bounds: an evaluation tool for quantitation. NMR in Biomedicine , 278–283.

Chang, C., Cunningham, J.P., Glover, G.H., 2009. Influence of heart rate on the BOLD signal: the cardiac response function. NeuroImage 44, 857–69.

Chang, L.J., Yarkoni, T., Khaw, M.W., Sanfey, A.G., 2012. Decoding the role of the insula in human cognition: functional parcellation and large-scale reverse inference. Cerebral Cortex 23, 739–49.

Chebib, M., Johnston, G.A.R., 1999. The 'abc' of gaba receptors: A brief review. Clinical and Experimental Pharmacology and Physiology 26, 937–940.

Chen, Z., Silva, A.C., Yang, J., Shen, J., 2005. Elevated endogenous GABA level correlates with decreased fMRI signals in the rat brain during acute inhibition of GABA transaminase. Journal of Neuroscience Research 79, 383–91.

Chen, Z.y., Jing, D., Bath, K.G., Ieraci, A., Khan, T., Siao, J., Herrera, D.G., Toth, M., Yang, C., Mcewen, B.S., Hempstead, L., Lee, F.S., 2006. Genetic Variant BDNF (Val66Met) Polymorphism Alters Anxiety-Related Behavior. Science 314, 140–143.

Chia-Feng, L., Shin, T., Hsiu-Mei, W., Wei-Yuan, H., Jen-Chuen, H., Yu-Te, W., 2012. Structural connectivity for human bilateral insulae using diffusion tensor imaging. OHBM Abstract 6432.

Ciampi de Andrade, D., Galhardoni, R., Pinto, L.F., Lancelotti, R., Jr, J.R., Marcolin, M.A., Teixeira, M.J., 2012. Into the Island: A new technique of non-invasive cortical stimulation of the insula Une nouvelle technique de stimulation corticale non invasive de l'insula. Clinical Neurophysiology 42, 363–368.

Cicchetti, D.V., 2001. The precision of reliability and validity estimates re-visited : Distinguishing between clinical and statistical significance of sample size requirements. Journal of Clinical and Experimental Neuropsychology 23, 695–700.

Clare, S., Francis, S., Morris, P.G., Bowtell, R., 2001. Single-shot T2* measurement to establish optimum echo time for fMRI: studies of the visual, motor, and auditory cortices at 3.0 T. Magnetic Resonance in Medicine 45, 930–3.

Cloutman, L.L., Binney, R.J., Drakesmith, M., Parker, G.J.M., Lambon Ralph, M.A., 2012. The variation of function across the human insula mirrors its patterns of structural connectivity: evidence from in vivo probabilistic tractography. NeuroImage 59, 3514–21.

Coelho, C.M., Purkis, H., 2009. The origins of specific phobias: Influential theories and current perspectives. Review of General Psychology 13, 335–348.

Cohen, E.R., Ugurbil, K., Kim, S., 2002. Effect of basal conditions on the magnitude and dynamics of the blood oxygenation level-dependent fMRI response. Journal of Cerebral Blood Flow and Metabolism 22, 1042–53.

Colden, A., Bruder, M., Manstead, A., 2008. Human content in affect-inducing stimuli: A secondary analysis of the international affective picture system. Motivation and Emotion 32, 260–269.

Coombs III, G., Loggia, M.L., Greve, D.N., Holt, D.J., 2014. Amygdala perfusion is predicted by its functional connectivity with the ventromedial prefrontal cortex and negative affect. PloS one 9, e97466.

Costafreda, S.G., Brammer, Michael, J., David, Anthony, S., Fu, Cynthia, H.Y., 2008. Predictors of amygdala activation during the processing of emotional stimuli: A meta-analysis of 385 PET and fMRI studies. Brain Research Reviews 58, 57–70.

Craig, A., 2009. How do you feel–now? The anterior insula and human awareness. Nature Reviews. Neuroscience 10, 59–70.

Craske, M.G., Rauch, S.L., Ursano, R., Prenoveau, J., Pine, D.S., Zinbarg, R.E., 2011. What Is an Anxiety Disorder? Depression and Anxiety 26, 1066–1085.

Critchley, H.D., Wiens, S., Rotshtein, P., Ohman, A., Dolan, R.J., 2004. Neural systems supporting interoceptive awareness. Nature Neuroscience 7, 189–95.

Dagli, M.S., Ingeholm, J.E., Haxby, J.V., 1999. Localization of cardiac-induced signal change in fMRI. NeuroImage 9, 407–15.

Dannlowski, U., Ohrmann, P., Konrad, C., Domschke, K., Bauer, J., Kugel, H., Hohoff, C., Schöning, S., Kersting, A., Baune, B.T., Mortensen, L.S., Arolt, V., Zwitserlood, P., Deckert, J., Heindel, W., Suslow, T., 2009. Reduced amygdala-prefrontal coupling in major depression: association with MAOA genotype and illness severity. The International Journal of Neuropsychopharmacology 12, 11–22.

Darwin, C., 1782. The Expression of the Emotions in Man and Animals.

Davis, M., 1998. Neurobiology of fear responses. The role of the amygdala., in: Salloway, S., Malloy, P., Cummings, J. (Eds.), The Neuropsychiatry of Limbic and Subcortical Disorders. American Psychiatric Press.

Davis, M., Rainnie, D., Cassell, M., 1994. Neurotransmission in the rat amygdala related to fear and anxiety. Trends in Neurosciences 17, 208–14.

Davis, T.L., Kwong, K.K., Weisskoff, R.M., Rosen, B.R., 1998. Calibrated functional MRI: mapping the dynamics of oxidative metabolism. Proceedings of the National Academy of Sciences of the United States of America 95, 1834–9.

Deen, B., Pitskel, N.B., Pelphrey, K.A., 2010. Three systems of insular functional connectivity identified with cluster analysis. Cerebral Cortex 21, 1498–506.

Del-Ben, C.M., Ferreira, C.A.Q., Sanchez, T.A., Alves-Neto, W.C., Guapo, V.G., de Araujo, D.B., Graeff, F.G., 2012. Effects of diazepam on BOLD activation during the processing of aversive faces. Journal of Psychopharmacology 26, 443–51.

Delplanque, S., N'diaye, K., Scherer, K., Grandjean, D., 2007. Spatial frequencies or emotional effects? A systematic measure of spatial frequencies for IAPS pictures by a discrete wavelet analysis. Journal of Neuroscience Methods 165, 144–50.

Dien, J., 1999. Differential lateralization of trait anxiety and trait fearfulness: Evoked potential correlates. Personality and Individual Differences 26, 333–356.

Dilger, S., Straube, T., Mentzel, H.J., Fitzek, C., Reichenbach, J.R., Hecht, H., Krieschel, S., Gutberlet, I., Miltner, W.H., 2003. Brain activation to phobia-related pictures in spider phobic humans: an event-related functional magnetic resonance imaging study. Neuroscience Letters 348, 29–32.

Donahue, M.J., Near, J., Blicher, J.U., Jezzard, P., 2010. Baseline GABA concentration and fMRI response. NeuroImage 53, 392–8.

Donahue, M.J., Rane, S., Hussey, E., Mason, E., Pradhan, S., Waddell, K.W., Ally, B.A., 2014. γ-Aminobutyric acid (GABA) concentration inversely correlates with basal perfusion in human occipital lobe. Journal of Cerebral Blood Flow and Metabolism 34, 532–541.

Donner, J., Pirkola, S., Silander, K., Kananen, L., Terwilliger, J.D., Lönnqvist, J., Peltonen, L., Hovatta, I., 2008. An association analysis of murine anxiety genes in humans implicates novel candidate genes for anxiety disorders. Biological Psychiatry 64, 672–80.

Drabant, E.M., McRae, K., Manuck, S.B., Hariri, A.R., Gross, J.J., 2009. Individual differences in typical reappraisal use predict amygdala and prefrontal responses. Biological Psychiatry 65, 367–73.

Duncan, N.W., Wiebking, C., Tiret, B., Marjaska, M., Hayes, D.J., Lyttleton, O., Doyon, J., Northoff, G., 2013. Glutamate concentration in the medial prefrontal cortex predicts resting-state cortical-subcortical functional connectivity in humans. PloS one 8, e60312.

Edden, R., Puts, N., Harris, A., Barker, P., Evans, C., in press. Gannet: a batch-processing tool for the quantitative analysis of GABA-edited MRS spectra. J Magn Reson Imag .

Eippert, F., Veit, R., Weiskopf, N., Erb, M., Birbaumer, N., Anders, S., 2007. Regulation of emotional responses elicited by threat-related stimuli. Human Brain Mapping 28, 409–23.

Ekman, P., Cordaro, D., 2011. What is meant by calling emotions basic. Emotion Review 3, 364–370.

El-Hage, W., Zelaya, F., Radua, J., Gohier, B., Alsop, D.C., Phillips, M.L., Surguladze, S.A., 2013. Resting-state cerebral blood flow in amygdala is modulated by sex and serotonin transporter genotype. NeuroImage 76, 90–7.

Engels, A.S., Heller, W., Spielberg, J.M., Warren, S.L., Sutton, B.P., Banich, M.T., Miller, G.A., 2010. Co-occurring anxiety influences patterns of brain activity in depression. Cognitive, Affective & Behavioral Neuroscience 10, 141–56.

Epperson, C.N., Haga, K., Mason, G.F., Sellers, E., Gueorguieva, R., Zhang, W., Weiss, E., Rothman, D.L., Krystal, J.H., 2002. Cortical gamma-aminobutyric acid levels across the menstrual cycle in healthy women and those with premenstrual dysphoric disorder: a proton magnetic resonance spectroscopy study. Archives of General Psychiatry 59, 851–858.

Ernst, T., Kreis, R., Ross, B., 1993. Absolute Quantification of Water and Metabolites in the Human Brain. I. Compartments and Water. Journal of Magnetic Resonance 102, 1–8.

Etkin, A., Klemenhagen, K.C., Dudman, J.T., Rogan, M.T., Hen, R., Kandel, E.R., Hirsch, J., 2004. Individual differences in trait anxiety predict the response of the basolateral amygdala to unconsciously processed fearful faces. Neuron 44, 1043–55.

Etkin, A., Prater, K.E., Hoeft, F., Menon, V., Schatzberg, A.F., 2010. Failure of anterior cingulate activation and connectivity with the amygdala during implicit regulation of emotional processing in generalized anxiety disorder. The American Journal of Psychiatry 167, 545–554.

Etkin, A., Schatzberg, A.F., 2011. Common anormalities and disorder-specific compensation during implicit regulation of emotional processing in generalized anxiety and major depressive disorders. Am J Psychiatr 9, 968–978.

Etkin, A., Wager, T.D., 2007. Functional neuroimaging of anxiety: A meta-analysis of emotional processing in PTSD, social anxiety disorder, and specific phobia. Am J Psychiatry 164, 1476–1488.

Evans, C.J., McGonigle, D.J., Edden, R.A.E., 2010. Diurnal stability of gamma-aminobutyric acid concentration in visual and sensorimotor cortex. Journal of Magnetic Resonance Imaging 31, 204–9.

Evans, C.J., Puts, N.A.J., Robson, S.E., Boy, F., McGonigle, D.J., Sumner, P., Singh, K.D., Edden, R.A.E., 2013. Subtraction artifacts and frequency (mis-)alignment in J-difference GABA editing. Journal of Magnetic Resonance Imaging 38, 970–5.

Evans, K.C., Banzett, R.B., Adams, L., McKay, L., Frackowiak, R.S.J., Corfield, D.R., 2002. BOLD fMRI identifies limbic, paralimbic, and cerebellar activation during air hunger. Journal of Neurophysiology 88, 1500–11.

Fergus, A., Lee, K.S., 1997. GABAergic regulation of cerebral microvascular tone in the rat. Journal of Cerebral Blood Flow And Metabolism 17, 992–1003.

Feusner, J., Ritchie, T., Lawford, B., Young, R.M., Kann, B., Noble, E.P., 2001. GABA(A) receptor beta 3 subunit gene and psychiatric morbidity in a post-traumatic stress disorder population. Psychiatry Research 104, 109–17.

Field, A.S., Laurienti, P.J., Yen, Y.f., Burdette, J.H., Moody, D.M., 2003. Dietary caffeine consumption and withdrawal: confounding variables in quantitative cerebral perfusion studies? Neuroradiology 227, 129–135.

Finn, D., Rutledge-Gorman, M.T., Crabbe, J.C., 2003. Genetic animal models of anxiety. Neurogenetics 4, 109–35.

Fino, E., Packer, A.M., Yuste, R., 2012. The logic of inhibitory connectivity in the neocortex. The Neuroscientist 19, 228–37.

Flodin, P., Gospic, K., Petrovic, P., Fransson, P., 2012. Effects of L-dopa and oxazepam on resting-state functional magnetic resonance imaging connectivity: a randomized, cross-sectional placebo study. Brain connectivity 2, 246–53.

Frank, T.C., Kim, G.L., Krzemien, A., Van Vugt, D.A., 2010. Effect of menstrual cycle phase on corticolimbic brain activation by visual food cues. Brain Research 1363, 81–92.

Franklin, T.R., Shin, J., Jagannathan, K., Suh, J.J., Detre, J.A., O'Brien, C.P., Childress, A.R., 2012. Acute baclofen diminishes resting baseline blood flow to limbic structures: a perfusion fMRI study. Drug and Alcohol Dependence 125, 60–6.

Franklin, T.R., Wang, Z., Sciortino, N., Harper, D., Li, Y., Hakun, J., Kildea, S., Kampman, K., Ehrman, R., Detre, J.A., O'Brien, C.P., Childress, A.R., 2011. Modulation of resting brain cerebral blood flow by the GABA B agonist, baclofen: a longitudinal perfusion fMRI study. Drug and Alcohol Dependence 117, 176–83.

Fraser, D.D., Mudrick-Donnon, L.A., Macvicar, B.A., 1994. Astrocytic GABA receptors. Glia 11, 83–93.

Fraser, L.M., Stevens, M.T., Beyea, S.D., D'Arcy, R.C.N., 2012. White versus gray matter: fMRI hemodynamic responses show similar characteristics, but differ in peak amplitude. BMC Neuroscience 13, article 91.

Fu, C.H.Y., Williams, S.C.R., Brammer, M.J., Suckling, J., Kim, J., Cleare, A.J., Walsh, N.D., Mitterschiffthaler, M.T., Andrew, C.M., Pich, E.M., Bullmore, E.T., 2007. Neural responses to happy facial expressions in major depression following antidepressant treatment. The American Journal of Psychiatry 164, 599–607.

Fusar-Poli, P., Placentino, A., Carletti, F., Landi, P., Allen, P., Surguladze, S., Benedetti, F., Abbamonte, M., Gasparotti, R., Barale, F., Perez, J., McGuire, P., Politi, P., 2009. Functional atlas of emotional faces processing: a voxel-based meta-analysis of 105 functional magnetic resonance imaging studies. Journal of Psychiatry Neuroscience 34, 418–432.

Geer, J.H., 1965. The development of a scale to measure fear. Beh. Res. Ther. 3, 45–53.

Geramita, M., van der Veen, J.W., Barnett, A.S., Savostyanova, A.a., Shen, J., Weinberger, D.R., Marenco, S., 2011. Reproducibility of prefrontal γ-aminobutyric acid measurements with J-edited spectroscopy. NMR in Biomedicine 24, 1089–98.

Gerull, F.C., Rapee, R.M., 2002. Mother knows best: effects of maternal modelling on the acquisition of fear and avoidance behaviour in toddlers. Behaviour Research and Therapy 40, 279–87.

Geuze, E., van Berckel, B.N.M., Lammertsma, A.A., Boellaard, R., de Kloet, C.S., Vermetten, E., Westenberg, H.G.M., 2008. Reduced GABAA benzodiazepine receptor binding in veterans with post-traumatic stress disorder. Molecular Psychiatry 13, 74–83, 3.

Gingnell, M., Morell, A., Bannbers, E., Wikström, J., Sundström Poromaa, I., 2012. Menstrual cycle effects on amygdala reactivity to emotional stimulation in premenstrual dysphoric disorder. Hormones and Behavior 62, 400–6.

Glover, G.H., Li, T.Q., Ress, D., 2000. Image-based method for retrospective correction of physiological motion effects in fMRI: RETROICOR. Magnetic Resonance in Medicine 44, 162–167.

Goddard, A.W., Mason, G.F., Almai, A., Rothman, D.L., Behar, K.L., Petroff, O.A.C., Charney, D.S., Krystal, J.H., 2001. Reductions in occipital cortex GABA levels in panic disorder detected with 1H-Magnetic Resonance Spectroscopy. Arch Gen Psychiatry 58.

Goddard, A.W., Mason, G.F., Appel, M., Rothman, D.L., Gueorguieva, R., Behar, K.L., Krystal, J.H., 2004a. Impaired GABA neuronal response to acute benzodiazepine administration in panic disorder. The American Journal of Psychiatry 161, 2186–93.

Goddard, A.W., Mason, G.F., Rothman, D.L., Behar, K.L., Petroff, O.A.C., Krystal, J.H., 2004b. Family psychopathology and magnitude of reductions in occipital cortex GABA levels in panic disorder. Neuropsychopharmacology 29, 639–40.

Goldberg, D., 1972. The Detection of Psychiatric Illness by Questionnaire. London: Oxford University Press.

Goldin, P.R., McRae, K., Ramel, W., Gross, J.J., 2008. The neural bases of emotion regulation: reappraisal and suppression of negative emotion. Biological Psychiatry 63, 577–86.

Goossens, L., Sunaert, S., Peeters, R., Griez, E.J.L., Schruers, K.R.J., 2007. Amygdala hyperfunction in phobic fear normalizes after exposure. Biological Psychiatry 62, 1119–25.

Graham, S.J., Scaife, J.C., Langley, R.W., Bradshaw, C.M., Szabadi, E., Xi, L., Crumley, T., Calder, N., Gottesdiener, K., Wagner, J.A., 2005. Effects of lorazepam on fear-potentiated startle responses in man. Journal of Psychopharmacology 19, 249–58.

Greicius, M.D., Kiviniemi, V., Tervonen, O., Vainionpää, V., Reiss, A.L., Menon, V., 2008. Persistent default-mode network connectivity during light sedation. Human Brain Mapping 29, 839–847.

Greicius, M.D., Krasnow, B., Reiss, A.L., Menon, V., 2003. Functional connectivity in the resting brain: A network analysis of the default mode hypothesis. PNAS 100(1), 253–258.

Greicius, M.D., Supekar, K., Menon, V., Dougherty, R.F., 2009. Resting-state functional connectivity reflects structural connectivity in the default mode network. Cerebral Cortex 19, 72–78.

Grillon, C., Baas, J.M.P., Pine, D.S., Lissek, S., Lawley, M., Ellis, V., Levine, J., 2006. The benzodiazepine alprazolam dissociates contextual fear from cued fear in humans as assessed by fear-potentiated startle. Biological Psychiatry 60, 760–6.

Gross, C., Hen, R., 2004. The developmental origins of anxiety. Nature Reviews. Neuroscience 5, 545–52.

Gross, C.T., Canteras, N.S., 2012. The many paths to fear. Nature Reviews. Neuroscience 13, 651–8.

Gross, J.J., Barrett, L.F., 2011. Emotion generation and emotion regulation: One or two depends on your point of view. Emotion Review 3, 8–16.

Guidotti, A., Auta, J., Davis, J.M., Dong, E., Grayson, D.R., Veldic, M., Zhang, X., Costa, E., 2005. GABAergic dysfunction in schizophrenia: new treatment strategies on the horizon. Psychopharmacology 180, 191–205.

Habel, U., Windischberger, C., Derntl, B., Robinson, S., Kryspin-Exner, I., Gur, R.C., Moser, E., 2007. Amygdala activation and facial expressions: Explicit emotion discrimination versus implicit emotion processing. Neuropsychologia 45, 2369–2377.

Hagmann, P., Cammoun, L., Gigandet, X., Meuli, R., Honey, C.J., Wedeen, V.J., Sporns, O., 2008. Mapping the structural core of human cerebral cortex. PLoS Biology 6, e159.

Ham, B.J., Sung, Y., Kim, N., Kim, S.J., Kim, J.E., Kim, D.J., Lee, J.Y., Kim, J.H., Yoon, S.J., Lyoo, I.K., 2007. Decreased GABA levels in anterior cingulate and basal ganglia in medicated subjects with panic disorder: a proton magnetic resonance spectroscopy (1H-MRS) study. Progress in Neuro-psychopharmacology & Biological Psychiatry 31, 403–11.

Hamann, S., 2012. Mapping discrete and dimensional emotions onto the brain: controversies and consensus. Trends In Cognitive Sciences 16, 458–66.

Handwerker, D.A., Gazzaley, A., Inglis, B.A., D'Esposito, M., 2007. Reducing vascular variability of fMRI data across aging populations using a breathholding task. Human Brain Mapping 28, 846–59.

Harada, M., Kubo, H., Nose, A., Nishitani, H., Matsuda, T., 2011. Measurement of variation in the human cerebral GABA level by in vivo MEGA-editing proton MR spectroscopy using a clinical 3 T instrument and its dependence on brain region and the female menstrual cycle. Human Brain Mapping 32, 828–33.

Hariri, A.R., Tessitore, A., Mattay, V.S., Fera, F., Daniel, R.W., 2002. The amygdala response to emotional stimuli: a comparison of faces and scenes. NeuroImage 17, 317–323.

Harris, A.D., Glaubitz, B., Near, J., John Evans, C., Puts, N.A.J., Schmidt-Wilcke, T., Tegenthoff, M., Barker, P.B., Edden, R.A.E., in press. Impact of frequency drift on gamma-aminobutyric acid-edited MR spectroscopy. Magnetic Resonance in Medicine .

Hasler, G., Van der Veen, J.W., Tumonis, T., Meyers, N., Shen, J., Drevets, W.C., 2007. Reduced prefrontal glutamate/glutamine and gamma-aminobutyric acid levels in major depression determined using proton magnetic resonance spectroscopy. Arch Gen Psychiatry 64, 193–200.

Hasler, G., van der Veen, J.W., Grillon, C., Drevets, W.C., Shen, J., 2010. Effect of acute psychological stress on prefrontal GABA concentration determined by proton magnetic resonance spectroscopy. The American Journal of Psychiatry 167, 1226–31.

Haydon, P.G., Carmignoto, G., 2006. Astrocyte control of synaptic transmission and neurovascular coupling. Physiol Rev 86, 1009–1031.

Heldt, S., Mou, L., Ressler, K.J., 2012. In vivo knockdown of GAD67 in the amygdala disrupts fear extinction and the anxiolytic-like effect of diazepam in mice. Translational Psychiatry 2, e181.

Heldt, S.A., Ressler, K.J., 2007. Training-induced changes in the expression of GABAA-associated genes in the amygdala after the acquisition and extinction of Pavlovian fear. Eur J Neurosci 26, 3631–3644.

Heller, W., Engels, A.S., Mohanty, A., Herrington, J.D., Banich, M.T., Miller, G.A., 2008. Specificity of regional brain activity in anxiety types during emotion processing. Brain and Cognition 67, S8–S9.

Henry, P.G., Dautry, C., Hantraye, P., Bloch, G., 2001. Brain GABA editing without macromolecule contamination. Magnetic Resonance in Medicine 520, 517–520.

Hettema, J.M., An, S.S., Neale, M.C., Bukszar, J., Van Den Oord, E.J.C.G., Kendler, K.S., Chen, X., 2006. Association between glutamic acid decarboxylase genes and anxiety disorders, major depression, and neuroticism. Molecular Psychiatry 11, 752–62.

Hettema, J.M., Annas, P., Neale, M.C., Kendler, K.S., Fredrikson, M., 2003. A twin study of the genetics of fear conditioning. Archives of General Psychiatry 60, 702–8.

Hettema, J.M., Neale, M.C., Kendler, K.S., 2001. A review and meta-analysis of the genetic epidemiology of anxiety disorders. Am J Psychiatry 158, 1568–1578.

Hoffmann, M., Lipka, J., Mothes-Lasch, M., Miltner, W.H.R., Straube, T., 2012. Awareness modulates responses of the amygdala and the visual cortex to highly arousing visual threat. NeuroImage 62, 1439–44.

Horn, D.I., Yu, C., Steiner, J., Buchmann, J., Kaufmann, J., Osoba, A., Eckert, U., Zierhut, K.C., Schiltz, K., He, H., Biswal, B., Bogerts, B., Walter, M., 2010. Glutamatergic and resting-state functional connectivity correlates of severity in major depression the role of pregenual anterior cingulate cortex and anterior insula. Frontiers in Systems Neuroscience 4, 1–10.

Huettel, S.A., Song, A.W., McCarthy, G., 2009. Functional Magnetic Resonance Imaging. 2nd ed., Sinauer.

Ihssen, N., Keil, A., 2012. Accelerative and decelerative effects of hedonic valence and emotional arousal during visual scene processing. Q J Exp Psych 66, 1276–301.

Isaacson, J.S., Scanziani, M., 2011. How inhibition shapes cortical activity. Neuron 72, 231–43.

Iversen, L.L., Iversen, S.D., Bloom, F.E., Roth, R.H., 2009. Introduction to Neuropharmacology. Oxford University Press.

Iwata, J., Chida, K., LeDoux, J.E., 1987. Cardiovascular responses elicited by stimulation of neurons in the central amygdaloid nucleus in awake but not anesthetized rats resemble conditioned emotional responses. Brain Research 418, 183–8.

Jaworska, N., Yang, X.R., Knott, V., MacQueen, G., in press. A review of fMRI studies during visual emotive processing in major depressive disorder. The World Journal of Biological Psychiatry .

Jenkinson, M., 2003. A fast, automated, n-dimensional phase unwrapping algorith. Magnetic Resonance in Medicine 49, 193–197.

Jenkinson, M., 2004. Improving the registration of B0-distorted EPI images using calculated cost function weights. Tenth Int. Conf. On Functional Mapping of the Human Brain .

Jenkinson, M., Bannister, P., Brady, M., Smith, S., 2002. Improved optimization for the robust and accurate linear registration and motion correction of brain images. NeuroImage 17, 825–841.

Jenkinson, M., Smith, S., 2001. A global optimisation method for robust affine registration of brain images. Medical Image Analysis 5, 143–56.

Johnston, S., Linden, D.E.J., Healy, D., Goebel, R., Habes, I., Boehm, S.G., 2011. Upregulation of emotion areas through neurofeedback with a focus on positive mood. Cognitive, Affective & Behavioral Neuroscience 11, 44–51.

Johnstone, T., Somerville, L.H., Alexander, A.L., Oakes, T.R., Davidson, R.J., Kalin, N.H., Whalen, P.J., 2005. Stability of amygdala BOLD response to fearful faces over multiple scan sessions. NeuroImage 25, 1112–1123.

Kaila, K., Voipio, J., 1987. Postsynaptic fall in intracellular pH induced by GABA-activated bicarbonate conductance. Nature 330, 163–165.

Kajimura, N., Nishikawa, M., Uchiyama, M., Kato, M., Watanabe, T., Nakajima, T., Hori, T., Nakabayashi, T., Sekimoto, M., Ogawa, K., Takano, H., Imabayashi, E., Hiroki, M., Onishi, T., Uema, T., Takayama, Y., Matsuda, H., Okawa, M., Takahashi, K., 2004. Deactivation by benzodiazepine of the basal forebrain and amygdala in normal humans during sleep: A placebo-controlled 15O H2O PET study. Am J Psychiatry 161, 748–751.

Kalueff, A.V., Nutt, D.J., 2007. Role of GABA in anxiety and depression. Depression and Anxiety 24, 495–517.

Kandel, E.R., Schwarz, J.H., Jessell, T.M., Siegelbaum, S.A., Hudspecht, A.J., 2013. Principles of Neural Science. Oxford University Press.

Kann, O., Papageorgiou, I., Draguhn, A., in press. Highly energized inhibitory interneurons are a central element for information processing in cortical networks. J Cereb Blood Flow Metab .

Kannurpatti, S.S., Biswal, B.B., 2008. Detection and scaling of task-induced fMRI-BOLD response using resting state fluctuations. NeuroImage 40, 1567–74.

Kannurpatti, S.S., Motes, M., Rypma, B., Biswal, B.B., 2011. Increasing measurement accuracy of age-related BOLD signal change: minimizing vascular contributions by resting-state-fluctuation-of-amplitude scaling. Human Brain Mapping 32, 1125–40.

Kannurpatti, S.S., Rypma, B., Biswal, B.B., 2012. Prediction of task-related BOLD fMRI with amplitude signatures of resting-state fMRI. Frontiers in Systems Neuroscience 6, article 7.

Kapogiannis, D., Reiter, D.A., Willette, A.A., Mattson, M.P., 2013. Posteromedial cortex glutamate and GABA predict intrinsic functional connectivity of the default mode network. NeuroImage 64, 112–119.

Kaschka, W., Festelt, H., Ebert, D., 1995. Reduced benzodiazepine receptor binding in panic disorder measured by Iomazenil SPECT. J. Psychiat. Res. 29, 427–434.

Kash, S.F., Tecott, L.H., Hodge, C., Baekkeskov, S., 1999. Increased anxiety and altered responses to anxiolytics in mice deficient in the 65-kDa isoform of glutamic acid decarboxylase. PNAS 96, 1698–703.

Kastrup, A., Krüger, G., Neumann-Haefelin, T., Moseley, M.E., 2001. Assessment of cerebrovascular reactivity with functional magnetic resonance imaging: comparison of CO2 and breath holding. Magnetic Resonance Imaging 19, 13–20.

Kastrup, A., Li, T.Q., Takahashi, A., Glover, G.H., Moseley, M.E., 1998. Functional magnetic resonance imaging of regional cerebral blood oxygenation changes during breath holding. Stroke 29, 2641–2645.

Kay, K.N., Rokem, A., Winawer, J., Dougherty, R.F., Wandell, B.A., 2013. GLMdenoise: a fast, automated technique for denoising task-based fMRI data. Frontiers in Neuroscience 7, article 247.

Kegeles, L.S., Mao, X., Stanford, A.D., Girgis, R., Ojeil, N., Xu, X., Gil, R., Slifstein, M., Abi-Dargham, A., Lisanby, S.H., Shungu, D.C., 2012. Elevated prefrontal cortex γ-aminobutyric acid and glutamate-glutamine levels in schizophrenia measured in vivo with proton magnetic resonance spectroscopy. Archives of General Psychiatry 69, 449–59.

Kim, J.J., Whan, M., 2006. Neural circuits and mechanisms involved in Pavlovian fear conditioning: A critical review. Neuroscience and Biobehavioral Reviews 30, 188–202.

Kim, M.J., Gee, D.G., Loucks, R.A., Davis, F.C., Whalen, P.J., 2011a. Anxiety dissociates dorsal and ventral medial prefrontal cortex functional connectivity with the amygdala at rest. Cerebral Cortex 21, 1667–73.

Kim, M.J., Loucks, R.A., Palmer, A.L., Brown, A.C., Solomon, K.M., Marchante, A.N., Whalen, P.J., 2011b. The structural and functional connectivity of the amygdala: From normal emotion to pathological anxiety. Behavioural Brain Research 223, 403–410.

Kim, M.J., Whalen, P.J., 2009. The structural integrity of an amygdala prefrontal pathway predicts trait anxiety. Journal of Neuroscience 29, 11614–11618.

Kittler, J.T., Moss, S.J., 2003. Modulation of GABAA receptor activity by phosphorylation and receptor trafficking: implications for the efficacy of synaptic inhibition. Current Opinion in Neurobiology 13, 341–347.

Kleinfeld, D., Blinder, P., Drew, P.J., Driscoll, J.D., Muller, A., Tsai, P.S., Shih, A.Y., 2011. A guide to delineate the logic of neurovascular signaling in the brain. Frontiers in Neuroenergetics 3, article 1.

Klumpp, H., Angstadt, M., Nathan, P.J., Phan, K.L., 2010. Amygdala reactivity to faces at varying intensities of threat in generalized social phobia: An event-related functional MRI study. Psychiatry Res 183, 167–169.

Koehler, R.C., Roman, R.J., Harder, D.R., 2009. Astrocytes and the regulation of cerebral blood flow. Trends in Neurosciences 32, 160–9.

Krause, B.W., Wijtenburg, S.A., Holcomb, H.H., Kochunov, P., Wang, D.J.J., Hong, L.E., Rowland, L.M., 2014. Anterior cingulate GABA levels predict whole-brain cerebral blood flow. Neuroscience Letters 561, 188–91.

Kreibig, S.D., 2010. Autonomic nervous system activity in emotion: A review. Biological Psychology 84, 394–421.

Kreibig, S.D., Wilhelm, F.H., Roth, W.T., Gross, J.J., 2007. Cardiovascular, electrodermal, and respiratory response patterns to fear- and sadness-inducing films. Psychophysiology 44, 787–806.

Laeger, I., Dobel, C., Dannlowski, U., Kugel, H., Grotegerd, D., Kissler, J., Keuper, K., Eden, A., Zwitserlood, P., Zwanzger, P., 2012. Amygdala responsiveness to emotional words is modulated by subclinical anxiety and depression. Behavioural Brain Research 233, 508–516.

Lambert, J.B., Mazzola, E.P., 2004. Nuclear Magnetic Resonance Spectroscopy. Pearson Education Inc.

Lang, P., Bradley, M., Cuthbert, B., 2008. International affective picture system (IAPS): Affective ratings of pictures and instruction manual. Technical Report A-8. University of Florida, Gainesville, FL.

Laurienti, P.J., Field, A.S., Burdette, J.H., Maldjian, J.A., Yen, Y.F., Moody, D.M., 2003. Relationship between caffeine-induced changes in resting cerebral perfusion and blood oxygenation level-dependent signal. American Journal of Neuroradiology 24, 1607–11.

Lauritzen, M., Mathiesen, C., Schaefer, K., Thomsen, K.J., 2012. Neuronal inhibition and excitation, and the dichotomic control of brain hemodynamic and oxygen responses. NeuroImage 62, 1040–50.

Lawrence, N.S., Williams, A.M., Surguladze, S., Giampietro, V., Brammer, M.J., Andrew, C., Frangou, S., Ecker, C., Phillips, M.L., 2004. Subcortical and ventral prefrontal cortical neural responses to facial expressions distinguish patients with bipolar disorder and major depression. Biological Psychiatry 55, 578–587.

LeDoux, J., 2012. Perspective rethinking the emotional brain. Neuron 73, 653–676.

LeDoux, J.E., 2000. Emotion circuits in the brain. Ann Rev Neurosc 23, 155–184.

Lee, H., Heller, A.S., van Reekum, C.M., Nelson, B., Davidson, R.J., 2012. Amygdala-prefrontal coupling underlies individual differences in emotion regulation. NeuroImage 62, 1575–81.

Licata, S.C., Nickerson, L.D., Lowen, S.B., Trksak, G.H., Maclean, R.R., Lukas, S.E., 2013. The hypnotic zolpidem increases the synchrony of BOLD signal fluctuations in widespread brain networks during a resting paradigm. NeuroImage 70, 211–22.

Linden, D.E.J., Habes, I., Johnston, S.J., Linden, S., Tatineni, R., Subramanian, L., Sorger, B., Healy, D., Goebel, R., 2012. Real-time self-regulation of emotion networks in patients with depression. PloS one 7, e38115.

Lindquist, K.A., Barrett, L.F., 2012. A functional architecture of the human brain: emerging insights from the science of emotion. Trends in Cognitive Sciences 16, 533–540.

Lindquist, K.A., Kober, H., Bliss-moreau, E., Barrett, L.F., 2012. The brain basis of emotion: A meta-analytic review. Behavioral and Brain Sciences 35, 121–202.

Lipp, I., Murphy, K., Caseras, X., Wise, R.G., submitted for publication. Agreement and repeatability of vascular reactivity estimates based on a breath-hold task and a resting state scan. NeuroImage .

Lipp, I., Murphy, K., Wise, R.G., Caseras, X., 2014. Understanding the contribution of neural and physiological signal variation to the low repeatability of emotion-induced BOLD responses. NeuroImage 86, 335–342.

Lissek, S., Powers, A.S., McClure, E.B., Phelps, E.A., Woldehawariat, G., Grillon, C., Pine, D.S., 2005. Classical fear conditioning in the anxiety disorders: a meta-analysis. Behaviour Research and Therapy 43, 1391–424.

Liu, G.X., Cai, G.Q., Cai, Y.Q., Sheng, Z.J., Jiang, J., Mei, Z., 2007. Reduced anxiety and depression-like behaviors in mice lacking GABA transporter subtype I. Neuropsychopharmacology 32, 1531–1539.

Liu, J., Qiu, M., Constable, R.T., Wexler, B.E., 2012. Does baseline cerebral blood flow affect task-related blood oxygenation level dependent response in schizophrenia? Schizophrenia Research 140, 143–8.

Liu, P., Hebrank, A.C., Rodrigue, K.M., Kennedy, K.M., Park, D.C., Lu, H., 2013. A comparison of physiologic modulators of fMRI signals. Human Brain Mapping 34, 2078–88.

Liu, T.T., Brown, G.G., 2007. Measurement of cerebral perfusion with arterial spin labeling: Part 1. Methods. Journal of the International Neuropsychological Society 13, 1–9.

LoBue, V., Rakison, D.H., 2013. What we fear most: A developmental advantage for threat-relevant stimuli. Developmental Review 33, 285–303.

Logothetis, N.K., 2008. What we can do and what we cannot do with fMRI. Nature 453, 869–878.

Logothetis, N.K., Wandell, B.A., 2004. Interpreting the BOLD signal. Annual Review of Physiology 66, 735–69.

Long, Z., Medlock, C., Dzemidzic, M., Shin, Y.W., Goddard, A.W., Dydak, U., 2013. Decreased GABA levels in anterior cingulate cortex/medial prefrontal cortex in panic disorder. Progress in Neuro-Psychopharmacology & Biological Psychiatry 44, 131–5.

Lonsdorf, T.B., Weike, A.I., Nikamo, P., Schalling, M., Hamm, A.O., 2009. Genetic gating of human fear learning and extinction. Psychological Science 20, 198–206.

Lu, H., Law, M., Johnson, G., Ge, Y., van Zijl, P.C.M., Helpern, J.A., 2005. Novel approach to the measurement of absolute cerebral blood volume using vascular-space-occupancy magnetic resonance imaging. Magnetic Resonance In Medicine 54, 1403–11.

Lu, Q., Li, H., Luo, G., Wang, Y., Tang, H., Han, L., Yao, Z., 2012. Impaired prefrontal-amygdala effective connectivity is responsible for the dysfunction of emotion process in major depressive disorder: a dynamic causal modeling study on MEG. Neuroscience Letters 523, 125–30.

Lueken, U., Daniel, J., Muehlhan, M., Siegert, J., Hoyer, J., Wittchen, H.U., 2011. How specific is specific phobia? Different neural response patterns in two subtypes of specific phobia. NeuroImage 56, 363–372.

Ma, C., Ding, J., Li, J., Guo, W., Long, Z., Liu, F., Gao, Q., Zeng, L., Zhao, J., Chen, H., 2012. Resting-state functional connectivity bias of middle temporal gyrus and caudate with altered gray matter volume in major depression. PloS one 7, e45263.

Maccaferri, G., Lacaille, J.C., 2003. Interneuron Diversity series: Hippocampal interneuron classifications–making things as simple as possible, not simpler. Trends in Neurosciences 26, 564–71.

Magon, S., Basso, G., Farace, P., Ricciardi, G.K., Beltramello, A., Sbarbati, A., 2009. Reproducibility of BOLD signal change induced by breath holding. NeuroImage 45, 702–12.

Makkar, S.R., Zhang, S.Q., Cranney, J., 2010. Behavioral and neural analysis of GABA in the acquisition, consolidation, reconsolidation, and extinction of fear memory. Neuropsychopharmacology 35, 1625–1652.

Malizia, A., 2000. Positron emitting ligands in the study of the clinical psychopharmacology of anxiety and anxiety disorders. Ph.D. thesis.

Malizia, A.L., 2002. Receptor binding and drug modulation in anxiety. European Neuropsychopharmacology 12, 567–574.

Malizia, A.L., Cunningham, V.J., Bell, C.J., Liddle, P.F., Jones, T., Nutt, D.J., 1998. Decreased brain GABAA-benzodiazepine receptor binding in panic disorder. Arch Gen Psychiatry 55, 715–720.

Manuck, S.B., Brown, S.M., Forbes, E.E., Hariri, A.R., 2007. Temporal stability of individual differences in amygdala reactivity. Am J Psychiatry 164, 1613–1614.

Manzanares, P.A.R., Isoardi, N.A., Carrer, H.F., Molina, V.A., 2005. Previous stress facilitates fear memory, attenuates GABAergic inhibition, and increases synaptic plasticity in the rat basolateral amygdala. The Journal of Neuroscience 25, 8725–34.

Marek, R., Strobel, C., Bredy, T.W., Sah, P., 2013. The amygdala and medial prefrontal cortex: partners in the fear circuit. The Journal of Physiology 591, 2381–91.

Maren, S., Quirk, G.J., 2004. Neuronal signalling of fear memory. Nature Reviews. Neuroscience 5, 844–52.

Marenco, S., Savostyanova, A.A., Veen, J.W.V.D., Geramita, M., Stern, A., Barnett, A.S., Kolachana, B., Radulescu, E., Zhang, F., Callicott, J.H., Straub, R.E., Shen, J., Weinberger, D.R., 2010. Genetic modulation of GABA levels in the anterior cingulate cortex by GAD1 and COMT. Neuropsychopharmacology 35, 1708–1717.

McAvoy, M., Larson-Prior, L., Nolan, T.S., Vaishnavi, S.N., Raichle, E., Avossa, G., 2008. Resting states affect spontaneous BOLD oscillations in sensory and paralimbic cortex resting states affect spontaneous BOLD oscillations in sensory and paralimbic cortex. J Neurophys 100, 922–931.

McCarthy, G., Puce, A., Gore, J.C., Allison, T., 1997. Fear-specific processing in the human fusiform gyrus. Journal of Cognitive Neuroscience 9, 605–610.

McRae, K., Hughes, B., Chopra, S., Gabrieli, J.D.E., Gross, J.J., Ochsner, K.N., 2009. The neural bases of distraction and reappraisal. Journal of Cognitive Neuroscience 22, 248–262.

Menon, V., Uddin, L.Q., 2010. Saliency, switching, attention and control: a network model of insula function. Brain Struct Funct 214, 655–667.

Mescher, M., Merkle, H., Kirsch, J., Garwood, M., Gruetter, R., 1998. Simultaneous in vivo spectral editing and water suppression. NMR in Biomedicine 11, 266–72.

Mesulam, M., Mufson, E.J., 1982. Insula of the old world monkey. architectonics in the insulo-orbito-temporal component of the paralimbic brain. The Journal of Comparative Neurology 22, 1–22.

Meyerhoff, D.J., Mon, A., Metzler, T., Neylan, T.C., 2014. Cortical gamma-aminobutyric acid and glutamate in posttraumatic stress disorder and their relationships to self-reported sleep quality. Sleep 37, 893–900.

Michels, L., Martin, E., Klaver, P., Edden, R., Zelaya, F., Brandeis, D., Gorman, R.L.O., Lythgoe, D.J., Lu, R., 2012. Frontal GABA levels change during working memory. PloS one 7, e31933.

Mikkelsen, M., Singh, K.D., Sumner, P., Evans, C., in preparation. Comparison of the repeatability of gaba-edited magnetic resonance spectroscopy with and without macromolecule suppression .

Millan, M.J., 2003. The neurobiology and control of anxious states. Progress in Neurobiology 70, 83–244.

Mombereau, C., Kaupmann, K., Gassmann, M., Bettler, B., Putten, H.V.D., Cryan, J.F., 2005. Altered anxiety and depression-related behaviour in mice lacking GABA B (2) receptor subunits. Motivation, Emotion, Feeding, Drinking 16, 307–310.

Morris, J., Friston, K., Büchel, C., Frith, C., Young, A., Calder, A., Dolan, R., 1998. A neuromodulatory role for the human amygdala in processing emotional facial expressions. Brain 121, 47–57.

Muller, J., Corodimas, K.P., Fridel, Z., LeDoux, J.E., 1997. Functional inactivation of the lateral and basal nuclei of the amygdala by muscimol infusion prevents fear conditioning to an explicit conditioned stimulus and to contextual stimuli. Behavioral Neuroscience 111, 683–91.

Mullins, P.G., McGonigle, D.J., O'Gorman, R.L., Puts, N.A.J., Vidyasagar, R., Evans, C.J., Edden, R.A.E., 2014. Current practice in the use of MEGA-PRESS spectroscopy for the detection of GABA. NeuroImage 86, 43–52.

Muris, P., Merckelbach, H., 1996. A comparison of two spider fear questionnaires. J. Behav. Ther. and Exp. Psychiatr. 27, 241–244.

Muris, P., Merckelbach, H., de Jong, P., Ollendick, T.H., 2002. The etiology of specific fears and phobias in children: a critique of the non-associative account. Behaviour Research and Therapy 40, 185–95.

Murphy, K., Birn, R.M., Handwerker, D.A., Jones, T.B., Bandettini, P.A., 2009. The impact of global signal regression on resting state correlations: Are anti-correlated networks introduced? NeuroImage 44, 893–905.

Murphy, K., Harris, A.D., Wise, R.G., 2011. Robustly measuring vascular reactivity differences with breath-hold: Normalising stimulus-evoked and resting state BOLD fMRI data. NeuroImage 54, 369–379.

Muthukumaraswamy, S.D., Edden, R.A.E., Jones, D.K., Swettenham, J.B., Singh, K.D., 2009. Resting GABA concentration predicts peak gamma frequency and fMRI amplitude in response to visual stimulation in humans. PNAS 106, 8356–8361.

Muthukumaraswamy, S.D., Evans, C.J., Edden, R.A.E., Wise, R.G., Singh, K.D., 2012. Individual variability in the shape and amplitude of the BOLD-HRF correlates with endogenous GABAergic inhibition. Human Brain Mapping 33, 455–465.

Napolitano, A., Kockenberger, W., Auer, D.P., 2013. Reliable gamma aminobutyric acid measurement using optimized PRESS at 3 T. Magnetic Resonance in Medicine 69, 1528–33.

Near, J., Ho, Y.C.L., Sandberg, K., Kumaragamage, C., Blicher, J.U., 2014. Long-term reproducibility of GABA magnetic resonance spectroscopy. NeuroImage 99, 191–6.

Niendam, T.A., Laird, A.R., Ray, K.L., Dean, Y.M., Glahn, D.C., Carter, C.S., 2012. Meta-analytic evidence for a superordinate cognitive control network subserving diverse executive functions. Cognitive, Affective & Behavioral Neuroscience 12, 241–68.

Nitschke, J.B., Heller, W., Palmieri, P.A., Miller, G.A., 1999. Contrasting patterns of brain activity in anxious apprehension and anxious arousal. Psychophysiology 36, 628–637.

Northoff, G., Heinzel, A., de Greck, M., Bermpohl, F., Dobrowolny, H., Panksepp, J., 2006. Self-referential processing in our brain–a meta-analysis of imaging studies on the self. NeuroImage 31, 440–57.

Northoff, G., Walter, M., Schulte, R.F., Beck, J., Dydak, U., Henning, A., Boeker, H., Grimm, S., Boesiger, P., 2007. GABA concentrations in the human anterior cingulate cortex predict negative BOLD responses in fMRI. Nature Neuroscience 10, 1515–1517.

Nutt, D.J., Malizia, A.L., 2001. New insights into the role of the GABAA benzodiazepine receptor in psychiatric disorder. British Journal of Psychiatry 179, 390–396.

O'Gorman, R.L.O., Michels, L., Edden, R.A., James, B., Martin, E., 2011. In vivo detection of GABA and glutamate with MEGA-PRESS: Reproducibility and gender effects. J Magn Reson Imaging 33, 1262–1267.

Öhman, A., 2002. Automaticity and the amygdala: nonconscious responses to emotional faces. Current Directions in Psychological Science 11, 62–66.

Öhman, A., 2008. Fear and anxiety: overlap and dissociations, in: Lewis, M., Haviland-Jones, J.M., Barrett, L.F. (Eds.), Handbook of Emotions. 3rd ed.. The Guilford Press.

Olatunji, B.O., 2006. Evaluative learning and emotional responding to fearful and disgusting stimuli in spider phobia. Journal of Anxiety Disorders 20, 858–876.

Olsson, A., Phelps, E.A., 2007. Social learning of fear. Nature Neuroscience 10, 1095–1102.

Oosterwijk, S., Lindquist, K.A., Anderson, E., Dautoff, R., Moriguchi, Y., Feldman, L., 2012. States of mind: Emotions, body feelings, and thoughts share distributed neural networks. NeuroImage 62, 2110–2128.

Ortigue, S., Grafton, S.T., Bianchi-Demicheli, F., 2007. Correlation between insula activation and self-reported quality of orgasm in women. NeuroImage 37, 551–60.

Panksepp, J., 1998. Affective Neuroscience. Oxford University Press.

Pannekoek, J.N., Veer, I.M., van Tol, M.J., van der Werff, S.J.A., Demenescu, L.R., Aleman, A., Veltman, D.J., Zitman, F.G., Rombouts, S.A.R.B., van der Wee, N.J.A., 2013. Resting-state functional connectivity abnormalities in limbic and salience networks in social anxiety disorder without comorbidity. European Neuropsychopharmacology 23, 186–95.

Paredes, R.G., Agmo, A., 1992. GABA and behavior: The role of receptor subtypes. Neuroscience and Biobehavioral Reviews 16, 145–170.

Patriat, R., Molloy, E.K., Meier, T.B., Kirk, G.R., Nair, V.A., Meyerand, M.E., Prabhakaran, V., Birn, R.M., 2013. The effect of resting condition on resting-state fMRI reliability and consistency: a comparison between resting with eyes open, closed, and fixated. NeuroImage 78, 463–73.

Paulus, M.P., Feinstein, J.S., Castillo, G., Simmons, A.N., Stein, M.B., 2005. Dose-dependent decrease of activation in bilateral amygdala and insula by Lorazepam during emotion processing. Arch Gen Psychiatry 62, 282–288.

Paulus, M.P., Stein, M.B., 2006. An insular view of anxiety. Biol. Psychiatry 60, 383–387.

Peng, T., Niazy, R., Payne, S.J., Wise, R.G., 2013. The effects of respiratory CO2 fluctuations in the resting-state BOLD signal differ between eyes open and eyes closed. Magnetic Resonance Imaging 31, 336–45.

Perlbarg, V., Bellec, P., Anton, J.l., Pélégrini-Issac, M., Doyon, J., Benali, H., 2007. CORSICA: correction of structured noise in fMRI by automatic identification of ICA components. Magnetic Resonance Imaging 25, 35–46.

Pernet, C.R., Wilcox, R., Rousselet, G.A., 2012. Robust correlation analyses: false positive and power validation using a new open source Matlab toolbox. Frontiers in Psychology 3, article 606.

Petrides, M., 2005. Lateral prefrontal cortex: architectonic and functional organization. Phil. Trans. R. Soc. B 360, 781–95.

Petty, F., 1994. Plasma concentrations of gamma-aminobutyric acid (GABA) and mood disorders: a blood test for manic depressive disease? Clinical Chemistry 40, 296–302.

Petty, F., Kramer, G.L., Fulton, M., Davis, L., Rush, A.J., 1995. Stability of plasma GABA at four-year follow-up in patients with primary unipolar depression. Biological Psychiatry 37, 806–10.

Petty, F., Kramer, G.L., Fulton, M., Moeller, F.G., Rush, A.J., 1993. Low plasma GABA is a trait-like marker for bipolar illness. Neuropsychopharmacology 9, 125–32.

Petty, F., Kramer, G.L., Gullion, C.M., Rush, A.J., 1992. Low plasma gamma-aminobutyric acid levels in male patients with depression. Biological Psychiatry 32, 354–63.

Phan, K.L., Wager, T., Taylor, S.F., Liberzon, I., 2002. Functional neuroanatomy of emotion : A meta-analysis of emotion activation studies in PET and fMRI. NeuroImage 348, 331–348.

Phillips, M., Drevets, W.C., Rauch, S.L., Lane, R., 2003. Neurobiology of emotion perception ii: Implications for major psychiatric disorders. Biol. Psychiatry 54, 515–528.

Phillips, M.L., Ladouceur, C.D., Drevets, W.C., 2008. A neural model of voluntary and automatic emotion regulation: implications for understanding the pathophysiology and neurodevelopment of bipolar disorder. Molecular Psychiatry 13, 833–857.

Phillips, M.L., Medford, N., Young, A.W., Williams, L., Williams, S.C.R., Bullmore, E.T., Gray, J.A., Brammer, M.J., 2001. Time courses of left and right amygdalar responses to fearful facial expressions. Human Brain Mapping 12, 193–202.

Plichta, M.M., Schwarz, A.J., Grimm, O., Morgen, K., Mier, D., Haddad, L., Gerdes, A.B.M., Sauer, C., Tost, H., Esslinger, C., Colman, P., Wilson, F., Kirsch, P., Meyer-Lindenberg, A., 2012. Test-retest reliability of evoked BOLD signals from a cognitive-emotive fMRI test battery. NeuroImage 60, 1746–1758.

Poldrack, R.A., 2010. The trouble with cognitive subtraction, in: Hanson, S.J., Bunzl, M. (Eds.), Foundational Issues In Human Brain Mapping. MIT Press, pp. 147–160.

Pollack, M.H., Jensen, J.E., Simon, N.M., Kaufman, R.E., Renshaw, P.F., 2008. High-field MRS study of GABA, glutamate and glutamine in social anxiety disorder: response to treatment with levetiracetam. Progress in Neuro-Psychopharmacology & Biological Psychiatry 32, 739–43.

Poulin, M.J., Liang, P.J., Robbins, P.A., Liang, P., 1996. Dynamics of the cerebral blood flow response to step changes in end-tidal PCO2 and PO2 in humans. J Applied Physiol 81, 1084–1095.

Poulton, R., Menzies, R.G., 2002. Fears born and bred: toward a more inclusive theory of fear acquisition. Behaviour Research and Therapy 40, 197–208.

Power, J.D., Barnes, K.A., Snyder, A.Z., Schlaggar, B.L., Petersen, S.E., 2012. Spurious but systematic correlations in functional connectivity MRI networks arise from subject motion. NeuroImage 59, 2142–2154.

Prater, K.E., Hosanagar, A., Klumpp, H., Angstadt, M., Phan, K.L., 2013. Aberrant amygdala-frontal cortex connectivity during perception of fearful faces and at rest in generalized social anxiety disorder. Depression and Anxiety 30, 234–41.

Putnam, R.W., Filosa, J.A., Ritucci, N.A., 2004. Cellular mechanisms involved in CO2 and acid signaling in chemosensitive neurons. Am J Physiol Cell Physiol 287, C1493–C1526.

Puts, N.A.J., Edden, R.A.E., 2012. In vivo magnetic resonance spectroscopy of GABA: A methodological review. Progress in Nuclear Magnetic Resonance Spectroscopy 60, 29–41.

Qin, S., Young, C.B., Duan, X., Chen, T., Supekar, K., Menon, V., 2014. Amygdala subregional structure and intrinsic functional connectivity predicts individual differences in anxiety during early childhood. Biological Psychiatry 75, 892–900.

Qiu, C., Liao, W., Ding, J., Feng, Y., Zhu, C., Nie, X., Zhang, W., Chen, H., Gong, Q., 2011. Regional homogeneity changes in social anxiety disorder: a resting-state fMRI study. Psychiatry Research 194, 47–53.

Rabinak, C.A., Angstadt, M., Welsh, R.C., Kenndy, A.E., Lyubkin, M., Martis, B., Phan, K.L., 2011. Altered amygdala resting-state functional connectivity in post-traumatic stress disorder. Frontiers in Psychiatry 2, article 62.

Raichle, M.E., MacLeod, A.M., Snyder, A.Z., Powers, W.J., Gusnard, D.A., Shulman, G.L., 2001. A default mode of brain function. PNAS 98, 676–682.

Ray, R.D., Zald, D.H., 2012. Anatomical insights into the interaction of emotion and cognition in the prefrontal cortex. Neuroscience and Biobehavioral Reviews 36, 479–501.

Reynolds, S.M., Zahm, D.S., 2005. Specificity in the projections of prefrontal and insular cortex to ventral striatopallidum and the extended amygdala. The Journal of Neuroscience 25, 11757–67.

Rhodes, R., Murthy, N.V., Dresner, M.A., Selvaraj, S., Stavrakakis, N., Babar, S., Cowen, P.J., Grasby, P.M., 2007. Human 5-HT transporter availability predicts amygdala reactivity in vivo. The Journal of Neuroscience 27, 9233–9237.

Riba, J., Rodríguez-Fornells, A., Urbano, G., Morte, A., Antonijoan, R., Barbanoj, M.J., 2001. Differential effects of alprazolam on the baseline and fear-potentiated startle reflex in humans: a dose-response study. Psychopharmacology 157, 358–67.

Riecker, A., Grodd, W., Klose, U., Schulz, J.B., Gröschel, K., Erb, M., Ackermann, H., Kastrup, A., 2003. Relation between regional functional MRI activation and vascular reactivity to carbon dioxide during normal aging. Journal of Cerebral Blood Flow and Metabolism 23, 565–73.

Robinson, O.J., Charney, D.R., Overstreet, C., Vytal, K., Grillon, C., 2012. The adaptive threat bias in anxiety: amygdala-dorsomedial prefrontal cortex coupling and aversive amplification. NeuroImage 60, 523–9.

Robson, S.E., 2012. Individual differences in excitation and inhibition in visual cortex. Ph.D. thesis. Cardiff University.

Rosso, I.M., Weiner, M.R., Crowley, D.J., Silveri, M.M., Rauch, S.L., Jensen, J.E., 2014. Insula and anterior cingulate GABA levels in posttraumatic stress disorder: preliminary findings using magnetic resonance spectroscopy. Depression and Anxiety 31, 115–123.

Roy, A.K., Ph, D., Fudge, J.L., Kelly, C., Ph, D., Perry, J.S.A., Carlisi, C., Benson, B., Ph, D., Castellanos, F.X., Milham, M.P., Ph, D., Pine, D.S., Ernst, M., Ph, D., 2013. Intrinsic functional connectivity of amygdala-based networks in adolescent generalized anxiety disorder. J Am Acad Child Adolesc Psychiatry 52, 290–299.

Sabatinelli, D., Fortune, E.E., Li, Q., Siddiqui, A., Krafft, C., Oliver, W.T., Beck, S., Jeffries, J., 2011. Emotional perception: Meta-analyses of face and natural scene processing. NeuroImage 54, 2524–2533.

Sah, P., Faber, E.S.L., Lopez De Armentia, M., Power, J., 2003. The amygdaloid complex: anatomy and physiology. Physiol Rev 83, 803–34.

Said, C.P., Baron, S.G., Todorov, A., 2008. Nonlinear amygdala response to face trustworthiness: contributions of high and low spatial frequency information. Journal of Cognitive Neuroscience 21, 519–528.

Sanacora, G., Mason, G.F., Rothman, D.L., Behar, K.L., Hyder, F., Petroff, O.A., Berman, R.M., Charney, D.S., Krystal, J.H., 1999. Reduced cortical gamma-aminobutyric acid levels in depressed patients determined by proton magnetic resonance spectroscopy. Arch Gen Psychiatry 56, 1043–1047.

Sanders, S.K., Shekhar, A., 1991. Blockade of GABA A receptors in the region of the anterior basolateral amygdala of rats elicits increases in heart rate and blood pressure. Brain Research 576, 101–110.

Satterthwaite, T.D., Elliott, M.A., Gerraty, R.T., Ruparel, K., Loughead, J., Calkins, M.E., Eickhoff, S.B., Hakonarson, H., Gur, R.C., Gur, R.E., Wolf, D.H., 2013. An improved framework for confound regression and filtering for control of motion artifact in the preprocessing of resting-state functional connectivity data. NeuroImage 64, 240–256.

Sauder, C.L., Hajcak, G., Angstadt, M., Phan, K.L., 2013. Test-retest reliability of amygdala response to emotional faces. Psychophysiology 50, 1147–56.

Sawchuk, C.N., Lohr, J.M., Tolin, D.F., Lee, T.C., Kleinknecht, R.A., 2000. Disgust sensitivity and contamination fears in spider and blood-injection-injury phobias. Behaviour Research and Therapy 38, 753–62.

Scaife, J.C., Hou, R.H., Samuels, E.R., Baqui, F., Langley, R.W., Bradshaw, C.M., Szabadi, E., 2007. Diazepam-induced disruption of classically-conditioned fear-potentiation of late-latency auditory evoked potentials is prevented by flumazenil given before, but not after, CS/US pairing. Journal of Psychopharmacology 21, 93–101.

Scaife, J.C., Langley, R.W., Bradshaw, C.M., Szabadi, E., 2005. Diazepam suppresses the acquisition but not the expression of 'fear-potentiation' of the acoustic startle response in man. Journal of Psychopharmacology 19, 347–56.

Schaefer, S.M., Abercrombie, H.C., Lindgren, K., Larson, C.L., Ward, R.T., Oakes, T.R., Holden, J.E., Perlman, S.B., Turski, P.A., Davidson, R.J., 2000. Six-month test-retest reliability of MRI-defined PET measures of regional cerebral glucose metabolic rate in selected subcortical structures. Human Brain Mapping 10, 1–9.

Schäfer, A., Leutgeb, V., Reishofer, G., Ebner, F., Schienle, A., 2009. Propensity and sensitivity measures of fear and disgust are differentially related to emotion-specific brain activation. Neuroscience Letters 465, 262–6.

Schäfer, A., Schienle, A., Vaitl, D., 2005. Stimulus type and design influence hemodynamic responses towards visual disgust and fear elicitors. International Journal of Psychophysiology 57, 53–59.

Schienle, A., Schäfer, A., Stark, R., Vaitl, D., 2009. Long-term effects of cognitive behavior therapy on brain activation in spider phobia. Psychiatry Research 172, 99–102.

Schienle, A., Schäfer, A., Walter, B., Stark, R., Vaitl, D., 2005. Brain activation of spider phobics towards disorder-relevant, generally disgust- and fear-inducing pictures. Neuroscience Letters 388, 1–6.

Schienle, A., Stark, R., Walter, B., Blecker, C., Ott, U., Kirsch, P., Sammer, G., Vaitl, D., 2002. The insula is not specifically involved in disgust processing: an fMRI study. Neuroreport 13, 2023–6.

Schlegel, S., Aldenhoff, J.B., Eissner, D., Lindner, P., Nickel, O., 1989. Regional cerebral blood flow in depression: associations with psychopathology. Journal of Affective Disorders 17, 211–8.

Schmahmann, J.D., Caplan, D., 2006. Cognition, emotion and the cerebellum. Brain 129, 290–2.

Schmahmann, J.D., Sherman, J.C., 1998. The cerebellar cognitive affective syndrome. Brain 121, 561–79.

Schüle, C., Eser, D., Baghai, T.C., Nothdurfter, C., Kessler, J.S., Rupprecht, R., 2011. Neuroactive steroids in affective disorders: target for novel antidepressant or anxiolytic drugs? Neuroscience 191, 55–77.

Schutter, D.J.L.G., van Honk, J., 2005. The cerebellum on the rise in human emotion. The Cerebellum 4, 290–4.

Schutter, D.J.L.G., van Honk, J., 2009. The cerebellum in emotion regulation: a repetitive transcranial magnetic stimulation study. Cerebellum 8, 28–34.

Scouten, A., Schwarzbauer, C., 2008. Paced respiration with end-expiration technique offers superior BOLD signal repeatability for breath-hold studies. NeuroImage 43, 250–7.

Seeley, W.W., Menon, V., Schatzberg, A.F., Keller, J., Glover, G.H., Kenna, H., Reiss, A.L., Greicius, M.D., 2007. Dissociable intrinsic connectivity networks for salience processing and executive control. The Journal of Neuroscience 27, 2349–56.

Sehlmeyer, C., Schöning, S., Zwitserlood, P., Pfleiderer, B., Kircher, T., Arolt, V., Konrad, C., 2009. Human fear conditioning and extinction in neuroimaging: a systematic review. PloS one 4, e5865.

Seligman, M.E.P., 1971. Phobias and preparedness. Behavior Therapy 2, 307–320.

Sen, S., Villafuerte, S., Nesse, R., Stoltenberg, S.F., Hopcian, J., Gleiberman, L., Weder, A., Burmeister, M., 2004. Serotonin transporter and GABA(A) alpha 6 receptor variants are associated with neuroticism. Biological Psychiatry 55, 244–249.

Sheehan, D., Lecrubier, Y., Sheehan, K., Amorim, P., Janavs, J., Weiller, E., Hergueta, T., Baker, R., Dunbar, G., 1998. The Mini-International Neuropsychiatric Interview (M.I.N.I.): the development and validation of a structured diagnostic psychiatric interview for DSM-IV and ICD-10. J Clin Psychiatry 59 Suppl20, 22–33.

Shirer, W.R., Ryali, S., Rykhlevskaia, E., Menon, V., Greicius, M.D., 2012. Decoding subject-driven cognitive states with whole-brain connectivity patterns. Cerebral Cortex 22, 158–65.

Shmueli, K., van Gelderen, P., de Zwart, J.A., Horovitz, S.G., Fukunaga, M., Jansma, J.M., Duyn, J.H., 2007. Low-frequency fluctuations in the cardiac rate as a source of variance in the resting-state fMRI BOLD signal. NeuroImage 38, 306–20.

Shrout, P., Fleiss, J., 1979. Intraclass correlations: uses in assessing rater reliability. Psychological Bulletin 86(2), 420–428.

Sicard, K.M., Duong, T.Q., 2005. Effects of hypoxia, hyperoxia, and hypercapnia on baseline and stimulus-evoked BOLD, CBF, and CMRO2 in spontaneously breathing animals. NeuroImage 25, 850–8.

Silveri, M.M., Sneider, J.T., Crowley, D.J., Covell, M.J., Acharya, D., Rosso, I.M., Jensen, J.E., 2013. Frontal lobe γ-aminobutyric acid levels during adolescence: associations with impulsivity and response inhibition. Biological Psychiatry 74, 296–304.

Simmons, A.N., Stein, M.B., Strigo, I.A., Arce, E., Hitchcock, C., Paulus, M.P., 2011. Anxiety positive subjects show altered processing in the anterior insula during anticipation of negative stimuli. Human Brain Mapping 32, 1836–1846.

Skre, I., 2000. The heritability of common phobic fear: A twin study of a clinical sample. The Journal of Anxiety Disorders 14, 549–562.

Sladky, R., Friston, K.J., Tröstl, J., Cunnington, R., Moser, E., Windischberger, C., 2011. Slice-timing effects and their correction in functional MRI. NeuroImage 58, 588–94.

Smith, K.S., Rudolph, U., 2012. Anxiety and depression: Mouse genetics and pharmacological approaches to the role of GABAA receptor subtypes. Neuropharmacology 62, 54–62.

Smith, S., 2002. Fast robust automated brain extraction. Human Brain Mapping 17, 143–155.

Sojkova, J., Najjar, S.S., Beason-Held, L.L., Metter, E.J., Davatzikos, C., Kraut, M.A., Zonderman, A.B., Resnick, S.M., 2010. Intima-media thickness and regional cerebral blood flow in older adults. Stroke 41, 273–9.

Spielberger, C., Gursuch, R., Lushene, R., 1970. State Trait Anxietory Inventory Manual. Palo Alto, Calif: Consulting Psychologist Press.

Sridharan, D., Levitin, D.J., Menon, V., 2008. A critical role for the right fronto-insular cortex in switching between central-executive and default-mode networks. PNAS 105, 12569–12574.

Sripada, R.K., King, A.P., Garfinkel, S.N., Wang, X., Sripada, C.S., Welsh, R.C., Liberzon, I., 2012. Altered resting-state amygdala functional connectivity in men with posttraumatic stress disorder. Journal Psychiatry Neurosci 37, 241–9.

Stagg, C.J., Bachtiar, V., Amadi, U., Gudberg, C.A., Ilie, A.S., Sampaio-Baptista, C., O'Shea, J., Woolrich, M., Smith, S.M., Filippini, N., Near, J., Johansen-Berg, H., 2014. Local GABA concentration is related to network-level resting functional connectivity. eLife 3, e01465–e01465.

Stagg, C.J., Bachtiar, V., Johansen-Berg, H., 2011. The role of GABA in human motor learning. Current Biology 21, 480–4.

Stan, A.D., Schirda, C.V., Bertocci, M.A., Bebko, G.M., Kronhaus, D.M., Aslam, H.a., LaBarbara, E.J., Tanase, C., Lockovich, J.C., Pollock, M.H., Stiffler, R.S., Phillips, M.L., in press. Glutamate and GABA contributions to medial prefrontal cortical activity to emotion: Implications for mood disorders. Psychiatry Research .

Stark, R., Kirsch, P., 2004. Hemodynamic effects of negative emotional pictures a test-retest analysis. Neuropsychobiology 50, 108–118.

Stefanacci, L., Amaral, D.G., 2000. Topographic organization of cortical inputs to the lateral nucleus of the macaque monkey amygdala: a retrograde tracing study. The Journal of Comparative Neurology 421, 52–79.

Stefanacci, L., Amaral, D.G., 2002. Some observations on cortical inputs to the macaque monkey amygdala: an anterograde tracing study. The Journal of Comparative Neurology 451, 301–23.

Stein, M.B., Goldin, P.R., Sareen, J., Zorrilla, L.T.E., Brown, G.G., 2002. Increased amygdala activation to angry and contemptuous faces in generalized social phobia. Archives of General Psychiatry 59, 1027–34.

Stein, M.B., Simmons, A.N., Feinstein, J.S., Paulus, M.P., 2007. Increased amygdala and insula activation during emotion processing in anxiety-prone subjects. The American Journal of Psychiatry 164, 318–27.

Stevens, J.S., Hamann, S., 2012. Sex differences in brain activation to emotional stimuli: A meta-analysis of neuroimaging studies. Neuropsychologia 50, 1578–1593.

Stevens, J.S., Jovanovic, T., Fani, N., Ely, T.D., Glover, E.M., Bradley, B., Ressler, K.J., 2013. Disrupted amygdala-prefrontal functional connectivity in civilian women with posttraumatic stress disorder. Journal of Psychiatric Research 47, 1469–78.

Stevenson, J., Batten, N., Cherner, M., 1992. Fears and fearfulness in children and adolescents: a genetic analysis of twin data. Journal of Child Psychology and Psychiatry 33, 977–85.

Stoléru, S., Fonteille, V., Cornélis, C., Joyal, C., Moulier, V., 2012. Functional neuroimaging studies of sexual arousal and orgasm in healthy men and women: a review and meta-analysis. Neuroscience and Biobehavioral Reviews 36, 1481–509.

Stork, O., Ji, F.Y., Obata, K., 2002. Reduction of extracellular GABA in the mouse amygdala during and following confrontation with a conditioned fear stimulus. Neuroscience Letters 327, 138–142.

Straube, T., Glauer, M., Dilger, S., Mentzel, H.J., Miltner, W.H.R., 2006a. Effects of cognitive-behavioral therapy on brain activation in specific phobia. NeuroImage 29, 125–135.

Straube, T., Mentzel, H.J., Glauer, M., Miltner, W.H.R., 2004. Brain activation to phobia-related words in phobic subjects. Neuroscience Letters 372, 204–8.

Straube, T., Mentzel, H.J., Miltner, W.H.R., 2006b. Neural mechanisms of automatic and direct processing of phobogenic stimuli in specific phobia. Biol Psychiatry 59, 162–170.

Streeter, C.C., Hennen, J., Ke, Y., Jensen, J.E., Sarid-Segal, O., Nassar, L.E., Knapp, C., Meyer, A.A., Kwak, T., Renshaw, P.F., Ciraulo, D.A., 2005. Prefrontal GABA levels in cocaine-dependent subjects increase with pramipexole and venlafaxine treatment. Psychopharmacology 182, 516–26.

Strelau, J., Zawadzki, B., 2011. Fearfulness and anxiety in research on temperament: Temperamental traits are related to anxiety disorders. Personality and Individual Differences 50, 907–915.

Stricker, R., Eberhart, R., Chevailler, M.C., Quinn, F.A., Bischof, P., Stricker, R., 2006. Establishment of detailed reference values for luteinizing hormone, follicle stimulating hormone, estradiol, and progesterone during different phases of the menstrual cycle on the Abbott ARCHITECT analyzer. Clin Chem Lab Med 44, 883–887.

Surguladze, S., Brammer, M.J., Keedwell, P., Giampietro, V., Young, A.W., Travis, M.J., Williams, S.C.R., Phillips, M.L., 2005. A differential pattern of neural response toward sad versus happy facial expressions in major depressive disorder. Biological Psychiatry 57, 201–9.

Surguladze, S., Marshall, N., Schulze, K., Hall, M.H., Walshe, M., Bramon, E., Phillips, M., Murray, R., McDonald, C., 2010. Exaggerated neural response to emotional faces in patients with bipolar disorder and their first-degree relatives. NeuroImage 53, 58–64.

Susskind, J.M., Lee, D.H., Cusi, A., Feiman, R., Grabski, W., Anderson, A.K., 2008. Expressing fear enhances sensory acquisition. Nature Neuroscience 11, 843–50.

Sylvers, P., Lilienfeld, S.O., Laprairie, J.L., 2011. Differences between trait fear and trait anxiety: Implications for psychopathology. Clinical Psychology Review 31, 122–137.

Sylvester, C.M., Corbetta, M., Raichle, M.E., Rodebaugh, T.L., Schlaggar, B.L., Sheline, Y.I., Zorumski, C.F., Lenze, E.J., 2012. Functional network dysfunction in anxiety and anxiety disorders. Trends In Neurosciences 35, 527–35.

Szymanski, J., Donohue, W.O., 1995. Fear of Spiders Questionnaire. J. Behav. Ther. and Exp. Psychiatr. 26, 31–34.

Tak, S., Wang, D.J.J., Polimeni, J.R., Yan, L., Chen, J.J., 2014. Dynamic and static contributions of the cerebrovasculature to the resting-state BOLD signal. NeuroImage 84, 672–80.

Takeuchi, H., Taki, Y., Hashizume, H., Sassa, Y., Nagase, T., Nouchi, R., Kawashima, R., 2011. Cerebral blood flow during rest associates with general intelligence and creativity. PloS one 6, e25532.

Tang, Y., Kong, L., Wu, F., Womer, F., Jiang, W., Cao, Y., Ren, L., Wang, J., Fan, G., Blumberg, H.P., Xu, K., Wang, F., 2013. Decreased functional connectivity between the amygdala and the left ventral prefrontal cortex in treatment-naive patients with major depressive disorder: a resting-state functional magnetic resonance imaging study. Psychological Medicine 43, 1921–7.

Thoeringer, C., Ripke, S., Unschuld, P., Lucae, S., Ising, M., Bettecken, T., Uhr, M., Keck, M., Mueller-Myshok, B., Holsboer, F., Binder, E., Erhardt, A., 2009. The GABA transporter 1 (SLC6A1): a novel candidate gene for anxiety disorders. J Neural Transm 116, 649–657.

Thomason, M.E., Burrows, B.E., Gabrieli, J.D.E., Glover, G.H., 2005. Breath holding reveals differences in fMRI BOLD signal in children and adults. NeuroImage 25, 824–837.

Thomason, M.E., Foland, L.C., Glover, G.H., 2007. Calibration of BOLD fMRI using breath holding reduces group variance during a cognitive task. Human Brain Mapping 28, 59–68.

Thomason, M.E., Glover, G.H., 2008. Controlled inspiration depth reduces variance in breath-holding induced BOLD signal. Neuroimage 39, 206–214.

Tillakaratne, N.J., Medina-Kauwe, L., Gibson, K.M., 1995. Gamma-Aminobutyric acid (GABA) metabolism in mammalian neural and nonneural tissues. Comparative Biochemistry and Physiology. 112A, 247–63.

Türe, U., Yasargil, D., Al-Mefty, O., Yasargil, M., 1999. Topographic anatomy of the insular region. J Neurosurg 90, 720–733.

Vaidyanathan, U., Patrick, C.J., Cuthbert, B.N., 2009. Linking dimensional models of internalizing psychopathology to neurobiological systems: affect-modulated startle as an indicator of fear and distress disorders and affiliated traits. Psychological Bulletin 135, 909–42.

Vaiva, G., Boss, V., Ducrocq, F., Fontaine, M., Devos, P., Ph, D., Brunet, A., Ph, D., Laffargue, P., Ph, D., Goudemand, M., Thomas, P., Ph, D., 2006. Plasma levels and PTSD at 1-year follow-up. Am J Psychiatry 163, 1446–1448.

Vaiva, G., Thomas, P., Ducrocq, F., Fontaine, M., Boss, V., Devos, P., Rascle, C., Cottencin, O., Brunet, A., Laffargue, P., Goudemand, M., 2004. Low posttrauma GABA plasma levels as a predictive factor in the development of acute posttraumatic stress disorder. Biological Psychiatry 55, 250–254.

van den Bulk, B.G., Koolschijn, P.C.M.P., Meens, P.H.F., van Lang, N.D.J., van der Wee, N.J.A., Rombouts, S.A.R.B., Vermeiren, R.R.J.M., Crone, E.A., 2013. How stable is activation in the amygdala and prefrontal cortex in adolescence? A study of emotional face processing across three measurements. Developmental Cognitive Neuroscience 4, 65–76.

van den Heuvel, M.P., Hulshoff Pol, H.E., 2010. Exploring the brain network: a review on resting-state fMRI functional connectivity. European Neuropsychopharmacology 20, 519–34.

van Dijk, K.R.A., Sabuncu, M.R., Buckner, R.L., 2012. The influence of head motion on intrinsic functional connectivity MRI. NeuroImage 59, 431–438.

van Tol, M.J., Veer, I.M., van der Wee, N.J.A., Aleman, A., van Buchem, M.A., Rombouts, S.A.R.B., Zitman, F.G., Veltman, D.J., Johnstone, T., 2013. Whole-brain functional connectivity during emotional word classification in medication-free Major Depressive Disorder: Abnormal salience circuitry and relations to positive emotionality. NeuroImage Clinical 2, 790–6.

van Wingen, G., van Broekhoven, F., Verkes, R., Petersson, K., Bäckström, T., Buitelaar, J., Fernández, G., 2008. Progesterone selectively increases amygdala reactivity in women. Molecular Psychiatry 13, 325–333.

van Wingen, G., Broekhoven, F.V., Verkes, R.J., Petersson, K.M., Buitelaar, J., 2007. How progesterone impairs memory for biologically salient stimuli in healthy young women. The Journal of Neuroscience 27, 11416–11423.

Vazquez, A.L., Cohen, E.R., Gulani, V., Hernandez-Garcia, L., Zheng, Y., Lee, G.R., Kim, S.G., Grotberg, J.B., Noll, D.C., 2006. Vascular dynamics and BOLD fMRI: CBF level effects and analysis considerations. NeuroImage 32, 1642–55.

Vlamings, P., Goffaux, V., Kemner, C., 2009. Is the early modulation of brain activity by fearful facial expressions primarily mediated by coarse low spatial frequency information? Journal of Vision 9, 1–13.

Vriends, N., Michael, T., Schindler, B., Margraf, J., 2012. Associative learning in flying phobia. Journal of Behavior Therapy and Experimental Psychiatry 43, 838–843.

Vuilleumier, P., Armony, J.L., Driver, J., Dolan, R.J., 2001. Effects of attention and emotion on face processing in the human brain: an event-related fMRI study. Neuron 30, 829–841.

Vuilleumier, P., Pourtois, G., 2007. Distributed and interactive brain mechanisms during emotion face perception: Evidence from functional neuroimaging. Neuropsychologia 45, 174–194.

Vytal, K., Hamann, S., 2010. Neuroimaging support for discrete neural correlates of basic emotions: A voxel-based meta-analysis. Journal of Cognitive Neuroscience 22, 2864–2885.

Vytal, K.E., Overstreet, C., Charney, D.R., Robinson, O.J., Grillon, C., 2014. Sustained anxiety increases amygdala - dorsomedial prefrontal coupling: a mechanism for maintaining an anxious state in healthy adults. J Psychiatry Neurosci 39, article 130145.

Wager, T.D., Davidson, M.L., Hughes, B.L., Lindquist, M.A., Ochsner, K.N., 2008. Prefrontal-subcortical pathways mediating successful emotion regulation. Neuron 59, 1037–1050.

Wang, J., Rao, H., Wetmore, G.S., Furlan, P.M., Korczykowski, M., Dinges, D.F., Detre, J.A., 2005. Perfusion functional MRI reveals cerebral blood flow pattern under psychological stress. PNAS 102, 17804–9.

Watson, J.B., Rayner, R., 1920. Conditioned emotional reactions. Journal of Experimental Psychology 3, 1–14.

Wendt, J., Lotze, M., Weike, A.I., Hosten, N., Hamm, A.O., 2008. Brain activation and defensive response mobilization during sustained exposure to phobia-related and other affective pictures in spider phobia. Psychophysiology 45, 205–215.

Wiebking, C., Duncan, N.W., Tiret, B., Hayes, D.J., Marjaska, M., Doyon, J., Bajbouj, M., Northoff, G., 2014. GABA in the insula - a predictor of the neural response to interoceptive awareness. NeuroImage 86, 10–18.

Wiech, K., Lin, C.S., Brodersen, K.H., Bingel, U., Ploner, M., Tracey, I., 2010. Anterior insula integrates information about salience into perceptual decisions about pain. The Journal of Neuroscience 30, 16324–31.

Wiens, S., Sand, A., Olofsson, J.K., 2011. Nonemotional features suppress early and enhance late emotional electrocortical responses to negative pictures. Biological Psychology 86, 83–89.

Wijtenburg, S.A., Rowland, L.M., Edden, R.A.E., Barker, P.B., 2013. Reproducibility of brain spectroscopy at 7T using conventional localization and spectral editing techniques. Journal of Magnetic Resonance Imaging 38, 460–7.

Wise, R.G., Ide, K., Poulin, M.J., Tracey, I., 2004. Resting fluctuations in arterial carbon dioxide induce significant low frequency variations in BOLD signal. NeuroImage 21, 1652–1664.

Wise, R.G., Lujan, B.J., Schweinhardt, P., Peskett, G.D., Rogers, R., Tracey, I., 2007. The anxiolytic effects of midazolam during anticipation to pain revealed using fMRI. Magnetic Resonance Imaging 25, 801–810.

Wolf, R.C., Thomann, P.A., Sambataro, F., Vasic, N., Schmid, M., Wolf, N.D., 2012. Orbitofrontal cortex and impulsivity in borderline personality disorder: an MRI study of baseline brain perfusion. European Archives of Psychiatry and Clinical Neuroscience 262, 677–685.

Wolpe, J., Lang, P., 1964. A fear survey schedule for use in behavior therapy. Beh. Res. Ther. 2, 27–30.

Worsley, K., 2001. Statistical analysis of activation images., in: Jezzard, P., Matthews, P., Smith, S. (Eds.), Functional MRI: An Introduction to Methods. OUP.

Wrase, J., Klein, S., Gruesser, S.M., Hermann, D., Flor, H., Mann, K., Braus, D.F., Heinz, A., 2003. Gender differences in the processing of standardized emotional visual stimuli in humans: a functional magnetic resonance imaging study. Neuroscience Letters 348, 41–45.

Wright, C.I., Fischer, H., Whalen, P.J., McInerney, S.C., Shin, L.M., Rauch, S.L., 2001. Differential prefrontal cortex and amygdala habituation to repeatedly presented emotional stimuli. Neuroreport 12, 379–83.

Wright, C.I., Martis, B., Mcmullin, K., Shin, L.M., Rauch, S.L., 2003. Amygdala and insular responses to emotionally valenced human faces in small animal specific phobia. Biol Psychiatry 54, 1067–1076.

Xu, G., Rowley, H.a., Wu, G., Alsop, D.C., Shankaranarayanan, A., Dowling, M., Christian, B.T., Oakes, T.R., Johnson, S.C., 2010. Reliability and precision of pseudo-continuous arterial spin labeling perfusion MRI on 3.0 T and comparison with 15O-water PET in elderly subjects at risk for Alzheimer's disease. NMR in Biomedicine 23, 286–93.

Yeo, B.T.T., Krienen, F.M., Sepulcre, J., Sabuncu, M.R., Lashkari, D., Hollinshead, M., Roffman, J.L., Smoller, J.W., Zöllei, L., Polimeni, J.R., Fischl, B., Liu, H., Buckner, R.L., 2011. The organization of the human cerebral cortex estimated by intrinsic functional connectivity. Journal of Neurophysiology 106, 1125–65.

Yeterian, E.H., Pandya, D.N., Tomaiuolo, F., Petrides, M., 2012. The cortical connectivity of the prefrontal cortex in the monkey brain. Cortex 48, 58–81.

Young, A., Perret, D., Calder, A., Sprengelmeyer, R., Ekman, P., 2002. Facial Expressions of Emotion: Stimuli and Tests (FEEST). Thames Valley Test Company, Bury St.Edmunds.

Zaki, J., Davis, J.I., Ochsner, K.N., 2012. Overlapping activity in anterior insula during interoception and emotional experience. NeuroImage 62, 493–9.

Zhao, X.H., Wang, P.J., Li, C.B., Hu, Z.H., Xi, Q., Wu, W.Y., Tang, X.W., 2007. Altered default mode network activity in patient with anxiety disorders: an fMRI study. European Journal of Radiology 63, 373–8.

Zigmond, A., Snaith, R., 1983. The Hospital Anxiety and Depression Scale. Acta Psychiatrica Scandinavica 67, 361–370.

Part VII

Supplementary Material

Appendix A

Supplement for Chapter 2

Task-related activation - ROI analysis (supplementary ANOVAs):

In the amygdala percent signal change did not differ between neutral, 50% fearful, and 100% fearful faces (session 1: $F[2,28] = 1.05$ ns; session 2: $F[2,28] = 1.49$, ns), and there was no interaction with hemisphere (session 1: $F[2,28] = 1.69$, ns; session 2: $F[2,28] = 0.608$, ns). In both sessions there was a trend for a main effect of hemisphere on activation. In session 1 the amygdala in the right hemisphere showed stronger activation ($F[1,28] = 3.36$, $p = .09$), while it was the left amygdala in session 2 ($F[1,28] = 3.80$, $p = .07$).

In the second region of interest, the fusiform gyrus, no significiant main effects or interaction between condition and hemisphere was found in either session.

Using the dataset corrected for physiological noise did not change these results, with the exception of the trend for a main effect hemisphere disappearing in session 1, but becoming significant for session 2 ($F[1,28] = 6.89$, p = .02).

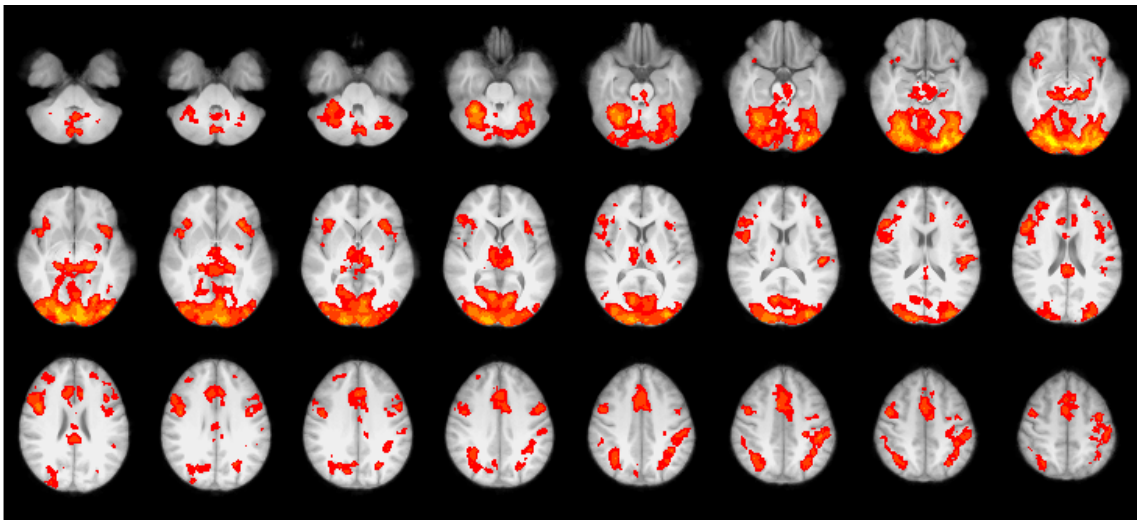

Figure A.1: Group-level activation for the main effect neutral faces. Results are displayed for a significance level of $Z > 2.3$ and a (corrected) cluster significance threshold of $P = 0.05$. Image in radiological convention.

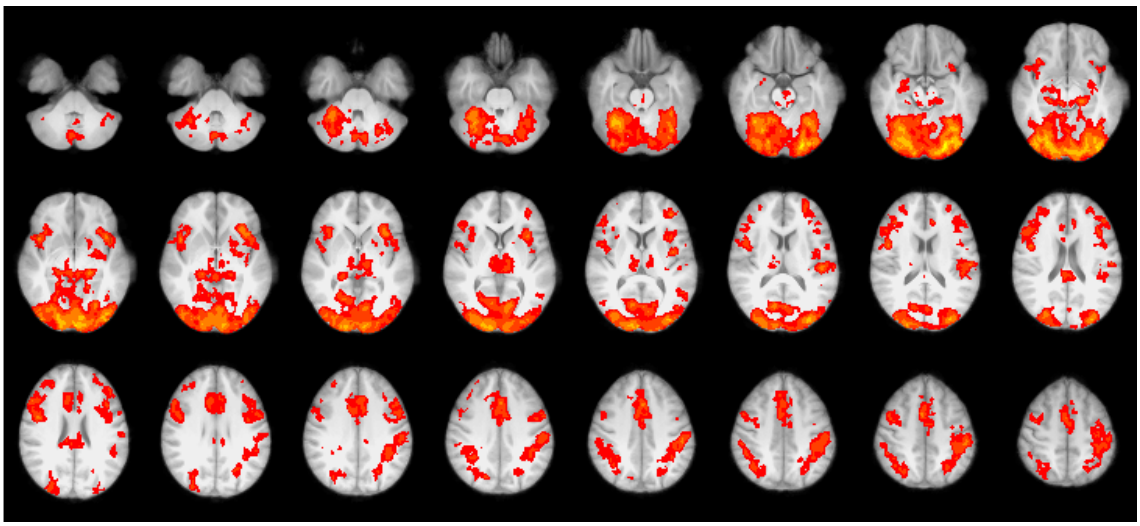

Figure A.2: Group-level activation for the main effect 50% fearful faces. Results are displayed for a significance level of $Z > 2.3$ and a (corrected) cluster significance threshold of $P = 0.05$. Image in radiological convention.

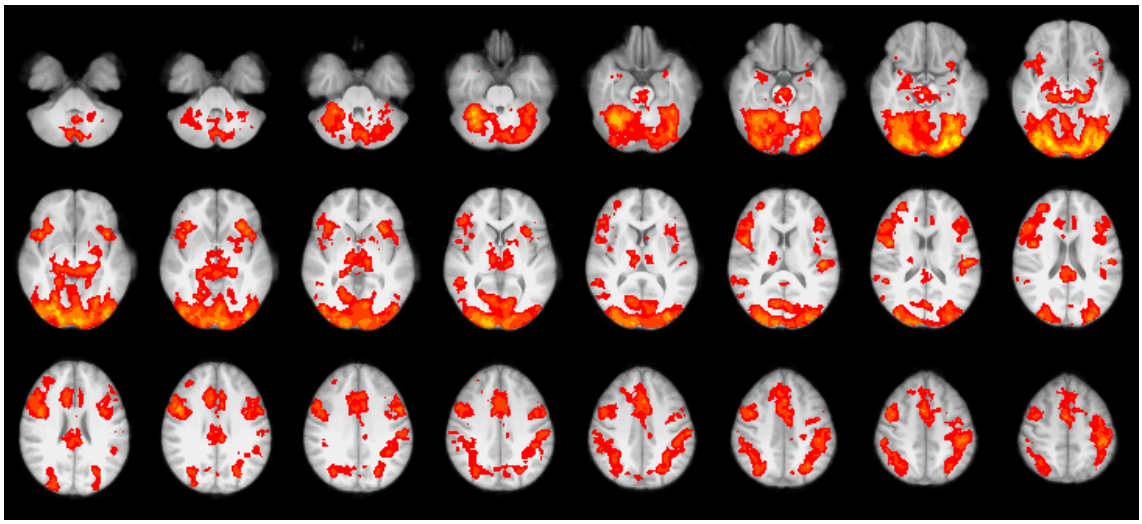

Figure A.3: Group-level activation for the main effect 100% fearful faces. Results are displayed for a significance level of $Z > 2.3$ and a (corrected) cluster significance threshold of $P = 0.05$. Image in radiological convention.

Table A.1: Correlation between vascular reactivity and percent signal change. This table presents correlation coefficient between the signal changes extracted from the breath-hold vs. emotion task.

N = 14	Uncorrected data		Physiological noise corrected data	
	Scan 1	Scan 2	Scan 1	Scan 2
Left amygdala				
neutral	-.18	.42	-.19	.18
50 % fear	-.17	.05	.08	.06
100 % fear	.03	.27	.19	-.03
fear > neutral	.16	-.27	.39	-.14
Right amygdala				
neutral	.01	.58*	.43	.46
50 % fear	.49	.14	.43	.08
100 % fear	.07	.19	.34	.10
fear > neutral	.26	-.51	.07	-.51
Left fusiform				
neutral	-.27	.60*	-.45	.36
50 % fear	-.19	.19	-.29	.14
100 % fear	-.42	.25	-.40	.23
fear > neutral	.05	-.43	.07	-.28
Right fusiform				
neutral	-.14	.26	-.24	.05
50 % fear	-.11	-.32	-.16	-.34
100 % fear	-.21	-.18	-.27	-.14
fear > neutral	-.02	-.54	-.09	-.37

Table A.2: Influence of the correction for vascular reactivity on repeatability. ICCs with and without correction for vascular reactivity are shown for the uncorrected and physiological noise corrected data set. Correction for vascular reactivity was performed by regressing out the influence of vascular reactivity on the emotion-task related BOLD signals, and by using the remaining signal to calculate the ICC. Note that values slightly differ from Table 2.1 because one participant was excluded due to bad breath-hold data.

N = 14	Uncorrected data		Physiological noise corrected data	
	without VR	with VR	without VR	with VR
Left amygdala				
neutral	.06(.41)	.15(.29)	-.04	.01
50 % fear	.00	-.06	-.11	-.06
100 % fear	.34(.10)	.34(.11)	.28(.16)	.32(.12)
fear > neutral	-.54	-.46	-.65	-.61
Right amygdala				
neutral	.00	-.12	-.06	.07(.40)
50 % fear	.39(.08)	.37(.09)	.19(.25)	.28(.16)
100 % fear	.30(.14)	.24(.19)	.17(.27)	.22(.22)
fear > neutral	-.52	-.56	-.44	-.34
Left fusiform				
neutral	.13(.32)	.30(.14)	0	.08(.40)
50 % fear	-.32	-.29	-.23	-.22
100 % fear	-.39	-.50	-.28	-.36
fear > neutral	-.10	-.15	-.05	-.09
Right fusiform				
neutral	.14(.31)	.13(.33)	.07(.40)	.04(.45)
50 % fear	-.04	-.08	-.07	-.16
100 % fear	-.05	-.12	-.07	-.17
fear > neutral	-.03	-.10	.11 (.35)	.10 (.36)

Table A.3: Variance of physiological changes explained by the task. Minimum, maximum and median R^2 for all scans and median R^2 for session 1 and session 2 separately are provided. Only R^2 above .13 reach significance at $P < .05$

Condition	Min. R^2	Max. R^2	Median R^2	Median R^2 Scan 1	Median R^2 Scan 2
all conditions	.03	.16	.08	.06	.09
neutral	.02	.21	.12	.11	.12
50 % fear	.03	.17	.09	.10	.09
100 % fear	.03	.23	.09	.08	.09
fear > neutral	.03	.20	.13	.13	.13

Table A.4: ROI analysis for uncorrected data when only first half of the task is considered. For each of the ROIs, mean and standard deviation for both scanning sessions (scan 1 and scan 2), the significance of the between- session difference, the repeatability of the value and its significance are provided.

	No correction				**Physiological noise correction**			
Area/condition	$M(Std.)$ 1	$M(Std.)$ 2	p	ICC(p)	$M(Std.)$ 1	$M(Std.)$ 2	p	ICC(p)
Left amy.								
neutral	0.16(0.45)	0.17(0.38)	.92	.39(.07)	0.16(0.28)	0.16(0.32)	.98	-.20
50% fearful	0.27(0.13)	0.19(0.31)	.29	.24(.18)	0.26(0.19)	0.20(0.28)	.45	.16(.28)
100% fearful	0.33(0.39)	0.25(0.25)	.40	.39(.07)	0.23(0.28)	0.20(0.31)	.80	-.15
Fear > Neutral	0.38(0.82)	0.16(0.30)	.31	.16(.28)	0.24(0.72)	0.14(0.50)	.69	-.20
Right amy.								
neutral	0.16(0.33)	0.03(23)	.14	.30(.13)	0.13(0.20)	0.10(0.24)	.75	-.33
50% fearful	0.26(0.19)	0.02(0.21)	< .01	.42(.05)	0.26(0.18)	0.10(0.19)	.03	.14(.31)
100% fearful	0.31(0.26)	0.05(0.18)	.02	-.34	0.24(0.25)	0.09(0.21)	.10	.09(.37)
Fear > Neutral	0.32(0.55)	0.02(0.45)	.15	-.12	0.29(0.42)	0.01(0.46)	.16	-.38
Left fusi.								
neutral	0.25(0.35)	0.19(0.30)	.56	.20(.23)	0.28(0.28)	0.11(0.32)	.20	-.28
50% fearful	0.39(0.23)	0.13(0.46)	.09	-.16	0.39(0.18)	0.11(0.33)	.02	-.24
100% fearful	0.46(0.32)	0.18(0.28)	.07	-.58	0.35(0.24)	0.14(0.21)	.07	-.59
Fear > Neutral	0.47(0.72)	-0.02(0.47)	.09	-.40	0.30(0.48)	0.07(0.44)	.28	-.41
Right fusi.								
neutral	0.31(0.42)	0.27(0.18)	.73	.06(.41)	0.32(0.29)	0.18(0.25)	.24	-.40
50% fearful	0.39(0.21)	0.17(0.36)	.10	-.30	0.42(0.19)	0.14(0.27)	.01	-.29
100% fearful	0.48(0.39)	0.21(0.24)	.08	-.51	0.40(0.31)	0.18(0.18)	.08	-.53
Fear > Neutral	0.38(0.76)	-0.10(0.44)	.10	-.43	0.29(0.38)	0.00(0.35)	.11	-.57

Appendix B

Supplement for Chapter 3

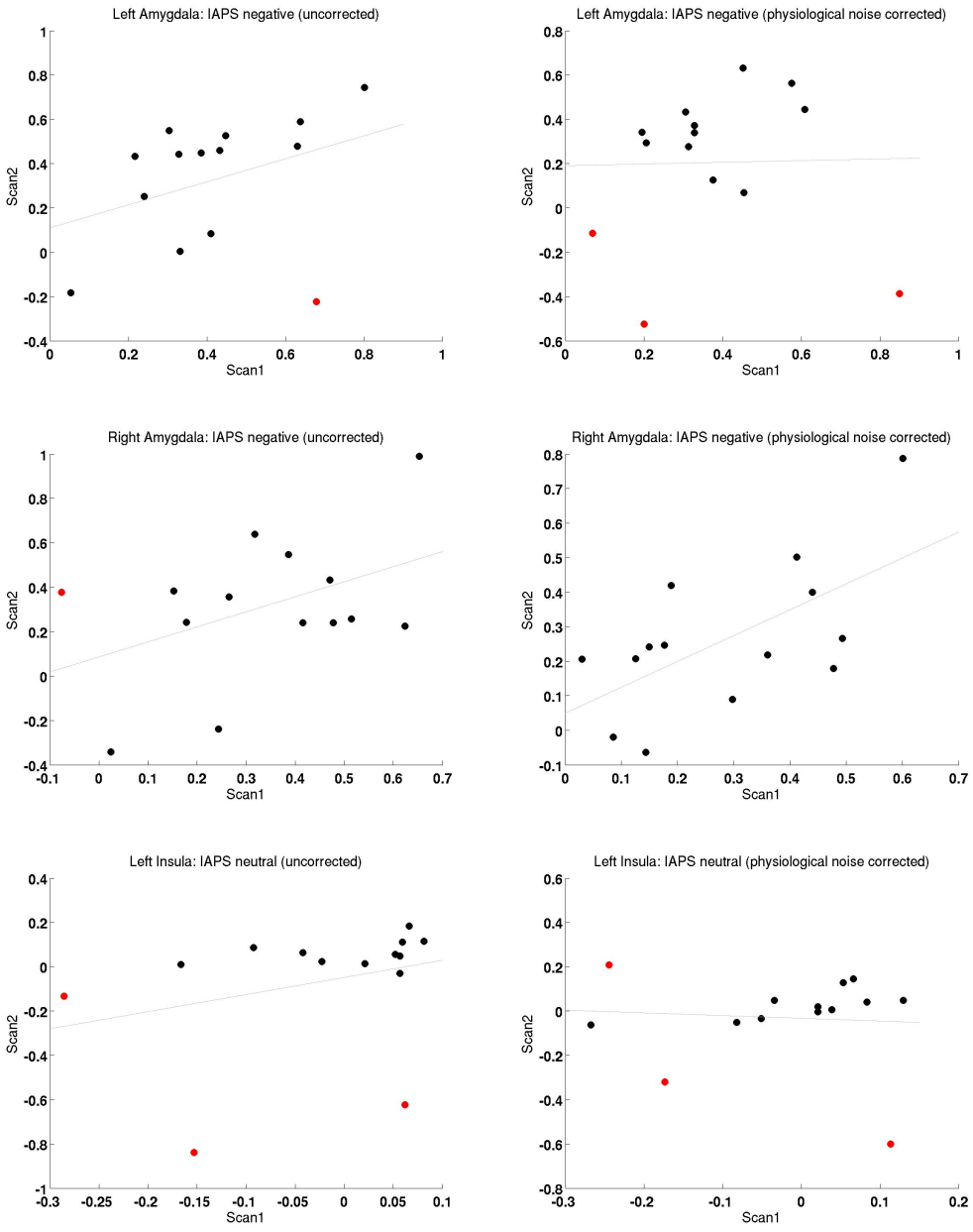

Figure B.1: Scatter plots for repeatability analysis (%SC session 1 on x-axis, %SC session 2 on y-axis). Red dots indicate outliers.

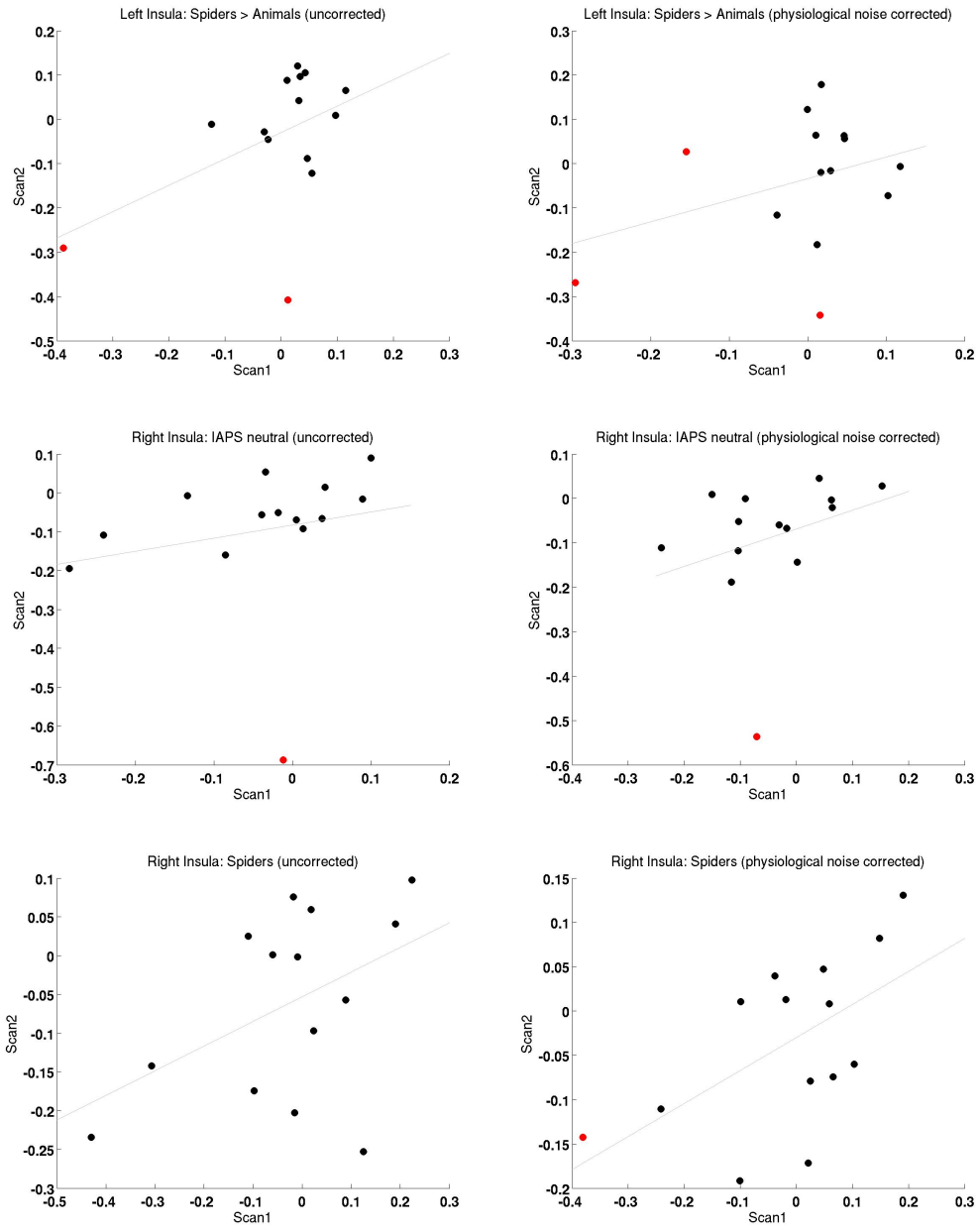

Figure B.2: Scatter plots for repeatability analysis (%SC session 1 on x-axis, %SC session 2 on y-axis). Red dots indicate outliers.

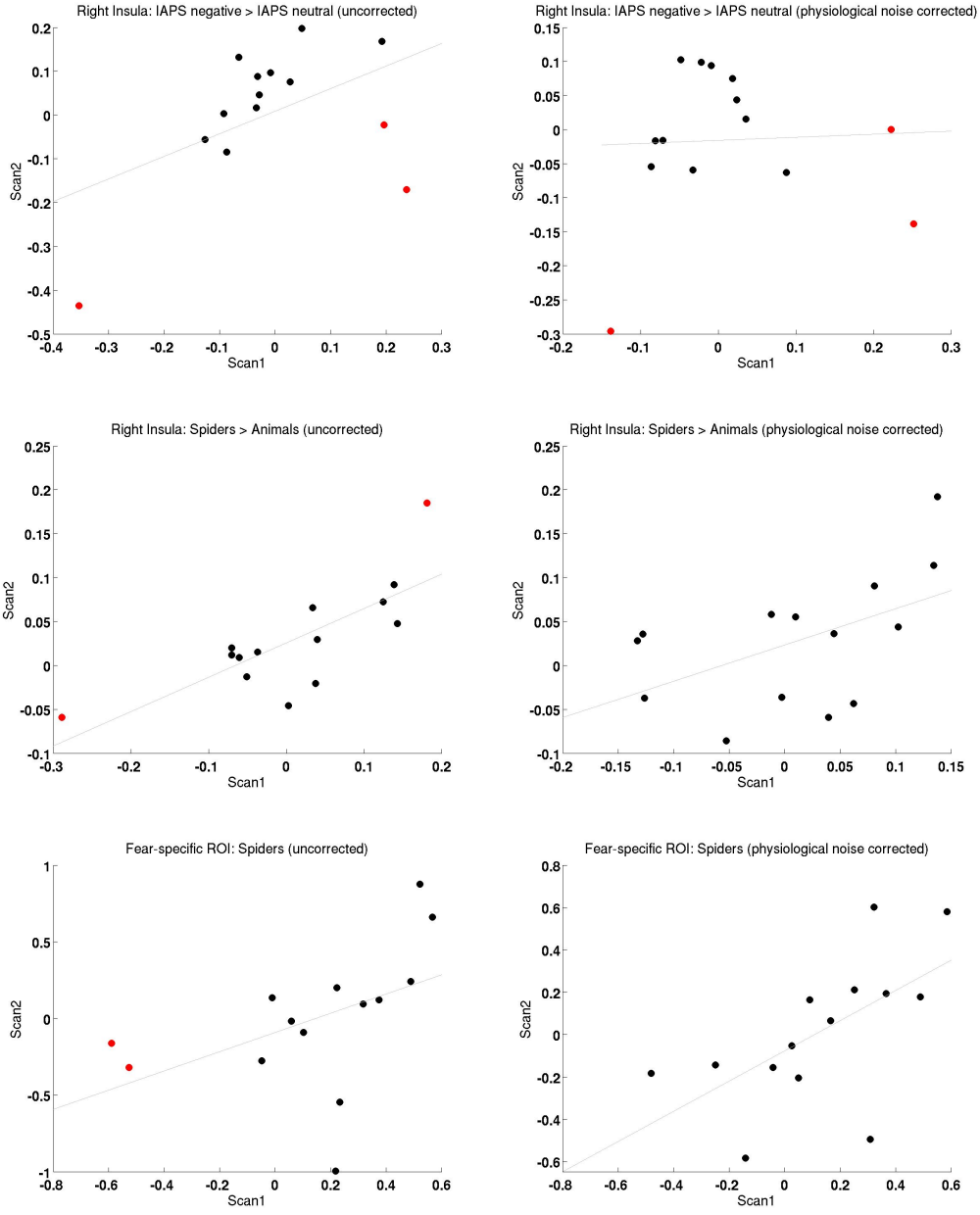

Figure B.3: Scatter plots for repeatability analysis (%SC session 1 on x-axis, %SC session 2 on y-axis). Red dots indicate outliers.

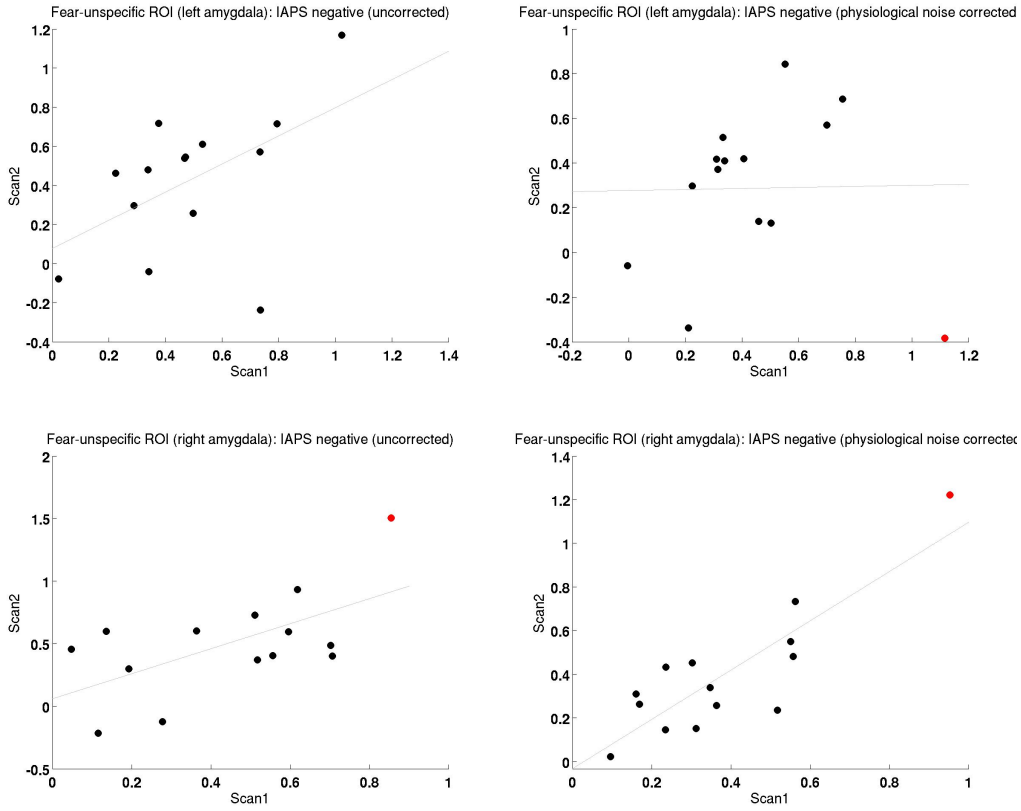

Figure B.4: Scatter plots for repeatability analysis (%SC session 1 on x-axis, %SC session 2 on y-axis). Red dots indicate outliers.

Appendix C

Supplement for Chapter 4

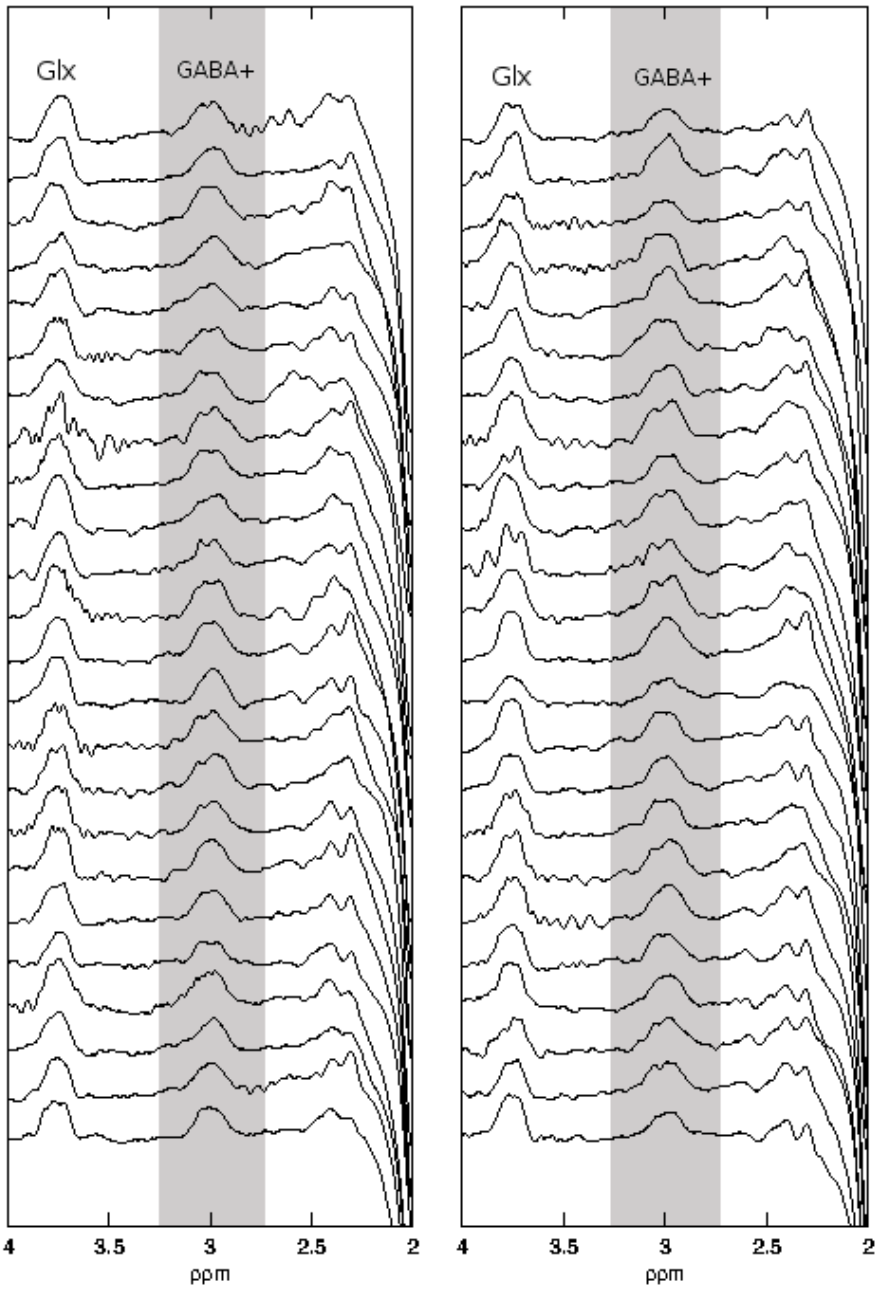

Figure C.1: All spectra from the insula that were included in the analysis.

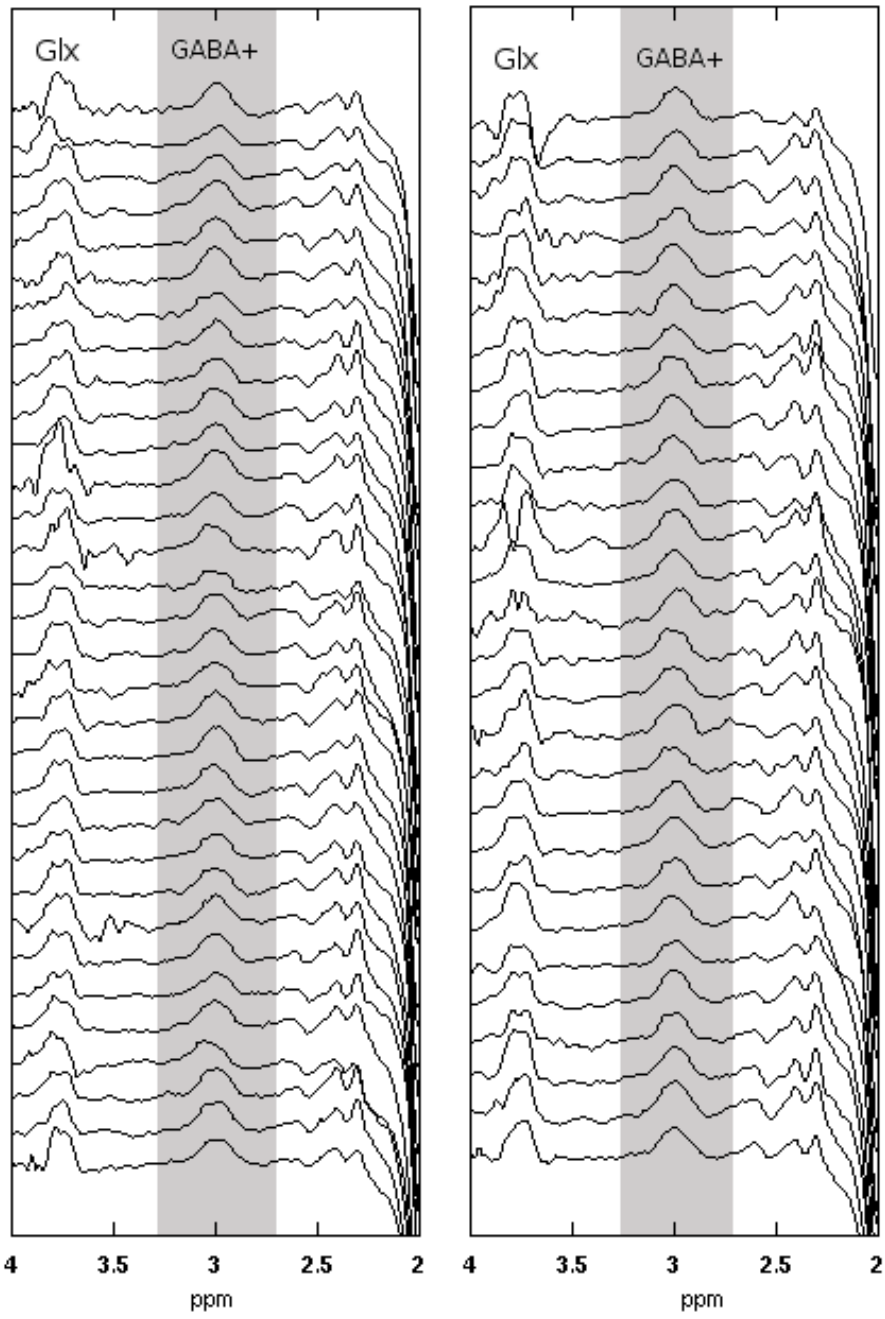

Figure C.2: All spectra from the DLPFC that were included in the analysis.

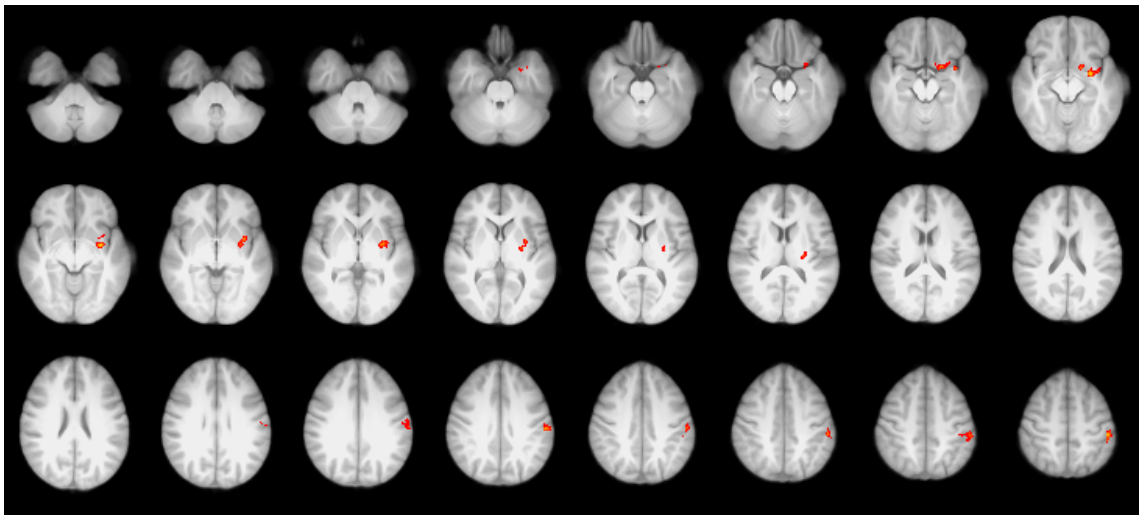

Figure C.3: Group effect for the GABA+ (insula) regressor on the contrast $SPIDERS > ANIMALS$ (N = 37).

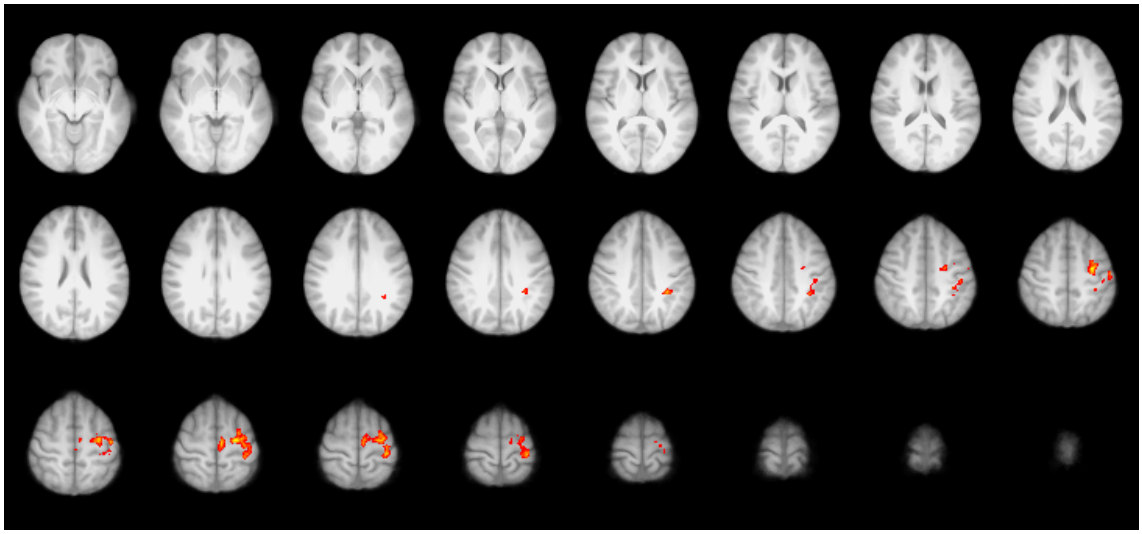

Figure C.4: Group effect for the GABA+ (DLPFC) regressor on the contrast $SPIDERS > ANIMALS$ (N = 37).

Table C.1: Correlations between insular GABA+ (reference: water) and BOLD %SC for a number of contrasts. $IAPS$ contrast refers to $IAPSnegative > IAPSneutral$, $SPIDERS$ contrast refers to $SPIDERS > ANIMALS$. The fear-specific ROI refers to the cluster in the anterior insula derived from the group level activation for the $SPIDERS$ contrast. GABA-sensitive ROI refers to the cluster derived from the analysis including the GABA+ regressor for the $SPIDERS$ contrast. Fear-unspecific ROI refers to the cluster in the anterior insula derived from the group level activation for the $IAPS$ contrast.

Area	$IAPS$ contrast	$SPIDERS$ contrast	$IAPSnegative$	$IAPSneutral$	$SPIDERS$	$ANIMALS$
fear-specific ROI (insula)	$r[23] = .05$, ns	$r[23] = .26$, ns	$r[25] = .32$, ns	$r[23] = -.37$, ns	$r[23] = .10$, ns	$r[24] = -.13$, ns
GABA-sensitive ROI (insula)	$r[24] = .19$, ns	$r[24] = .67$, $p < .001$	$r[26] = .09$, ns	$r[24] = -.13$, ns	$r[23] = .03$, ns	$r[24] = -.74$, $p < .0001$
fear-unspecific ROI (insula)	$r[24] = -.01$, ns	$r[24] = .42$, $p = .03$	$r[23] = -.10$, ns	$r[24] = .00$, ns	$r[24] = -.02$, ns	$r[25] = -.30$, ns

Appendix D

Supplement for Chapter 5

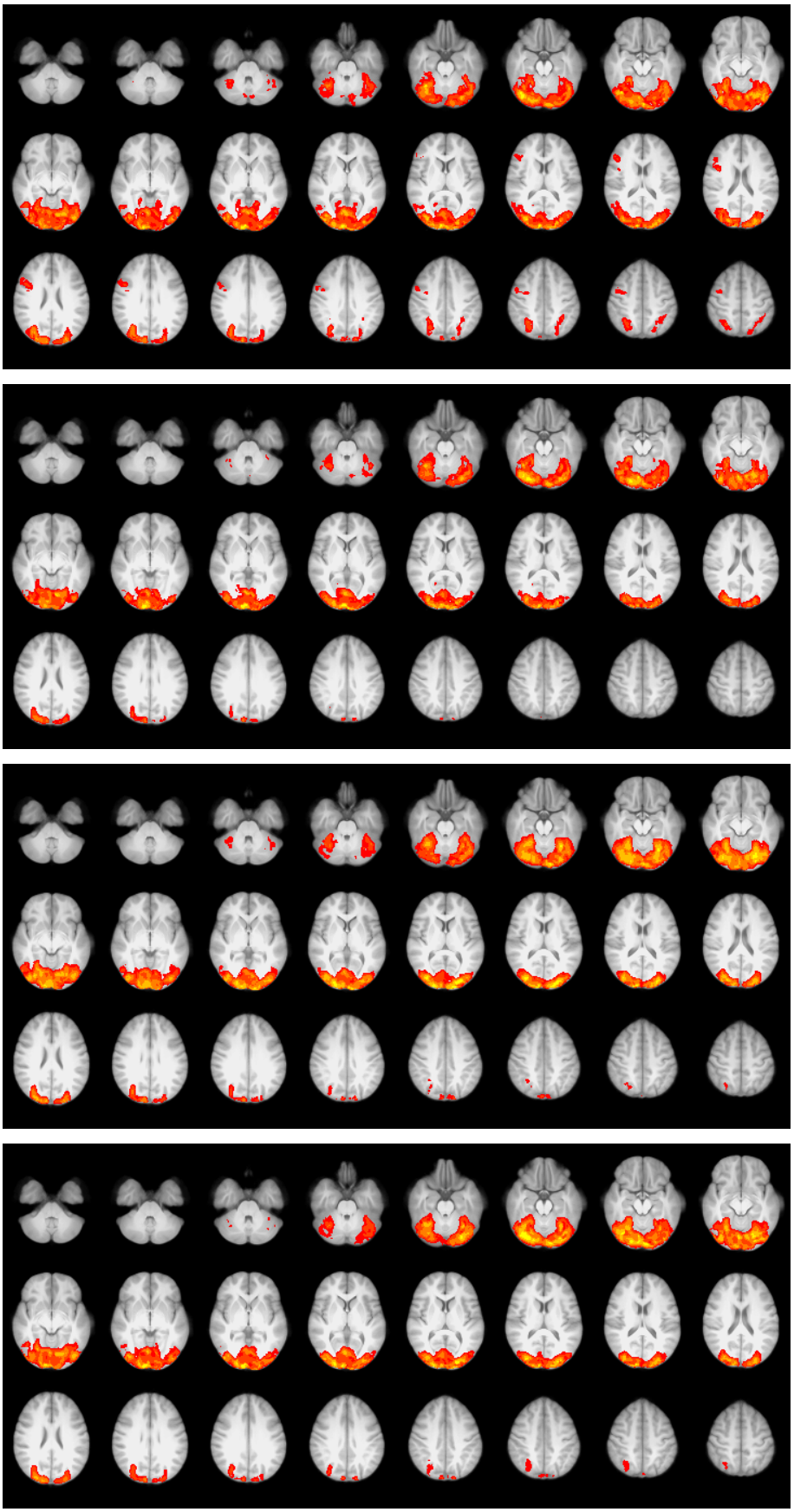

Figure D.1: Uncorrected > corrected. Statistical parametrical maps are shown for *IAPSnegative*, *IAPSneutral*, *SPIDERS*, *ANIMALS* (all vs. fixation cross baseline) in that order. The maps show in which regions the uncorrected dataset leads to stronger BOLD signals than the dataset corrected for physiological noise. The statistical threshold was set to $Z > 5$ and corrected cluster threshold of $P < .05$. Image displayed in radiological convention. No results were found for the opposite contrast.

Appendix E

Supplement for Chapter 9

Table E.1: Within-session repeatability dependent on spectrum exclusion criteria for GABA+/Cr. For each exclusion criterion (top rows: based on fit error; bottom rows: based on ratings), the number of remaining participants, the ICC and its significant value, as well as CV_{within} and $CV_{between}$ based on the remaining sample are shown. ICC(av) refers to the estimated ICC for averaged measures (based on Spearman-Brown).

Fit error												
	DLPFC						Insula					
thr.	N	ICC	p(ICC)	ICC(av)	CV_{ws}	CV_{bs}	N	ICC	p(ICC)	ICC(av)	CV_{ws}	CV_{bs}
20.0	34	0.00	N.A.	0.00	14.80	23.58	35	0.23	0.09	0.37	16.07	25.46
19.5	33	0.00	N.A.	0.00	14.73	23.81	35	0.23	0.09	0.37	16.07	25.46
19.0	33	0.00	N.A.	0.00	14.73	23.81	35	0.23	0.09	0.37	16.07	25.46
18.5	33	0.00	N.A.	0.00	14.73	23.81	35	0.23	0.09	0.37	16.07	25.46
18.0	33	0.00	N.A.	0.00	14.73	23.81	35	0.23	0.09	0.37	16.07	25.46
17.5	33	0.00	N.A.	0.00	14.73	23.81	35	0.23	0.09	0.37	16.07	25.46
17.0	33	0.00	N.A.	0.00	14.73	23.81	34	0.25	0.07	0.40	15.62	25.54
16.5	33	0.00	N.A.	0.00	14.73	23.81	34	0.25	0.07	0.40	15.62	25.54
16.0	32	0.00	N.A.	0.00	13.06	17.89	34	0.25	0.07	0.40	15.62	25.54
15.5	32	0.00	N.A.	0.00	13.06	17.89	34	0.25	0.07	0.40	15.62	25.54
15.0	31	0.00	N.A.	0.00	13.15	17.69	34	0.25	0.07	0.40	15.62	25.54
14.5	31	0.00	N.A.	0.00	13.15	17.69	34	0.25	0.07	0.40	15.62	25.54
14.0	29	0.00	N.A.	0.00	13.60	18.22	31	0.26	0.07	0.42	16.11	26.32
13.5	28	0.00	N.A.	0.00	13.69	18.52	31	0.26	0.07	0.42	16.11	26.32
13.0	27	0.03	0.44	0.06	12.70	16.57	30	0.26	0.08	0.41	16.20	26.50
12.5	26	0.02	0.45	0.05	12.76	16.85	30	0.26	0.08	0.41	16.20	26.50
12.0	23	0.00	N.A.	0.00	13.46	16.19	27	0.27	0.08	0.43	16.36	27.01
11.5	22	0.00	N.A.	0.00	12.96	15.28	25	0.30	0.07	0.46	15.80	24.01
11.0	17	0.08	0.37	0.15	10.57	14.53	23	0.08	0.36	0.14	15.87	21.68
10.5	16	0.24	0.18	0.39	9.12	13.97	20	0.11	0.31	0.21	15.58	21.00
10.0	11	0.52	0.04	0.68	6.94	13.98	20	0.11	0.31	0.21	15.58	21.00
9.5	8	0.44	0.12	0.61	7.47	14.57	17	0.04	0.43	0.09	16.52	21.24
9.0	4	0.66	0.11	0.79	6.58	11.72	12	0.25	0.21	0.40	14.65	19.76
8.5	1	N.A.	N.A.	N.A.	N.A.	N.A.	12	0.25	0.21	0.40	14.65	19.76
8.0	0	N.A.	N.A.	N.A.	N.A.	N.A.	12	0.25	0.21	0.40	14.65	19.76
7.5	0	N.A.	N.A.	N.A.	N.A.	N.A.	5	0.36	0.24	0.53	13.82	17.62
7.0	0	N.A.	N.A.	N.A.	N.A.	N.A.	2	0.52	0.32	0.69	9.13	5.54
6.5	0	N.A.	N.A.	N.A.	N.A.	N.A.	2	0.52	0.32	0.69	9.13	5.54
6.0	0	N.A.	N.A.	N.A.	N.A.	N.A.	1	N.A.	N.A.	N.A.	N.A.	N.A.
Rating												
	DLPFC						Insula					
thr.	N	ICC	p(ICC)	ICC(av)	CV_{ws}	CV_{bs}	N	ICC	p(ICC)	ICC(av)	CV_{ws}	CV_{bs}
1.0	34	0.00	N.A.	0.00	14.80	23.58	35	0.23	0.09	0.37	16.07	25.46
1.2	33	0.00	N.A.	0.00	14.73	23.81	29	0.31	0.05	0.48	14.74	26.33
1.5	32	0.00	N.A.	0.00	13.93	22.14	25	0.08	0.35	0.15	14.16	20.27
1.8	31	0.00	N.A.	0.00	13.39	22.31	24	0.10	0.31	0.19	14.00	20.46
2.0	29	0.00	N.A.	0.00	11.83	15.03	21	0.21	0.17	0.35	13.13	20.32
2.2	25	0.00	N.A.	0.00	12.40	15.44	19	0.23	0.16	0.38	13.41	20.83
2.5	24	0.00	N.A.	0.00	11.51	15.18	18	0.43	0.03	0.60	11.99	17.71
2.8	22	0.05	0.41	0.09	10.06	13.14	13	0.48	0.04	0.65	12.40	19.74
3.0	21	0.00	N.A.	0.00	10.37	12.18	9	0.51	0.06	0.68	12.77	21.50
3.2	18	0.00	N.A.	0.00	10.07	11.24	8	0.54	0.07	0.70	13.26	22.77
3.5	13	0.00	N.A.	0.00	10.83	12.55	7	0.33	0.21	0.50	13.23	19.91
3.8	10	0.01	0.48	0.03	10.36	13.17	3	0.73	0.13	0.85	8.15	19.30
4.0	6	0.00	N.A.	0.00	9.60	11.58	3	0.73	0.13	0.85	8.15	19.30
4.2	4	0.00	N.A.	0.00	13.33	10.57	2	0.94	0.11	0.97	8.10	14.50
4.5	2	0.00	N.A.	0.00	8.28	8.26	1	N.A.	N.A.	N.A.	N.A.	N.A.
4.8	1	N.A.	N.A.	N.A.	N.A.	N.A.	1	N.A.	N.A.	N.A.	N.A.	N.A.

Table E.2: Between-session repeatability dependent on spectrum exclusion criteria for GABA+/Cr. For each exclusion criterion (top rows: based on fit error; bottom rows: based on ratings), the number of remaining participants, the ICC and its significant value, as well as CV_{within} and $CV_{between}$ based on the remaining sample are shown. ICC(av) refers to the estimated ICC for averaged measures (based on Spearman-Brown).

Fit error

	DLPFC						Insula					
thr.	N	ICC	p(ICC)	ICC(av)	CV_{ws}	CV_{bs}	N	ICC	p(ICC)	ICC(av)	CV_{ws}	CV_{bs}
20.0	13	0.00	N.A.	0.00	18.38	27.01	14	0.10	0.36	0.18	15.74	25.76
19.5	13	0.00	N.A.	0.00	17.77	26.90	14	0.10	0.36	0.18	15.74	25.76
19.0	13	0.00	N.A.	0.00	17.77	26.90	14	0.10	0.36	0.18	15.74	25.76
18.5	13	0.00	N.A.	0.00	17.77	26.90	14	0.10	0.36	0.18	15.74	25.76
18.0	13	0.00	N.A.	0.00	17.77	26.90	14	0.10	0.36	0.18	15.74	25.76
17.5	13	0.00	N.A.	0.00	17.77	26.90	14	0.10	0.36	0.18	15.74	25.76
17.0	13	0.00	N.A.	0.00	17.77	26.90	14	0.10	0.36	0.18	15.74	25.76
16.5	13	0.00	N.A.	0.00	17.77	26.90	14	0.10	0.36	0.18	15.74	25.76
16.0	13	0.00	N.A.	0.00	17.77	26.90	14	0.10	0.36	0.18	15.74	25.76
15.5	13	0.00	N.A.	0.00	17.77	26.90	14	0.10	0.36	0.18	15.74	25.76
15.0	13	0.00	N.A.	0.00	17.77	26.90	14	0.09	0.38	0.16	15.81	25.80
14.5	13	0.00	N.A.	0.00	17.47	26.71	14	0.09	0.38	0.16	15.81	25.80
14.0	11	0.06	0.43	0.11	12.52	19.21	14	0.11	0.35	0.20	15.65	25.75
13.5	11	0.11	0.37	0.20	12.85	19.60	14	0.11	0.35	0.20	15.65	25.75
13.0	7	0.07	0.44	0.13	12.35	14.57	14	0.09	0.38	0.16	16.25	25.57
12.5	5	0.10	0.42	0.19	13.29	16.51	13	0.20	0.24	0.34	14.46	24.06
12.0	5	0.10	0.42	0.19	13.29	16.51	13	0.20	0.24	0.34	14.46	24.06
11.5	5	0.01	0.49	0.02	11.57	13.56	13	0.16	0.29	0.27	15.16	25.88
11.0	5	0.48	0.17	0.65	7.91	14.32	13	0.15	0.30	0.27	14.69	24.65
10.5	4	0.78	0.06	0.88	5.99	14.82	13	0.23	0.22	0.37	13.49	25.30
10.0	2	0.00	N.A.	0.00	6.56	6.55	13	0.23	0.22	0.37	13.49	25.30
9.5	1	N.A.	N.A.	N.A.	9.85	9.85	12	0.22	0.24	0.36	14.12	26.08
9.0	1	N.A.	N.A.	N.A.	10.37	10.37	10	0.18	0.29	0.31	16.02	27.19
8.5	0	N.A.	N.A.	N.A.	N.A.	N.A.	8	0.37	0.16	0.54	11.24	21.77
8.0	0	N.A.	N.A.	N.A.	N.A.	N.A.	7	0.32	0.22	0.49	13.91	23.19
7.5	0	N.A.	N.A.	N.A.	N.A.	N.A.	5	0.22	0.34	0.37	17.50	26.95
7.0	0	N.A.	N.A.	N.A.	N.A.	N.A.	3	0.00	N.A.	0.00	10.99	10.30
6.5	0	N.A.	N.A.	N.A.	N.A.	N.A.	1	N.A.	N.A.	N.A.	7.14	7.14
6.0	0	N.A.	N.A.	N.A.	N.A.	N.A.	1	N.A.	N.A.	N.A.	7.14	7.14

Rating

	DLPFC						Insula					
thr.	N	ICC	p(ICC)	ICC(av)	CV_{ws}	CV_{bs}	N	ICC	p(ICC)	ICC(av)	CV_{ws}	CV_{bs}
1.0	13	0.00	N.A.	0.00	18.38	27.01	14	0.10	0.36	0.18	15.74	25.76
1.2	12	0.09	0.39	0.16	13.42	19.60	14	0.11	0.35	0.19	15.67	25.73
1.5	12	0.09	0.39	0.16	13.42	19.60	14	0.16	0.29	0.27	13.97	24.24
1.8	11	0.28	0.18	0.44	11.31	14.78	13	0.18	0.27	0.30	13.84	24.96
2.0	11	0.28	0.18	0.44	11.31	14.78	13	0.09	0.38	0.17	15.20	26.06
2.2	10	0.31	0.18	0.47	12.38	15.46	12	0.20	0.26	0.33	13.43	25.56
2.5	8	0.33	0.19	0.49	11.89	16.42	12	0.17	0.29	0.29	14.07	25.70
2.8	6	0.72	0.04	0.83	8.09	16.72	11	0.33	0.15	0.49	12.10	22.86
3.0	6	0.69	0.04	0.81	8.44	16.99	10	0.37	0.13	0.54	12.04	24.57
3.2	4	0.85	0.03	0.92	8.17	17.42	9	0.50	0.07	0.67	11.09	20.00
3.5	3	0.80	0.10	0.89	8.26	18.76	6	0.54	0.10	0.70	8.29	17.20
3.8	3	0.52	0.24	0.68	10.60	15.69	5	0.47	0.17	0.64	11.07	19.44
4.0	2	0.53	0.32	0.69	18.15	18.74	4	0.03	0.48	0.06	10.64	14.77
4.2	1	N.A.	N.A.	N.A.	9.62	9.62	2	0.38	0.38	0.55	7.55	3.92
4.5	1	N.A.	N.A.	N.A.	9.62	9.62	2	0.38	0.38	0.55	7.55	3.92
4.8	0	N.A.	N.A.	N.A.	N.A.	N.A.	1	N.A.	N.A.	N.A.	10.21	10.21
5.0	0	N.A.	N.A.	N.A.	N.A.	N.A.	1	N.A.	N.A.	N.A.	7.14	7.14

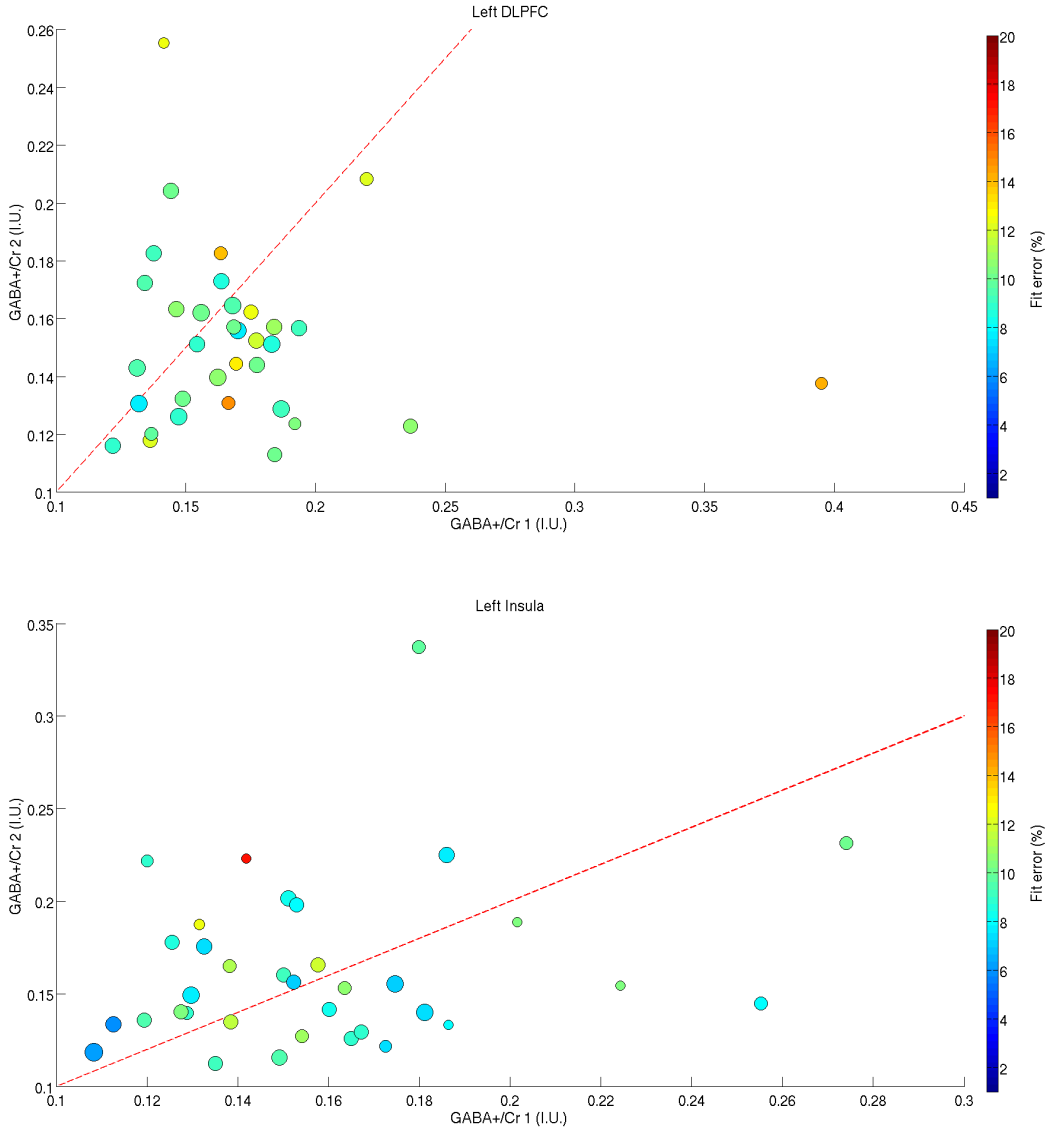

Figure E.1: Within-session repeatability. Scatter plot of GABA+/Cr measure obtained in run 1 with GABA+/Cr measure obtained in run 2 (top: DLPFC, bottom: insula). The colour of the dot refers to the mean fit error, the size of the bubble to the mean rating (the bigger, the better rated the spectrum quality). The red line indicates the ideal slope of data.

Table E.3: Effect of inclusion criterion on number of participants. Number of participants are shown for participants with two spectra meeting the inclusion criterion (N 2spec), and number of participants with one spectrum meeting the criterion (N 1spec).

Fit error		DLPFC		Insula	
	thresh.	N 2spec	N 1spec	N 2spec	N 1spec
	20.0	33	40	36	41
	19.5	33	40	36	41
	19.0	33	38	36	41
	18.5	33	38	36	41
	18.0	32	38	36	41
	17.5	32	38	36	41
	17.0	32	38	36	40
	16.5	32	38	36	39
	16.0	32	38	36	39
	15.5	32	38	36	39
	15.0	32	37	36	39
	14.5	32	37	35	39
	14.0	32	37	35	39
	13.5	31	37	35	38
	13.0	31	37	32	38
	12.5	31	37	32	38
	12.0	30	37	32	38
	11.5	30	37	31	38
	11.0	28	37	29	38
	10.5	28	37	27	38
	10.0	26	37	25	38
	9.5	24	35	21	35
	9.0	23	34	21	35
	8.5	23	31	19	35
	8.0	19	31	16	32
	7.5	17	26	8	29
	7.0	15	23	6	26
	6.5	11	22	6	23
	6.0	5	20	4	14
	5.5	3	16	1	10
	5.0	0	9	1	9
Rating		DLPFC		Insula	
	thresh.	N 2spec	N 1spec	N 2spec	N 1spec
	1.0	33	40	36	41
	1.2	32	39	29	34
	1.5	31	38	25	33
	1.8	30	37	24	33
	2.0	29	35	21	33
	2.2	25	35	19	32
	2.5	24	34	18	32
	2.8	22	32	13	30
	3.0	21	31	9	30
	3.2	18	29	8	25
	3.5	13	26	7	21
	3.8	10	21	3	14
	4.0	6	18	3	13
	4.2	4	13	2	10
	4.5	2	9	1	8
	4.8	1	7	1	4
	5.0	0	0	0	1

Appendix F

Supplement for Chapter 10

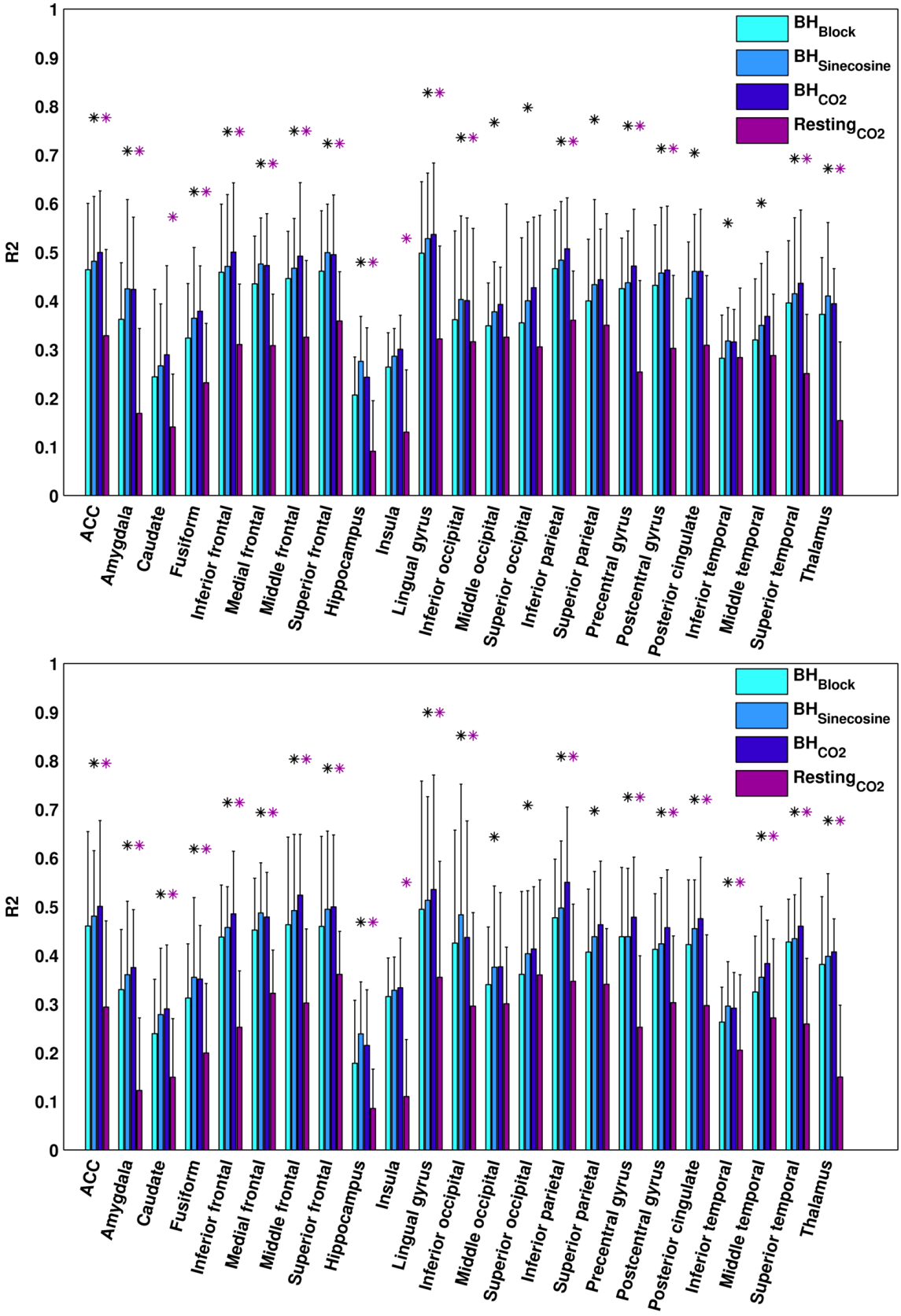

Figure F.1: The median amount of variance (error bars: interquartile range) explained by each of the methods in each region of interest in the left hemisphere (left) and right hemisphere (right). A black asterisk indicates a significant difference between the three breath-hold based analyses. A purple asterisk indicates a significant difference between the resting state based analysis and the mean of the breath-hold based analyses.

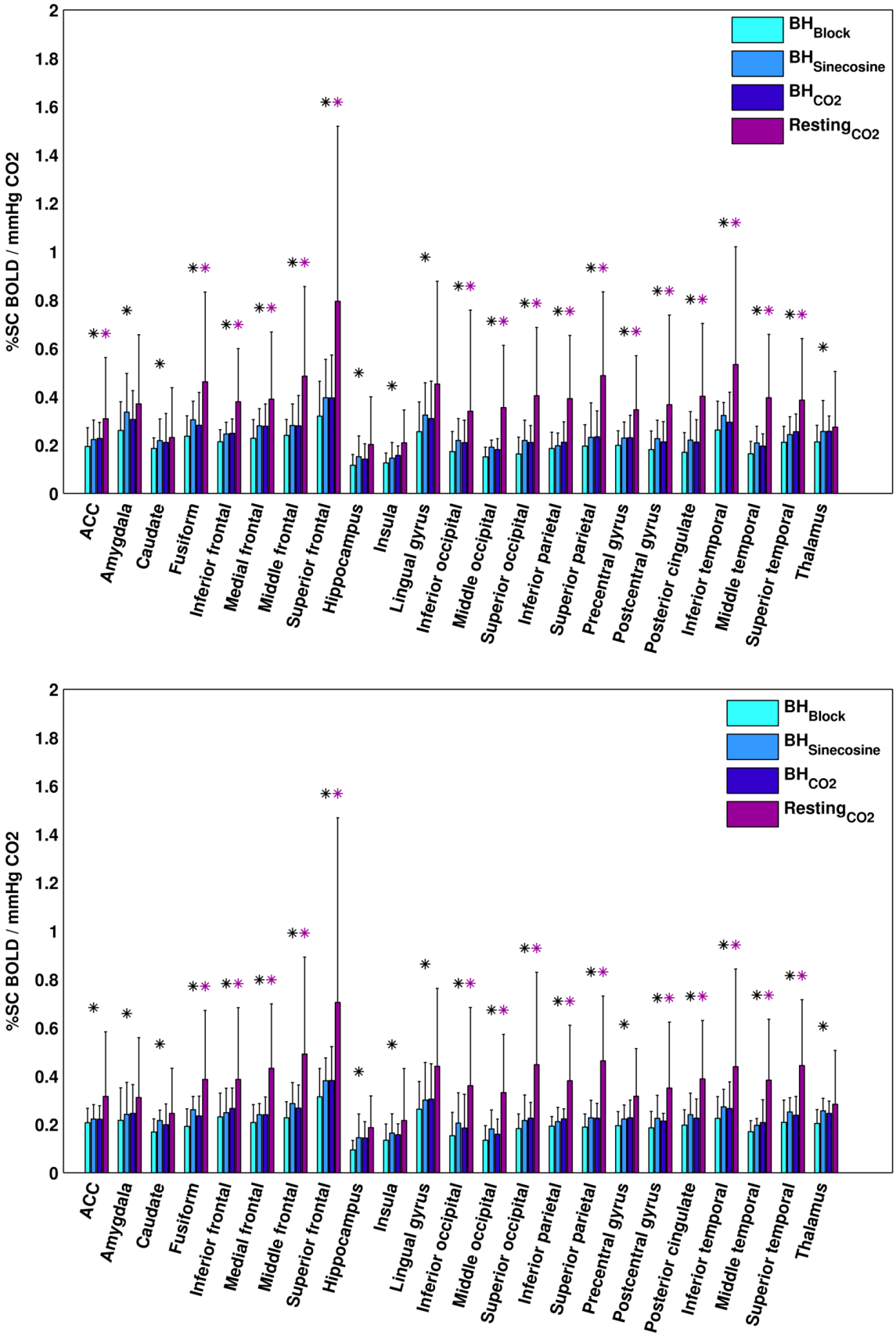

Figure F.2: The median estimated vascular reactivity (error bars: interquartile range) by each of the methods in each region of interest in the left hemisphere (left) and right hemisphere (right). A black asterisk indicates a significant difference between the three breath-hold based analyses. A purple asterisk indicates a significant difference between the resting state based analysis and the mean of the breath-hold based analyses.

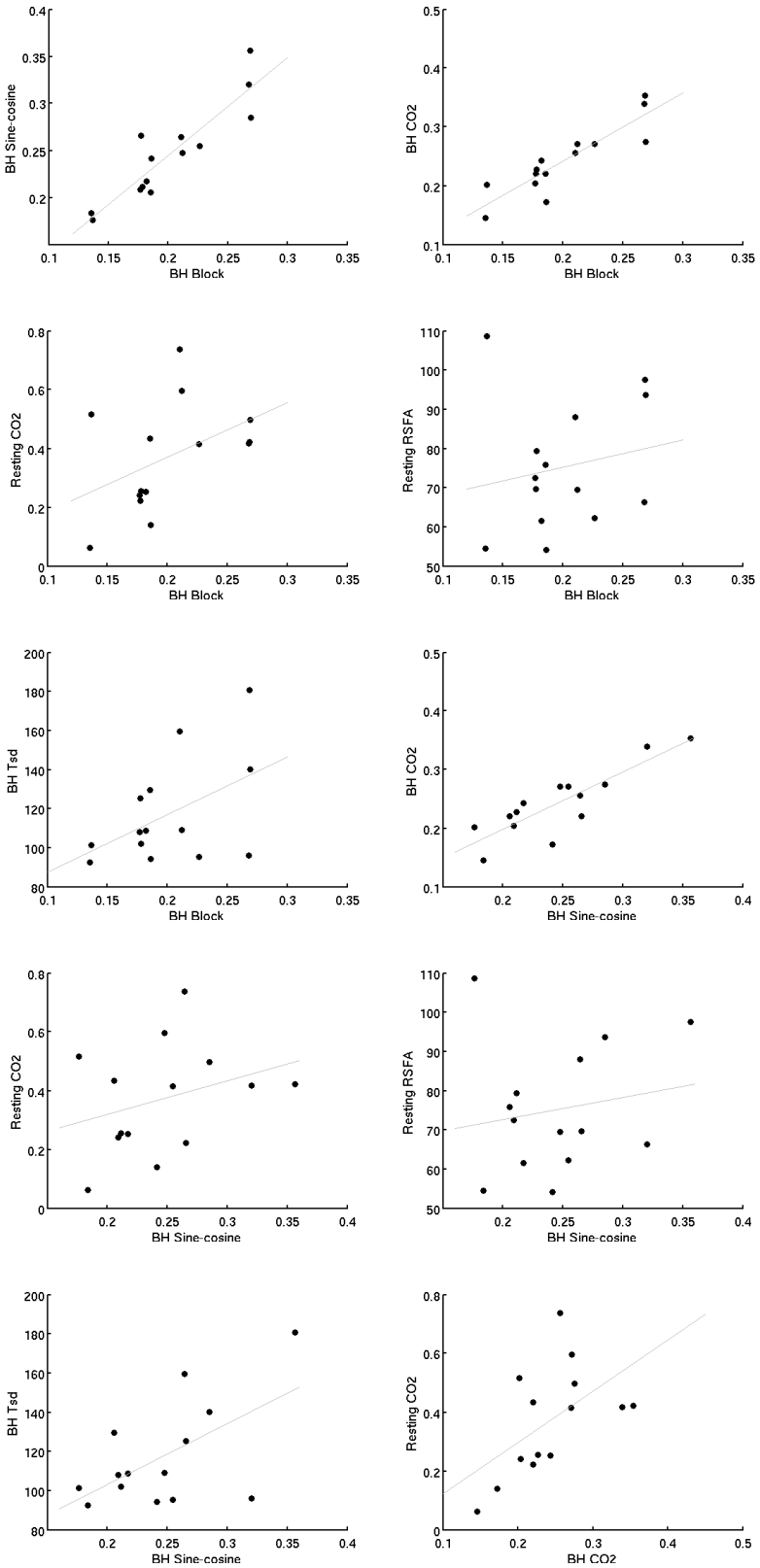

Figure F.3: Scatter plots for between-subject correlations of vascular reactivity estimates (averaged over gray matter) obtained by the six different methods BH_{Block}, $BH_{\text{Sine-Cosine}}$, BH_{CO2}, $Resting_{\text{CO2}}$, $Resting_{\text{RSFA}}$ and BH_{Tsd}.

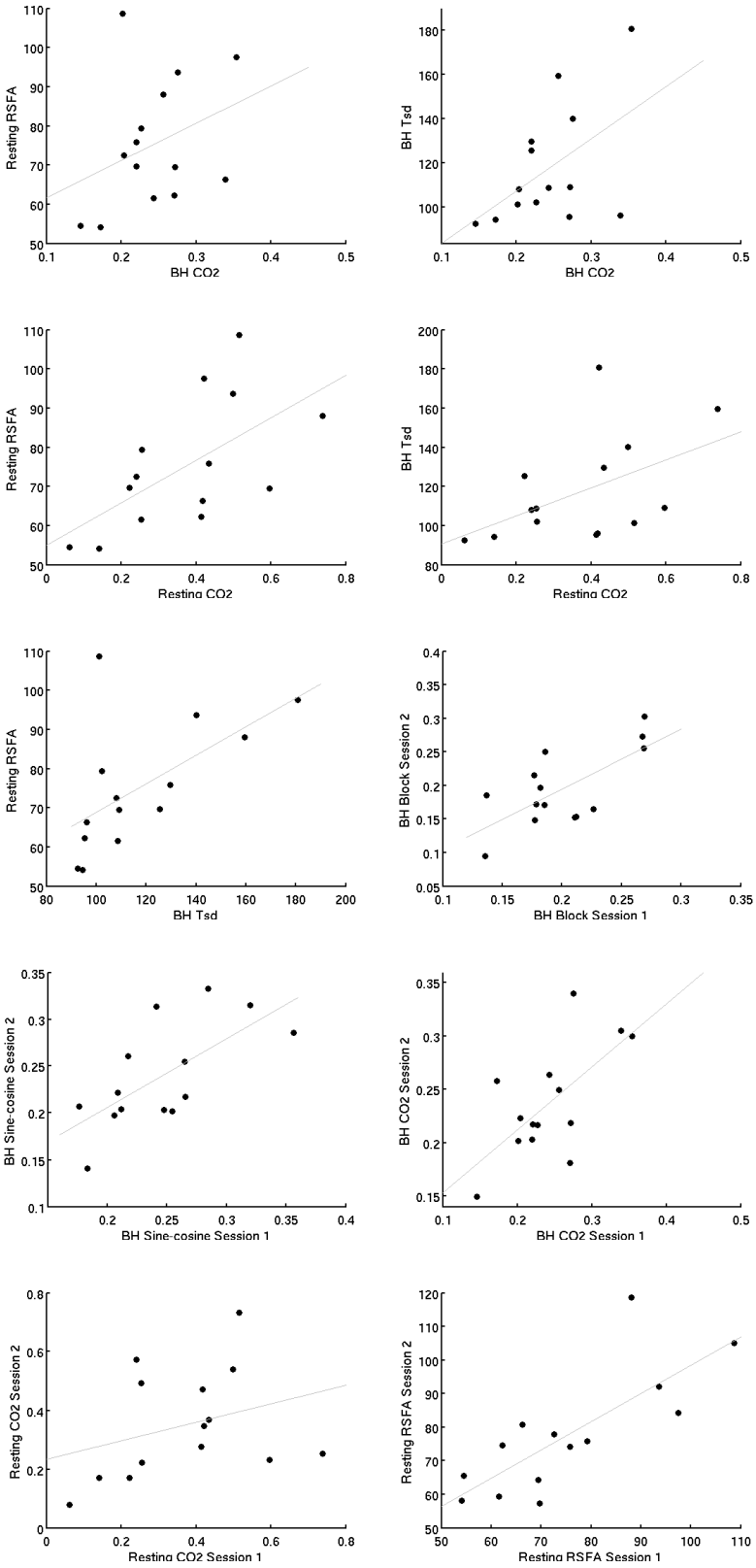

Figure F.4: ... continued

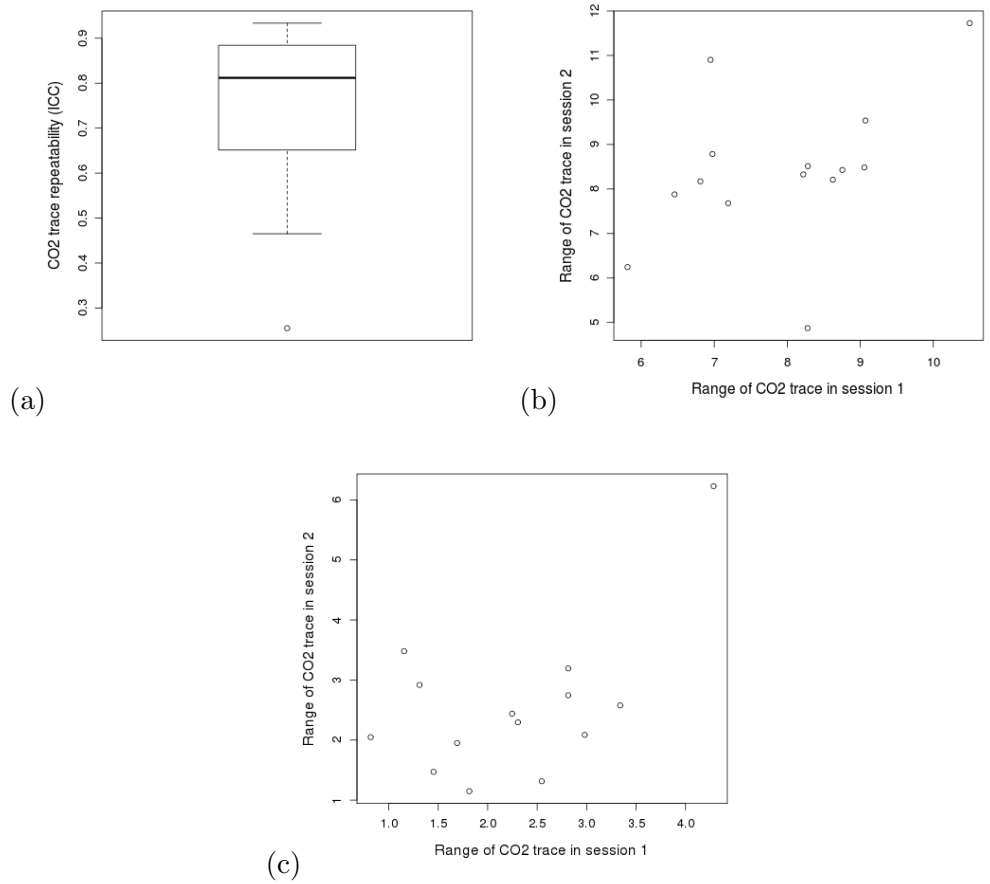

Figure F.5: a) Repeatability of the CO_2 trace during the breath-hold task. b) Scatterplot of the CO_2 range obtained during the breath-hold task in session 1 vs. in session 2. 3) Scatterplot of the CO_2 range obtained during the resting scan in session 1 vs. in session 2.